PB83-251322

Environmental Engineering and Pollution Control Processes State-of-the-Art Seminar

(U.S.) Environmental Protection Agency
Washington, DC

Sep 82

U.S. Department of Commerce
National Technical Information Service
NTIS

TECHNICAL REPORT DATA

(Please read Instructions on the reverse before completing)

1. REPORT NO. EPA 600/9-82-018	2.	3. RECIPIENT'S ACCESSION NO. PB83-251322
4. TITLE AND SUBTITLE Environmental Engineering and Pollution Control Processes State-of-the-Art Seminar		5. REPORT DATE September, 1982
		6. PERFORMING ORGANIZATION CODE
7. AUTHOR(S) Donald F. Carey & Jerry Y.C. Huang, editors		8. PERFORMING ORGANIZATION REPORT NO.
9. PERFORMING ORGANIZATION NAME AND ADDRESS Office of Exploratory Research (RD-675) U.S. Environmental Protection Agency Washington, D.C. 20460		10. PROGRAM ELEMENT NO.
		11. CONTRACT/GRANT NO.
12. SPONSORING AGENCY NAME AND ADDRESS Office of Exploratory Research Office of Research and Development U.S. Environmental Protection Agency Washington, DC 20460		13. TYPE OF REPORT AND PERIOD COVERED Final
		14. SPONSORING AGENCY CODE EPA-600/20

15. SUPPLEMENTARY NOTES

16. ABSTRACT

This publication will compile all of the papers and comments presented at the July State-of-the Art Seminar.

17. KEY WORDS AND DOCUMENT ANALYSIS

a. DESCRIPTORS	b. IDENTIFIERS/OPEN ENDED TERMS	c. COSATI Field/Group

18. DISTRIBUTION STATEMENT Release unlimited	19. SECURITY CLASS *(This Report)* Unclassified	21. NO. OF PAGES 284
	20. SECURITY CLASS *(This page)* Unclassified	22. PRICE

EPA Form 2220-1 (Rev. 4-77) PREVIOUS EDITION IS OBSOLETE

United States
Environmental Protection
Agency

Office of
Exploratory Research
Washington DC 20460

EPA-600/9-82-018
September 1982

Research and Development

PB83-251322

EPA

Environmental Engineering and Pollution Control Processes State-of-the-Art Seminar

REPRODUCED BY
NATIONAL TECHNICAL
INFORMATION SERVICE
U.S. DEPARTMENT OF COMMERCE
SPRINGFIELD, VA 22161

ENVIRONMENTAL ENGINEERING AND POLLUTION CONTROL PROCESSES
STATE-OF-THE-ART SEMINAR

Donald F. Carey and
Jerry Y.C. Huang, Editors

1981
Organized by Environmental Protection Agency,
Office of Research Grants and Centers
Held at Andrew W. Breidenbach Research Center,
Cincinnati, Ohio 45268, July 22-24, 1981
Published by Office of Exploratory Research,
Environmental Protection Agency
Washington, D.C.

Preface

By direction of Congress, the Office of Research and Development, Environmental Protection Agency, implemented a new process for solicitation and evaluation of research grants in late 1979. An Office of Research Grants and Centers (ORGC) began operation in January 1980. Research grants funded under the auspices of ORGC are not necessarily representative of the kinds of projects which the Agency funds as cooperative agreements and contracts through other programs at Headquarters and the regional research laboratories.

In April 1980, the first annual generalized solicitation was issued. Initially, proposals were requested in four major areas, i.e. Environmental Engineering and Pollution Control Processes; Health Research; Environmental Chemistry and Physics; and Environmental Biology. Usually, eligibility is limited to universities and other non-profit institutions.

The program is extremely competitive with scientific merit of every proposal being evaluated by an extramural Peer Review Panel comprised of experts selected from the academic community; state, local and Federal governmental agencies; and industry. A chairperson approved by the Science Advisory Board administers the Peer Review Process. Only those proposals recommended for consideration for funding by the Peer Review Panel are considered further by ORGC. The final funding decision for each competitive research grant is made within the Agency relative to scientific merit, relevance to current Agency programs, and availability of monies.

Arthur C. Stern, Professor Emeritus of the University of North Carolina, served as the first chairperson of the Environmental Engineering and Pollution Control Processes Peer Review Panel. His skills in organization and appreciation of detail have been important assets in the inauguration of the competitive grants program.

Each Principal Investigator is required to present a seminar detailing his research. The discussant for each paper, in most instances, was one of the initial reviewers of the proposal.

The Agency wishes to compliment both Professor Stern and the Principal Invetigators for the quality and depth of work presented.

CONTENTS

Preface ii

Seminar Program v

Papers:

1. Coagulation of Natural Organic Substances in Water Treatment. Charles R. O'Melia and Brian A. Dempsey 1
   Comments: George E. Wilson

2. Cyst Inactivation With Chlorine and Chlorine Dioxide. Otis J. Sproul, Y.S.R. Chen, John P. Engel, and Alan J. Rubin 24
   Comments: Harold W. Wolf

3. Electrosorption of Phenol Onto Activated Carbon. Peter S. Fedkiw, Carlton F. Dwiggins, and Joseph McGuire 39
   Comments: James O. Leckie

4. Effect of Turbidity and Other Factors on the Virus Disinfection Process Using Free and Combined Chlorine Forms. Pasquale V. Scarpino 56
   Comments: Richard F. Unz

5. Measurement of Aqueous Particle Size Distributions. James R. Hunt 84
   Comments: Charles R. O'Melia

6. Analytical Fourier Transform Mass Spectrometry. Michael L. Gross 105
   Comments: S. A. Hoenig

7. The Investigation and Demonstration of a Hydroperm Microfiltration System for the Treatment of Electroplating Wastewater Effluent. Han-Lieh Liu 121
   Comments: E. Robert Baumann

8. Wet Oxidation of the Waste Water From Coal Gasification Installations. O. J. Hahn, J. C. Carter and O. W. Stewart 134
   Comments: Rolf T. Skrinde

9. Theory for Penetration in a Pulse-Jet Cleaned Fabric Filter. David Leith, Michael Ellenbecker and Melvin W. First 149
   Comments: Richard B. Engdahl

10. Integrated Swine Waste Management System for Pollution Control and Energy and Food Production. P. Y. Yang..............163
Comments: Richard I. Dick

11. The Removal of Heavy Metals by Activated Carbon Process from Water and Wastewater. C. P. Huang, M. O. Corapcioglu, D. W. Blankenship, A. E. Boomhower and P. L. K. Fu...............174
Comments: Walter J. Weber

12. Heterogeneous Catalytic Oxidation of Model Chlorinated Hydrocarbons. Michael P. Manning................................200
Comments: H. William Prengle, Jr.

13. Combustion of Chlorinated Hydrocarbons. Selman M. Senkan, Ashwani K. Gupta, John M. Robinson and Horacio Valeras...........219
Comments: Richard Chaddock

14. The Effect of Aeration Basin Configuration on Activated Sludge Bulking at Low Organic Loading. Sang-Eun Lee, Ben L. Koopman, David Jenkins and Ronald F. Lewis...............................236
Comments: G. Wolfgang Fuhs

Appendix

A. Environmental Engineering Research Seminar Attendees.............266

STATE-OF-THE-ART RESEARCH SEMINAR
IN
ENVIRONMENTAL ENGINEERING AND POLLUTION CONTROL PROCESSES

JULY 22-24, 1981
Andrew W. Breidenbach Environmental Research Center
Cincinnati, Ohio 45268
(513) 684-7771

Wednesday, July 22, 1981

1:00 - 4:30 p.m.	Registration and Tour of Laboratory Facilities
6:00 p.m.	Banquet—Vernon Manor Hotel Mr. Dennis A. Tirpak Director Office of Exploratory Research Office of Research and Development Washington, D.C. 20460

Thursday, July 23, 1981

8:00 a.m.	Welcome and Introduction Mr. Lou Lefke Deputy Director Municipal Environmental Research Laboratory Cincinnati, OH 45268 Moderator: Professor Arthur C. Stern
8:15 a.m.	Coagulation/Precipitation of Natural Organic Substances in Water Treatment Charles O'Melia Department of Geography and Environmental Engineering, The Johns Hopkins University Baltimore, Maryland 21218
9:00 a.m.	Cyst Inactivation with Chlorine and Chlorine Dioxide Otis Sproul Department of Civil Engineering Ohio State University Columbus, Ohio 43212

9:45 a.m. Electrosorption of Phenol onto Activated Carbon
Peter Fedkiw
Department of Chemical Engineering
North Carolina State University
Raleigh, North Carolina 27650

10:30 a.m. BREAK

10:45 a.m. Effect of Turbidity and Other Factors on
the Virus Disinfection Process Using Free
and Combined Chlorine Forms
Pasquale Scarpino
Department of Civil and Environmental
Engineering, University of Cincinnati
Cincinnati, Ohio 45221

11:30 a.m. Particle Size Distribution Dynamics during
Coagulation
James Hunt
Department of Civil Engineering
University of California
Berkeley, California 94720

12:15 noon LUNCH

Moderator: Professor Arthur Stern

1:15 p.m. Application of Fourier Transform Mass
Spectrometry to the Analysis of Organic
Emission Samples
Charles Wilkins
Department of Chemistry
University of Nebraska
Lincoln, Nebraska 68588

2:00 p.m. The Investigation and Demonstration of a
Hydroperm Microfiltration System for the
Treatment of Electroplating Wastewater
Effluent
H.L. Liu
Hydronautics, Inc.
Laurel, Maryland 20810

2:45 p.m. Wet Oxidation of the Waste Water from Coal
Gasification Installations
O.J. Hahn
Department of Mechanical Engineering
University of Kentucky
Lexington, Kentucky 40506

3:30 p.m.	BREAK
3:45 p.m.	Pulse-jet Fabric Filter Performance David Leith School of Public Health, Environmental Engineering Division Harvard University Boston, Massachusetts 02115
4:40 p.m.	Integrated Swine Waste Management System for Pollution Control and Energy and Food Production P.I. Yang Department of Agricultural Engineering University of Hawaii Honolulu, Hawaii 96822
5:15 p.m.	ADJOURN

Friday, July 24, 1981

Moderator: Professor Arthur C. Stern

8:30 a.m.	The Removal of Heavy Metals by Activated Carbon Process from Water and Wastewater C.P. Huang Department of Civil Engineering University of Delaware Newark, Delaware 19711
9:15 a.m.	Heterogeneous Catalytic Oxidation of Model Chlorinated Hydrocarbons Michael P. Manning Department of Chemical Engineering Massachusetts Institute of Technology Cambridge, Massachusetts 02139
10:00 a.m.	BREAK
10:15 a.m.	Thermal Destruction Kinetics of Chlorinated Hydrocarbons Selim M. Senkan Department of Chemical Engineering Massachusetts Institute of Technology Cambridge, Massachusetts 02139

11:00 a.m. The Effect of Aeration Basin Configuration on Activated Sludge Bulking at Low Organic Loading
David Jenkins
Department of Civil Engineering
University of California-Berkeley
Richmond, California 94804

11:45 a.m. Conference Summary

12:00 noon ADJOURN

COAGULATION OF NATURAL ORGANIC SUBSTANCES IN WATER TREATMENT

Charles R. O'Melia and Brian A. Dempsey
Department of Geography and Environmental Engineering
The Johns Hopkins University
Baltimore, Maryland 21218

INTRODUCTION

Humic substances are ubiquitous in surface water supplies. They are of natural origin, derived from the soil or produced within surface waters by biological processes. They cause several problems in water treatment plants including (1) the formation of trihalomethanes and other chlorinated organics, (2) the presence of color in the water, (3) utilization of the adsorption capacity of activated carbon beds, (4) exertion of chlorine demand, and (5) possible transport of organic and inorganic pollutants through the water treatment facility.

Many water treatment plants use coagulation and filtration to remove solid particles and use chlorination to destroy pathogens. Practice has evolved over many decades, and these processes can function effectively. It is plausible, however, that design and operating procedures that are effective in removing turbidity will not be identical to those that are effective in removing humic substances. The objective of this research is to determine conditions for the design and operation of coagulation facilities that are effective in removing natural organic substances from water supplies. This can result in reduced formation of chlorinated organics, more effective utilization of granular activated carbon, and reduced chlorine demand; it could also provide increased removals of pollutants that may be associated with humic substances such as toxic metals and pesticides.

EARLY INVESTIGATIONS

Some excellent investigations of the properties of humic substances were conducted by Black, Packham, and their coworkers (e.g., 1-4). These studies provide much of the base for our present understanding of the coagulation of humic substances. A brief review of their work is useful for understanding and evaluating the research presented herein.

The studies by Black and Packham and their coworkers were prompted by a need to remove color from water supplies. As a result, their investigations used waters containing high concentrations of color and humic substances. Correspondingly, the waters studied contained high concentrations of organic carbon. Although not measured, the TOC of these waters probably ranged upward from 25 mg/L. Our present interest in the removal of TOC from water supplies extends to TOC concentrations an order of magnitude lower. This difference in TOC concentrations may cause differences in treatment practice, as discussed subsequently.

Hall and Packham (2) ably summarized knowledge about the conditions for and the mechanisms of removal of turbidity and color. Their summary is presented in Table 1. There are important differences noted by these authors between the removal of clays and humic substances by coagulation with alum. These differences indicate the necessity of considering coagulant-humic interactions when applying present coagulation and filtration practice based on the removal of turbidity to the removal of natural organic substances.

TABLE 1.

COMPARISON OF THE COAGULATION OF CLAYS AND HUMICS WITH ALUM
(after Hall and Packham, (2))

Clay Suspensions	Humic Substances
Optimum pH = 6.5-7.5 (for precipitation of $Al(OH)_3(s)$ to increase flocculation kinetics).	Optimum pH = 5-6 (for precipitation of Al-humate).
Required coagulant dosage decreases slightly with increased clay concentration.	Required coagulant dosage increases with increased humic concentration.
Minimum residual turbidity independent of pH.	Minimum residual color dependent on pH.

Hall and Packham note that coagulation for the removal of turbidity from dilute suspensions (equivalent to 50 mg/L or less of kaolin) is best under conditions that promote the precipitation of amorphous aluminum hydroxide. This corresponds to a pH range of 6.5 to 7.5. The presence of clay particles actually increases the rate of precipitation of $Al(OH)_3(s)$, so that the required coagulant dosage decreases slightly with increasing turbidity. The function of the alum here is to provide floc volume, "targets" in suspension to increase the rate of interparticle contacts or flocculation, thereby producing a settleable aggregate in a reasonable flocculation time. Because the process is primarily a physical one, pH has little effect on turbidity removal within the optimum pH range of 6.5-7.5.

In contrast, coagulation for the removal of color from concentrated solutions of humic substances (probably equivalent to 25 mg/L or more of TOC) is best under conditions which promote chemical interaction between the pollutant (humic substances) and the coagulant (alum), leading to the formation of an aluminum-humate precipitate/aggregate. Hence, there is a direct stoichiometry between the coagulant requirement and the color of the water. Because of the chemical nature of the process, and because the speciation of both aluminum and humic substances varies with pH, residual color depends upon pH even within the pH zone of effective treatment, pH 5-6.

A PRESENT-DAY PERSPECTIVE

The studies summarized by Hall and Packham and described above focused on "dilute" suspensions of particles and "concentrated" solutions of humic substances. Let us consider next some other applications of coagulation, viz., the treatment of concentrated suspensions of particles and dilute solutions of humic substances. Understanding of the coagulation of concentrated suspensions begins with the work of LaMer and coworkers (e.g., 5). These researchers demonstrated that organic polymers destabilize colloids by adsorbing at the solid-liquid interface. Because the suspensions are concentrated, mass transport is fast and flocculation kinetics are rapid. The polymers function by neutralizing the charge on the colloidal particles (polymer and particle of opposite charge) or by forming bridges across repulsive energy barriers between particles (polymer and particle of like charge). Because adsorption is required, there is a direct stoichiometry between polymer dosage and particle concentration.

Studies of the coagulation of concentrated suspensions by metal salts were performed by Stumm and coworkers (e.g., 6). These investigators concluded that iron(III) and aluminum(III) salts form polymeric species (hydroxometal polymers) under certain pH conditions in water and that these inorganic polymers adsorb at solid-liquid interfaces. Coagulation is accomplished primarily by charge neutralization (positive polymers, negative colloids). Because the suspensions tested are concentrated, flocculation kinetics are rapid. Because destabilization involves adsorption, increased solids concentrations require increased coagulant dosages (stoichiometry).

The investigations to be reported here have focused on the coagulation of dilute solutions of humic substances. Some experiments have involved the coagulation of a fulvic acid extracted from a lake water using alum as the coagulant. Jar tests were performed and the concentrations of fulvic acid remaining after settling and after membrane filtration were determined. Fulvic acid removal is plotted as a function of pH at a constant aluminum dosage of 10^{-4} M (2.7 mg Al/L; 33.3 mg alum/L) in Figure 1. These results do not agree with the conclusions of earlier investigators studying more concentrated solutions. For treatment involving coagulation and settling, the pH region providing the best removal is about pH 6 to 7, where aluminum hydroxide precipitates readily. When coagulation, settling, and membrane filtration are used, effective fulvic acid removal occurs in these tests over a broad pH range from 4.8 to 7.

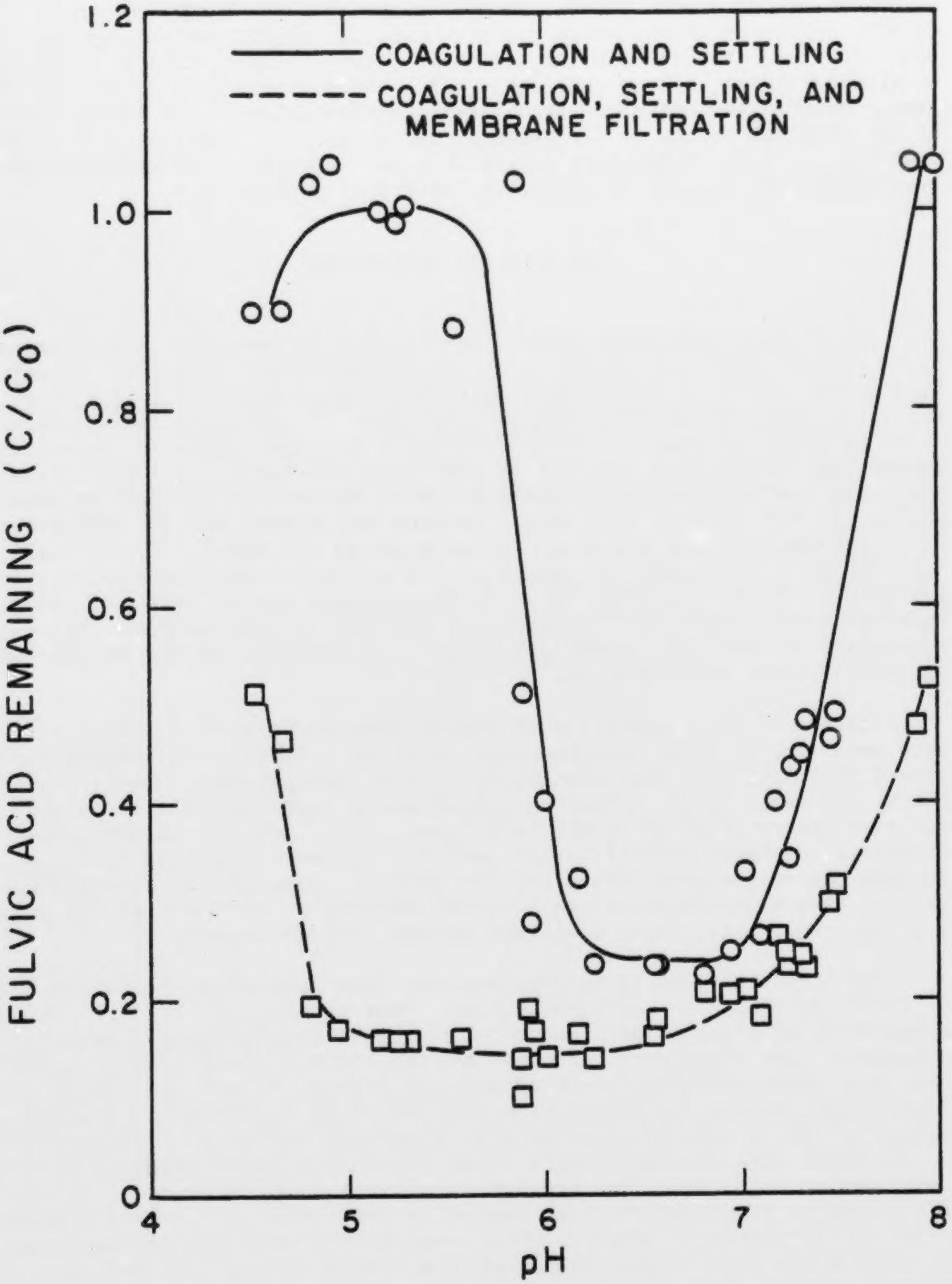

Figure 1. Coagulation of FA-4. Raw Water TOC=3.5 mg/L. Coagulant = Alum ($Al_2(SO_4)_3 \cdot 18 H_2O$). Aluminum Dosage = 10^{-4} M = 2.7 mg Al/L = 33.3 mg Alum / L.

Based on these studies of the coagulation of concentrated particle suspensions and dilute humic solutions, the comparison of Hall and Packham can be extended, as in Table 2.

TABLE 2.

EXPANDED COMPARISON OF THE COAGULATION OF CLAYS AND HUMICS WITH ALUM

	Clay Suspensions	Humic Substances
Dilute Systems	Optimum pH = 6.5-7.5 (pptn. of $Al(OH)_3(s)$ to increase flocculation kinetics).	Optimum pH = 6-7 (pptn. of $Al(OH)_3(s)$ to adsorb humics).
	No stoichiometry.	Stoichiometry plausible but not tested.
Concentrated Systems	Optimum pH = 5-6 (Formation of metal polymers, destabilization by adsorption, rapid flocculation).	Optimum pH = 5-6 (Formation of metal polymers, coagulation/pptn. of humics, rapid flocculation).
	Stoichiometry	Stoichiometry

Before considering this summary, it is useful to consider some aspects of the chemistry of aluminum in water. The results presented here are based on the work of Baes and Mesmer (7). These investigators critically reviewed several studies of aluminum speciation and concluded that, for the ranges of aluminum concentration and ionic strength studied, aluminum hydrolysis can be accurately but not uniquely explained by invoking three polymeric species ($Al_2(OH_2{}^{4+}$, $Al_3(OH)_4{}^{5+}$, and $Al_{13}O_4(OH)_{24}{}^{7+}$) and five monomers ($Al^{3+}$, $AlOH^{2+}$, $Al(OH)_2{}^{+}$, $Al(OH)_3$, and $Al(OH)_4{}^{-}$). Based on these species, a solubility diagram for freshly precipitated, amorphous $Al(OH)_3(s)$ is presented in Figure 2. Lines corresponding to the $Al(OH)_2{}^{+}$ and $Al(OH)_3$ species are dashed to indicate that their concentrations are uncertain because of questionable thermodynamic data (7). The pH of minimum solubility of $Al(OH)_3(s)$ is about 6.2. A 10^{-4} M solution of Al(III) can precipitate $Al(OH)_3(s)$ in the pH range 5.8 to 8. Below pH 5.7, freshly precipitated $Al(OH)_3(s)$ is quite soluble and the polymeric species $Al_{13}O_4(OH)_{24}{}^{7+}$ can predominate.

With this background consider the coagulation results summarized in Table 2. For dilute clay suspensions representative of many surface waters, the kinetics of mass transport limit the coagulation process and additional mass must be introduced to provide effective aggregation. This is commonly done by precipitating $Al(OH)_3(s)$. Precipitation is best accomplished in the

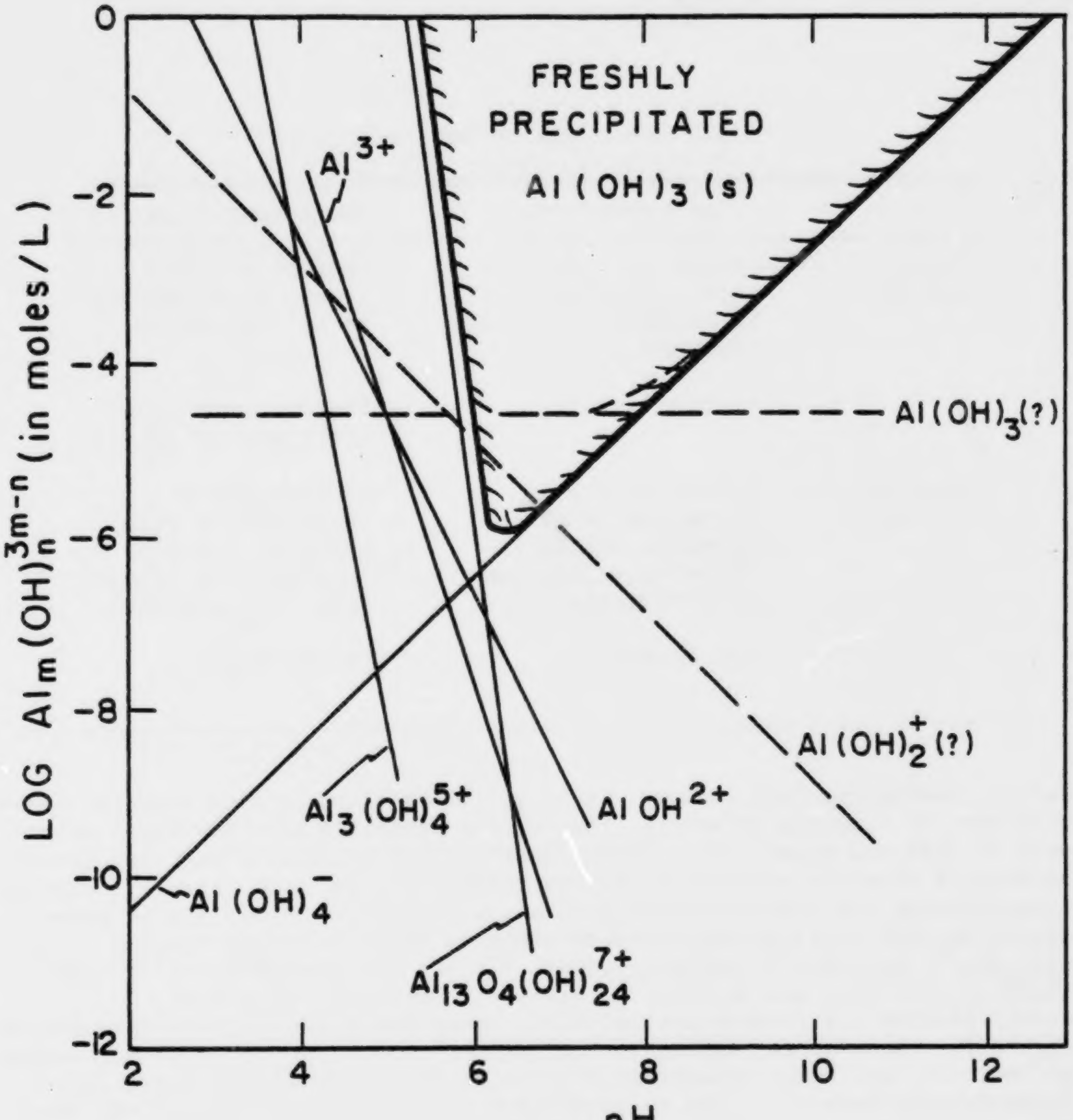

Figure 2. Solubility of Freshly Precipitated, Amorphous Al $(OH)_3$ (s).

neutral pH range; stoichiometry is not observed. It is valuable to recognize that particles in such dilute suspensions can be destabilized by aluminum polymers, but the destablished particles cannot be brought into contact effectively in flocculation tanks. One alternative coming into practice is direct filtration; particles are destablished chemically and then contacted with filter media. Flocculation kinetics are less important and sedimentation is not required. The analysis presented here indicates that the pH range 5 to 6 would be effective for direct filtration using alum.

For the coagulation of concentrated suspensions such as sludges and very turbid surface water supplies, flocculation kinetics do not limit plant performance. Destabilization by adsorption of aluminum polymers such as $Al_{13}O_4(OH)_{24}^{7+}$ is possible in the pH range 5 to 6. Stoichiometry is observed.

For the coagulation of concentrated solutions of humic substances representative of highly colored waters in parts of the southeastern United States and Great Britain, flocculation kinetics are again not limiting. Removal of humic substances is probably brought about by interaction between negatively charged humic molecules and positively charged aluminum polymers, resulting in the formation of colloidal precipitates that can be flocculated readily if the overall charge of the Al-humic solid is near zero.

Finally, for the removal of humic substances from dilute solutions characteristic of many surface waters and the subject of this research, flocculation kinetics limit aggregation and removal by gravity settling. As with the coagulation of dilute clay suspensions, two removal processes are suggested. First, aluminum polymers can interact with humic molecules in the pH range 5 to 6. The resulting colloid will not aggregate to a settleable size because of slow flocculation kinetics, but could be removed by direct filtration. Edzwald and coworkers (e.g., 8) have demonstrated the effectiveness of direct filtration of humic substances using cationic organic polymers. Second, aluminum hydroxide can be precipitated in the pH range 6 to 7.5. This solid may adsorb humic substances from dilute solution, leading to their removal. The study of the removal of humic substances from most natural waters by conventional coagulation and sedimentation processes thus involves the study of the factors affecting the adsorption of humic substances on solid surfaces. Some preliminary results obtained in this research follow.

PREPARATION AND CHARACTERIZATION OF FULVIC ACIDS

The humic substances used to date in this study have been extracted from samples from Lake Drummond, Virginia. A schematic diagram of the separation and fractionation procedures is presented in Figure 3. This water source was selected because it contains a high concentration of humic substances (TOC from 30 to 50 mg/L, almost entirely fulvic acids (FA)). To obtain FAs for laboratory studies, water from Lake Drummond was acidified to pH 2 with HCl, stored for 24 hours, filtered using glass fiber filters, and applied to columns containing Amberlite XAD-7 resin. After washing with 0.01 M HCl and distilled, deionized water, four fractions of FA were eluted from the column

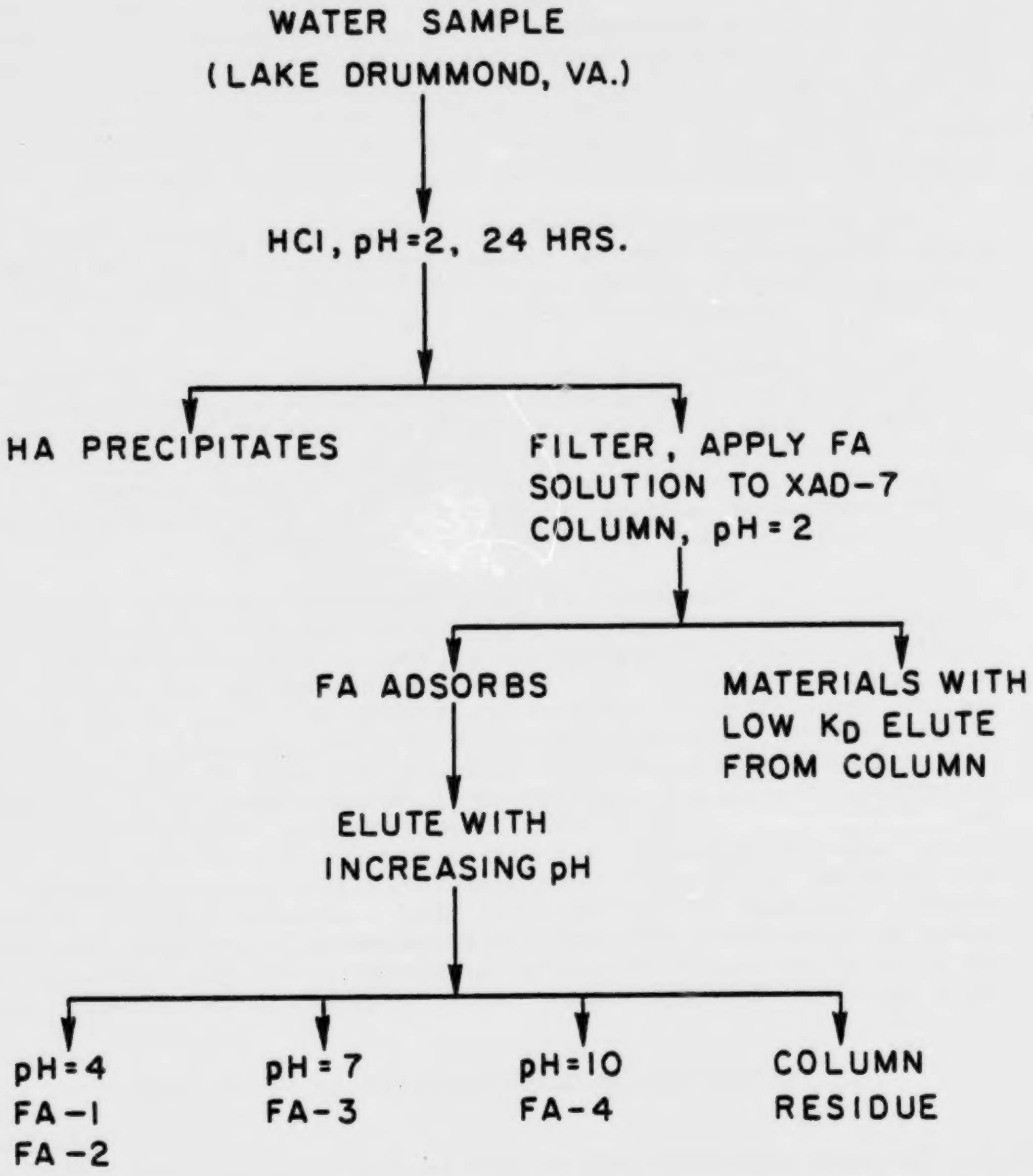
WATER SAMPLE
(LAKE DRUMMOND, VA.)
HCl, pH=2, 24 HRS.
HA PRECIPITATES
FILTER, APPLY FA SOLUTION TO XAD-7 COLUMN, pH=2
FA ADSORBS
MATERIALS WITH LOW K_D ELUTE FROM COLUMN
ELUTE WITH INCREASING pH
pH=4
FA-1
FA-2
pH=7
FA-3
pH=10
FA-4
COLUMN RESIDUE

Figure 3. Separation and Fractionation of Fulvic Acids (FAs).

at successively higher pH values (two fractions were eluted at pH 4, a third fraction at 7, and a fourth FA fraction at pH 10). The four fractions were stored at 4°C in dark glass bottles under nitrogen.

The interactions of the four fulvic acid fractions with protons were determined using acid-base titrations and a charge balance. Some results are presented in Figure 4. Residual negative charge on each fulvic acid fraction is plotted as a function of pH. Two results were unexpected. First, the fulvic acids maintain a significant negative charge in acid solutions at pH less than 3. Second, the fractions did not differ significantly in their proton chemistry, even though they were eluted from the XAD-7 column at different pH levels.

The effects of calcium ions on the fulvic acid fractions were evaluated using calcium titrations and a calcium selective ion electrode. Some results are presented in Figure 5. The extent of calcium complexation by fulvic acid, expressed as meq Ca complexed per gram of TOC, is plotted versus the free calcium concentration for two fulvic acid fractions at two pH levels. There are extensive differences between the two fulvic acids (FA-1 and FA-4) with respect to their interactions with calcium ions. Calcium complexation increases with increasing pH for FA-1 and decreases with pH for FA-4. At pH = 9, FA-1 interacts more extensively with calcium ions than FA-4, while at pH = 5 this order is reversed. Subsequent experiments indicate that calcium complexation affects the adsorption of these fulvic acids on solid surfaces. Unlike their proton chemistry, in which the interactions of the four fulvic acid fractions were similar, the calcium complexing ability of the four fractions differed significantly. This, in turn, affected their adsorbability on solid surfaces and hence could affect their removal from solution in natural waters and in water treatment plants.

The reactions between fulvic acid and calcium neutralized up to one-half of the charge on the FAs, but did not induce precipitation or coagulation of these organics under the TOC, Ca, and pH conditions used in these experiments. This illustrates the affinity of fulvic acids for the water phase and exemplifies the difficulty in removing them in natural waters and in water treatment plants.

ADSORPTION OF FULVIC ACIDS

The adsorption of fulvic acid on $MnO_x(s)$, amorphous $Fe(OH)_3(s)$, and $CaCO_3(s)$ at several pH levels and calcium concentrations has been studied. Results of a determination of FA adsorption on $MnO_x(s)$ are presented in Figure 6. The adsorption of FA-1 as measured by TOC removal is plotted as a function of pH in the absence of calcium and in the presence of a total calcium concentration of 5×10^{-3} M. Initial TOC = 3.49 mg/L and total manganese = 3.8×10^{-3} M. MnO_x is negatively charged in the absence of FA and TOC at pH levels above about 2. In the absence of calcium, FA adsorption is negligible over the pH range tested (4.5 to 9.5). In the presence of calcium, FA adsorption is significant, ranging from 35 per cent at pH 4.5 to about 65 per cent at pH 9. The increased adsorption of FA-1 with pH resembles the

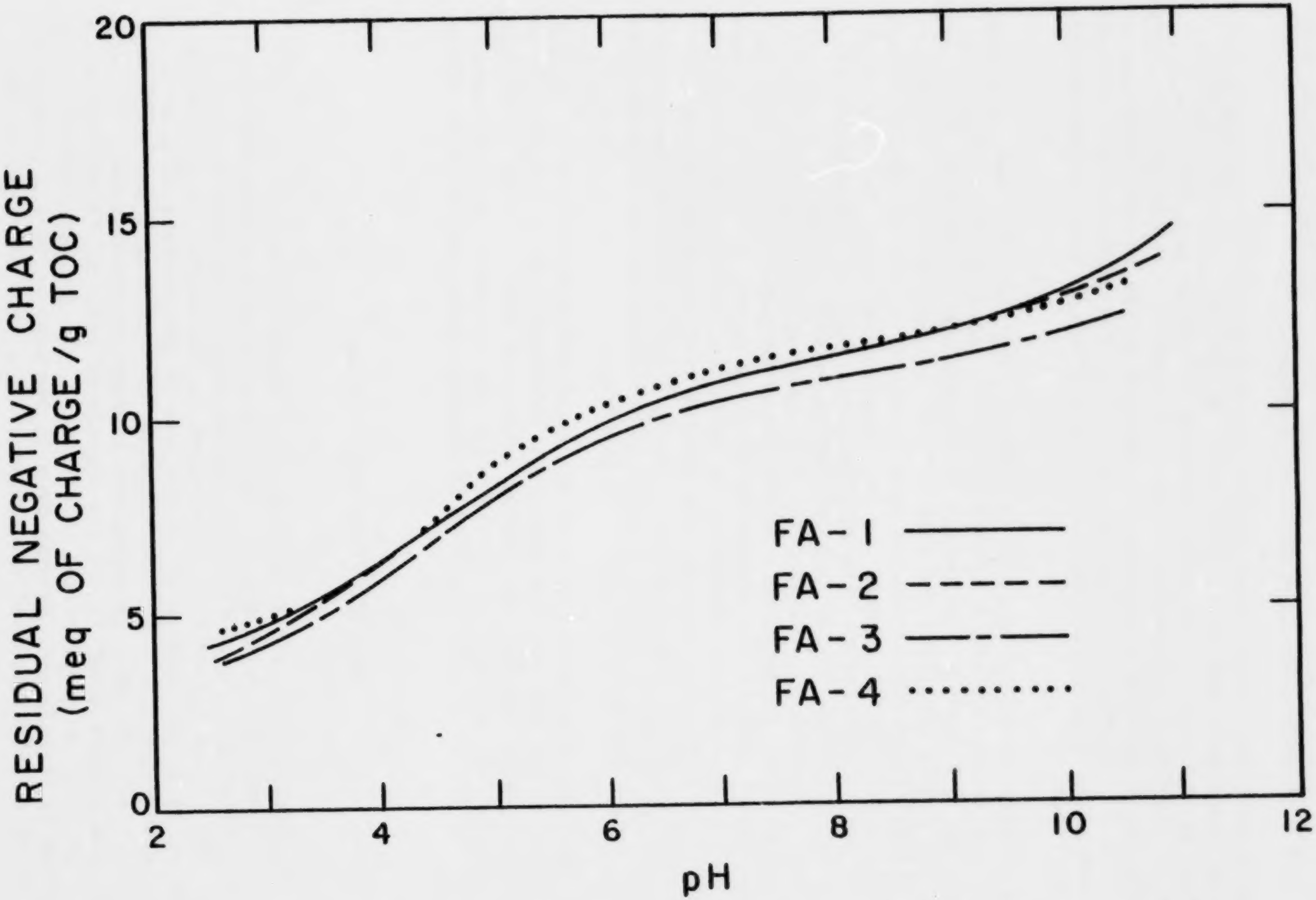

Figure 4. Effect of pH on Residual Charge of Four Fulvic Acids. I = 0.01.

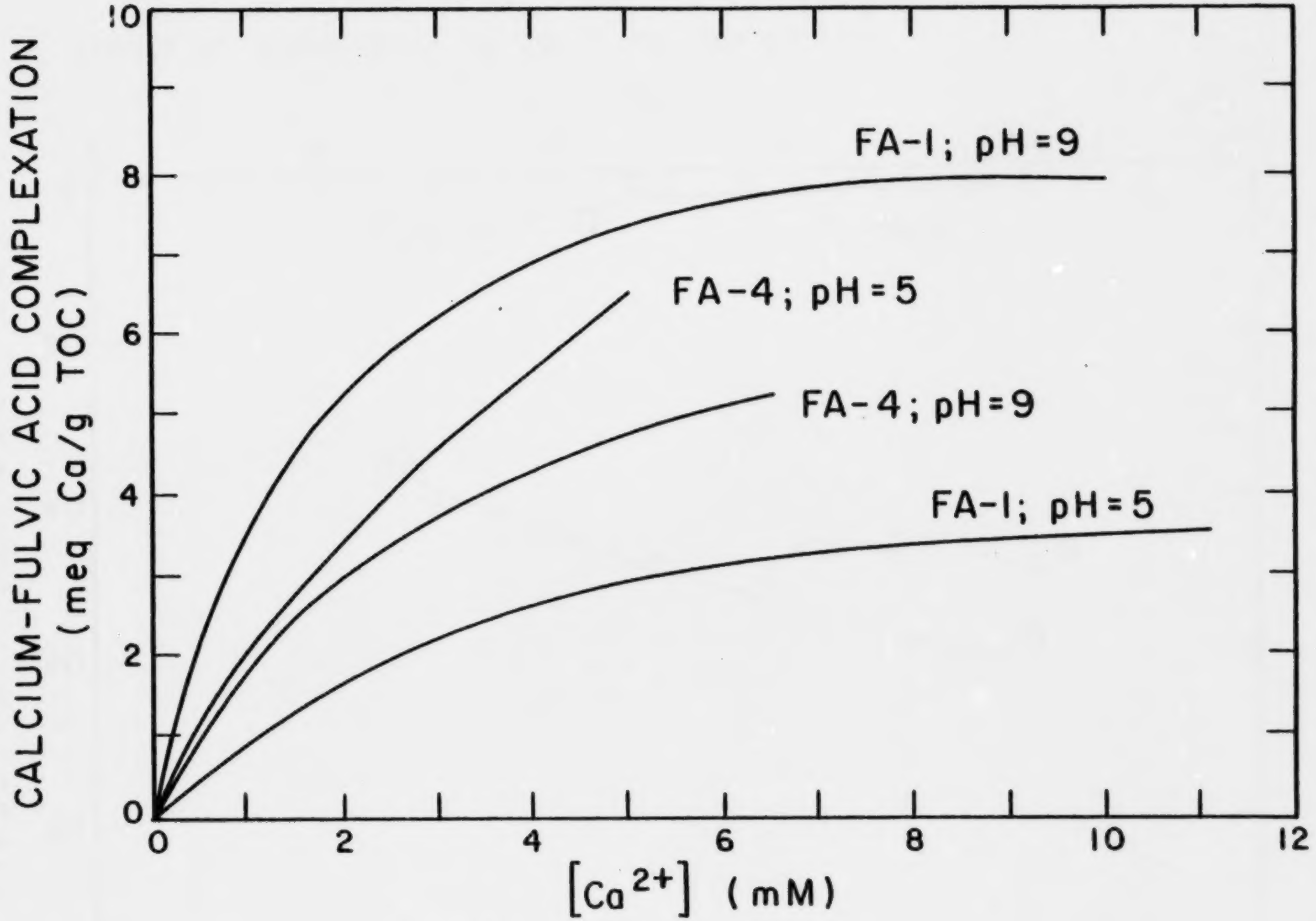

Figure 5. Calcium Complex Formation of Two Fulvic Acids.

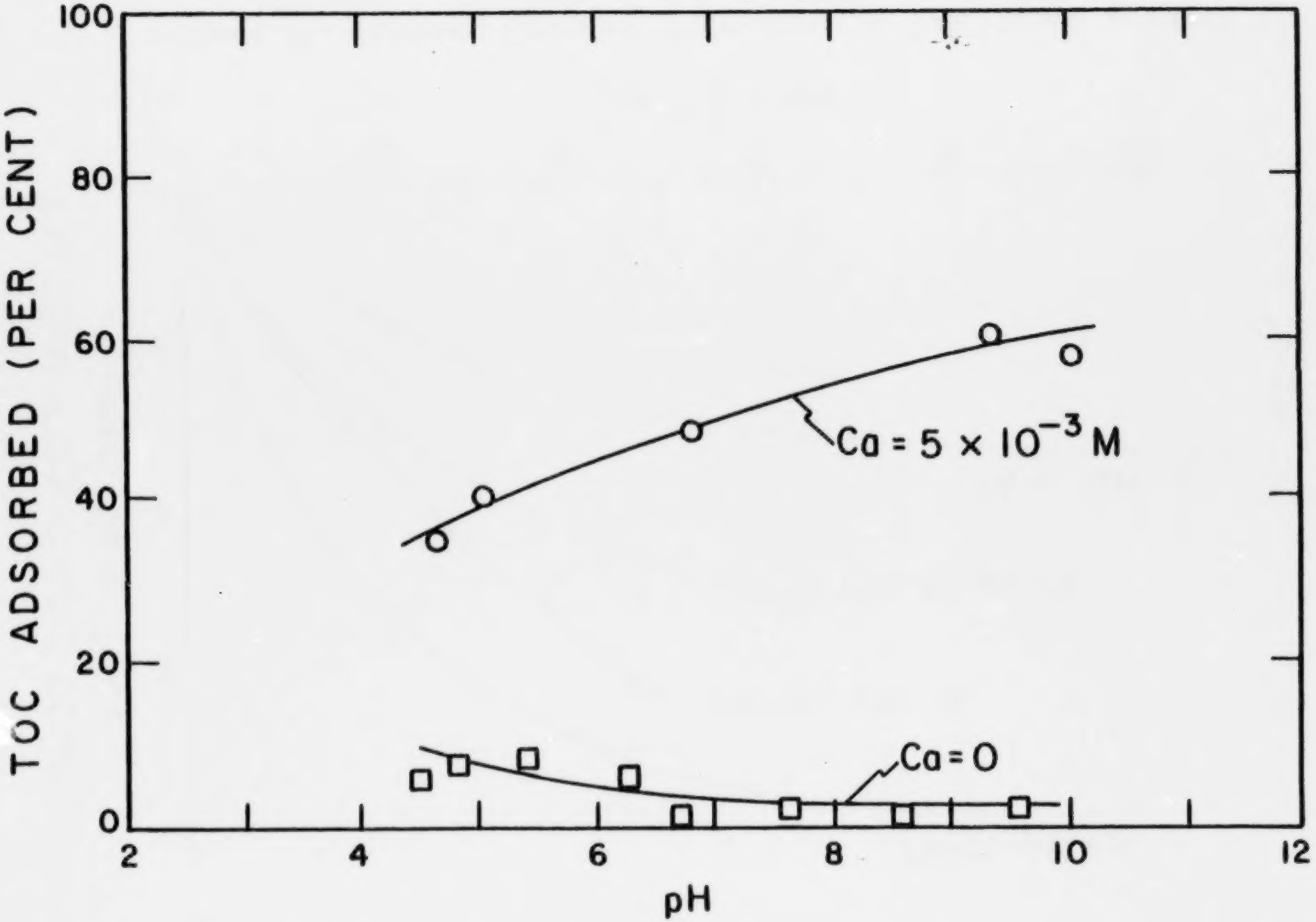

Figure 6. Adsorption of FA-I on Mn O_x (s).
TOC = 3.49 mg/L; Mn_T = 3.8 × 10^{-3} M.

increased Ca complex formation of FA-1 with pH (Figure 5). One possible descriptive explanation (among others) for this effect is that calcium fulvate complexes are less hydrophilic and less negatively charged than uncomplexed FAs, making them more adsorbable at solid surfaces. These effects are particularly important with negatively charged surfaces such as MnO_x.

The results of several adsorption experiments are summarized in Figure 7. Fulvic acid adsorption is expressed as moles of TOC adsorbed per mole of metal in the solid adsorbant and plotted versus the dissolved organic carbon (DOC) remaining in solution. Amorphous $Fe(OH)_3(s)$ adsorbs up to 2 moles C/mole Fe, about an order of magnitude more TOC than $CaCO_3(s)$ and $MnO_x(s)$. The lower curve for adsorption by $Fe(OH)_3(s)$ corresponds to the removal of FA-4 at pH 8 in the absence of calcium; the upper curve summarizes results for FA-2 at pH 6 with total calcium = 5×10^{-3} M.

Similar effects are noted for $MnO_x(s)$ and $CaCO_3(s)$. For MnO_x, the lower boundary (negligible adsorption) corresponds to the absence of calcium and the upper curve is based on experiments using FA-2 in the presence of total calcium = 5×10^{-3} M. For $CaCO_3(s)$, the lower curve corresponds to results using preformed $CaCO_3(s)$ with a low concentration of free calcium ions ($[Ca^{2+}] \simeq 2 \times 10^{-4}$). The upper curve with $CaCO_3(s)$ describes FA removal at pH = 8.5 when $CaCO_3(s)$ is formed in the presence of fulvic acid and $[Ca^{2+}] \simeq 6 \times 10^{-3}$ M.

These results demonstrate the adsorbability of fulvic acids on solid surfaces and indicate some of the chemical factors affecting this adsorption (type of solid, pH, calcium concentration). They support the hypothesis that amorphous $Al(OH)_3(s)$ may be capable of removing FA from dilute solution in water treatment practice. The factors affecting this adsorption will be studied in future experimental work.

POLYALUMINUM CHLORIDE (PAC)

Aluminum forms a variety of species in water treatment, ranging from the free aluminum ion (Al^{3+}) to amorphous $Al(OH)_3(s)$. It now appears probable that most of these aluminum species can react with fulvic acids. Some products of these reactions are removed by coagulation and sedimentation and some are not. For example, FA adsorbed on amorphous $Al(OH)_3(s)$ is removed by settling, while the products of reactions at low pH between Al^{3+} and FA may be soluble and not removed by precipitation, coagulation, settling, or filtration. In the pH region 5 to 6, polymeric hydroxoaluminum complexes are formed when alum is added to water. These can react with FA molecules forming a precipitate or aggregate that can under certain circumstances be removed by solid-liquid separation processes.

It is possible to prepare solutions of polymeric hydroxocomplexes prior to adding aluminum to water. This has been accomplished by Japanese and French investigators (e.g., 9). Both groups prepare stock coagulant solutions by partial neutralization of concentrated aluminum chloride solutions. The composition of the resulting coagulant (termed polyaluminum chloride,

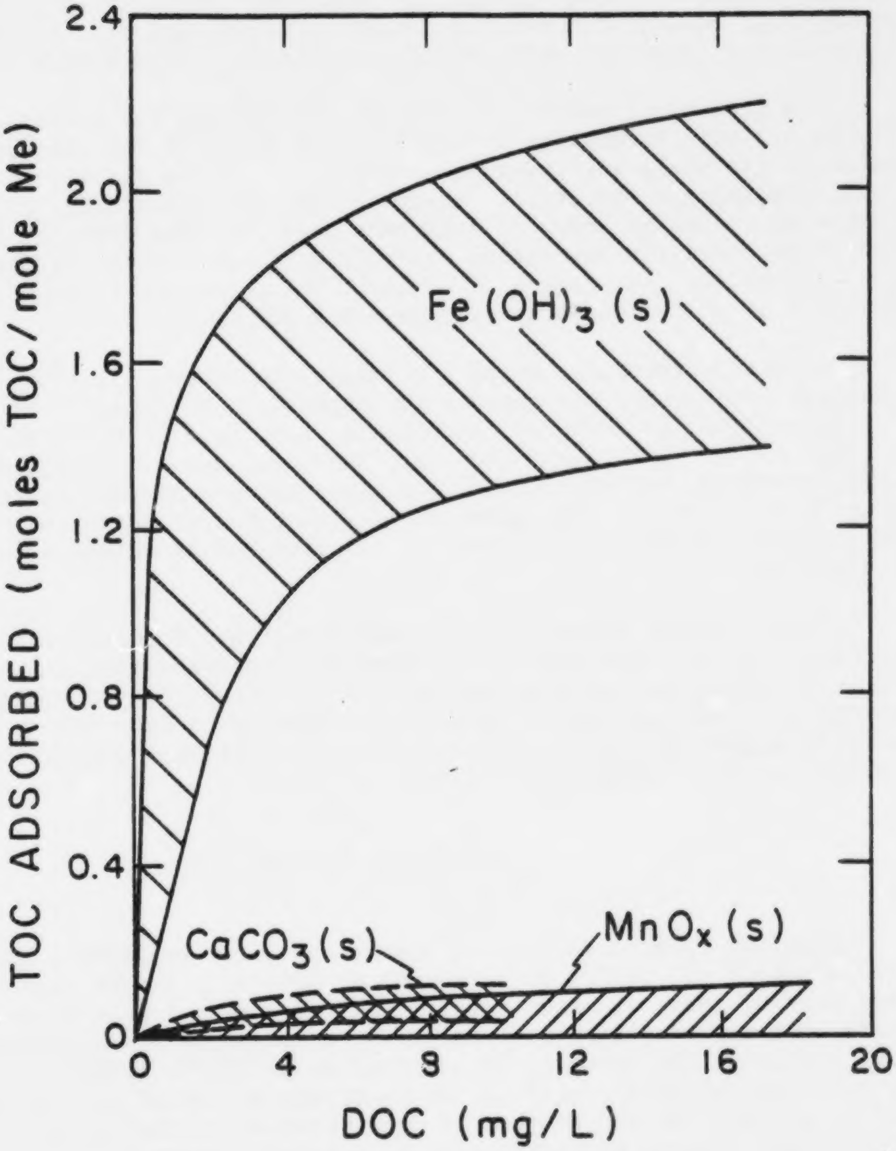

Figure 7. Adsorption of Fulvic Acid on Three Solids

PAC) is uncertain. Bottéro et al. (9) provide evidence for the presence of an Al_{13} polymer such as $Al_{13}O_4(OH)_{24}{}^{7+}$. The PAC used to date in this research has been obtained through the courtesy of Dr. Norihito Tambo, Hokkaido University, Japan and consists of an aluminum chloride solution with a concentration equivalent to 10 per cent Al_2O_3. The solution has been 60 per cent neutralized with base.

Some results of jar tests using PAC are presented in Figure 8. Fulvic acid removal by settling and by settling and membrane filtration are plotted as functions of pH. Aluminum dosage = 10^{-4} M; original FA as TOC = 3.5 mg/L. The results indicate some important differences when compared to similar tests using alum (Figure 1). For treatment involving coagulation and settling, the pH for optimum TOC removal is about 7.5, higher than the pH 6 to 7 region noted for alum. In fact removal by coagulation and settling does not occur at all at pH < 6.5. When removal occurs by coagulation, settling, and membrane filtration, two pH optima occur, one in a narrow region around pH 5.1 and a second broader region at pH 6 to 7. This contrasts with the single broad optimum region from pH 4.8 to 7 when alum was used as the coagulant.

Consider again that these solutions are oversaturated with respect to amorphous $Al(OH)_3(s)$ at pH levels greater than about 5.7 and undersaturated below it. It is probable that polymeric species such as $Al_{13}O_4(OH)_{24}{}^{7+}$ will form $Al(OH)_3(s)$ in the pH range 6 to 7 more slowly than alum solutions. Since removal of FA can be effectively accomplished by adsorption on $Al(OH)_3(s)$ in the pH range, PAC is a less effective coagulant than alum for dilute FA solutions at these pH levels. Thermodynamic calculations indicate that $Al_{13}O_4(OH)_{24}{}^{7+}$ can exist in significant concentrations in the pH range 5 to 5.7 for $Al_T = 10^{-4}$ M. This suggests that PAC can function effectively in destabilizing dilute FA solution in this pH range. This is confirmed by the effective removal of FA by PAC using membrane filtration at pH = 5.1. In the pH region from 5.1 to 5.7, it is probable that PAC restabilizes the FA solutions by producing colloidal PAC-FA aggregates that are positively charged. Other experiments in this pH range using lower aluminum dosages produced effective removal by filtration.

These preliminary experiments do not indicate which coagulant, alum or PAC, is better for removing FA at pH levels below 6. They do indicate that they can function differently and produce dissimilar results. This evaluation will continue in future experiments.

SUMMARY

The removal of natural organic substances from water by coagulation and filtration processes is divided into two categories, depending upon the concentration of soluble organic matter present. For waters containing high concentrations of TOC, removal by coagulation and sedimentation can be accomplished in the pH region from 5 to 6 using alum and probably also with polyaluminum chloride. Removal is accomplished by the formation of a precipitate/aggregate comprised of polymeric aluminum species and humic substances. Because of the high concentration of material present, flocculation

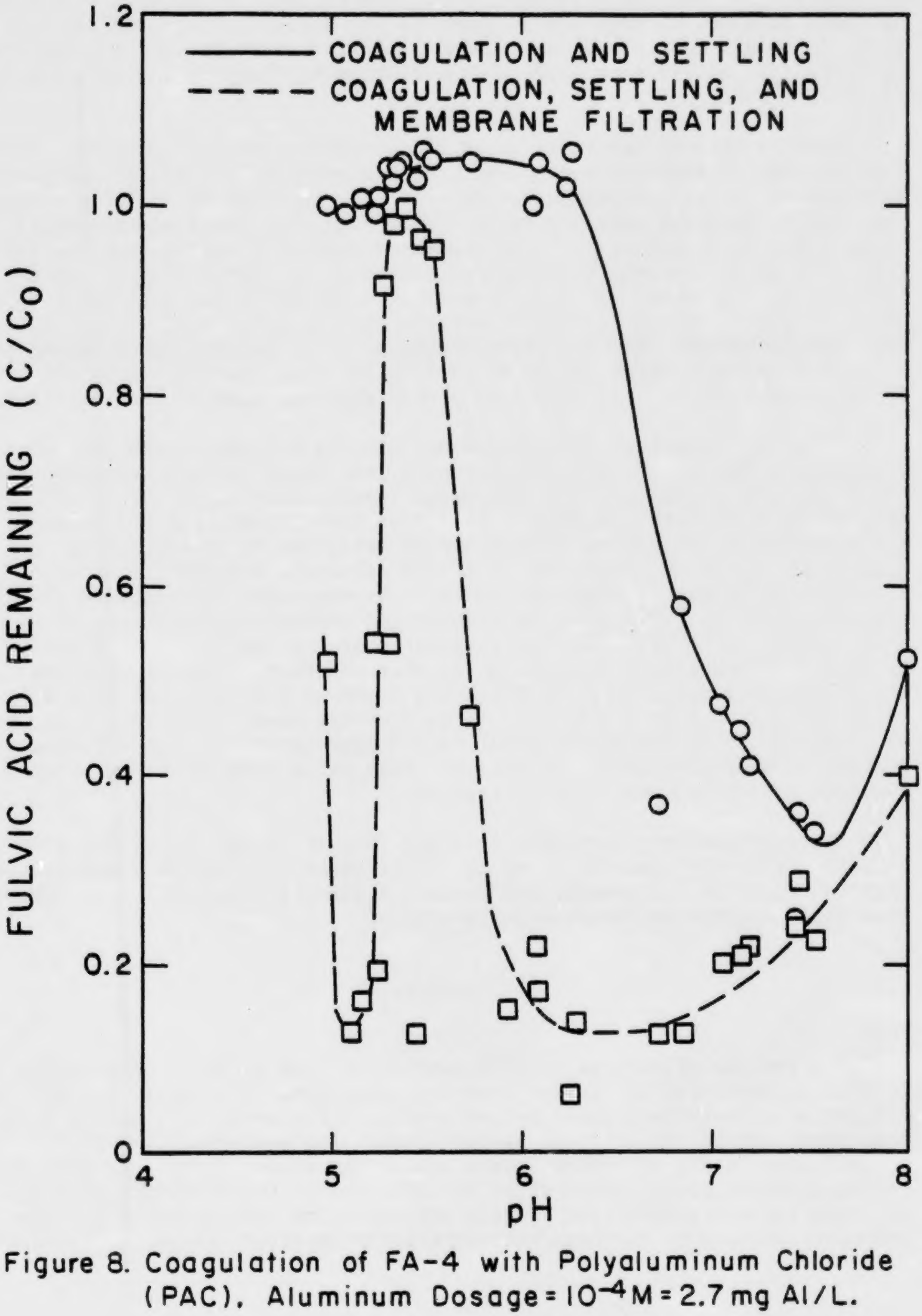

Figure 8. Coagulation of FA-4 with Polyaluminum Chloride (PAC), Aluminum Dosage = 10^{-4} M = 2.7 mg Al/L.

is rapid and settleable aggregates can be produced using flocculation periods normal in practice (30 to 60 minutes).

For low concentrations of TOC, removal by coagulation and sedimentation can be accomplished in the pH region 6 to 7 with alum, probably by adsorption of humic substances on amorphous $Al(OH)_3(s)$. Because PAC is less effective then alum in precipitating $Al(OH)_3(s)$ in this pH range, it is less effective in removing humic substances under these conditions. Removal of TOC by coagulation and direct filtration is plausible in the pH region 5 to 6 by both alum and PAC. Settleable aggregates are not produced because flocculation kinetics are slow.

Future studies to be conducted in the remainder of this research will focus on the factors affecting the adsorption of humic substances on $Al(OH)_3(s)$ and $Fe(OH)_3(s)$, the testing of other coagulants and coagulant combinations, determination of the effects of rapid mix conditions on coagulant effectiveness, testing of organics from other natural waters, and an evaluation of the effects of turbulence on the breakup of aggregates comprised of the products of metal-humic interactions.

REFERENCES

1. Packham, Ronald F., "Studies of Organic Colour in Natural Water", *Proceedings of the Society for Water Treatment and Examination*, Vol. 13, pp. 316-334 (1964).

2. Hall, Eric S., and Packham, Ronald F., "Coagulation of Organic Color with Hydrolyzing Coagulants", *Journal American Water Works Association*, Vol. 57, pp. 1149-1166 (1965).

3. Black, A.P., and Willems, Donald G., "Electrophoretic Studies of Coagulation for the Removal of Organic Color", *Journal American Water Works Association*, Vol. 53, pp. 589-604 (1961).

4. Black, A. P., and Christman, Russell F., "Characteristics of Colored Surface Waters", *Journal American Water Works Association*, Vol. 55, pp. 753-770 (1961).

5. LaMer, Victor K., and Healy, Thomas W., "Adsorption-Flocculation Reactions of Macromolecules at the Solid-Liquid Interface", *Review of Pure and Applied Chemistry*, Vol. 13, pp. 112-132 (1963).

6. Stumm, Werner, and O'Melia, Charles R., "Stoichiometry of Coagulation", *Journal American Water Works Association*, Vol. 60, pp. 514-539 (1968).

7. Baes, C.F., Jr., and Mesmer, R.E., *The Hydrolysis of Cations*, John Wiley and Sons (1976).

8. Glaser, Harold T. and Edzwald, James K., "Coagulation and Direct Filtration of Humic Substances with Polyethyleneimine", *Environmental Science and Technology*, Vol. 13, pp. 299-305 (1979).

9. Bottéro, Jean Yves, Poirier, Jean Eric, and Fiessinger, Francois, "Study of Partially Neutralized Aqueous Aluminum Chloride Solutions: Identification of Aluminum Species and Relation Between the Composition of the Solutions and Their Efficiency as a Coagulant", *Progress in Water Technology*, Vol. 12, pp. 601-612 (1980).

Comments on
Coagulation/Precipitation of Natural
Organic Substances in Water Treatment

George E. Wilson
President, Eutek Systems
Sacramento, California

OBJECTIVES OF THE RESEARCH

The overall objective of the research is to determine conditions for the design and operation of coagulation facilities that are effective in removing natural organic matter (NOM) from water supplies. Three sub-goals have been identified to meet the overall objective:

1. To characterize NOM removal by conventional coagulants and NOM residual after treatment.

2. To study the chemical conditions affecting the ability of metal salts to remove NOM.

3. To determine the influence of reactor design (initial mixing intensity, flocculator residence time and residence time distribution, and the root mean square (rms) velocity gradient on coagulant dispersion and floc particle growth and breakup.

These sub-goals are concerned with identifying the nature of NOM, chemical factors involved in its removal, and physical factors governing coagulant dispersion and subsequent flocculation.

Once the sub-goals have been met, the information will be utilized to determine the maximum extent to which NOM can be removed in water treatment systems designed for turbidity removal.

The first year research objectives were fourfold:

1. To collect samples of lake water containing NOM.

2. To extract and isolate NOM.

3. To develop the laboratory procedures for evaluation studies.

4. To study NOM removal with alum and polymers individually.

CONSISTENCY OF WORK WITH FIRST YEAR OBJECTIVES

Based on the work accomplished and reported in the paper, the first year objectives have been met for collection and extraction of NOM. Preliminary laboratory work on NOM removal by alum and other metal salts has begun. However, laboratory procedures have not been explicitly stated.

It is not clear how some of the work reported in the paper relates to the overall research objectives. Specifically, the adsorption of NOM on dispersed solids other than $Al(OH)_3$ to draw conclusions regarding their adsorption on $Al(OH)_3$ has not been clearly linked with the research objectives. The study of the direct chemical interaction of NOM with $Al(OH)_3$ would be a more direct path toward meeting the overall study objective.

QUALITY OF RESEARCH

The general objective of the research is very timely and promises to have great potential value for water treatment design and operation. Specifically, the use of NOM extracted from surface waters as the primary performance variable and the use of amorphous $Al(OH)_3$ as in conventional coagulation/flocculation facilities occurs as the dispersed solid phase for NOM adsorption will provide the greatest assurance that the results will be directly applicable to conventional water treatment facilities. However, alum coagulation is an extremely complex process involving interaction of numerous chemical and physical factors. It is unfortunate that most of the research carried on in this area to date has failed to define and measure the primary chemical and physical factors affecting the process. Consequently, it is generally impossible to compare ongoing research results with previous results and, in fact, to draw unambiguous conclusions based on previous work. If research in alum coagulation is to provide progress, all chemical and physical factors affecting the process should be explicitly defined and measured in all investigations. This applies both to comparisons to previous work as well as discussion of current work.

In the present paper, comparisons are made with previous investigations and conclusions drawn without a complete definition of the chemical and physical factors affecting all work under consideration. The reported results would be greatly strengthened if, in addition to pH and NOM concentrations, the following factors were clearly defined, measured, and/or estimated:

Anion Composition of Water: Perhaps more than any other variable, the anion composition of the water can have a strong influence on the alum coagulation/flocculation process. Anion composition of the water affects the optimum pH of coagulation, the total floc volume, and the resulting floc strength. (6-11,18)

Total Alum Concentration: At a given pH, this variable directly affects the total floc volume, the floc strength, and depending on the anion composition of the water, will influence the optimum pH of coagulation. (18)

Physical Mixing Conditions: In the research proposal, the term "power input" has been used loosely to represent turbulence. Also, reference has been made to a "mixing intensity parameter." The factors that influence the rate and degree of turbulent mixing applicable to the dispersion of metal salt coagulants in water supplies are reasonably well defined. Power input is only indirectly related to turbulence but both can be independently measured. In the mixing process, turbulence plays the more important role.

Factors which should be directly measured or estimated in the present research in order to evaluate the role of mixing in removal of NOM from water are the following (17,18):

a. Stock alum concentration.

b. Final dispersed alum concentration.

c. Characteristic scale of mixing.

d. Specific turbulent energy dissipation rate.

e. Residence time distribution.

f. Overall residence time.

There are of course other combinations of these independent variables which can also be measured to define the initial mixing conditions. However, these present a sufficient list to intelligently evaluate the importance of initial mixing in removal of NOM and in comparing the results of present research with previous investigations.

Physical Flocculation Conditions: It has been established by previous research over the past several decades that $Al(OH)_3$ floc properties generally govern the achievable performance of conventional water treatment facilities designed for turbidity removal. (1,2,3,5,7,8,10,11,12,14,18)

Analysis of batch flocculation reactor kinetics revealed that alum floc properties as influenced by pH, water anion composition, total alum concentration, and clay/alum floc structure, affected the performance of the flocculation process through effects on both aggregation and breakup rates. Tentative conclusions were drawn regarding probable mechanisms explaining these effects. The following factors would represent a minimum list of variables which should be identified and measured or estimated in the present research:

a. Floc volume.

b. Floc strength (as influenced by floc volume, clay/alum distribution in the floc structure, and water anion composition). (4,15,18)

c. Intensity of turbulence. (14,16,18)

d. Total specific energy dissipation rate. (This relates to the rms velocity gradient below the microscale of turbulence.)

e. Residence time distribution.

f. Overall residence time.

CONCLUSIONS

The research is timely and should be of real value in improving design and operation of conventional coagulation/flocculation water treatment facilities for NOM removal. The value of the reported research would be strengthened through explicit descriptions of laboratory procedures and clearly linking study efforts with the general research objective. To provide maximum progress, the research should clearly define and measure or estimate the major chemical and physical factors known to govern the performance of the initial mixing and flocculation processes.

REFERENCES

1. Baylis, J.R., "The Use of Acids with Alum in Water Purification and the Importance of Hydrogen Ion Concentration", JAWWA, 10, 365 (1923)
2. Black, A.P., and C. Chen, "Electrokinetic Behavior of Aluminum Species in Dilute Dispersed Kaolinite Systems", JAWWA, 59, 1173 (1967)
3. Black, A.P., and C. Chen, "Electrophoretic Studies of Coagulation and Flocculation of River Sediments Suspensions with Aluminum Sulfate", JAWWA, 57, 354 (1965)
4. Camp, T.R., "Floc Volume Concentration", JAWWA, 60, 656 (1968)
5. Kim, W., H.F. Ludwig, and W.D. Bishop, "Cation-Exchange Capacity and pH in the Coagulation Process", JAWWA, 65, 327 (1965)
6. Miller, L.B., "Adsorption by Aluminum Hydrate Considered as a Solid Solution Phenomenon", Public Health Repts., 39, 1502 (1924)

7. Miller, L.B., "A Study of the Effects of Anions Upon the Properties of 'Alum Floc'", Public Health Repts., 40, 351 (1925^a)

8. Miller, L.B., "Notes on the Clarification of Colored Water", Public Health Repts., 40, 1472 (1925^b)

9. Miller, L.B., "On the Composition of the Precipitate from Partially Alkalized Alum Solutions", Public Health Repts., 38, 1995 (1923)

10. Packham, R.F., "The Coagulation Process. I. Effect of pH and the Nature of Turbidity", J. Appl. Chem., 12, 556 (1962)

11. Packham, R.F., "The Coagulation Process. II. Effect of pH on the Precipitation of Aluminum Hydroxide", J. Appl. Chem., 12, 564 (1962)

12. Peterson, B.H., and E. Bartow, "Effects of Salts on the Rate of Coagulation and the Optimum Precipitation of Alum Floc", IEC, 20, 51 (1928)

13. Schwartzberg, H.G., and R.E. Treybal, "Fluid and Particle Motion in Turbulent Stirred Tanks, I. Fluid Motion", IEC Fund., 7, 1 (1968)

14. Stumm, W., and C.R. O'Melia, "Chemical Aspects of Coagulation II. Stoichiometry of Coagulation", JAWWA, 60, 514 (1968)

15. Thomas, D.G., "Turbulent Disruption of Flocs in Small Particle Size Suspensions", A.I. Ch. E., J., 10, 517 (1964)

16. Townsend, A.A., The Structure of Turbulent Shear Flow, Cambridge U. Press (1966)

17. Uhl, V.W., and J.B. Gray, Eds., Mixing - Theory and Practice, Vol. I., Academic Press (1966)

18. Wilson, G.E., "Initial Mixing and Turbulent Flocculation", Ph.D. Thesis. Univ. of California, Berkeley. (March, 1972)

CYST INACTIVATION WITH CHLORINE AND CHLORINE DIOXIDE

Otis J. Sproul*, Y.S.R. Chen**,
John P. Engel**, and Alan J. Rubin*
*Professor, **Graduate Research Assistant,
The Ohio State University,
Columbus, Ohio 43210

INTRODUCTION

Protozoan cysts, and more particularly that for Giardia lamblia, are the most commonly identified biological agent in waterborne disease outbreaks in the United States today. In 1975 and 1976, a total of 95 outbreaks were reported from 23 states in the United States and Puerto Rico (1-3). In these 95 outbreaks an etiological agent was determined in only 16; 4 were associated with Giardia lamblia. The remaining outbreaks were associated with Shigella sonnei, Shigella flexneri, E. coli, Typhimurium, one by infectious hepatitis, and 6 were associated with chemicals. In Camus, Washington, in the spring of 1976, 600 individuals from a population of 6,000 were diagnosed with giardiasis. This was the first documented outbreak of giardiasis from a filtered water supply. It was pointed out that the disinfection practices at Camus were evidently inadequate in that sufficiently high concentrations of chlorine and contact times were not provided. It is interesting to note in this case that coliform organisms were not found in the finished water supply, yet Giardia cysts were able to pass through the system.

In the spring of 1977, 205 cases of giardiasis were reported in Berlin, New Hampshire in a population of 15,000 (4). In this case, Giardia cysts were recovered from the raw water supply and from three sites within the distribution system. Another outbreak of giardiasis occurred in late 1974 and 1975 in Rome, New York (5,6). Clinical confirmation of giardiasis was made in 350 cases. In Rome, New York, the water supply was chlorinated only, and the chlorination process did not protect the residents consuming the water. Wright et al. (7) concluded that giardiasis is endemic in Colorado and that the consumption of untreated mountain water was an important source of the disease transmission.

Recent reports are available which present information on giardiasis outbreaks in California, Oregon, Pennsylvania and Colorado (8,9,10).

Most of the data which are available on the inactivation of cysts have been done using chlorine and iodine with cysts of Endamoeba histolytica. Chang and Fair (11) determined that a dosage of approximately 3 mg/L of chlorine resulting in a 2 mg/L residual after 15 minutes at pH 7 and 20°C was necessary to reduce an initial 60-100 cysts/ml of *E. histolytica* to 0. Interpretation of that data, however, is hampered by the fact that they were unable to quantitatively measure the number of viable cysts remaining. Stringer, *et al*. (12) obtained about 99 percent inactivation of *E. histolytica* in 10 minutes at pH 6.0 with 0.38 mg/L residual chlorine. In the same time only 50 percent inactivation was obtained at pH 8.0 with a residual of 1.3 mg/L. De Jonckheere and Van de Poorde (13) found a decreasing sensitivity of cysts to chlorine in the following order: *Acanthamoeba* spp. 4A, *A. culbertsoni* A-1, *N. gruberi* 1518/LE, and *N. fowleri* HB-1. Their data are somewhat difficult to interpret since they were not able to count the individual number of organisms which survived, but were forced to determine the point where the first negative sample was obtained in a suspension of cysts exposed to various levels of chlorine. They found that the *Acanthamoeba* spp. 4A was just inactivated by an initial and final chlorine residual of 16 mg/L for one hour, while the *N. fowleri* HB-1 was able to withstand only an initial and final residual of 2 mg/L for 15 minutes. They also demonstrated that the pathogenic *N. fowleri* was more sensitive to chlorine than the non-pathogenic *N. gruberi*. Their work was done at a pH 7.3 to 7.4 and at a temperature of 25°C.

In the first apparent report in the literature on the determination of cyst inactivation by the plaque technique, Chang (14) found that about 4 mg/L of free chlorine was necessary to obtain 99.9 percent destruction or inactivation of pathogenic *Naegleria* in water at 25°C and at a pH of 7.2 to 7.3.

There does not appear to be any information in the literature on the inactivation of cysts with chlorine dioxide and little on ozone. Newton and Jones (15), in a study performed in 1949, reported the inactivation of 99 to 99+ percent of the cysts of *E. histolytica* in water with residuals of ozone as low as 0.3 mg/L. The initial ozone dose required to obtain this residual varied from 0.7 to 0.9 mg/L. The causative agent for human giardiasis was used in an inactivation study by Jarroll *et al*. (16) using several halagen disinfectants with various pH's at 3° and 20°C. They reported an inactivation of 93 percent at 3°C with a chlorine residual of 5.1 mg/L at a pH of 7.7. Greater than 99.8 percent were inactivated with 6.2 mg/L of chlorine residual at 20°C with a pH of 7.9. Other conditions of inactivation with chlorine were not investigated.

Objectives

The objective of this research report is to present data on the inactivation of *Naegleria gruberi* with chlorine and chlorine dioxide.

MATERIALS AND METHODS

Cyst Preparation

Cysts of *Naegleria gruberi* strain NEG obtained from R. Neal Bond, Department of Zoology, Michigan State University, were prepared from procedures of Fulton (17) and Chang (18). *Escherichia coli*, food source for the *N. gruberi*, were maintained on trypticase soy agar with suspensions prepared as needed by culturing in trypticase soy broth tubes at 28°C for 24 hours. For Naegleria stocks petri dishes prepared with Fulton's PM agar were spread with 0.2 ml of the E. coli and one loop of cysts and/or trophozoites inoculated at one side. The plates were incubated at 28°C for up to 7 days. Cysts were washed from the dishes with 5 to 10 ml of 0.2 percent sodium lauroyl sarcosine in distilled water. The recovered cysts were washed 5 to 10 times in distilled water to remove extraneous matter and filtered through a 28 μm nylon screen to remove clumped cysts.

Solutions

All solutions were prepared from chlorine demand free water. Buffer solutions used were from acetic acid and sodium acetate for pH 5; phosphate for pH 7 and 8 and sodium carbonate and bicarbonate for pH 9.

Chlorine stock solutions were made up in concentrations of 1,000 mg/L with sodium hypochlorite (Clorox). Stock chlorine dioxide in concentrations of 200-300 mg/L was prepared as described for the iodometric method for measurement of chlorine dioxide described in Standard Methods (19).

Analytical Procedures

Chlorine residuals were measured by titration with phenylarsine oxide with the endpoint determined amperometrically and are reported in this paper as mg/L Cl (19). Chlorine dioxide was measured by the DPD method of Palin and reported as mg/L ClO_2 (20).

Disinfection Procedures

The inactivation experiments were carried out in 2.5 liter amber glass bottles fitted with an immersion heater and sampling ports. Chlorine demand free distilled water was added to the bottle, buffer added, heated to 25°C, disinfectant added and final pH adjustments made. Naegleria cysts were added to give a final concentration of about 1000 cysts/ml. Samples for cyst determination were taken at suitable intervals and mixed with 0.04 N or 0.1 N sodium thiosulfate for disinfectant neutralization.

Cyst survival was determined by spreading a small aliquot of the sample with 0.15 ml of the E. coli broth over the surface of a petri dish containing the Fulton's PM agar and incubated at 28°C. The amoebic colonies, or plaques in the bacterial lawn were counted after about 40, 48 and 64 hours. Two or more sample dilutions were used with triplicate plates prepared for each dilution. These plate counts were averaged. At low survivals 10 ml sample aliquots were centrifuged to concentrate the cysts for plating.

Control bottles were treated in the same way with the exception that the disinfectant was not added. Survivals in the disinfected samples were determined as a fraction of the survivors in the control bottle.

RESULTS

Chlorine Dioxide Inactivation

The inactivation data of N. gruberi cysts at pH 7 with four different concentrations of chlorine dioxide are presented in Figure 1. These plots are typical of those seen at other pH values. There was an initial lag in the inactivation rate which gradually increased to a steady state value. The initial and final chlorine dioxide concentrations varied by only several hundredths of a mg/L indicating close control over the experimental procedures.

Concentration-time plots for 99 percent cyst inactivation are presented in Figure 2. These data indicate that the inactivation of N. gruberi with chlorine dioxide is most efficiently done at pH 7.0 since less ClO_2 and/or contact time is required for the inactivation than at pH 6.0 or 8.0. It is unclear at this time why inactivation at pH 7.0 should be better than at other values.

Chlorine Inactivation

Cyst inactivation data using chlorine at pH 7.0 are shown in Figure 3. Inactivation rates gradually increased reaching a steady state value as occurred with chlorine dioxide. The initial free chlorine residuals were 0.78, 1.27, 2.28 and 3.44 mg/L. The lowest concentration used 0.78 mg/L had the greatest decrease to 0.64 mg/L.

Figure 4 shows the concentration time plots for 99 percent cyst inactivation with free chlorine at pH 5.0, 7.0 and 9.0. These data indicate the ineffectiveness of hypochlorite as a disinfectant since the concentrations of free chlorine for 99 percent inactivation at pH 9.0 are well over an order of magnitude greater than at pH 5.0 or 7.0.

A comparison of concentration and time products for chlorine and chlorine dioxide at pH 7.0 for 99 percent inactivation is shown in Table 1. Chlorine dioxide's 6.05 mg-min/L indicates rather clearly its superiority as a disinfectant for Naegleria over free chlorine's 12.1 mg-min/L. Conversion of the free chlorine to hypochlorous acid and expressing this as a concentration-time product, 9.34 mg-min/L, still indicates that chlorine dioxide is a better disinfectant than hypochlorous acid.

DISCUSSION

Cyst inactivation in water is accomplished by the use of chlorine or chlorine dioxide but with dosages and residuals well above that required for similar levels of inactivation of bacteria and viruses. Representative concentration-time products for 99 percent inactivation of several organisms using chlorine and chlorine dioxide are presented in Table 2. The data are not exactly comparable since there are minor differences in pH and temperature but the differences do not seriously detract from the comparison. Inactivation of cysts of either E. hisolytica or N. gruberi requires either more disinfectant or contact time than is required for either poliovirus 1 or

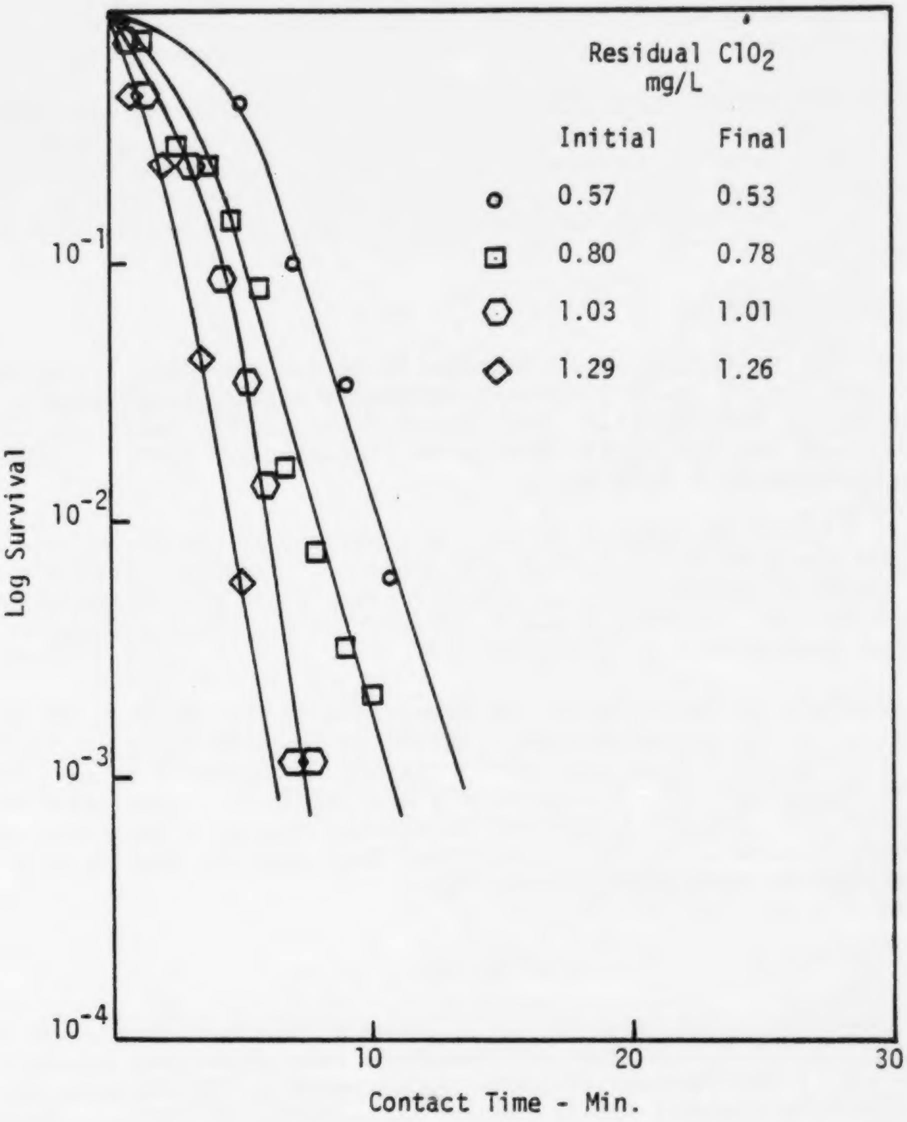

Figure 1. Cyst Inactivation by Chlorine Dioxide at pH 7.0 and 25°C

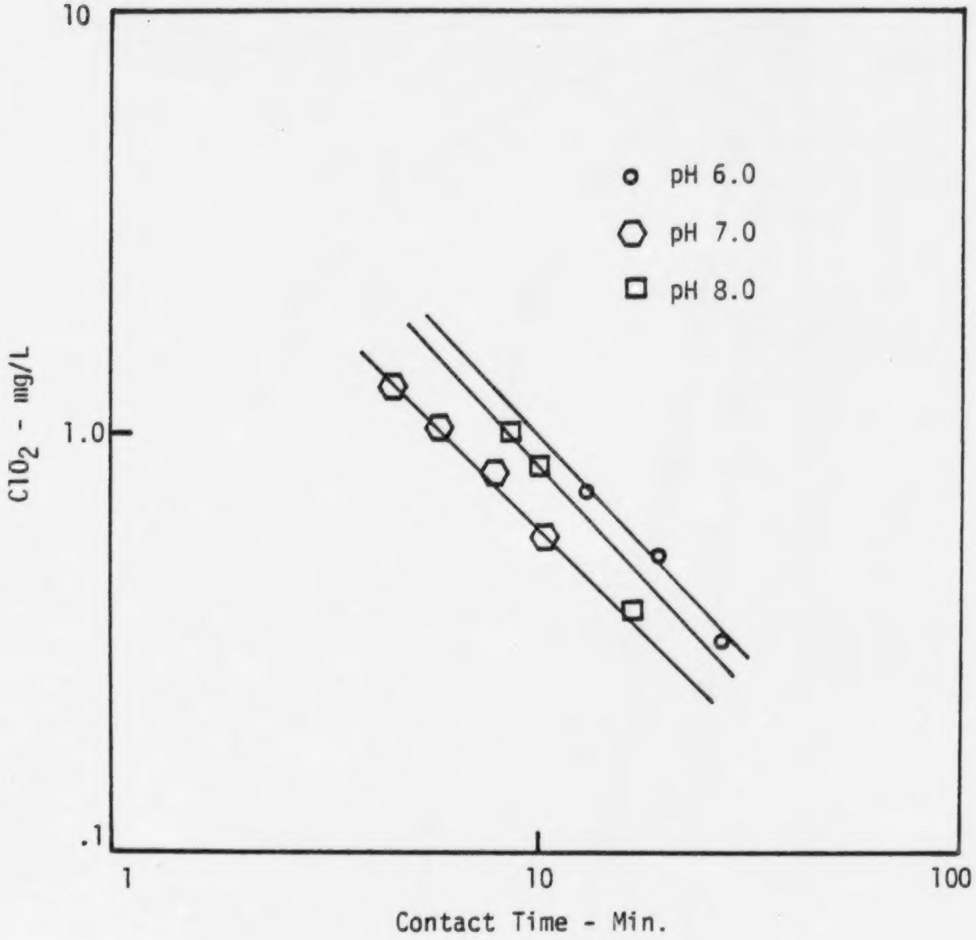

Figure 2. Concentration-Time Relationship for 99 Percent Cyst Inactivation at 25°C.

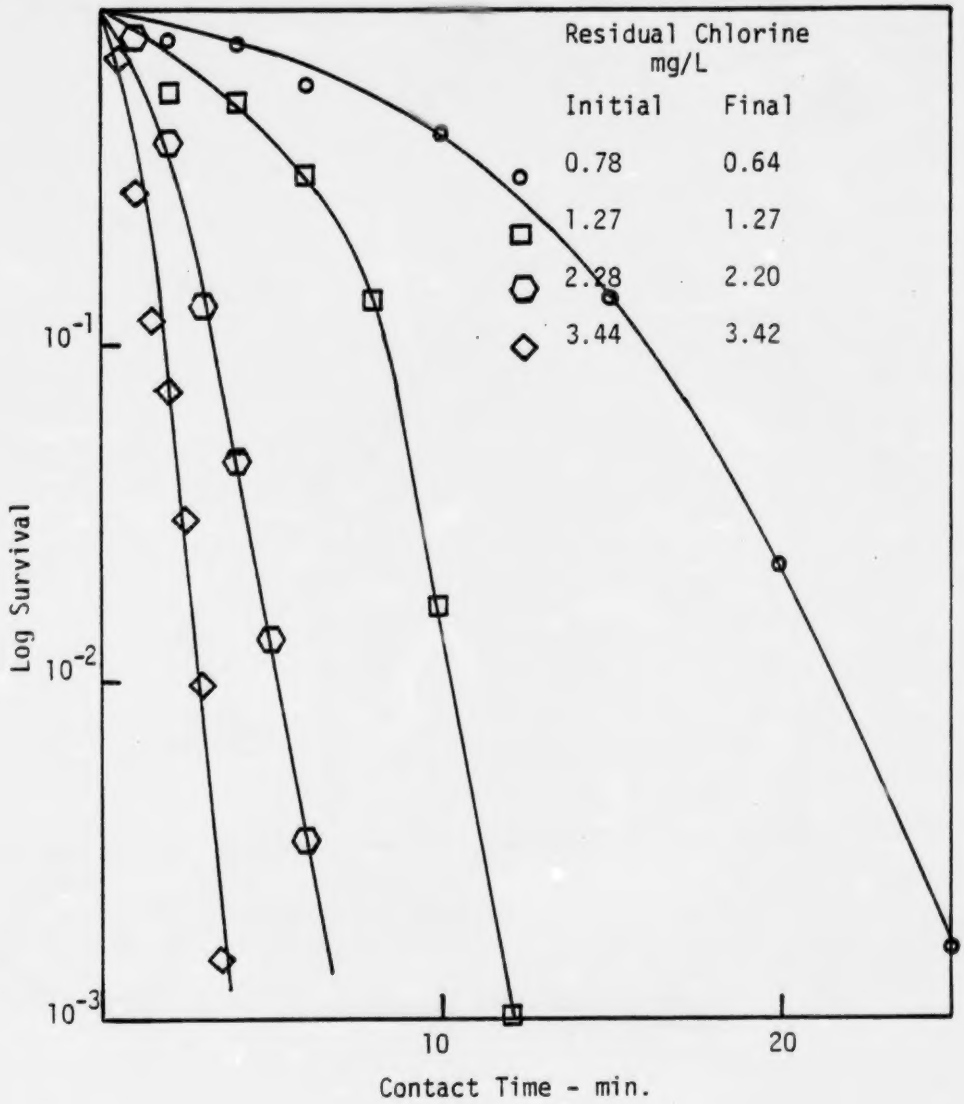

Figure 3. Cyst Inactivation by Free Chlorine at pH 7.0 and 25°C.

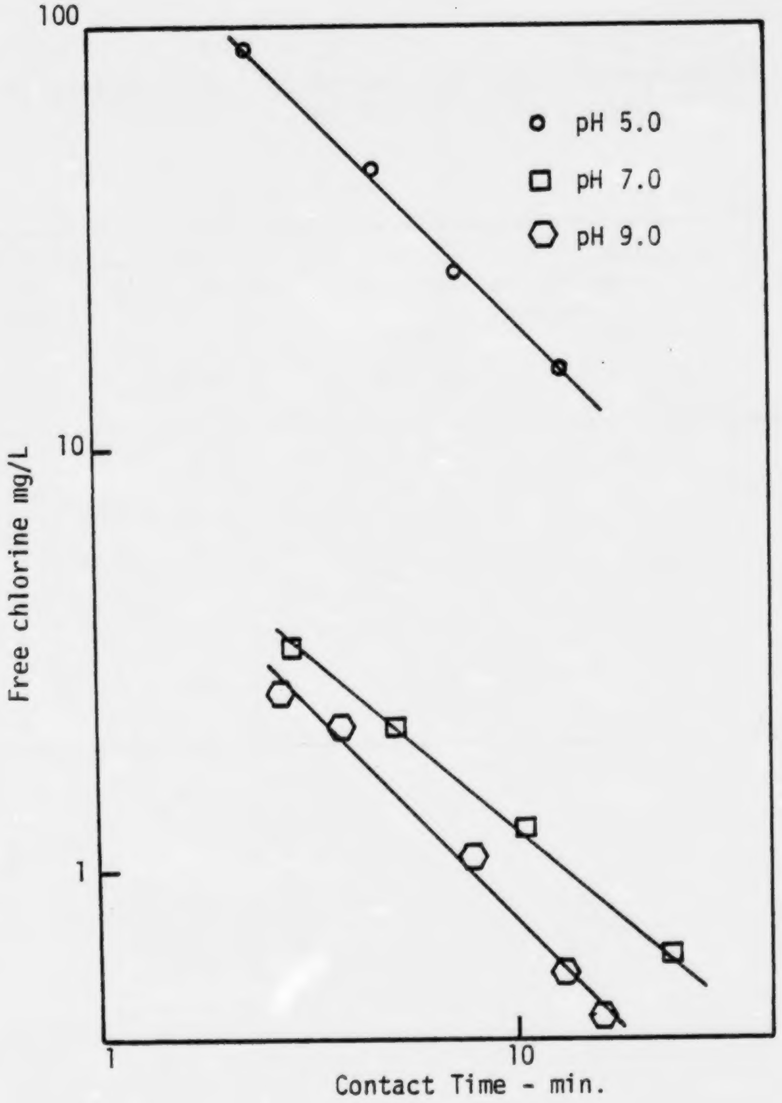

Figure 4. Concentration-Time Relationship for 99 Percent Cyst Inactivation at 25°C.

TABLE 1. TIME-CONCENTRATION DATA FOR 99 PERCENT INACTIVATION OF N. gruberi AT pH 7.0 AND 25°C

	Chlorine		Chlorine Dioxide	
Initial Cl_2	Concentration Time Product		Initial ClO_2	Concentration Time Product
mg/L	Free Cl_2 $\frac{\text{mg-min}}{\text{L}}$	HOCl $\frac{\text{mg-min}}{\text{L}}$	mg/L	$\frac{\text{mg-min}}{\text{L}}$
0.78	13.8	10.7	0.57	5.87
1.27	13.0	10.1	0.80	6.32
2.28	11.4	8.86	1.03	6.08
3.44	10.1	7.70	1.29	5.93
Average	12.1	9.34		6.05

TABLE 2. COMPARATIVE CONCENTRATION-TIME DATA FOR 99 PERCENT INACTIVATION

	Free Chlorine						Chlorine Dioxide					
	Conc. mg/L	Time min.	Temp °C	pH	C·T $\frac{\text{mg-min}}{\text{L}}$	Ref.	Conc. mg/L	Time min.	Temp °C	pH	C·T $\frac{\text{mg-min}}{\text{L}}$	Ref.
Virus												
Poliovirus 1	0.55	0.6	24	7.0	0.33	21	0.3	3.6	25	7.0	1.1	22
Bacteria												
E. coli	0.1	0.4	5	6.0	0.04	23	0.3	0.98	25	7.0	0.29	22
Cysts												
E. histolytica	1.8	10	30	7.0	18	24						
N. gruberi	*	*	25	7.0	12	this study	*	*	25	7.0	6.0	this study

*Average from 4 experiments.

E. coli. Nearly an order of magnitude more is required for chlorine dioxide and significantly more than one order for chlorine.

Chlorine appears to be a more effective disinfectant for poliovirus 1 and for E. coli but the reverse is true for N. gruberi cysts. Other data for comparison purposes are not available for cyst inactivation with chlorine dioxide. Final conclusions on this point must await more data. The concentration-time product of 12 mg-min/L for the N. gruberi for 99 percent inactivation with chlorine at 25°C is close to the 18 mg-min/L at 30°C for E. histolytica considering the latter's higher temperature.

CONCLUSIONS

The following conclusions can be drawn from this work:

(1) A concentration-time product of 12 mg-min/L was required for 99 percent inactivation of Naegleria gruberi with chlorine at 25°C and pH 7.0

(2) A product of 6.0 mg-min/L was required for 99 percent cyst inactivation with chlorine dioxide under similar conditions.

(3) Of the three common disease organisms in water, bacteria, viruses and protozoan cysts, the cysts require an order of magnitude or more combination of disinfectant and contact time than do either bacteria or viruses for the same level of inactivation.

ACKNOWLEDGEMENTS

This work was supported in part by Grant #R808150-01 from the Office of Exploratory Research, U.S. Environmental Protection Agency.

REFERENCES

1. Craun, G.F., "Impact of the Coliform Standard in the Transmission of Disease." Symposium on the Evaluation of the Microbiology Standards for Drinking Water, U.S.E.P.A., April 13-14, 1977.

2. Center for Disease Control, Food-Borne and Water-Borne Disease Outbreaks, Annual Summary 1975, 75 pp., 1976.

3. Center for Disease Control, Food-Borne and Water-Borne Disease Outbreaks, Annual Summary 1976, 82 pp., 1977.

4. Center for Disease Control, Morb. and Mort. Weekly Report, 26, 169 (1977).

5. Craun, G.F., "Microbiology - Water-borne Outbreaks," J. Water Pollut. Control Fed., 48, 1378 (1976).

6. Center for Disease Control, Morb. and Mort. Weekly Report, 26, 299 (1977).

7. Wright, R.A., et al., "Giardiasis in Colorado: An Epidemiological Study," Amer. J. Epidemiol., 105, 330 (1977).

8. Center for Disease Control, Morb. and Mort. Weekly Report, 29, 11, 121 (1980).

9. Center for Disease Control, Morb. and Mort. Weekly Report, 27, 19, 155 (1978).

10. Center for Disease Control, Morb. and Mort. Weekly Report, 27, 20, 167 (1978).

11. Chang, S.L., and G.M. Fair, "Viability and Destruction of the Cysts of Endamoeba histolytica," J. Amer. Water Works Assoc., 33, 1705 (1941).

12. Stringer, R.P., W.N. Cramer, and C.W. Kruse, "Comparison of Bromine, Chlorine and Iodine as Disinfectants for Amoebic Cysts," chapter in Disinfection: Water and Wastewater, J.D. Johnson, editor, Ann Arbor Science, Ann Arbor, Mich., 1975.

13. DeJonekheere, J., and H. Van de Voorde, "Difference in Destruction of Cysts of Pathogenic and Nonpathogenic Naegleria and Acanthamoeba by Chlorine," App. Environ. Microbiol., 31, 294 (1976).

14. Chang, S.L., "Resistance of Pathogenic Naegleria to Some Common Physical and Chemical Agents," Appl. Environ. Microbiol., 35, 368 (1978).

15. Newton, W.L., and M.F. Jones, "Effect of Ozone in Water on Cysts of Endamoeba histolytica," Amer. J. Trop. Med., 29, 669 (1949).

16. Jarroll, E.L., A.K. Bingham and E.A. Meyer, "Giardia Cyst Destruction: Effectiveness of Six Small-Quantity Water Disinfection Methods," Am. J. Trop. Med. Hyg., 29, 8 (1980).

17. Fulton, C., "Amebo-flagellates as Research Partners: The Laboratory Biology of Naegleria and Tetramitus," chapter in Methods in Cell Physiology, Volume 4, D. Prescott, Editor, Academic Press, New York, 1970.

18. Chang, S.L., "Small Free-Living Amoebae: Cultivation, Quantitation, Identification, Classification, Pathogenesis, and Resistance," in Current Topics in Comparative Pathobiology, T.C. Cheng, editor, Vol. 1. Academic Press, New York (1971).

19. APHA, AWWA, WPCF, Standard Methods for the Examination of Water and Waste-Water, 14th Ed., Am. Pub. Health Assoc., Washington, D.C., 1975.

20. Palin, A.T.,"Analytical Control of Water Disinfection with Special Reference to Differential DPD Methods for Chlorine, Chlorine Dioxide, Bromine, Iodine and Ozone," J. Institution of Water Engineers, 28, 139 (1974).

21. Engelbrecht, R.S., B.F. Severin, M.T. Masarik, S. Farooq, S.H. Lee, C.N. Haas, and A. Lalchandani, "New Microbial Indicators of Disinfection Efficiency," Final Report under Interagency Agreement EPA-IAG-D4-0432, U.S. Environmental Protection Agency, 82 pp (1975).

22. Cronier, S.D., Destruction by Chlorine Dioxide of Viruses and Bacteria in Water, M.Sc. thesis, University of Cincinnati, Cincinnati, OH, 85 pp. (1977).

23. Scarpino, P.V., M. Lucas, D.R. Dahling, G. Berg, and S.L. Chang, "Effectiveness of Hypochlorous Acid and Hypochlorite Ion in Destruction of Viruses and Bacteria," in Chemistry of Water Supply, Treatment and Distribution, A.J. Rubin, Editor, Ann Arbor Science, Ann Arbor, MI (1974).

24. Stringer, R. and C.W. Kruse, "Amoebic Cysticidal Properties of Halogens in Water," in Proceedings National Speciality Conference on Disinfection, American Society of Civil Engineers, New York, 1970.

Comments on
Cyst Inactivation with Chlorine and Chlorine Dioxide

Harold W. Wolf
Texas A&M University
College Station, Texas

This is a progress report on a grant titled "Disinfection of Giardia lamblia Cysts with Chlorine, Chlorine Dioxide, and Ozone."

Just two weeks ago I checked into a motel in Red Lodge, Montana, and observed a sign "Don't Drink Our Water." Under the sign was a newspaper item describing a Giardia problem in the city's water supply. This Red Lodge infestation is not mentioned in Dr. Sproul's report or in his grant application; hence, the problem of giardiasis may be more widespread than we realize.

The objectives set forth in the grant application which funds this work are as follows:

> "The objectives of this project are to determine inactivation kinetics of Giardia lamblia and Naegleria gruberi using chlorine, chlorine dioxide and ozone as disinfectants. The effects of the following specific parameters will be included: pH, contact time, cyst and disinfectant concentration, and temperature."
>
> "A secondary objective for this project is to increase the data pool available on the inactivation of protozoan cysts by the commonly used water disinfectants. This information is nonexistent for chlorine dioxide and little information is available on ozone."

The pH values to be investigated were specified as 5, 6, 7, and 8; temperatures 5, 15, 25, and 30°C. Initial experiments were to be done at pH 7.0, 25°C, and a cyst concentration of about 500/ml; these conditions were defined as "standard conditions."

Dr. Sproul's data show that he has developed standard condition data for N. gruberi using chlorine dioxide. He has also developed data for pH values of 5, 6, 7, and 8. Although his grant makes no mention of pH 9, he may want to include this pH because of the bunching obvious from his data. He has also developed standard condition data for N. gruberi using free chlorine and pH values of 5, 7, and 9. The very large effect of pH is obvious and in agreement with what would be expected.

A table is presented which compares his findings thus far with data from the literature for polio 1, E. coli, and E. histolytica. These comparisons show quite clearly that approximately one to two orders of magnitude more of disinfectant concentration-contact time are needed by the amoebic cysts—an observation that should give water treatment engineers, biologists, operators, health department personnel, and the like some thoughtful moments. Note that these data are derived using a chlorine-demand-free water—not with the complications of natural water. Certainly, no one will increase disinfectant concentrations to the values necessary. Prolonged contact times are contrary to the minimizing of trihalomethane concentrations—unless a "fixed" chlorine such as chloramine or chlorine dioxide is used. The importance of good coagulation, flocculation, and sedimentation processes preceding filtration is, therefore, again emphasized.

The work plan shows that standard condition data for N. gruberi should be completed by the end of 12 months; Dr. Sproul and his colleagues are well on their way. The plan also shows that background chemistry (analytical procedures) and the laboratory manipulation of G. lamblia should have been completed by this time. Only the latter is lacking because of the lack of a human host for G. lamblia. Perhaps contact with state health departments in endemic areas might be rewarding.

ELECTROSORPTION OF PHENOL ONTO ACTIVATED CARBON

Peter S. Fedkiw, Carlton F. Dwiggins, and Joseph McGuire
Department of Chemical Engineering
North Carolina State University
Raleigh, North Carolina 27650-5035

ABSTRACT

Adsorption of a nonionic organic species at a solid electrode under the influence of an applied potential is called electrosorption. We have postulated that electrosorption can be used to increase the adsorptive capacity of an activated carbon for phenol. After a brief review of phenol adsorption and electrosorption in general, data are presented which substantiate this claim. Anodic polarizations enhance the adsorption capacity, whereas cathodic polarizations decrease the adsorption capacity of the activated carbon used in this study. Future work to be performed in this study is outlined.

INTRODUCTION

This manuscript is an interim report of the work being performed in our laboratory studying the feasibility of increasing the adsorption capacity of activated carbon for nonionic organic species by applying an electrical potential to the carbon. The applied potential polarizes the surface relative to the solution. An additional electrostatic force can thereby operate to aid the adsorption process at the surface. This process is called electrosorption to distinguish it from an ordinary, nonelectrically driven adsorption. Phenol in a dilute aqueous solution (<100 mg/l) is chosen as our model adsorbate. Phenol is unionized in acidic and slightly basic solutions ($pK_a = 9.9$, 20°C) and is an example of nonionic adsorbate. Removal of phenols from an aqueous stream is relevant to pollutant control in this country's developing coal gasification technology. Phenolic compounds are a major constituent of the condensate water from a gasifier, with the monohydric phenol concentration near 2000 ppm (1, 2, 3). The removal of phenols has been classified as a high priority objective (4). A guideline effluent of 0.005 ppm has been recommended for the effluent of a coal-gasifier plant.

The results obtained so far in our work will be presented after a brief review of activated carbon adsorption of phenol and electrosorption in general.

PHENOL ADSORPTION ONTO ACTIVATED CARBON

Much work has been reported on conventional adsorption of phenols by activated carbon. An evaluation (6) of applying pollutant control technology developed for coke ovens to gasifiers cites a commercial scale activated carbon adsorber used to recover phenol from an effluent stream. An overview of treatment techniques for phenolic wastes, including activated carbon adsorption, has been presented (7). A thorough laboratory-scale study on phenol adsorption at a carbon surface has been reported by Zogorski and Faust (8, 9, 10) who performed an extensive study of the effects of carbon source, solution pH, phenol concentration, flowrate, bed depth, etc... for a variety of phenolic compounds on the adsorption capacity of a carbon bed. A dramatic decrease in the adsorption capacity of the carbon as the pH increased above the pK_a of the phenol was observed which they attributed to the phenol existing as a phenoxy anion at the solution pH. Singer et al. (11) studied the equilibrium adsorption isotherms of a variety of substituted phenols on activated carbon and Takeuchi et al. (12) have examined the effects of multiple phenolic solutes on the performance of a carbon adsorbent. All of the above workers found that the adsorption isotherm was Langmurian at low concentrations (less than 50 ppm).

Detailed studies attempting to elucidate the mechanism of the phenol-activated carbon surface interaction have been reported. There are at least three probable explanations for the adsorption process. Coughlin et al. (13) propose a dispersive force pi electron interaction of the phenol with the graphitic plane pi electron system. Mattson et al. (14, 15) suggest an electron donor-acceptor complex is formed between carbonyl oxygen ($>C = O$) on the surface and the aromatic ring of phenol. Walker and his coworkers (16) propose a competition between phenol and water which is hydrogen bonded to the surface for available adsorption sites.

ADSORPTION IN AN APPLIED ELECTRIC FIELD

Dameskin et al. (17) present 14 different adsorption isotherms which have been developed by various investigators to describe the adsorption of an organic at an electrode. The simplest of these is the Langmuir adsorption isotherm and it will be used to demonstrate in a semiquantitive manner the effect of an imposed potential on the sorption process.

The Langmuir adsorption isotherm may be derived by considering the electrode surface to consist of a fixed number of active sites at which adsorption may take place. We then write

$$A_{soln} + \square \rightleftarrows A_{ad} \qquad (1)$$

where □ denotes an empty adsorption site and A_{ad} the adsorbed molecule A. A simple accounting of the total number of occupied and vacant adsorption sites, and assuming equilibrium for Equation 1 leads to the Langmuir isotherm

$$\theta/(1-\theta) = KC \qquad (2)$$

where θ is the fraction of occupied adsorption sites, K is the equiblibrium constant for Equation 1, and C is the bulk concentration of the adsorbate. Equation 2 may also be rearranged in terms of the surface concentration

$$\theta = \Gamma/\Gamma_{max} = KC/(1 + KC) \qquad (3)$$

where Γ is the amount adsorbed per unit area of the electrode and Γ_{max} is the maximum amount of adsorbate corresponding to a monolayer coverage. The equilibrium constant is related to the free energy change $\overline{\Delta G^\circ}$ for the adsorption,

$$-RT \ln K = \overline{\Delta G^\circ} \qquad (4)$$

The free energy of adsorption is in turn dependent upon the electrical state of the adsorbent-solution interface. Frumkin (as reviewed in 17) developed a phenomenological model to account for the electrical potential dependence of $\overline{\Delta G^\circ}$ at an ideal polarized electrode (i.e. where no Faradaic current is passed).

$$\overline{\Delta G^\circ} = \Delta G^\circ + C' (E_z)(E-E_{z,\theta=0}) A + (C-C')(E-E_{z,\theta=0})^2 A/2 \qquad (5)$$

Here E_z is the potential of zero charge (p.z.c) relative to a given reference electrode. At this potential there is no net charge on the electrode surface. At potentials negative relative to the p.z.c, a net negative charge exists on the electrode, and for potentials positive relative the p.z.c, a net positive charge exists on the electrode. $E_{z,\theta=0}$ is the p.z.c. at zero coverage. E_z is the shift of p.z.c., $E_{z,\theta=1} - E_{z,\theta=0}$. C is the double-layer capacitance at zero coverage and the superscript prime refers to C at $\theta = 1$. A is the area of the electrode and ΔG° is the free energy of adsorption at the p.z.c.

The first term on the right-hand side of Equation 5 accounts for an energy change due to a change in the dipole moment at the adsorbate-adsorbent interface. The last term accounts for the variation of energy due to a decrease in the solvent's dielectric constant when the adsorbate is introduced (18). Equation 5 is parabolic in E, hence the free energy change $\overline{\Delta G^\circ}$ may reach a maximum depending upon the values of C' and E_z which are both measured experimentally.

Bockris and coworkers (as reviewed in reference 19) have derived a molecular based model whose predictions qualitatively agree with Equation 5. They reason that since water molecules are replaced by the adsorbate, the largest $\overline{\Delta G^\circ}$ will occur when the electrode's attraction for the water molecule is at a minimum. This takes place at the p.z.c. because at potentials positive to p.z.c. the oxygen of water is preferentially adsorbed and at potentials negative to the p.z.c. the hydrogen is preferentially adsorbed.

It is clear that the efficiency of an adsorber can be increased if the potential can be manipulated. Equations (5) and (2) predict that, at a given bulk concentration, the adsorption goes through a maximum as the potential is increased in the anodic direction past E_z. However, this maximum is rarely seen for the adsorption of organic species at solid electrodes because oxidation of the compound usually takes place.

POTENTIAL BOUNDS IMPOSED BY ELECTROCHEMICAL REACTIONS

The preceding discussion has assumed that the potential of the electrode may be varied arbitrarily over a large range; however, there are practical limitations to the potential span which can be applied in electrosorption. Undesired electrochemical reactions will take place if too positive or too negative a potential is applied.

Consider a carbon electrode in contact with an aqueous solution of phenol The potential of zero charge for carbon is in the range of 0.2 to 0.3 volts (versus a H_2 reference electrode) (20). The exact value of E_z is dependent upon the solution composition, but for sake of the presentation, let us assume the upper limit reported above. At a potential positive to 0.3 volt a net positive charge is placed on the electrode. The electrode is electron deficient and it is energetically favorable to remove an e^- from a species in contact with the electrode/electrolyte interface. Three possibilities exist: (1) a carbon atom at the surface may be oxidized, (2) the solvent may be oxidized, (3) the adsorbate may be oxidized. Carbon requires a very large overpotential (electrical driving force) to react and it behaves essentially as an inert material (thus it makes an excellent anode for Cl_2 cells, 21). Furthermore at a pH = 7, the carbon electrode must be polarized to 0.816 volts (versus a H_2 electrode) before it is possible thermodynamically to oxidize H_2O. In an aqueous solution, the phenol will be oxidized before the carbon or water. Phenol is oxidized irreversibly in an acidic, neutral or basic solution to the phenoxy radical

$$\mathrm{Ph} \xrightarrow[C]{} e^- + \mathrm{Ph}^\bullet$$

which further chemically reacts to quinones, hydroquinones or polymeric species (22). Figure one presents a measure of the rate of this reaction at a carbon electrode as a function of the solution pH. The dashed lines show the thermodynamic potential limits imposed by electrolysis of water. The ordinate for the solid line is, in the voltametry vocabulary, the "half-wave potential." The half-wave potential is that potential at which the reaction proceeds at one-half of its mass-transfer limited rate at a stationary electrode when the potential is linearly scanned. There exists a quantitative relationship between the half-wave potential and the rate constant of the oxidation step but for our purposes, it suffices to note that the larger $E_{1/2}$, the more difficult is the oxidation. From the data it can be seen an applied potential approximately 0.1 to 0.2 volts anodic of the p.z.c. on carbon is required before an appreciable oxidation of the phenol proceeds in an acidic or neutral solution. If the carbon is to act as an electrosorber, too large of an anodic oxidation potential is to be avoided, otherwise a polymeric film may form on the carbon and occlude its surface and/or an oxidized phenol product may leave the electrosorber.

On the negative polarity of the p.z.c., the carbon becomes electron rich and thus a reductive medium. No data has been found by the authors on the direct electrolytic reduction of phenol at a carbon surface; however, an indirect electrolytic reduction of resorcinol by a Na(Hg) amalgam has been reported (23) wherein the double bonds were reduced. It is speculated in this same reference that a direct electrolysis could reduce the double bonds if

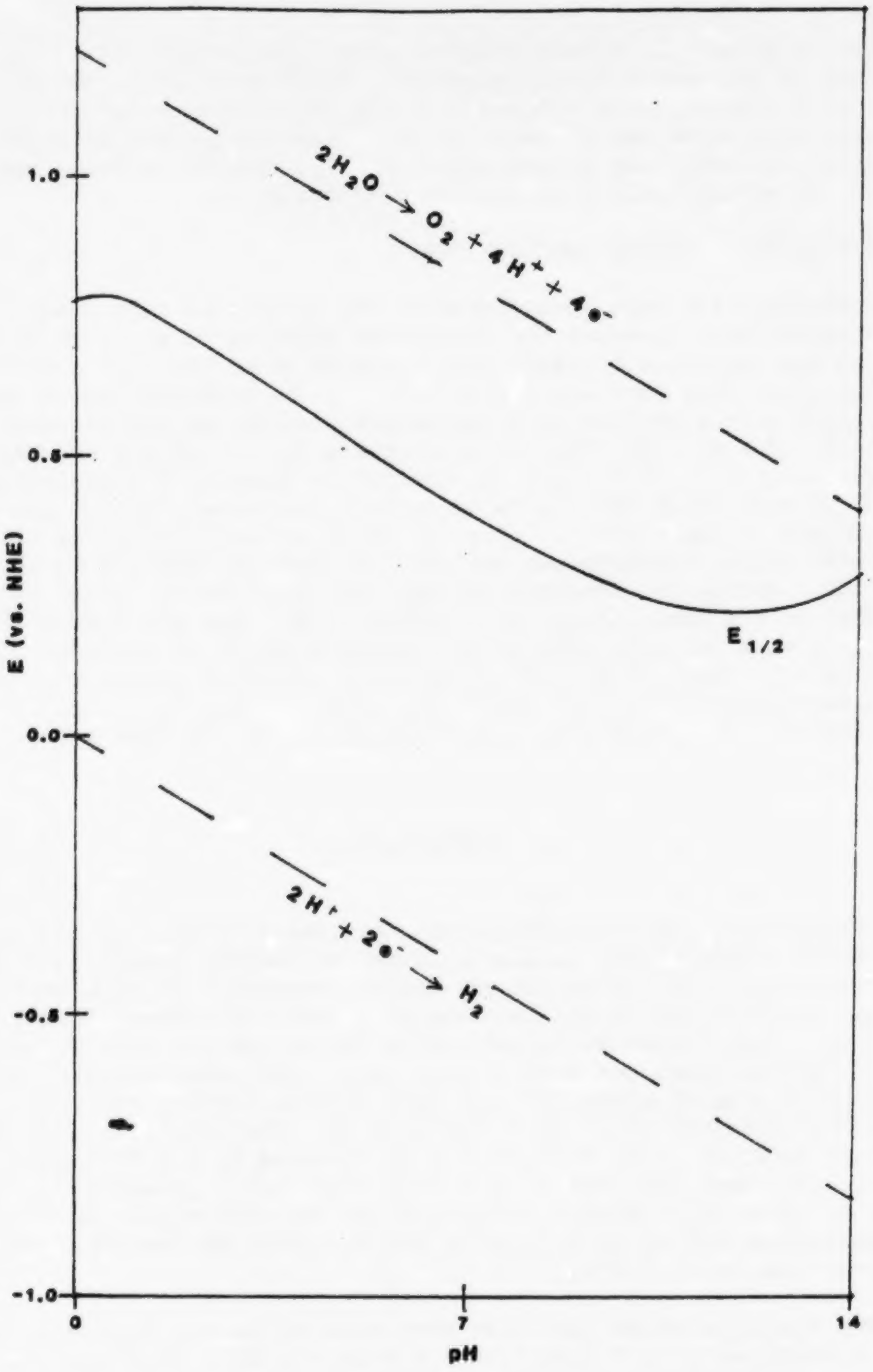

Figure 1. Potential limits imposed by electrolysis of water and oxidation of phenol at a graphite electrode.

the applied potential is made slightly more negative than the decomposition potential of the medium at the given pH. In water H_2 would be evolved and this is, of course, to be avoided. In the desorption cycle of the bed, the potential must never become more cathodic than the H_2 evolution potential on the carbon surface. Any oxygen which is dissolved in the water may be reduced at both the adsorption and desorption potentials.

PREVIOUS RELEVANT ELECTROSORPTION WORK

Precedence has been established in the literature that electrosorption will substantially increase the adsorption capacity of a carbon bed. Electrosorption has been used to desalinate brackish water (24, 25). In this process the adsorbates were charged species and the adsorbent was a carbon bed. The utility of electrosoprion of uncharged species was demonstrated by Strohl and Dunlap (26) who explored electrosorption in a fixed bed of graphite as a possible analytical technique. Figure two is taken from their publication. A solution containing the indicated quinone was passed through the packing. The ordinate is the volume of solution which passed through the bed until a detectable solute breakthrough was observed and the abscissa is the applied potential. Notice the dramatic increase in the capacity of the bed for each component over a small change in potential. Eisinger and Alkire (27) have recently presented their work on the electrosorption of β-napthol on graphite. Figure three, taken from their publication, shows an increase in adsorption with a more positive applied potential. They claimed that a modified Langmuir isotherm (19) correlated their data up to surface coverages of 63 percent.

EXPERIMENTAL

The activated carbon used in this work was a coconut based material with a BET surface area of approximately $10^3 m^2/gm$ (Barneby Cheney Company, type UU). Prior to usage the carbon was washed repeatedly in warm 4M HCl until no material was detected in the leachate by a spectrophotometric scan from 190 to 400 nm. The cleaned and dried carbon was sieved and only the portion between 50 and 120 mesh was used in this work. All chemicals used were Fisher Scientific's reagent grade and were used without further purification except the phenol which was purified by sublimation. The solutions were made with deionized water and were deoxygenated by bubbling N_2 gas through the solution. The solutions were buffered at pH = 6.86 with sodium phosphate salts and contained 0.5 $\underline{M}$ Na_2SO_4. Phenol concentrations were determined by adsorbance measurements at 270 nm on a Shimadzu 210 UV spectrophotometer. The experiments were performed at 23 ± 2°C.

The electrosorption isotherms were measured in the flow cell appratus shown schematically in Figure four. A Princeton Applied Research potentiostat (model 179) with a coulometer (model 179) was used to control the potential between the carbon bed and the calomel reference electrode at any adjustable value. [For further information on the functioning of a potentiostat see (28).]

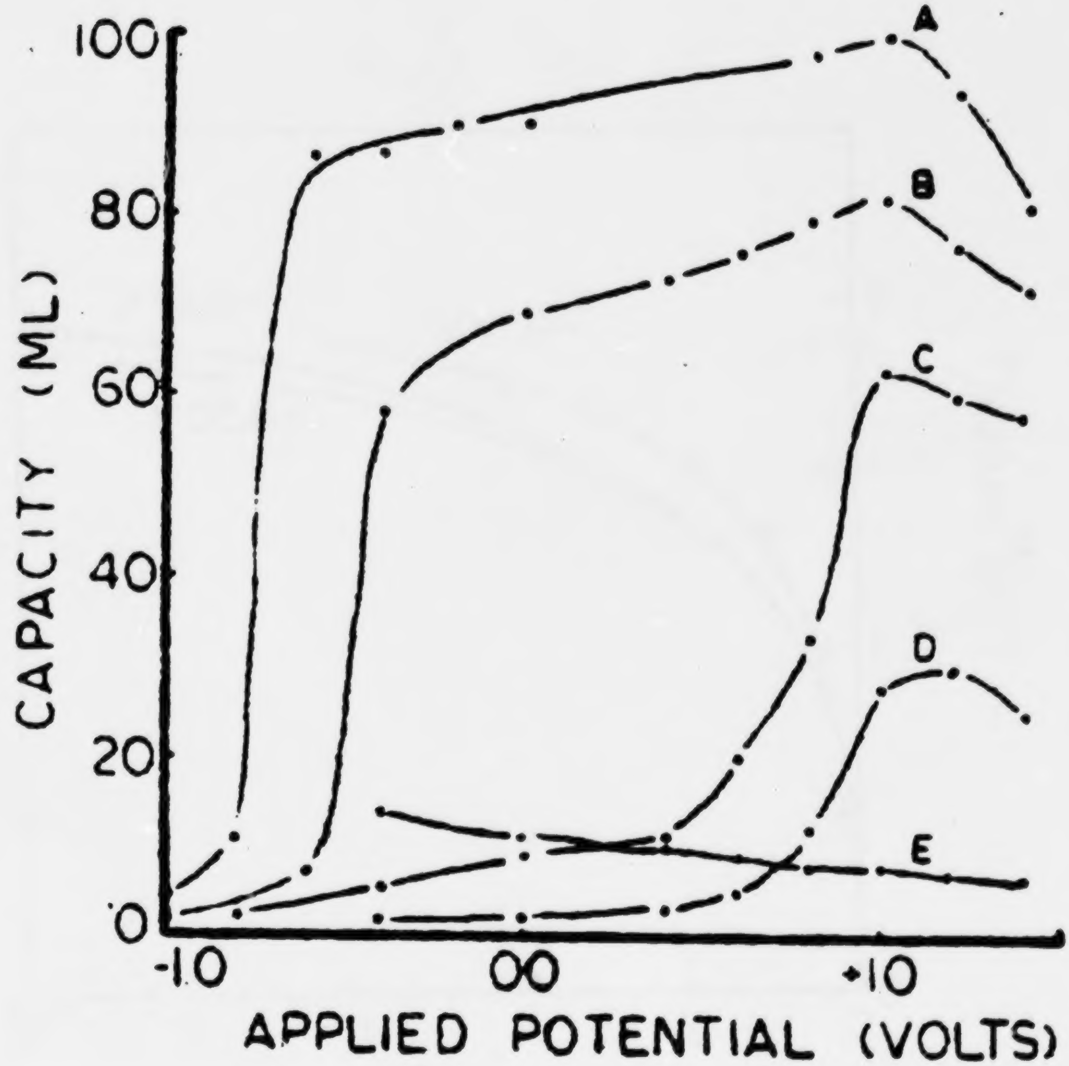

Figure 2. Capacity as a function of potential. 1.0×10^{-4}M solutions used, and flow rate was 1 ml/min.

A. 1.8-Dichloro-9,10-anthraquinone
B. Phenanthrenequinone
C. 9,10-Anthraquinone-1-sulfonic acid Na salt
D. 1,2-Naphtoquinone-4-sulfonic acid Na salt
E. Duroquinone

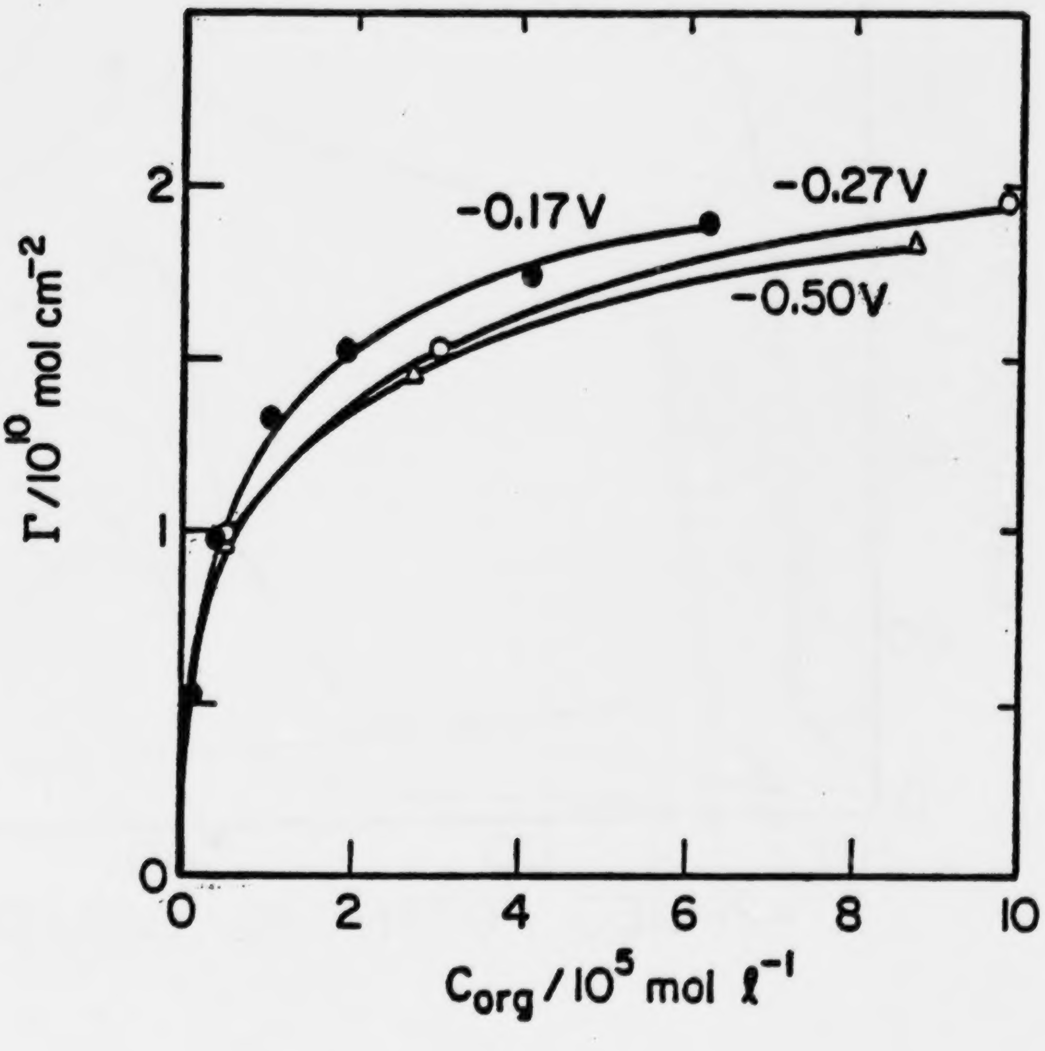

Figure 3. Electrosorption of ß-napthol on graphite(27).

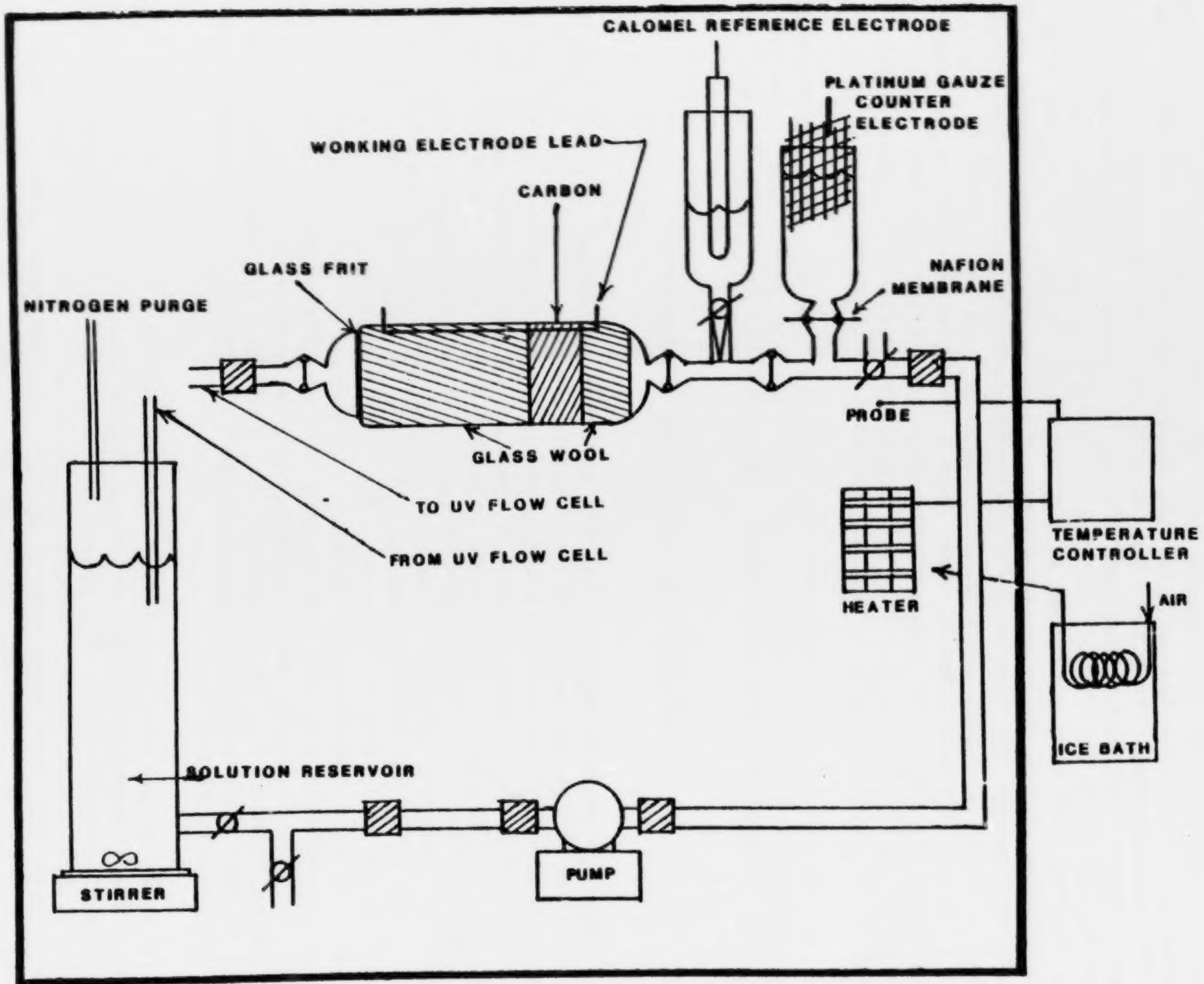

NOTE : ELECTRODE COMPARTMENTS AND SOLUTION RESERVOIR ARE GLASS.CONNECTING TUBING IS TEFLON.

CALOMEL REFERENCE ELECTRODE
PLATINUM GAUZE COUNTER ELECTRODE
WORKING ELECTRODE LEAD
CARBON
NAFION MEMBRANE
GLASS FRIT
NITROGEN PURGE
PROBE
GLASS WOOL
TO UV FLOW CELL
FROM UV FLOW CELL
TEMPERATURE CONTROLLER
AIR
HEATER
ICE BATH
SOLUTION RESERVOIR
STIRRER
PUMP

Figure 4. Recirculating-fluid electrosorption cell. Electrode compartments and solution reservoir are glass. Connecting tubing is teflon.

The procedure used in measuring an isotherm was as follows. A weighed portion of the activated carbon (usually near 1.5 gm) was boiled in a small beaker containing the electrolyte solution. After cooling, the carbon was carefully packed into the cell so that no air bubbles were included. The packed cell assembly was placed in the constant temperature air bath and the remaining flow and electrical connections were made. The potentiostat was then engaged into the circuit to control the potential between the carbon bed and calomel reference electrode at a preselected value. An initial slug of concentrated phenol solution was placed in the reservoir and allowed to recirculate through the flow cell-UV spectrophotometer flow loop for approximately 2 hours at which point an absorbance reading was recorded. Since the fluid volume of the system is known from a previous calibration, a mass balance gives the amount of phenol adsorbed on the carbon surface, hence, a single point on the isotherm. This procedure was continually repeated by the addition of known volumes of the concentrated stock solution.

At the end of the an isotherm run, the fluid in the solution reservoir was analyzed for reaction products by a spectrophotometric scan from 190 to 400 nm. No species other than phenol were detected by this procedure.

PRELIMINARY RESULTS AND DISCUSSION

The flow cell arrangement (to the author's knowledge) has not been used in previous activated carbon isotherm measurements. In previous work it has been convenient to use batch isotherm measurements in which a known amount of carbon is added to a known volume of phenol solution at some initial concentration. The mixture is continously stirred and after a period of time(usually a day or more) the final solution concentration of the adsorbate is measured. In order to assess the validity of the isotherms measured in the flow cell a series of batch isotherms were measured as outlined above. The equilibration period was 22 ± 2 hours. The ordinary isotherms were also measured in the flow cell following the procedure presented in the previous section except the potentiostat was not engaged. Figure five shows a comparison between the flow cell and batch isotherm. There is no statistically significant difference between the two measurements. Thus, it is concluded that the time frame in which our concentration measurements were made very nearly represent the true equilibrium.

At this point in our work four electrosorption isotherms have been measured. These measurements are shown on Figure six in relation to the ordinary adsorption isotherm. The polarization of the carbon-reference electrode potential difference about its equilibrium value is shown for each of the runs. Three runs have been made at anodic polarizaitons (+55mV, + 95mV, + 220 mV) and one at a cathodic polarization (-460mV). We have not collected any data in the low concentration region (<5 mg/l) as of yet, but certainly in the higher concentration regions the application of the external potential has a decidedly beneficial (anodic polarizations) or detrimental (cathodic polarization) effect. For example, at an equilibrium concentration of 40 mg phenol/l, a 25 percent increase in the adsorption capacity of the carbon is obtained if the carbon is polarized 220 mV positive to its open circuit

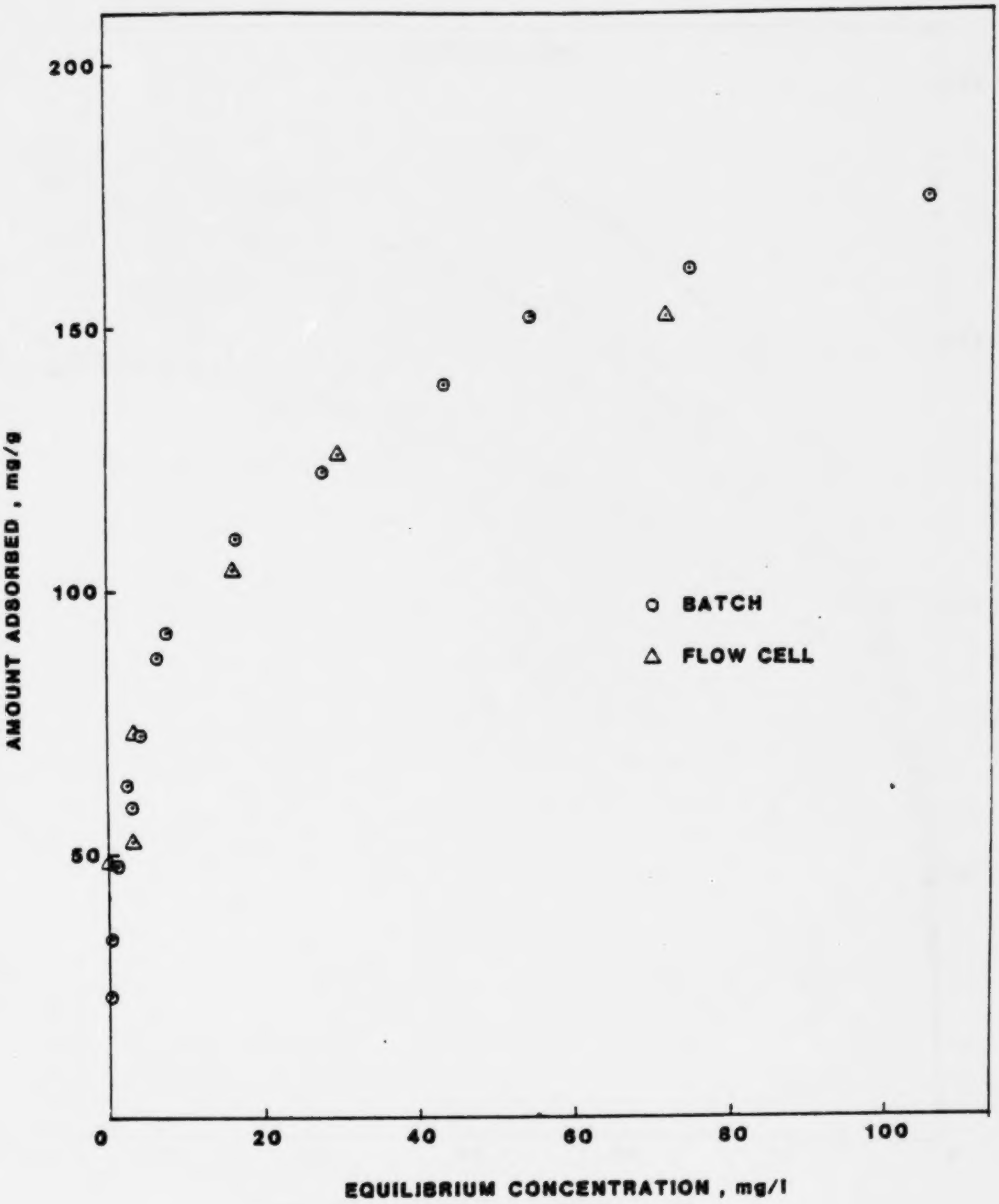

Figure 5. Adsorption isotherm of phenol onto activated carbon determined by two independent procedures.

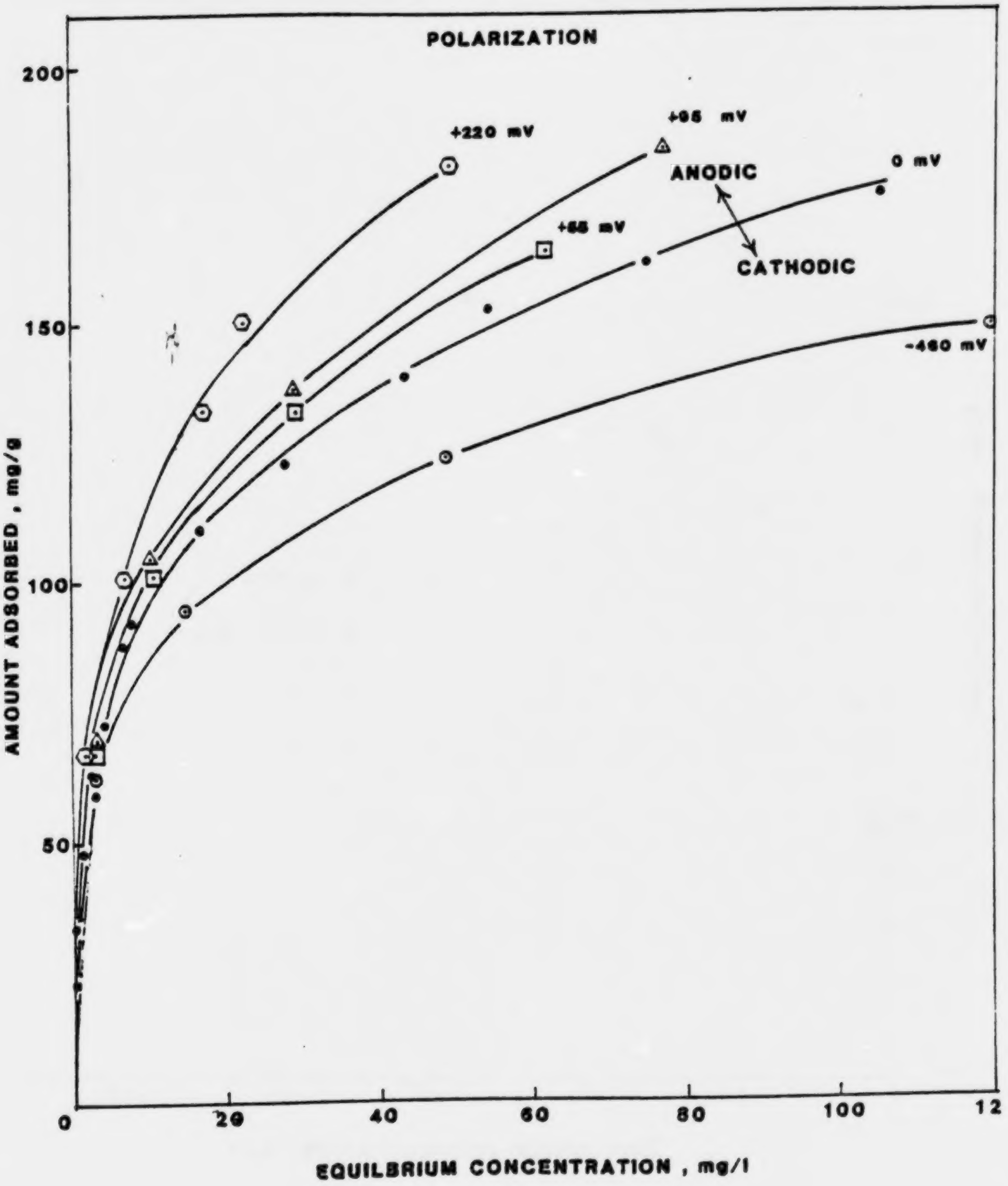

Figure 6. Electrosorption isotherm of phenol onto activated carbon.

value. This increase in adsorption capacity is not due to any electrochemical oxidation of the phenol. The measured faradaic coulombs passed during the experiment amounts to less than a 1 percent correction to the adsorption isotherm, which is insignificant.

The thesis upon which this work is predicated, the application of an electric field can enhance the adsorption capacity of activated carbon, has been substantiated by the data shown in Figure six. It is interesting to speculate on the cause-effect relationship of the imposed electric field. It seems plausible that the anodic polarizations show an increase in the adsorption of phenol because they tend to weaken the effect of hydrogen bonding of water to the surface sites, therefore making the surface sites more accessible to phenol. This reasoning would also explain the drop in adsorption during cathodic polarizations since the hydrogen side of the water will be more strongly attracted to the surface.

WORK TO BE PERFORMED

We have reported some of our early results in this manuscript. There are many items in this work which are presently being explored: The effect of (1) pH (in an unsupported electrolyte, i.e. no Na_2SO_4) and (2) temperature on the electrosorption isotherm. An integral part of this work is also to demonstrate how electrosorption can be applied in a fixed bed, activated carbon adsorber. For this purpose, a packed-bed electrosorber has been constructed (Figure seven) and will be used to measure the breakthrough curve characteristics in electrosorption. Finally the possibility of electrochemically regenerating the used adsorbent will be explored. This work will be reported in a future communication.

ACKNOWLEDGEMENTS

Professor Vivian Stannett permitted the use of his UV spectrophotometer. Mr. Ellis McGaughy performed some of the routine laboratory work.

REFERENCES

1. R. E. Hicks, D. J. Goldstein, F. B. Seufert, and I. W. Wei, Wastewater Treatment in Coal Conversion, EPA-600/7-79-133, p. 6, June (1979).

2. P. C. Singer, J. C. Lamb, III, F. K. Pfaender and R. Goodman, Treatment and Assessment of Coal Conversion Wastewaters: Phase 1, EPA-600/7-79-248, p. 40, (1979).

3. P. C. Singer, F. K. Pfaender, J. Chinchilli, and J. C. Lamb, III, "Composition and Biodegradability of Organics in Coal Conversion Wastewaters," in Symp Proc.: Environmental Aspects of Conversion Technology, III, EPA-600/7-78-063 (1978).

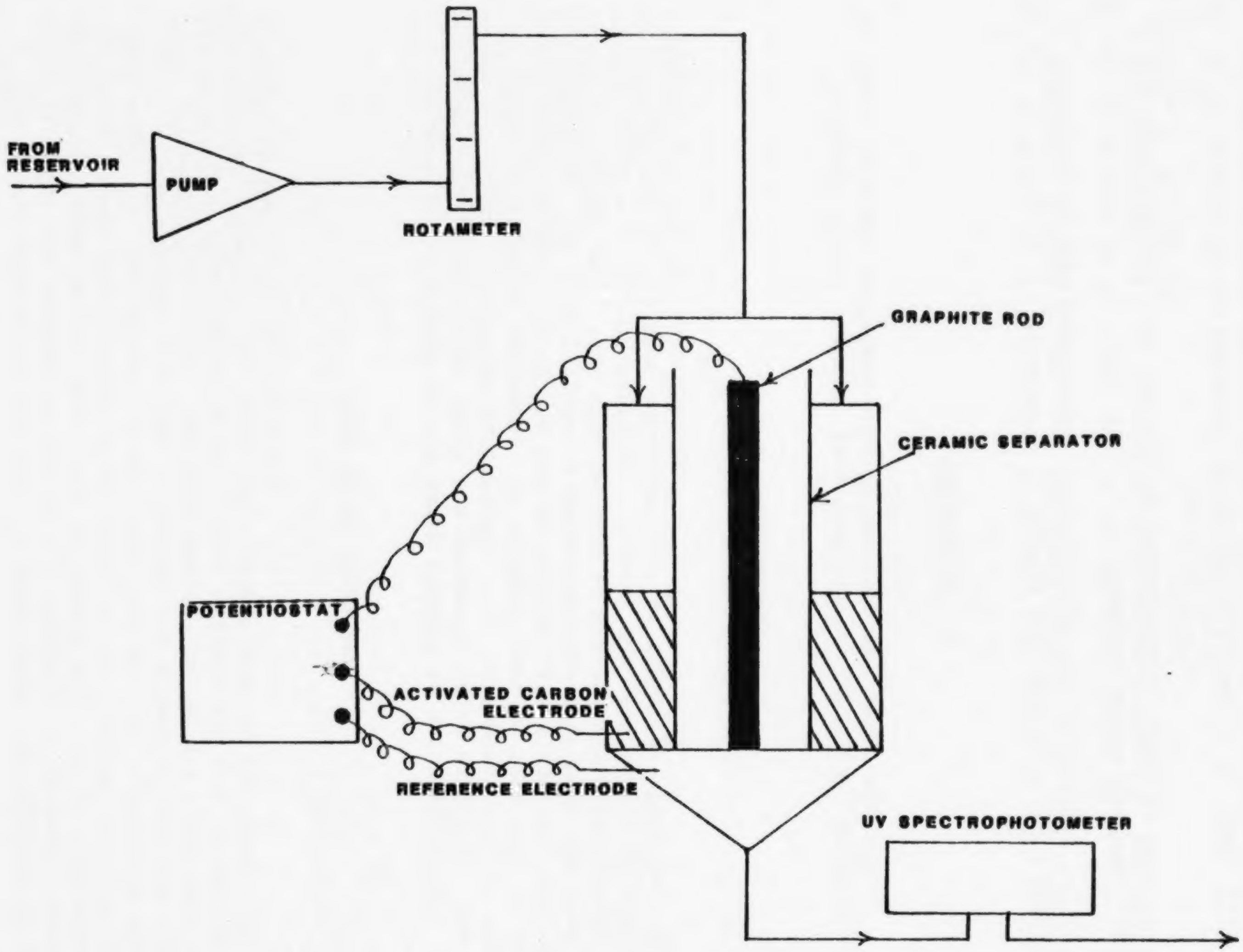
FROM RESERVOIR
PUMP
ROTAMETER
GRAPHITE ROD
CERAMIC SEPARATOR
POTENTIOSTAT
ACTIVATED CARBON ELECTRODE
REFERENCE ELECTRODE
UV SPECTROPHOTOMETER

Figure 7. **ANNULAR PACKED-BED ELECTROSORBER**

4. G. C. Page, *Environmental Assessment: Source Test and Evaluation Report-Chapman Low - BTU Gasification*, EPA-600/7-78-202 (1978).

5. L. E. Bostwick, N. R. Smith, D. O. Moore, and D. K. Webber, *Coal Conversion Control Technology, Volume 1, Environmental Regulations; Liquid Effluents*, EPA-600/7-79-228a, p. 119 (1979).

6. S. M. Hossain, P. F. Cilione, A. B. Cherry, and W. J. Wasylenko, Jr., *Applicability of Coke Plant Control Technologies to Coal Conversion*, EPA-600/7-79-184, p. 137 (1979).

7. K. H. Lanouette, "Treatment of phenolic wastes," *Chem. Engr.*, October 17, 99 (1977).

8. J. S. Zogorski and S. D. Faust, "Operational Parameters for Optimum Removal of Phenolic Compounds from Polluted Waters by Columns of Activated Carbon," Chapter 20 in reference 1.

9. J. S. Zogorski and S. D. Faust, "Removing Phenols via Activated Carbon," *Chem. Engr. Prog.*, May, 65 (1977).

10. J. S. Zogorski and S. D. Faust, "Removal of Phenols from Polluted Waters," final report to Water Resources Research Institute, Rutgers State University, NJ, June (1974).

11. P. C. Singer, F. K. Pfaender, et al., *op. cit.*, p. 172.

12. Y. Takeuchi, T. Wasai, and S. Suginaka, "Fixed-Bed Breakthrough Curves in Binary and Ternary Component Adsorption from Aqueous Solutions," *J. Chem. Engr. Japan*, *11*, 458 (1978).

13. R. W. Coughlin, F. S. Ezra, and R. N. Tan, "Influence of Chemisorbed Oxygen in Adsorption onto Carbon from Aqueous Solution," *J. Coll. Interface Sci.*, *28*, 386 (1968).

14. J. S. Mattson, H. B. Mark, M. D. Malbin, W. J. Weber, and J. C. Crittenden, "Surface Chemistry of Active Carbon: Specific Adsorption of Phenols," *J. Coll. Interface Sci.*, *31*, 116 (1969).

15. B. D. Epstein, E. Dalle-Molle, and J. S. Mattson, "Electrochemical Investigations of Surface Functional Groups on Isotropic Pyrolytic Carbon," *Carbon*, *9*, 609 (1971).

16. O. P. Mahajan, C. Moreno-Castilla, and P. L. Walker, "Surface-Treated Activated Carbon for Removal of Phenol from Water," *Separation Science Techn.*, *15*, 1733 (1980).

17. B. B. Damaskin, O. A. Petrii, and V. V. Batrakov, *Adsorption of Organic Compounds on Electrodes*, Plenum Press, New York (1971).

18. P. Delahay, *Double Layer and Electrode Kinetics*, John Wiley and Sons, New York, p. 91 (1965).

19. J. O'M Bockris and A. K. N. Reddy, *Modern Electrochemistry*, *Vol. 2*, Plenum Press, New York (1970).

20. A. J. Bard (ed), "Carbon," Chapter 1 in *Encyclopedia of Electrochemistry of the Elements*, *Vol. VII*, Marcel Dekker, New York, p. 37 (1976).

21. A. J. Bard (ed), *op. cit.* p. 127ff.

22. A. J. Bard and H. Lund (ed), "Hydroxy Compounds," Chapter XI-2, in *Encyclopedia of Electrochemistry of the Elements*, Vol. XI, Marcel Dekker, New York, p. 2433ff (1978).

23. M. M. Balzer (ed), *Organic Electrochemistry*, Marcel Dekker, New York, p. 814 (1973).

24. J. A. Blair and G. W. Murphy, "Electrochemical Demineralization of Water with Porous Electrodes of Large Surface Area," *Adv. Chem. Series*, *27*, 206 (1960).

25. A. M. Johnson and J. Newman, "Desalting by Means of Porous Carbon Electrodes," *J. Electrochem. Soc.*, 118, 510 (1971).

26. J. H. Strohl and K. L. Dunlap, "Electrosorption and Separation of Quinones on a Column of Graphite Particles," *Anal. Chem.*, *44*, 2166 (1972).

27. R. S. Eisinger and R. C. Alkire, "Electrosorption of β-Naphol on Graphite," *J. Electroanly. Chem. Inter. Electrochem.*, *112*, 237 (1980).

28. E. Gileadi, E. Kirowa-Eisner and J. Penciner, *Interfacial Electrochemistry* Addison-Wesley Publishing Co., Reading, MA, (1975).

Comments on
Electrosorption of Phenol onto Activated Carbon

James O. Leckie
Environmental Engineering and Science
Department of Civil Engineering
Stanford University
Stanford, California

This paper represents an interim report on progress achieved during the first six months of work on a grant titled "Electrosorption of Phenol on Activated Carbon from Dilute Aqueous Solutions." The study tests the feasibility of increasing the adsorptive capacity of activated carbon, specifically for nonionic organics, by imposing an applied electrical potential to the carbon, thus inducing a polarization of the carbon and by reversing the potential, increase the desorption process as well. This is a novel application of a phenomenon well known in electrode electrochemistry based on the fact that making a surface more anodic by an applied potential, we can induce polarizable molecules to approach and attach to the surface. The mode of attachment of nonionic organic species is not well known. We do not know whether the water layer is removed from the surface or whether bonding is through the hydrated layer. Nevertheless, the question at hand is whether the process can be made to work in a manner that is predictable and reversible. The project has two parts: 1) investigation of the electrosorption isotherms as a function of applied potential, and 2) evaluation of breakthrough curve characteristics of a fixed-bed activated carbon electrosorber using phenol as the test solute. The concept is innovative and has potential for: 1) increasing the capacity of adsorption for polarizable nonionic organics at low concentration, and 2) increasing the efficiency (and ease) of regeneration of the expended carbon. If the process proves feasible and sufficiently efficient, it would be useful to explore the details of the mechanism of binding at the carbon surface.

Preliminary results are promising. Enhanced adsorption of up to 25% was shown for anodic polarizations of +220 mv. In addition significant rejection occurs at cathodic voltages of -460 mv indicating a rejection of the adsorbate by reversal of the polarizing voltage. Future work will explore the effect of pH, temperature, and enhanced adsorption at lower solute concentrations. Considerable work must be completed before feasibility can be determined.

EFFECT OF TURBIDITY AND OTHER FACTORS ON THE VIRUS DISINFECTION PROCESS USING FREE AND COMBINED CHLORINE FORMS

Pasquale V. Scarpino, Ph.D.
Professor of Environmental Engineering
Department of Civil and Environmental Engineering
University of Cincinnati
Cincinnati, Ohio 45221

ABSTRACT

This research study is a direct extension of continuing efforts to learn more about factors influencing viral and bacterial water disinfection processes in the presence of turbidity (in the form of organic and inorganic particulate matter). Organic suspended solids in the form of BGM cell-associated poliovirus 1 were evaluated to determine their influence upon disinfection using hypochlorous acid, monochloramine, and dichloramine. The effect of ionic presence on disinfection was investigated in order to assess why ionic presence (i.e., KCl) was initiating differences in the viral inactivation studies. I believe it vitally important that the latter effect be evaluated to alleviate the uncertainties surrounding the effect of ion presence on the disinfection process in the presence of particulates. It is hoped that most of the research goals outlined in the original proposal will be completed in year one of the grant.

INTRODUCTION

This research grant was awarded on October 27, 1980, which means that we are in the eighth month of the first grant year.

Only minor departures have occurred from the original research schedule and these all involved re-assembling priorities to mesh the actual experimental data that developed, and to take advantage of what we regarded as significant findings.

It is of course unfortunate that we cannot make final conclusions today based on the data accumulated over the past 8 months. However, we will be able to make you aware of the direction of our research, and hopefully indicate its relevancy to you.

During the first eight months (see Figure 1) of this study, the literature review was completed to fill any gaps in research information, especially in regard to particulate-interference with the disinfection process. A "singles" preparation of poliovirus 1 was prepared to be used in the study, along with poliovirus 1 in the aggregated state. I decided to delay working with rotavirus at this time because of the lack of manpower required to provide rotavirus tissue cultures for the experimentation. Although the necessary protocol and supplies were assembled to commence work on the effect of particulates on the virus disinfection process, difficulties arose because of the uncertainties surrounding the effect of ion presence on the disinfection process. It was decided to delay the initiation of inorganic particulate studies, and instead determine why ionic presence was causing differences in the viral inactivation studies. However, additional cell-viral associated studies were commenced during this time period. At this time I am initiating additional cell-viral associated studies, and inorganic particulate experimentation. I believe that although I have been delayed longer than I anticipated in regard to the ionic presence research, I will be able to complete most of the research goals outlined in Figure 1 before the end of grant year one. I believe that it was imperative to resolve the ionic presence problem before I could progress to the rest of the proposed year one experimentation. I firmly believe that the experimentation that I am doing is unique and vital to the final solution of the problems associated with particulate presence in water and wastewater and its effect on the disinfection of microbes, especially animal viruses.

BACKGROUND OF THE STUDY

Precise knowledge concerning the inactivation of viruses in water assumes greater importance as we turn to an ever increasing degree to the re-use of our neighbor's upstream wastewater. Since sewage contaminated water is a potential health hazard (1), an awareness of the efficiency of applied disinfectants (i.e., free and combined forms of chlorine) on human enteric pathogens has continued increased significance. This is particulary true with animal viruses which are considerably more resistant than the bacteria.

Over 100 new human enteric viruses have been described since the investigations of Enders _et al_. (2) on viral propagation techniques using tissue cultures. Enteric viruses are the most important virus agents infective for man known to be present in water and wastewater. This group includes all viruses known to be excreted in quantity in the feces of man; they are listed in Table 1 along with their associated diseases. Thus, the enteric viruses consist, among others, of the enteroviruses (poliovirus, coxsackievirus, and echovirus), hepatitis type A (i.e., infectious hepatitis), Norwalk type agents, adenoviruses, reoviruses, and rotaviruses.

First Three-Month Period

(a) Complete literature review necessary to fill any gaps in information needed for the research.

(b) Prepare virus particles to be used in the experimentation in either the single state or in an aggregated one.

(c) Prepare the tissue cultures needed for the growth of the rotavirus.

(d) Commence free and combined chlorine studies for test microbes using varying level of particulates (bentonite, kaolin, and alum), and single virus inocula.

Second Three-Month Period

(e) Continue (b) and (d) above.

(f) Commence virus studies with disinfectants using cell-associated virus preparations.

Third Three-Month Period

(g) Continue (d) above.

(h) Continue (f) above.

(i) Prepare the fecal-associated virus suspensions for disinfection studies.

Fourth Three-Month Period

(j) Continue studies on the effect of organic solids (i.e., feces) on the viral disinfection process.

(k) Evaluate our performance during Year One to determine the schedule for the second year.

Figure 1. Research Schedule For Year One.

TABLE 1. HUMAN ENTERIC VIRUSES THAT MAY BE PRESENT IN WATER AND THEIR ASSOCIATED DISEASES (3)

Virus group	No. of types	Disease caused
Enteroviruses:		
Poliovirus	3	Paralysis, meningitis, fever
Echovirus	34	Meningitis, respiratory disease, rash, diarrhoea, fever
Coxsackievirus A	24	Herpangina, respiratory disease, meningitis, fever
Coxsackievirus B	6	Myocarditis, congenital heart anomalies, rash, fever, meningitis, respiratory disease, pleurodynia
New enteroviruses	4	Meningitis, encephalitis, respiratory disease, acute haemorrhagic conjunctivitis, fever
Hepatitis type A (probably an enterovirus)	1	Infectious hepatitis
Gastroenteritis virus (Norwalk type agents)	2	Epidemic vomiting and diarrhoea, fever
Rotavirus (Reoviridae family)	?	Epidemic vomiting and diarrhoea, chiefly of children
Reovirus	3	Not clearly established
Adenovirus	30	Respiratory disease, eye infections
Parvovirus (adeno-associated virus)	3	Associated with respiratory disease in children, but etiology not clearly established

Note: Other viruses which, because of their stability, might contaminate water are the following:

(1) SV40 like papovaviruses, which appear in the urine. The JC subtype is associated with progressive multifocal leukoencephalopathy

(2) Creutzfeld-Jakob (C-J) disease virus. Like scrapie virus, the C-J virus resist heat and formaldehyde. It causes a spongiform encephalopathy, characterized by severe progressive dementia and ataxia.

This research study is a direct extension of our continuing efforts to learn more about factors effecting the disinfection of viruses and bacteria in water and wastewater by free and combined forms of chlorine. One of the basic objectives of our laboratory is to evaluate the effect of turbidity and other factors such as ionic presence on the virus disinfection process. The need to understand more properly the factors affecting the virus disinfection process by chlorine and its compounds is more imperative in light of the inclusion of a Maximum Contaminant Level (MCL) of 1 Nephelometric Turbidity Unit (NTU) in the National Interim Primary Drinking Water Regulations. Since turbidity may interfere with disinfection efficiency, these investigations will provide further insight into the observed differences of the effect of different levels of turbidity on the virus disinfection process.

This work has or will be involved with both the free and combined chlorine forms. Perhaps, a quick review of chlorine chemistry might be productive at this point. Equation 1 shows the formation of the free chlorine forms of hypochlorous acid (HOCl) and hypochlorite ion (OCl^-):

$$Cl_2 + H_2O \rightleftharpoons HOCl + H^+ + Cl^- \qquad \text{(Equation 1)}$$

$$HOCL \rightleftharpoons H^+ + OCl^- \qquad \text{(Equation 2)}$$

Equations 3 & 4 show the formation of monochloramine (NH_2Cl), as ammonia (NH_3) interacts with hypochlorous acid; and the formation of dichloramine ($NHCl_2$) as monochloramine reacts chemically with hypochlorous acid:

$$NH_3 + HOCl \rightleftharpoons NH_2Cl + H_2O \qquad \text{(Equation 3)}$$

$$NH_2Cl + HOCl \rightleftharpoons NHCl_2 + HOH \qquad \text{(Equation 4)}$$

The pH has a definite impact on the form of chlorine that will be present in the water. For instance, with the free chlorine forms, a pH above or at 10 will give mainly OCl^- (hypochlorite ion), whereas a pH at 6 will give mainly HOCl (hypochlorous acid). In the case of the combined chlorine forms, a pH of 8.5 will give NH_2Cl (monochloramine), whereas that of 4.4 to 5.0 will give only $NHCl_2$ (dichloramine).

Although this work has or will be involved with both the free and combined chlorine forms, monochloramine has been emphasized in the initial start-up phase of this project. This is because of the problem inherent in the chlorination of water supplies, where chlorine plus precursor organics leads to the formation of chlorinated organics.

5

The use of combined chlorine (i.e., chloramines) as a disinfectant in water supplies thus assumes great importance when consideration is given to their reduced reactivity with precursor organics in water to form chlorinated organic compounds (i.e., trihalomethanes) which may be later identified as carcinogenic (4). Investigations have shown that chloramines either do not cause trihalomethane (i.e., chloroform, bromo-dichloromethane, dibromochloromethane, and bromoform) formation, or cause reduced quantities of trihalomethanes to be formed (5). The 1975 National Organics Reconnaissance Survey (NORS) (6) initially had noted that the finished water of utilities disinfecting with chloramines contained total trihalomethane (TTHM) levels that ranged from 1 to 81 ug/l with an average level of 19 ug/l, whereas those water utilities using breakpoint chlorination had total trihalomethane (TTHM) concentrations ranging from 1 to 472 ug/l in their finished water with an average level of 72 ug/l. It has been noted (5) that the reason that some of the water utilities in the NORS study using chloramines had high TTHM's was probably due to free chlorine being used prior to the addition of ammonia, with the resultant formation of TTHM's in the water. Subsequently, Stevens, et al. (7) applied both free and combined chlorine for varying contact times to untreated Ohio River water. Their results are presented in Figure 2, and shows that the TTHM's in the chlorinated sample reached 160 ug/l after 72 hours, whereas the sample dosed with combined chlorine formed only 16 ug/l TTHM's during the study.

Further information is thus essential concerning not only the usefulness of chloramines in minimizing chlorinated organic formation, the possible toxicity of the organic byproducts resulting from the reaction of chloramines with organic matter in water, but also concerning chloramine disinfecting capability in regard to both turbidity and microbes of pathogenic significance, especially animal viruses, in water supplies (5,8).

Monitoring of environmental virus levels must account for not only free virus but also for those that are solids-associated. These studies will extend these cited particulate virus studies by viewing the survival characteristics of a test enteric virus associated with particulates after dosing with free chlorine forms and with pre-formed and forming chloramines, i.e., monochloramine and dichloramine, to evaluate their disinfecting capability in the presence of varying concentrations of particulate matter. The use of enteric virus-associated animal cells will also focus attention on the survival characterisitics of such cell-associated viruses after application of varying levels of chlorine. Waterborne animal viruses may be transported either inside or on the surface of cells that are excreted from the intestinal tract of man and animals. The possibility exists that under natural conditions these cell-associated viruses may be protected during disinfection.

Factors such as ionic presence are also essential in understanding the effects of inorganic and organic turbidities in disinfection of viruses by free and combined chlorine forms. Recently, Sharp et al. (9), pointed out the importance of considering not only the pH, but also the ionic strength of the suspending buffer when studying the reasons for virus dieaway during the disinfection process.

6

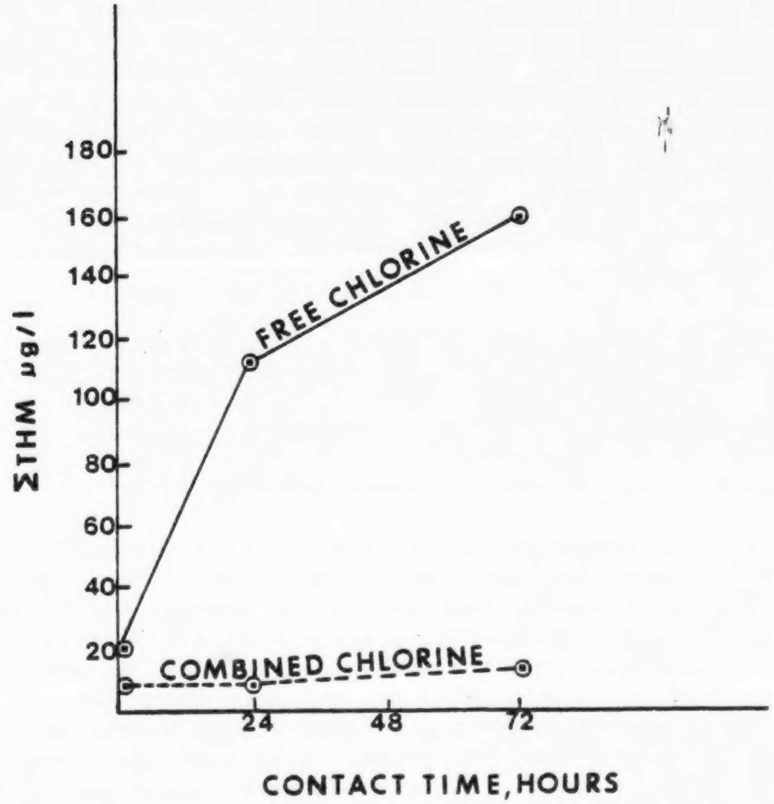

Figure 2. Comparison of Free and Combined Chlorine on the Formation of Trihalomethanes in Ohio River Water (7).

Several years ago, this researcher (10), noted that poliovirus (Mahoney) was inactivated more rapidly by chlorine in the form of OCl^- at pH 10 than by HOCl at pH 6. This was contrary to existing concepts as initially reported by Weidenkopf (11). As commented on later (12), subsequent studies indicated that the borate buffer system (containing KCl) had an influence on the OCl^- and HOCl microbiocidal relationships. The admonitions of Sharp *et al*. (9) should thus be heard, i.e., that all researchers in the area of disinfection, control for and clearly state in their publications the following variables: (a) the time of contact of the virus with the disinfectant, (b) the temperature of the reaction, (c) the total ionic strength of the reaction mixture, (d) the pH of the reaction mixture, (e) the type of buffer used to maintain the pH, (f) the total chlorine concentration and the relative amounts of HOCl and OCl^-, and (g) the state of aggregation of the virus. It is hoped that our present studies will provide us with some of the information needed to understand not only the effects of ionic presence in regard to pure systems of virus and buffer, but also the survival effects that may occur in disinfection reaction systems containing inorganic and/or organic solids.

METHODS

PREPARATION OF VIRUS STOCKS

Poliovirus 1 (Mahoney strain), and coxsackievirus A9 were used in these studies. Poliovirus 1 was grown in monolayers of Buffalo Green Monkey (BGM) kidney continuous cell line obtained from the *Cercopithecus aethiops* African green monkey. Coxackievirus A9 was grown in monolayers of primary rhesus monkey (*Macaca* sp.) kidney cell cultures. Appropriate host cell monolayers were inoculated with their respective viruses at a multiplicity of 100 plaque forming units (PFU) per cell. The viruses were allowed to absorb to the cells for one hour at 37C before a maintenance medium was added. The infected cells were incubated until complete cytopathological effect (CPE) was observed. Infected cells and fluids were frozen at -70C and thawed twice, then centrifuged for thirty minutes at 2000 rpm, and the supernatant again at 10,000 rpm for one hour. The supernatant was frozen at -70C, thawed and centrifuged at 19,000 rpm for twenty-one hours. The pellet containing the virus was now suspended in demand-free deionized distilled water and respun for a second time at 19,000 rpm for twenty-one hours. The virus was now resuspended in chlorine demand-free deionized distilled water and frozen at -70C. The stock virus was tested for chlorine-demand, and when the demand was demonstrated to be negative, the virus was dispersed in 1.2 ml quantities into chlorine demand-free vials and frozen at -70C. The virus titer was 10^7 PFU/ml. For test purposes the virus was thawed and diluted 1:10 before use. This preparation was considered to be aggregated.

PREPARATION OF PURIFIED VIRUS

Poliovirus 1 preparations of high purity, consisting mostly of single virions as determined by electron microscopy, were prepared by the method of Floyd *et al*. (13). Appropriate host cell monolayers were again inoculated with the virus at a multiplicity of 100 PFU per cell.

The virus was allowed to absorb for one hour, after which a maintenance medium was added and the cells further incubated at 37C for eleven hours. The cells were then removed from incubation and chilled to 4C. The BGM monolayers are scraped from the bottles into their surrounding maintenance medium, collected, and centrifuged to harvest the cells. The infected cells were then washed twice with phosphate buffered saline. The cells were resuspended with phosphate buffered saline and the virus extracted by the addition of Freon 113 followed by homogenization in a Waring blender, with separation of the aqueous phase from the freon phase by centrifugation. This freon extraction was carried out three times, each time with the virus-containing aqueous phase being collected and pooled. The virus was further purified and concentrated by density gradient centrifugation. The aqueous-virus phase was layered onto a 10 to 30% (wt/wt) sucrose gradient and centrifuged at 25,000 rpm in a Beckman L2-65B Ultra-centrifuge for two hours and fifteen minutes. Fractions of 2 ml each were collected from the centrifuge tubes and examined by electron microscopy for the presence of the virus. All relevant fractions were pooled and stored at refrigerator temperature without any attempt to remove the sucrose. The greatest concentration of purified virus was found at a concentration of 22% sucrose. The resultant virus contained no cell debris, or debris of any kind, and consisted of greater than 93% single virus particles.

PREPARATION OF BACTERIA

Escherichia coli (ATCC 11229) was grown on trypticase soy agar slants 16-18 hours at 35°C, removed from the slant surface and washed with 10 ml of demand-free phosphate buffer, centrifuged for ten minutes at 2500 rpm, and the pellet was resuspended in the demand-free phosphate buffer. This was repeated three times. The final suspension was adjusted to an optical density equal to a cell concentration of 10^8 bacteria/ml. The suspension was found usually to be demand-free using this procedure. If not, the cells were rewashed with demand-free phosphate buffer until the demand-free state was obtained.

The buffer solutions were prepared as follows:

BUFFER

The buffer systems for the hypochlorous acid (HOCl) and hypochlorite ion (OCl^-) studies consist of 0.05 Molar, pH 6 phosphate buffer (KH_2PO_4-K_2HPO_4) and 0.05 Molar, pH 10 borate buffer (H_3BO_3-NaOH) (10,12). For the monochloramine (NH_2Cl) work, the test buffer is 0.05 Molar borate (H_3BO_3-NaOH) at pH 9.0. For the dichloramine ($NHCl_2$) work, the test buffer is 0.05M potassium phthalate at pH 4.5. The buffers are made demand-free by the addition of chlorine to provide a residual of 3 to 5 mg/liter. The water is dechlorinated at room temperature for at least twenty-four hours under ultraviolet light (chlorine is highly photoreactive at ultraviolet wavelengths of about 2600A and decomposes rapidly) or until the titration by the orthotolidine spot plate test method is negative. Such water is then demand-free.

Chlorine determinations are conducted as follows:

CHLORINE DETERMINATION

The amperometric titration method employing the Wallace and Tiernan Amperometric titrator, is used to determine free chlorine and monochloramine at the time of the experimentation. Dichloramine is determined by the FAS: DPD method according to Standard Methods (14) with one exception. Since the titrations are required to be carried out at a pH of 6.2-6.5, the pH effect of the phthalate-buffered dichloramine samples has to be overcome. To accomplish this, pH 6 phosphate buffer is added as necessary to bring the pH of the titration sample to the proper range. The total recommended titration volume of 100 ml is held constant, as is the added amount of the DPD color indicator.

Chlorine solutions are prepared as follows:

PREPARATION OF STOCK CHLORINE SOLUTION

Chlorine stock solutions were prepared as required by bubbling chlorine gas into distilled water for thirty minutes, and storing the solution in an amber bottle at 4°C.

The neutralizer for monochloramine, dichloramine, and chlorine consists of enough sodium thiosulfate to give a final concentration of 6 mg/liter in the samples removed from the test and control beakers.

The test procedure will be accomplished as follows:

On the day of the tests using hypochlorous acid or hypochlorite ion, the desired chlorine concentrations are prepared in demand-free buffer by the addition of calculated amounts of the stock chlorine solution. The monochloramine test solutions are prepared the day before each experiment by first chlorinating the buffer to the desired level. Sufficient ammonium sulfate $(NH_4)_2(SO_4)$ is then added to produce an ammonia (NH_4) to chlorine ration of 6:1. All monochloramine determinations are made using the amperometric titrator as described by Wallace and Tiernan. Dichloramine is formed by adding ammonium sulfate to hypochlorous acid in one to two liter quantities of sterile demand-free 0.05M phthalate buffer of pH 4.5. The chlorine to nitrogen weight ratio (Cl:N) is approximately 3:1 to insure rapid formation of the dichloramine. The solution, loosely capped, is allowed to mix on a magnistir for two hours at room temperature to allow maximum dichloramine formation. Since dichloramine is found to be unstable over a 24-hour period, test solutions are freshly prepared on the day of the experiment.

Four hundred ml volumes of the chlorine-treated water are then placed in 600 ml test beakers according to the test scheme used by Scarpino et al. (10,12) (Figure 3). These beakers are covered by a loose metal lid through the center of which passes a glass stirring rod. One buffer control beaker contains 400 ml of the untreated (no monochloramine, dichloramine, or chlorine is added) demand-free buffer, while a second neutralizer control beaker contains a treated buffer (containing the highest free chlorine

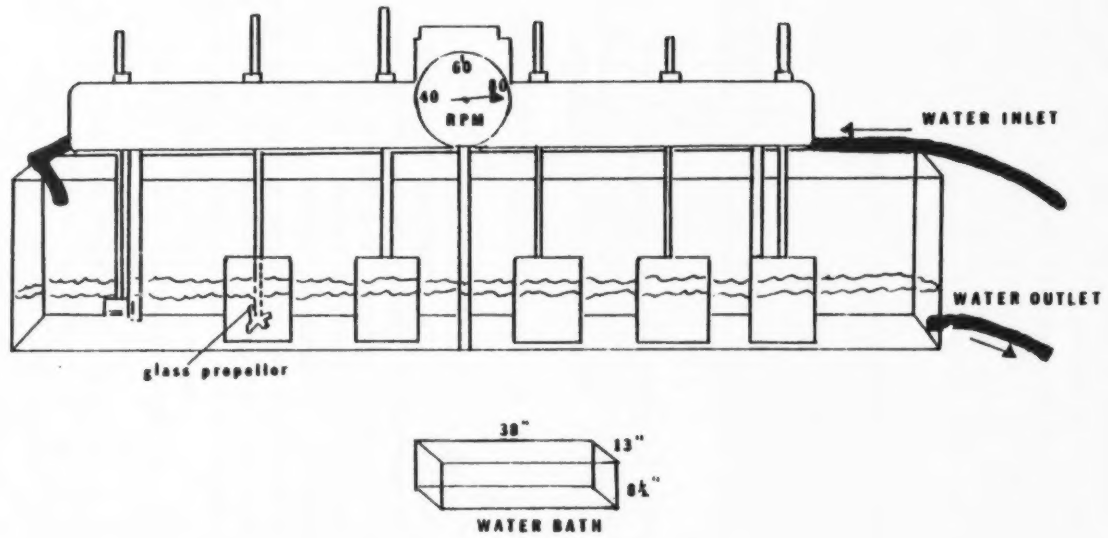
60
40
80
RPM
WATER INLET
WATER OUTLET
glass propeller
38"
13"
8¼"
WATER BATH

Figure 3. Kinetic Disinfection Apparatus Used by Scarpino et al. (10,12).

(HOCl and OCl^-), monochloramine or dichloramine (NH_2Cl and $NHCl_2$) concentrations being used that day]. The chlorine species in the second beaker is neutralized with sodium thiosulfate just before the start of the experiment. Disinfectant control beakers are also prepared that are similar in every aspect to the test beakers except that the test virus or bacterium are not added. The glass stirring rods are connected to an overhead variable-speed stirring device that is adjusted to 100 rpm, and all beakers are allowed to equilibrate to the test temperature in a carefully regulated water bath. After temperature equilibrium is obtained, the disinfectant control beakers are titrated at the start (and end) of each experiment, whereas the test beakers are titrated at the end of each study. One-millimeter standardized amounts of the test virus or bacterium are added to the buffer control, neutralizer control, and the test beakers, and 5 ml samples are removed at intervals and rapidly blown into 5 ml of the neutralizer. The neutralized samples are assayed immediately at the conclusion of the test. The pH of all test and control solutions are also determined at this time.

VIRAL AND BACTERIAL ASSAYS

The animal viruses are assayed either in the continuous cell line of African green monkey (Cercopithecus aethiops) kidney cells, designated Vero, by the plaque technique of Dulbecco and Vogt (15), as modified by Hsiung and Melnick (16), or a continuous cell line, BGM, derived from primary African Green monkey kidney cells. The BGM cell line has been found to be more sensitive to many enteroviruses and to reovirus 1 (17).

In order to characterize the viral inoculum used in these studies, the Sharp (18) kinetic attachment-electron microscopic virus assay technique was used. In the kinetic attachment procedure, a drop 1 mm thick of the virus suspension (10^{10} particles/ml or greater is the best concentration) is placed on an aluminum stabilized collodian coated copper electron microscope grid. To prevent drying of the suspension, humid conditions are provided. Virus particles, by diffusion and Brownian motion, come into contact with the grid surface, and due to the difference in charges between the aluminum and virus, they attach to the grid. After a thirty minute attachment period the unattached virus is washed away. The washing is continued for at least thirty minutes to insure the removal of all unattached virus before grid drying. After drying, the viruses are shadowcast with chromium for easier examination and enumeration of the virus particles. The grids are examined at a low magnification (5000X) in a JEOL 100B transmission electron microscope with the resulting randomly-taken micrographs being projected onto a gridded screen for virus counting. The number of particles (Nc) counted per unit area of picture at the magnification (M) used depends upon the number (No) of particles per ml of the original virus suspension, the diffusion constant (D), the viscosity (N), the absolute temperature (T) and the time (t) in seconds of contact, as follows (19):

$$Nc = 1.13\ No\ \sqrt{Dt/M^2}$$

PREPARATION OF POLIOVIRUS 1-ASSOCIATED BGM CELLS

Poliovirus 1-associated BGM (Buffalo Green Monkey) continuous kidney tissue culture cells were prepared as inocula to be used in our disinfection studies. First, BGM cells were inoculated at a multiplicity of infection of 100 pfu/cell of poliovirus 1. The virus was allowed to adsorb one hour at 37°C prior to addition of MEM maintenance medium and further incubation at 37°C for 11 hours. The infected cells were then chilled at 4°C. The monolayers were then scraped from the bottles and they and their fluids were spun at 2000 RPM. The BGM cell-associated poliovirus 1 were then washed and spun 6 times prior to experimentation with chlorine demand-free 0.05M phosphate buffer. This preparation retained a chlorine-demand due to the animals cells. Cells were harvested, washed, and enumerated using a hemocyctometer, and appropriate aliquots were used for the inoculation of hypochlorous acid - (HOCl), monochloramine - (NH_2Cl) and dichloramine - ($NHCl_2$) containing buffer solutions, following the disinfection experimental protocol already outlined. Initial determinations were made of both the free and cell-associated poliovirus 1 viruses, as follows: The infected cell aliquots are placed in contact with chloroform to lyse the cells present, thus releasing the viruses to give the total quantity present in the cell-associated virus preparation, while titration of the supernatant after centrifugation of the BGM cell-associated poliovirus 1 preparation gave the quantity of free virus that was present originally in the cell preparation (6).

RESULTS AND DISCUSSION

DISINFECTION OF BGM CELL-ASSOCIATED POLIOVIRUS 1 WITH HYPOCHLOROUS ACID, MONOCHLORAMINE, AND DICHLORAMINE

Inactivation of poliovirus 1-associated BGM cells at different turbidities was studied using three disinfectants, i.e. hypochlorous acid (HOCl) at pH 6.0 and 15°C, monochloramine (NH_2Cl) at pH 9.0 and 15°C, and dichloramine ($NHCl_2$) at pH 4.5 and 15°C. Figure 4 shows the extended survival (i.e., "tailing") due to the poliovirus' association with the BGM cells while being disinfected with HOCl. Similar tailing was also apparent when NH_2Cl and $NHCl_2$ (see Figure 5) disinfectants were used. Figure 6 is a comparison between BGM cell-associated poliovirus 1 disinfection with HOCl and NH_2Cl at similar turbidities and disinfectant concentrations. Ninety percent of the viruses are disinfected in 15 seconds with HOCl, whereas 95 minutes are required to achieve 90% disinfection inactivation by NH_2Cl of the test virus-associated cells. Hypochlorous acid is thus 380 times more effective than NH_2Cl. Figure 7 is a concentration-time relationship for 99% inactivation by NH_2Cl of poliovirus 1 singles and BGM cell associated-poliovirus 1 (at various turbidity and NH_2Cl levels) at 15°C at pH 9.0. The curve in the graph represents the unassociated "singles" poliovirus control, showing the data points for the 99% inactivation of the unassociated "singles" poliovirus 1 control. The other data points on the graph represented the 99% viral inactivation points at various turbidity levels that ranged from 0.65 to 1.98 NTU, and at various NH_2Cl levels that ranged from 3.16 to 7.00 ppm.

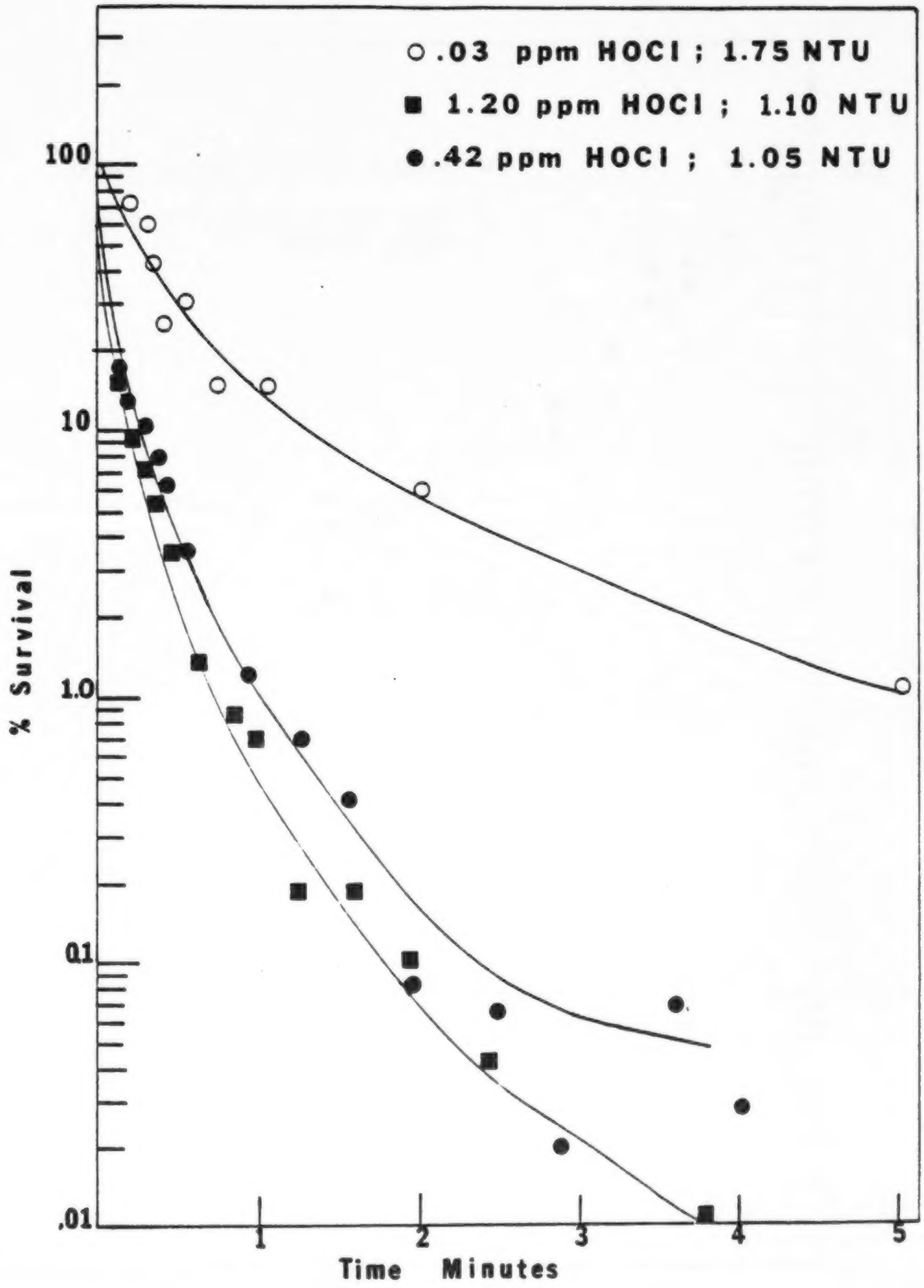

Figure 4. Disinfection of BGM Cell-Associated Poliovirus 1 with 0.42, 1.20, and 0.03 ppm of Hypochlorous Acid at Turbidities of 1.05, 1.10, and 1.75 NTU, respectively, at 15°C and pH 6.0.

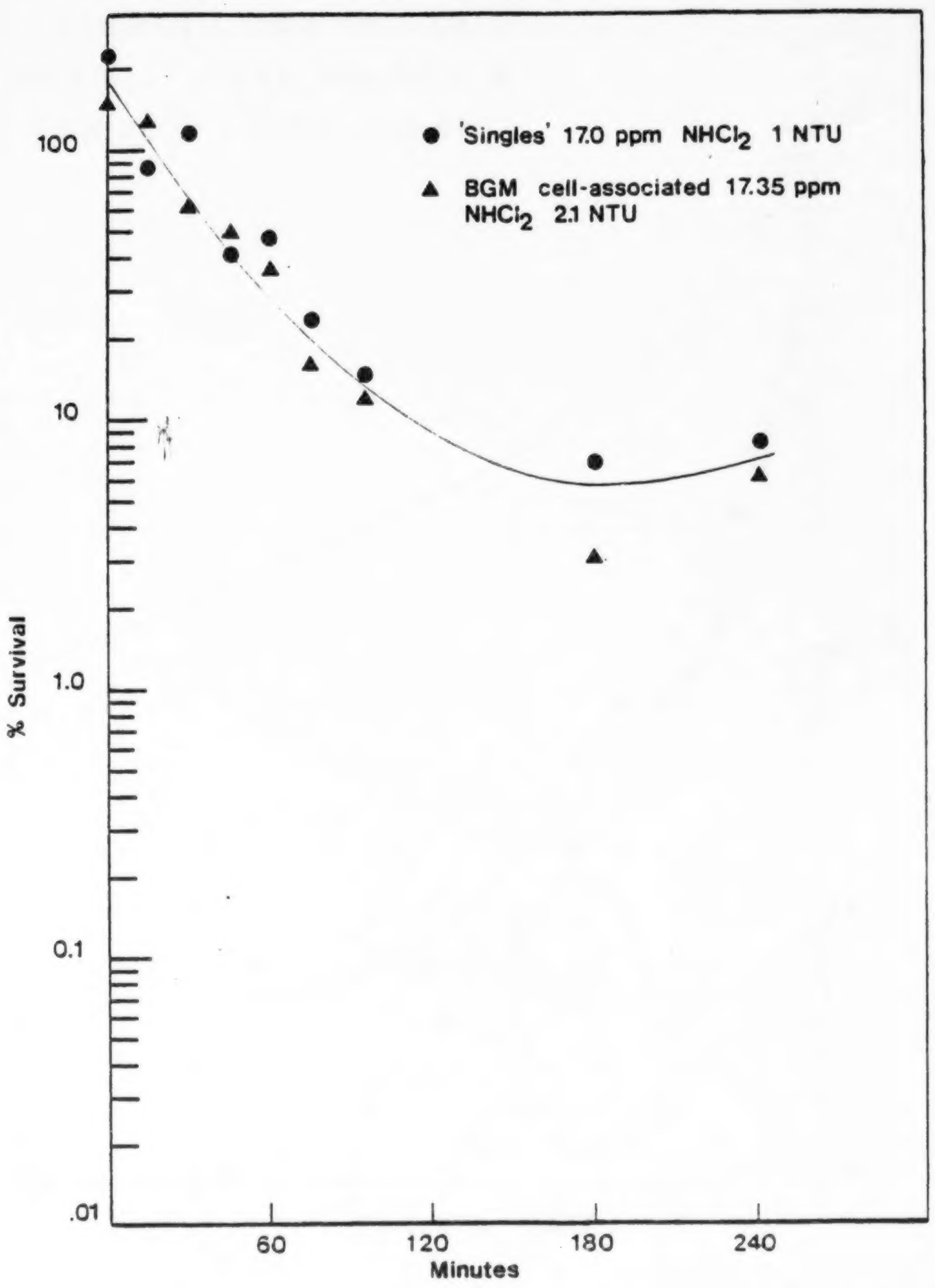

Figure 5. Disinfection of Poliovirus 1 "Singles" and BGM Cell-Associated Poliovirus 1 with Dichloramine at pH 4.5 and 5°C.

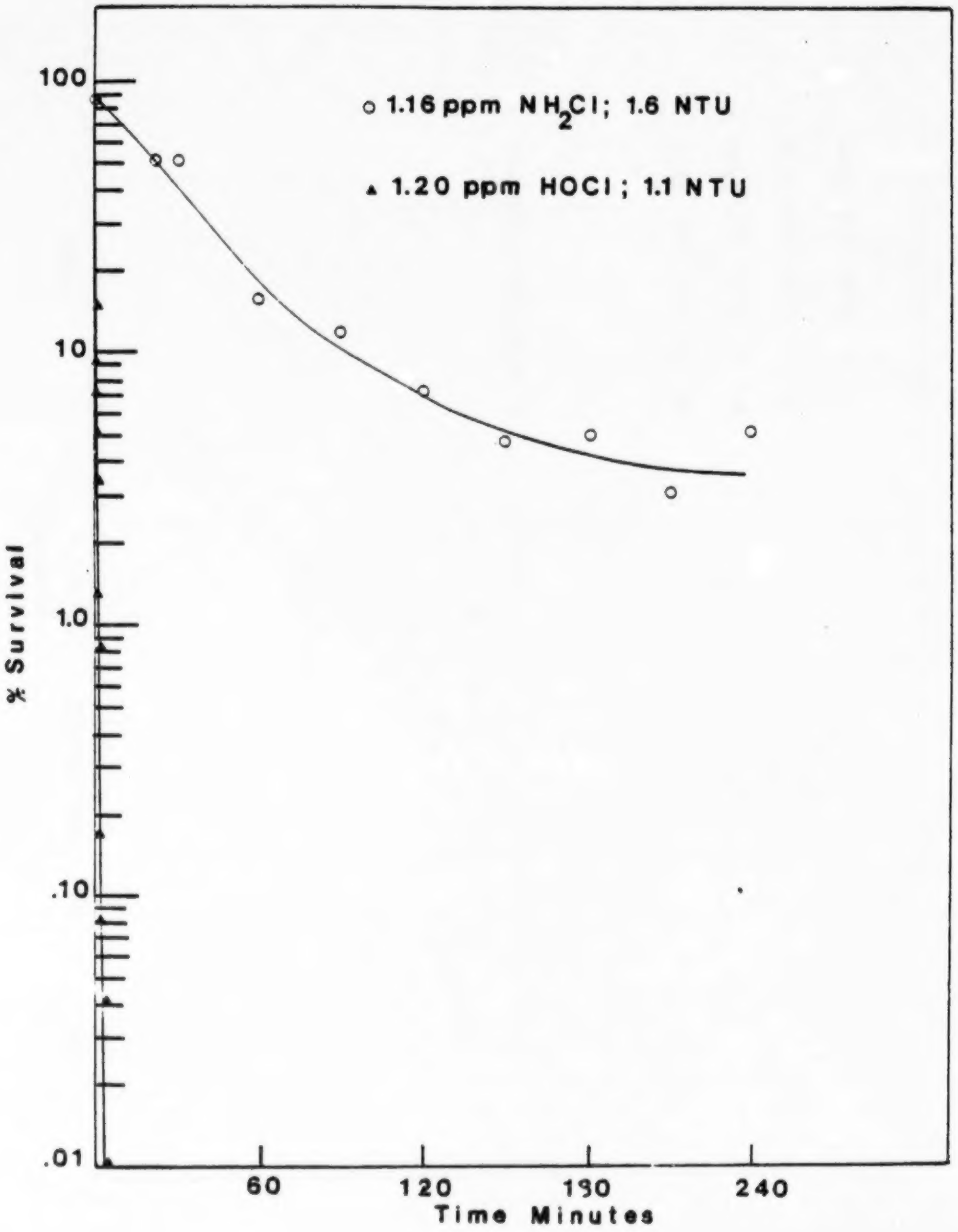

Figure 6. Comparison of Disinfection of BGM Cell-Associated Poliovirus 1 with Hypochlorous Acid at pH 6.0 and Monochloramine at pH 9.0 at 15°C.

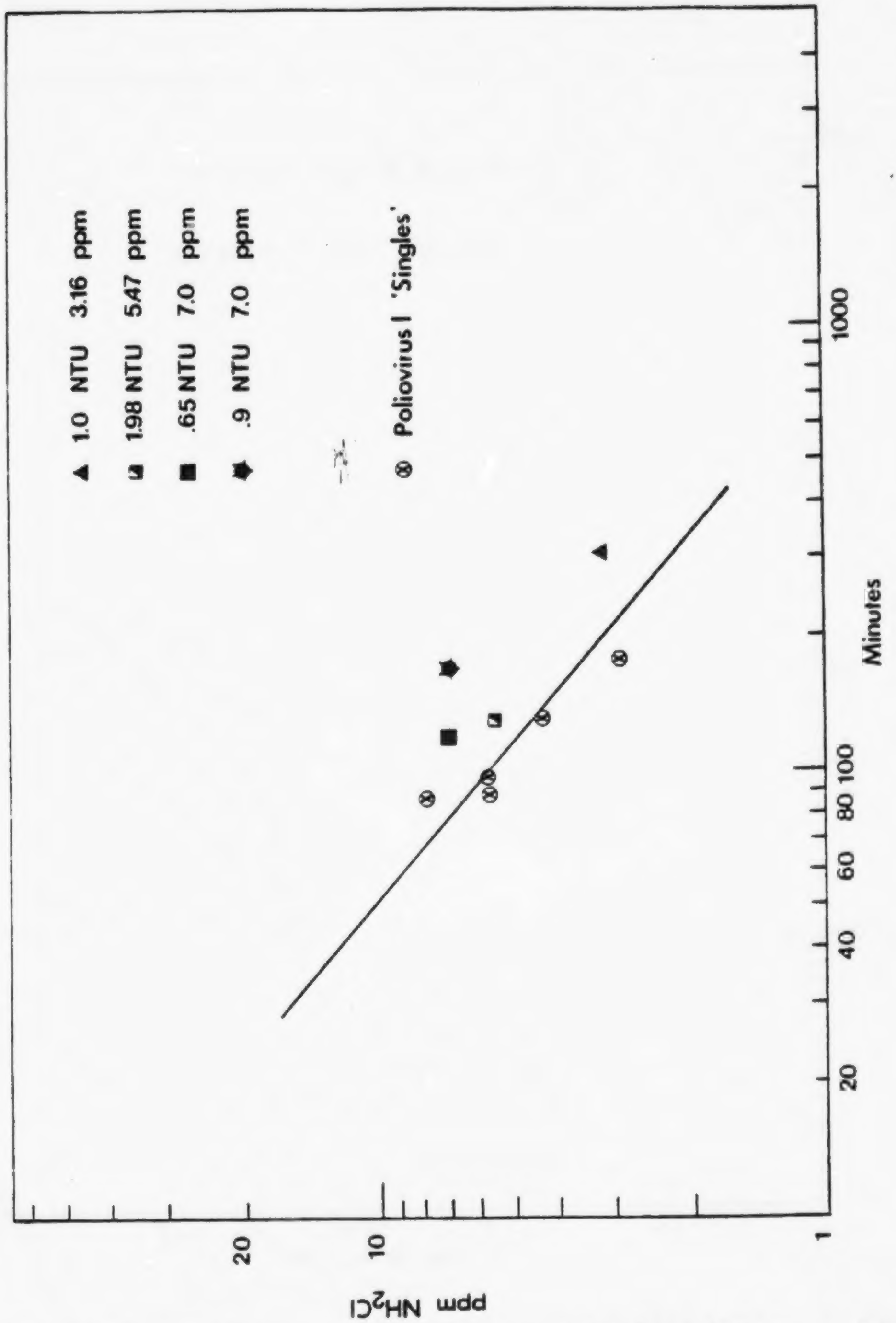

Figure 7. Concentration-Time Relationship for 99% Inactivation of Poliovirus 1 "Singles" and BGM Cell-Associated Poliovirus 1 with Monochloramine at 15°C and pH 9.0

The cell-associated poliovirus 1 data points are above the poliovirus 1 singles line, demonstrating a trend towards protection by the cells in the presence of NH_2Cl.

Figure 5's results were extremely interesting since they show that the "singles" preparation of poliovirus 1 was being inactivated at the same rate as the BGM cell-associated poliovirus 1. Apparently, the "singles" preparation was aggregating at the pH of 4.5 necessary to maintain the dichloramine in the solution. Such aggregation is protective, and will result in a delay (i.e. tailing) in the inactivation curve. This explanation is consistent with the findings of Floyd and Sharp (13), who found poliovirus "singles" aggregating at pH 4.5.

EFFECT OF IONIC PRESENCE ON DISINFECTION

Work by Scarpino in 1972 indicated that disinfection rates are affected by ionic presence. When disinfecting coxackievirus A9 with HOCl at pH 6.0 in the presence of 0.05M KCl the effect is to increase the disinfection rate 50 times (10). Disinfection of coxackievirus A9 at pH 10.0 shows also that 0.05M KCl increases the disinfection rate 10 times. This rate difference due to 0.05M KCl between the two pH's may be due to the charge on the hypochlorite ion, the change of charge on the surface of the virion, or to a change in the chemical equilibrium of chlorine due to the pH. Studies with poliovirus 1 and 0.05M KCl showed the same ion effect. When the disinfection of poliovirus 1 with hypochlorous acid (HOCl) was compared with the disinfection of E. coli, the E.coli was disinfected quicker than poliovirus 1. This relationship that viruses are more resistant than the fecal indicator organism E.coli is generally accepted. However, poliovirus 1 was more sensitive to hypochlorite ion (OCl^-) than E.coli, when 0.05M KCl was present in the buffer. Whereas the ion effect was present for coxsackievirus A9 and poliovirus 1, it was not present for E.coli.

We have been persuing this ion effect phenomenon using not only chlorine but also chloramines. Figure 8 is a survival curve showing the effect of 0.05M KCl on the disinfection of poliovirus 1 'singles' using OCl^- as the disinfectant. Open symbols denote buffers without KCl present and solid symbols denote KCl presence in buffers. As can be seen from this graph, the presence of KCl increases the efficiency of the inactivation of the viruses. To determine whether this effect is present with chloramines, similar tests were run using monochloramine (NH_2Cl) as the disinfectant. Figure 9 shows that again the effect holds. That is, the presence of KCl in the buffers increases the efficiency of the disinfectant. This ion-effect is dose dependent between 0.05M KCl and 0.1M KCl where the effect is greater with 0.1M KCl. The OCl^- and NH_2Cl studies were both run at pH 10.0 and at 5°C. Tests were then run to determine whether the effect holds for dichloramine ($NHCl_2$) at pH 4.5. Figure 10 shows that indeed the ion-effect is present using dichloramine. The level of dichloramine dropped from 11.5 ppm to 6.5 ppm during the test. Somehow the chloramine was disappearing from the system. The chloramine loss may be due to the shift of equilibrium as represented by the following equation.

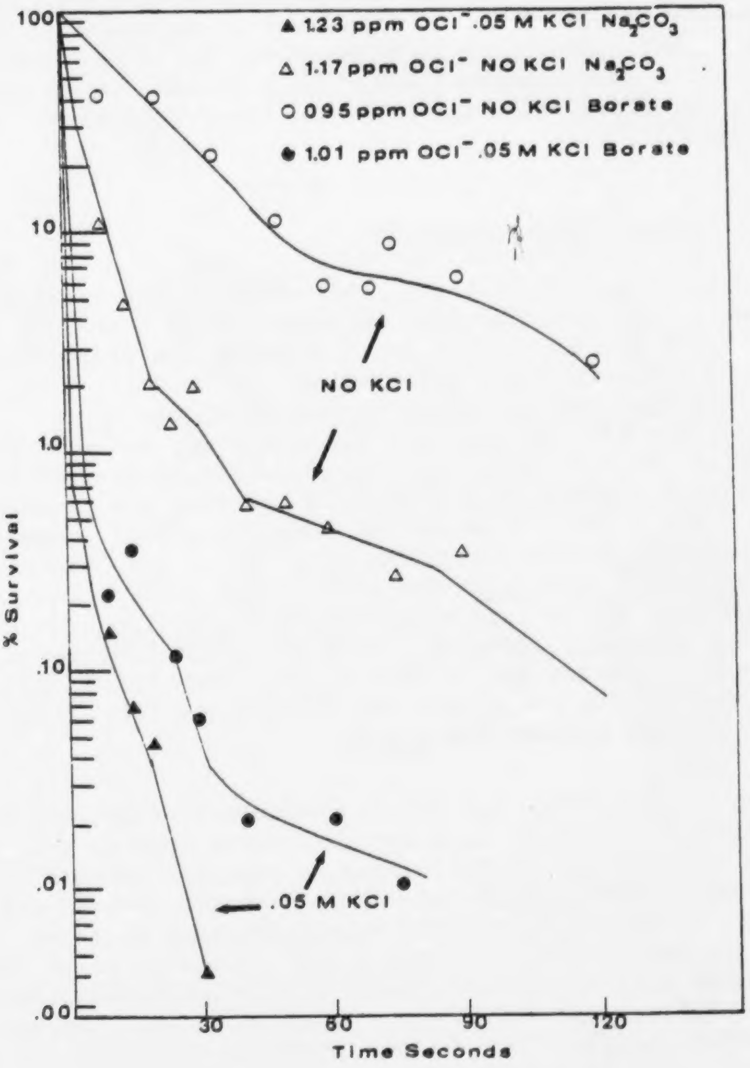

Figure 8. Effect of 0.05M KCl on Disinfection of Poliovirus 1 "Singles" with OCl^- at pH 10.0 and 5°C, in 0.05M $Na_2CO_3$and 0.05M Borate-NaOH Buffer.

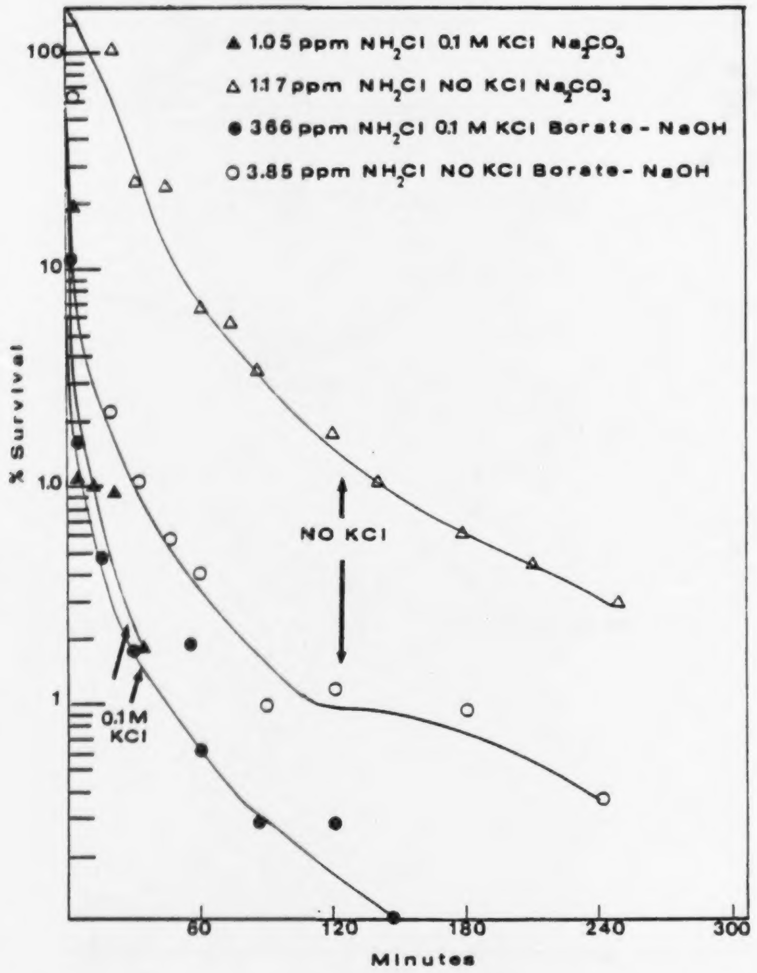

Figure 9. Effect of 0.1M KCl on Disinfection of Poliovirus 1 "Singles" with NH_2Cl at pH 10 and at 5°C, in 0.05M Borate-NaOH Buffer.

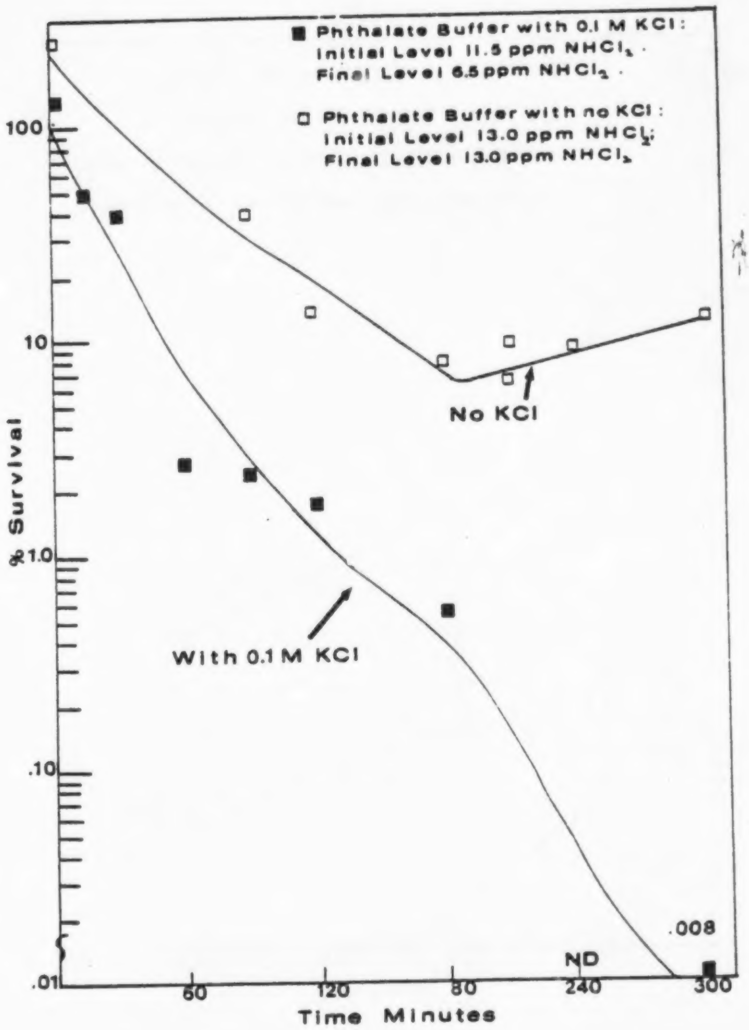

Figure 10. Effect of 0.01M KCl on Disinfection of Poliovirus 1 "Singles" with $NHCl_2$ at pH 4.5 and at $5^{\circ}C$, in 0.05M Phthalate Buffer.

$$Cl^- + NHCl_2 \rightleftharpoons NCl_3 \uparrow$$

The ion-effect can be dissipated if the addition of KCl is made at a different time. Figure 11 shows the disinfection of poliovirus 1 'singles' with and without 0.1M KCl. The open symbols depict a survival curve of polioviruses in borate buffer and NH_2Cl only. The 0.1M KCl was added at two different times. First, the hypochlorite ion and monochloramine was formed in borate buffer that contained 0.1M KCl. The solid symbols depict the survival of polioviruses when KCl is present. The ion-effect holds, that is the viruses are dying faster when the KCl is present. Second, the half and half symbols depict the event of making the borate-NH_2Cl buffer 0.1M with respect to KCl immediately before the addition of the polioviruses to the disinfection system. In this case the presence of 0.1M KCl has no effect on the disinfection rate of poliovirus 1. Therefore the time of the KCl addition to the system is critical to ion-effect phenomenon.

ACKNOWLEDGEMENTS

I wish to thank Ms. Sandy Cronier and Ms. Constance Wells for assistance in the preparation of this manuscript and for providing technical assistance. This study was partially supported by E.P.A. Grant No. R-808248010.

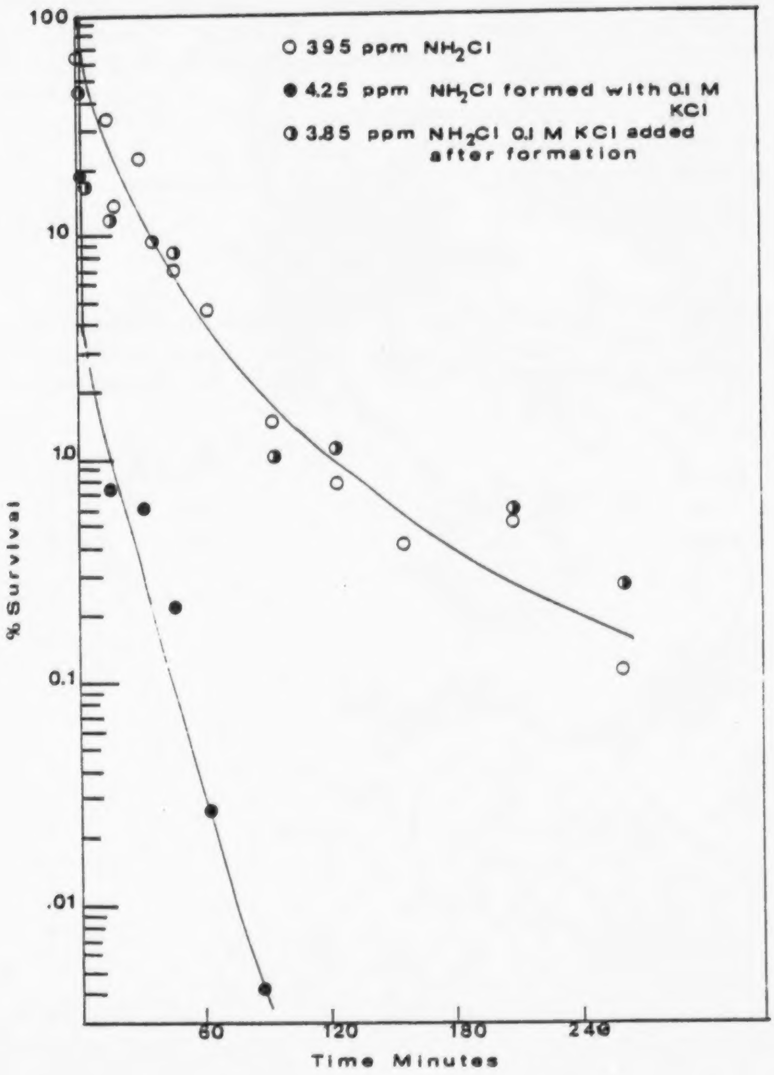

Figure 11. Effect of 0.1M KCl on Disinfection of Poliovirus 1 "Singles" with NH_2Cl at pH 10.0 and 5°C, in 0.05M Borate-NaOH Buffer.

REFERENCES

(1) Mosley, J.W. 1966. In Transmission of Viruses by the Water Route (G. Berg, Ed.), Interscience, New York, p. 5.

(2) Enders, J.F., Weller, T.H., and Robbins, F.C. 1949. Science, 109, 85.

(3) World Health Organization Scientific Group, 1979. Human Viruses in Water, Wastewater and Soil, World Health Organization, Geneva, Switzerland.

(4) Symons, J.M., Carswell, J.K., Clark, R.M., Love, O.T., Jr., Miltner, R.J., and Stevens, A.A. June 1976. "Interim Treatment Guide for the Control of Chloroform and Other Trihalomethanes," Water Supply Research Division, Municipal Environmental Research Laboratory, U.S. EPA, Cincinnati, Ohio, 96 pp.

(5) Anon. November, 1977. "Ozone, Chlorine Dioxide, and Chloramines as Alternatives to Chlorine for Disinfection of Drinking Water," Water Supply Research Division, Municipal Environmental Research Laboratory, U.S. EPA, Cincinnati, Ohio.

(6) Symons, J.M., and Hoff, J.C. Presented at Third Water Quality Technology Conference, American Water Works Association, Atlanta, Georgia, December 8-10, 1975.

(7) Stevens, A.A., Slocum, C.J., Seeger, D.R., Robeck, G.G. 1976. In Proceedings, Conference on the Environmental Impact of Water Chlorination, CONF-751096 (R.L. Jolley, Ed.), Oak Ridge National Laboratory, Oak Ridge, Tennessee.

(8) Anon. 1978. "Statement of the American Water Works Association on Proposed Amendments to the National Interim Primary Drinking Water Regulation for Control of Organic Chemical Contaminants in Drinking Water," 6 pages.

(9) Sharp, D.G., Young, D.C., Floyd, R., and Johnson, J.D. 1980. Appl. Environ. Microbial., 39, 530.

(10) Scarpino, P.V., Berg, G., Chang, S.L., Dahling, D., and Lucas, M. 1972. Water Research, 6, 959.

(11) Weidenkopf, S.J. 1958. Virology, 5, 56.

(12) Scarpino, P.V., Lucas, M., Dahling, D.R., Berg, G., and Chang, S.L. 1974. Chapter 15 in Chemistry of Water Supply, Treatment and Distribution. (A.J. Rubin, Ed.), Ann Arbor Science Publishers, Inc., p. 359.

(13) Floyd, R., and Sharp, D.G. 1977. Appl. Environ. Microbiol. 33, 159.

(14) American Public Health Assoc. 1974. "Standard Methods for the Examination of Water and Wastewater" 14th Edition, Am. Public Health Assoc., New York.

(15) Dulbecco, R., and Vogt, M. 1954. "Plaque Formation and Isolation of Pure Lines with Poliomyelitis Virus," J. Exp. Med., 99, 167.

(16) Hsiung, G.D., and Melnick, J.L. 1955. "Plaque Formation with Poliomyelitis, Coxsackie, and Orphan (Echo) Virus in Bottle Cultures of Monkey Epithelial Cells," Virology, 1, 533.

(17) Dahling, D.R., Berg, G., and Berman, D. 1974. Health Lab. Sci., 11, 275.

(18) Sharp, D.G., 1974. In Proc. 32nd Annual Meeting of the Electron Microscopy Society of America (C.J. Arceneaux, Ed.), Claitor's Publishing Division, Baton Rouge, La., p. 264.

(19) Valentine, R.C., and Allison, A.C. 1959. "Virus Particle Adsorption: Theory of Adsorption and Experiments on the Attachment of Particles to Non-Biological Surfaces," Biochem. Biophys. Acta., 34, 10.

Comments on
Effect of Turbidity and Other Factors on the Virus Disinfection Process Using Free and Combined Chlorine Forms

Richard F. Unz
Pennsylvania State University
University Park, Pennsylvania

Concern exists for the well being of consumers of chlorinated water, primarily with respect to the potential presence of suspected mutagenic and carcinogenic molecules arising through reaction between free chlorine and parent organic compounds. Solutions to the vexing problems have been sought along two lines, namely, (a) replacement of chlorine by a more suitable alternative disinfectant and (b) improved management and understanding of the use and action of chlorine such that the disinfectant may be employed more effectively in a decidedly judicious fashion.

The subject of this discussion is an ongoing research project which has its major thrust examining the effect of turbidity forms on the efficiency of chlorine species typically employed to inactivate candidate enteric viruses, e.g., poliovirus 1, coxsackie virus A9, and simian rotavirus SA-11. The materials contributing to the turbidities to be studied are (a) inorganic suspended solids, e.g., bentonite and kaolin clays and aluminum hydroxide floc, (b) simulated intestinal tissue moult, e.g., available laboratory cell lines, and (c) fecal matter. The experimental conditions involve a range of pH, temperature values, contact periods, chlorine dosages, and salt species.

The project has a designated two-year period of study. At this writing, 9 months of activity have elapsed during which experiments have been conducted to demonstrate the effect of certain soluble salts on the rate of inactivation by free chlorine of coxsackie A9 and poliovirus 1 suspended in various buffer solutions, pH values, and temperatures (5 and 15C). The work was prompted by the results of earlier research in the principal investigator's laboratory where it was found that poliovirus became inactivated more rapidly in the presence of hypochlorite (OCL^-) than hypochlorous acid (HOCl), a finding contradictory to general knowledge about the relative effectiveness of these free chlorine species as disinfectants (Scarpino et al., 1972).

The disinfection experiments were performed with a set of 600-ml beakers partly immersed in a temperature controlled water bath. Each beaker contained coxsackie A9 virus and either OCl^- or HOCl resulted in an enhancement of viral inactivation. For example, 0.1 mg/l of HOCl at pH 6 in the presence of the KCl resulted in 99% inactivation of coxsackie virus in approximately 50 seconds whereas in the absence of KCl an equivalent level of disinfection required 130 seconds. At pH 10, OCL^- is the predominant free chlorine species and the effect of KCL was to increase the rate of disinfection by the hypochlorite, also. No enhancement of OCL^- disinfection was observed when either NaCl or KNO_3 appeared as the sole salt additive to the buffer.

The time of addition of KCl to the buffer appeared to govern the effect of disinfection enhancement. In studies with poliovirus 1, presence of 0.1 M KCl in the reactor mixture before OCl^- and monochloramine were formed resulted in the improved inactivation of virus. However, if the monochloramine was developed in the reactor at a molar level equivalent to that of the KCl, no enhancement of virus inactivation occurred due to the presence of KCl. It has been proposed by the principal investigator that the observed enhancement of viral inactivation when KCl was available resulted from reaction with Cl^- and OCL^- to produce HOCl. It is not clear why NaCl did not produce a similar effect unless it is the cation rather than the anion which is active. It should be noted, however, that Sharp et al. (1980) have demonstrated that 0.1 M NaCl enhanced inactivation of poliovirus 1, although the effect could not be demonstrated with t_2 coliphage by Sproul et al. (1970). Jensen et al. (1980) indicated that other salts in addition to KCl contribute to enhanced inactivation of coxsackie B3 and B5 at pH 10 with OCl^-. Sharp and Leong (1980) noted a 31-fold increase in OCL^- inactivation rate of poliovirus 1 (Brunhilde) single particles at pH 10 in the presence of 0.1 M NaCl.

Explanations for the effect of chloride salts on virus disinfection rates are still unclear. Sharp and Leong (1980) suggested that the combination of a high pH (pH 10) and increased ionic strength of the medium may alter the protective capacity of the capsid. Jensen et al. (1980) indicated the possibility of a weakening of the capsid for better penetration of chemical agents.

In summary, interest in the effect of salinity on disinfection power has been shown independently by several investigators. The principal investigator could not have been aware of several of these developments judging from the newness of publications. The original intent of the work, that is, investigation of the relationships between viral inactivation efficiency with free and combined chlorine forms and qualitative and quantitative presence of turbidity should be focused upon for the project duration.

REFERENCES

Jensen, H., et al. 1980. Appl. Environ. Microbiol. 40: 633-640.

Scarpino, P.V., et al. 1972. Water Res. 6: 959-965.

Sharp, D.G. and J. Leong. 1980. Appl. Environ. Microbiol. 40: 381-385.

Sharp, D.G., et al. 1980. Appl. Environ. Microbiol. 39: 530-534.

Sproul, O.J., et al. 1970. Proc. Nat. Spec. Conf. Disinfect., Am. Soc. Civil Eng., pp. 385-396.

MEASUREMENT OF AQUEOUS PARTICLE SIZE DISTRIBUTIONS

James R. Hunt
Department of Civil Engineering
University of California
Berkeley, CA 94720

ABSTRACT

Rapid particle sizing procedures are needed to understand particle size distribution dynamics during water and wastewater treatment. Particle sizing instrumentation is briefly reviewed followed by a detailed discussion of necessary electronic signal processing, which includes logarithmic conversion and multichannel analysis. Calibration of particle sizing systems and calculation of particle size districutions are discussed. Procedures are illustrated using a Coulter Counter based sizing system to measure solid and aggregate particle size distributions.

INTRODUCTION

Research has shown that suspended particles transport the majority of the pollutants found in water. These pollutants include toxic metals, persistent organic compounds, bacteria, and viruses. Understanding the removal of these pollutants during water and wastewater treatment requires consideration of particle removal mechanisms based on theoretical and experimental study of particle size distribution dynamics.

The current techniques for particle removal, sedimentation, filtration, and flotation, have removal efficiencies which are strongly dependent on the size of the particles. In sedimentation, the settling velocity of a particle depends on the square of the diameter, while in filtration, the diameter dependence is more complex because of multiple collection mechanisms (Yao et al., 1; Spielman and FitzPatrick, 2). In flotation, the collision of bubbles and particles is also dependent on particle size. To understand particle removal by these processes, information is needed on the particle size distribution and on techniques for modifying the size distribution to improve removal efficiencies.

Measurement of particle size distributions is common in many fields, including blood analysis, food and drug processing, mineral processing, paint manufacturing, quality control for lubricating fluids, oceanography, and environmental engineering (air and water). In spite of this broad concern with particle sizing, a detailed discussion of procedures for rapidly measuring particle size distributions is needed using available instrumentation, noting the accuracy and limitations of such techniques. Furthermore, a standard notation for particle size data presentation is needed to avoid reporting data that are dependent upon the instrument used for measurement. Procedures for reporting volume distributions measured with Coulter Counters have suffered from this problem (Sheldon and Parsons, 3).

This paper discusses available techniques for measuring particles suspended in liquids and presents methods for calibrating the instruments and calculating particle size distributions. Procedures are illustrated with data obtained from a Coulter Counter based sizing system demonstrating calibration, size distribution calculation, and data presentation for solid and aggregate suspensions.

TECHNIQUES FOR PARTICLE SIZING

Treweek and Morgan (4) have presented a summary of experimental techniques for particle sizing. Only a few of the available techniques will be reviewed here along with recent references to their useage. The chief concerns are instrumental techniques which can rapidly count and size individual particles or aggregates.

The sizing techniques considered are microscopy, light scattering, light blockage, and electrical resistivity. The oldest sizing technique is optical or electron microscopy, but in application it is time consuming, even in automated systems, and requires considerable sample preparation (Kavanaugh et al., 5). Light scattering by individual particles is commonly used for aerosol measurements but has not been extensively applied to counting and sizing particles suspended in liquids (Kaye, 6; Diehl et al., 7). Light blockage has been used more recently to count and size particles in suspension, and has been applied in analyzing particle removal during water and wastewater treatment operations (Beard and Tanaka, 8; Tate and Trussell, 9). Particle sizing by electrical resistivity is probably the most common technique for suspended particle size analysis, with a number of instruments manufactured by Coulter Electronics and Particle Data, Inc. This technique has been used recently to measure particle size distributions during thickening (Lawler, 10), during clay particle coagulation in seawater (Hunt, 11), and to size anaerobically digested sewage sludge (Faisst, 12).

To investigate the kinetics of particle removal during water and wastewater treatment, instrumentation is needed for rapidly measuring particle size distributions. At this time the techniques available for rapid measurement are limited to electrical resistivity and light blockage. The two techniques differ only in that the electronic signal produced by the instrument is either proportional to particle volume in electrical resistivity sizing or maximum projected area for light blockage sizing. Both techniques required passage of particle suspensions through a small sensing zone called an orifice or aperture. Sensing zones come in various sizes for detecting particles over different size intervals. The particle suspension must be sufficiently dilute so that there is only a small probability of more than one particle in the sensing zone at a given time. Particle counts are related to number concentration by collecting electronic signals over a known fluid volume, using either a timer and a known flow rate, or a volume sensing device such as start and stop sensors in a volumetric section. The electronic signal processing and calibration procedures required for arriving at particle size distributions are the subject of the following sections.

CONTINUOUS SIZE DISTRIBUTION MEASUREMENT

The adopted notation for hydrosol particle size distributions (Lawler et al., 13) follows closely the notation used in characterizing aerosols (Friedlander, 14). The particle size distribution function $n(d_p)$ is defined as the number concentration of particles, ΔN, with diameters in the interval d_p to $d_p + \Delta d_p$, divided by the width of the interval, Δd_p, or

$$n(d_p) = \frac{\Delta N}{\Delta d_p} \tag{1}$$

where the units for $n(d_p)$ are #/mL-μm. With a particle size distribution, various other properties of the distribution can be calculated including surface area and volume distributions along with cumulative distributions of number, area, and volume.

While the particle size distribution is convenient for calculations, it is not usually appropriate for data presentation. Many size distributions are observed to be power law distributions of the form

$$n(d_p) = \alpha d_p^{-\beta} \tag{2}$$

where β ranges from 2 to 5 (Bader, 15). This rapid decrease in $n(d_p)$ with increasing diameter makes $\log n(d_p)$ vs. $\log d_p$ plots inconvenient and difficult to interpret. The particle volume distribution $dV/d(\log d_p)$ is a better distribution for plotting size distributions and represents the total suspended particle volume concentration within an interval divided by the change in the logarithm of the diameter over the interval. The transformation from particle size distribution to particle volume distribution is

$$\frac{dV}{d(\log d_p)} = \frac{2.3\pi}{6} d_p^4 \; n(d_p) \tag{3}$$

as derived by Friedlander (14) and Lawler et al.(13). The typical units for the volume distribution are either μm³/mL or parts per million by volume (1 ppm by volume = 10^6 μm³/mL).

The particle diameter appearing in Equations 1, 2, and 3 is the diameter of the particle assuming it is spherical, or equivalent spherical diameter. For a particle determined by electrical resistivity sizing to have a volume v, the equivalent spherical diameter is $d_p = (6v/\pi)^{1/3}$. Similarly, if the maximum projected area of a particle is a, the equivalent spherical diameter is $d_p = (4a/\pi)^{1/2}$. While most particles are not spherical, use of equivalent spherical diameter is a consistent method for reporting data.

Electronic signal processing is required to count only particles within a narrow size interval, corresponding to diameters in the range d_p to $d_p + \Delta d_p$. Earlier in oceanic particle sizing (Sheldon and Parsons, 3) and particle coagulation kinetics studies (Birkner and Morgan, 16) signal processing was limited to a single channel with the size and width of the channel determined by upper level and lower level thresholds. Particle size distributions could be obtained in two ways. First, the upper level threshold was set at the maximum and the lower level threshold was increased by small steps, at each step determining the number concentration of particles greater than or equal to the threshold (cumulative distribution). The second method of sizing with a single channel analyzer was to fix the upper and lower thresholds so that particle volume varied by a factor of $\sqrt{2}$ or 2 between thresholds. This "window" was then incrementally moved through the available sizes by adjusting instrument settings giving a differential measure of the distribution. Both procedures required repetitive counting of the same sample to give size distribution information and these procedures are not suitable for rapid collection of sizing data.

The alternative to size distribution measurement using single channel analyzers is the use of multiple channel analyzers. In this case the electronic signal pulse from the particle sensor is compared with thresholds for each of many channels. When the magnitude of the signal pulse is greater than the lower level threshold but less than the upper threshold, then the total count in that channel is incremented by one. Use of multichannel analyzers, either. hardwired or software programmed into a microprocessor, allows rapid collection of data from which particle size distributions can be calculated. The number of channels in a multichannel analyzer ranges from six to over a thousand with one hundred being a reasonable number for particle size analysis.

Prior to multichannel analysis, logarithmic conversion of electronic signals from the particle sensor is needed for two reasons. The first reason is related to the range in signal pulses from different sized particles, and second, because size distribution data are usually presented on a log d_p axis and logarithmic conversion distributes the data points evenly on a logarithmic axis. To size particles in the range of 1 to 10 μm in diameter, an electrical resistivity particle sensor produces signal pulses over a range of three orders of magnitude, say 1 to 1000 volts, because the signal is proportional to particle volume. For a light blockage particle sensor, the signal magnitudes would vary over two orders of magnitude because the signal is proportional to projected area.

Consider signal pulses from an electrical resistivity sensor in the range of 1 to 1000 volts corresponding to 1 to 10 μm particles. If these pulses were analyzed linearly by a 100 channel analyzer where the upper threshold of the last channel was 1000 volts, then the relationship between signal S and channel number i would be

$$\frac{i}{100} = \frac{S}{1000} \tag{4}$$

or

$$i = \frac{1}{10} S \quad . \tag{5}$$

With signal equal to particle diameter (in micrometers) cubed, the sizing system response is

$$i = \frac{1}{10} d_p^3 \quad . \tag{6}$$

In the first channel corresponding to signals in the range 0 to 10 volts by Equation 5, the corresponding diameter range is 0 to 2.15 μm. The last channel, 990 to 1000 volts, would have a diameter range of 9.97 to 10.μm. For linear multichannel analysis, far too wide a range would be covered in the lower channels and too narrow a range in the higher channels.

With a logarithmic converter between the particle sensor and the multichannel analyzer, data collection is improved. For a log base ten amplifier, the relationship between sensor signal, S, and channel is

$$\frac{i}{100} = \frac{1}{3} \log_{10} S \tag{7}$$

or

$$i = \frac{100}{3} \log_{10} S \tag{8}$$

so that the upper limit of channel 100 corresponds to 1000 volts. With the signal equal to particle diameter cubed, the sizing system response is

$$i = 100 \log_{10} d_p \quad . \tag{9}$$

In the first channel the diameter range would be 1. to 1.023 μm, and the last channel would count particles with diameter from 9.77 to 10. μm. With logarithmic conversion of sensor signal, the change in logarithm of the diameter over all channels is fixed, that is, $\Delta \log d_p = 0.010$.

The examples to follow will be for a Model ZBI Coulter Counter based sizing system. Output from the main amplifier of the Coulter Counter was input to a particle sizing amplifier (Nuclear Data PSA) for logarithmic conversion. Output from the PSA was processed by a multichannel analyzer with 128 channels for data storage (Nuclear Data MCA 555). Multichannel analyzer data were displayed on an oscilloscope (Hewlett Packard 1208 B) and the data were saved for later analysis by punching paper tape on a Teletype (ASR 33) with a teletype interface module (Nuclear Data TTY IN/OUT). The PSA, MCA, and TTY IN/OUT modules plugged into a System Power Supply (Nuclear Data Series 1100). The MCA had been modified by Nuclear Data for volumetric control (81-0335) to allow the mercury manometer of the Coulter Counter to control data acquisition. All calibration and sizing was done in artificial seawater.

CALIBRATION OF PARTICLE SIZING SYSTEMS

The sizing system composed of the particle sensor and electronic signal processing must be calibrated to determine the particle diameter for each channel of the multichannel analyzer. More than one calibration is usually required because of changing instrument settings, sensor sizes, and sometimes, suspending solution ionic composition. Calibration consists of determining the log base of the logarithmic amplifier and the diameter at one channel of the multichannel analyzer. With this information, particle diameters at other channels can be calculated along with particle size distributions.

For sizing systems using light blockage or electrical resistivity combined with logarithmic amplification and multichannel analysis, a particle of diameter d_i will be recorded in channel i according to the following relationship

$$i = \log_b d_i^t + \text{constant}. \qquad (10)$$

In Equation 10 b is the log base, and t is 2 for light blockage sizing, or 3 for electrical resistivity sizing since the signal from the particle sensor is proportional to the particle's projected area or volume, respectively. There are two unknowns in Equation 10, the log base and the constant. With two calibration particle diameters d_i and d_j appearing in channels i and j, there are two equations and two unknowns. Eliminating the constant and solving for the log base gives

$$b = \left(\frac{d_i}{d_j}\right)^{t/(i-j)} . \qquad (11)$$

Once the log base has been determined for the sizing system, then at specific instrument settings and sensor sizes, determining that a calibration particle of diameter d_c appears in channel c allows calculation of the diameter, d_i, at any channel i, according to

$$d_i = d_c b^{(i - c)/t} . \qquad (12)$$

The Coulter Counter Counter based sizing system with 30, 70, 140, and 280 μm diameter apertures was calibrated with seven different sized particles. The characteristics of these latex microspheres are summarized in Table I. The 40 μm particles were supplied dry and were dispersed in artificial seawater by sonication; the other microspheres were supplied as concentrated suspensions which were diluted with artificial seawater before counting.

Table I LATEX MICROSPHERE CALIBRATION PARTICLES

Diameter (μm)	Composition	Reported Standard Deviation Per Cent of Mean	Lot Number	Supplier
1.011	Polystyrene	0.5	2G4H	Dow Diagnostics
2.02	Polyvinyltoluene	0.7	1177	Duke Scientific
5.1	Polystyrene DVB	1.	3750	Duke Scientific
5.17	Polystyrene	2.	1177	Duke Scientific
10.12	Polystyrene	2.	1177	Duke Scientific
19.87	Polystyrene	1.4	1077	Duke Scientific
40.	Polystyrene DVB	10.	3769	Duke Scientific

Assigning a channel number to a given calibration particle requires judgment. For latex microspheres of diameters 1.011 and 2.02 μm, the size distributions were not monodisperse, but unimodal and had well defined maxima. For these particles the peak channel number was used for calibration. The larger calibration particles were either bimodal or had a broad distribution so that the mean channel number of the distribution was used to calculate the log base. Plots of the MCA counts for the 5.1 and 10.12 μm particles are shown in Figure 1 for different apertures. All distributions have been normalized to contain 1000 counts. The narrow microsphere distributions are seen to change when measured with different aperture sizes. The 5.1 μm particles measured with a 30 μm aperture have a bimodal distribution with the second peak eleven channels above the first, too close for a doublet which should appear 19 channels above the singlet. With the 70 μm μm aperture, the 5.1 μm distribution becomes narrower, skewed, and unimodal,

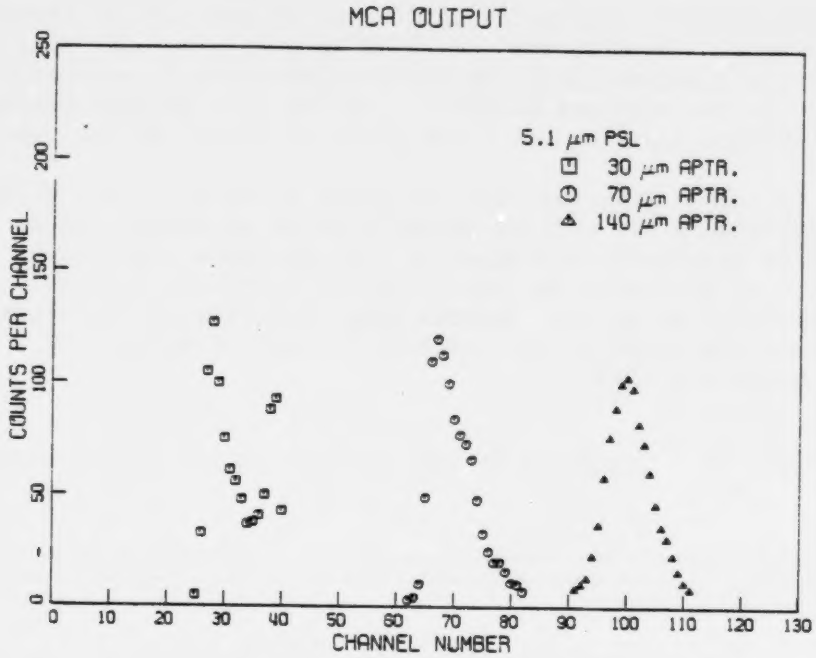

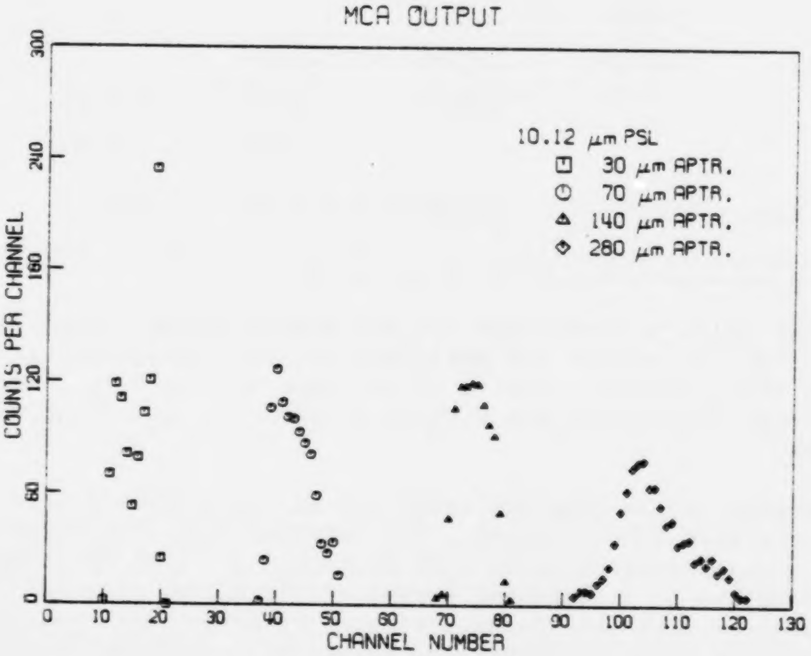

Figure 1. Latex microsphere distributions measured with Coulter Counter based sizing system.

while the distribution obtained with the 140 μm aperture is broader, symmetrical, and unimodal. Results for the 10.12 μm particles show similar patterns of detailed distributions when the particle diameter is greater than five to ten per cent of the aperture diameter, and the distribution broadens as the particle diameters approach the lower limit of detection for the aperture.

Using the above procedure for assigning a diameter to a channel, log bases are calculated for various particle pairs as summarized in Table II. While there is considerable scatter in the log bases, the values obtained for each pair of particles for the different apertures are close, indicating possible inaccuracies in the reported mean diameters of the microspheres which has been discussed in the literature (Cassatt et al., 17). The mean of the log bases was 1.038.

Table II. LOG BASES OF THE COULTER COUNTER SIZING SYSTEM

Particle Pair	Aperture Diameter (μm)			
	30	70	140	280
1.011-2.02	1.0392			
2.02-5.17	1.0367	1.0377		
5.17-10.12	1.0384	1.0388	1.0374	
10.12-19.87		1.0375	1.0375	1.0397
19.87-40.			1.0366	1.0365
mean log base = 1.0378		standard deviation = 0.0011		

With the log base determined for the sizing system, specific Coulter Counter settings of current and amplification were determined and calibrated during each sizing period. Choice of settings was based on a need for small diameter sizing information but without substantial interference from electronic noise.

Calibration is not complete until the sizing system is used to measure broad particle size distributions. The measured size distributions can be for either a suspension of known size distribution, such as glass beads available from the U. S. National Bureau of Standards, or a solid suspension which is analyzed with the sizing system at different settings and aperture sizes. Sizing of broad distributions serves as a check on the calibration and sensing system as discussed by Birkner and Morgan (16) and Venolia (18).

CALCULATION OF PARTICLE SIZE DISTRIBUTION

The purpose to this section is to present the mechanics of converting particle counts in the channels of the MCA into size distributions. The discussion includes calculation of size distributions, noise, and multiple aperture sizing techniques. The particle size distribution, $n(d_p)$, is calculated by

$$n(d_i) = \frac{N_i}{\Delta d_i} \tag{13}$$

where N_i is the number of particles recorded per milliliter of fluid in channel i over the narrow range of particle diameters d_i to $d_i + \Delta d_i$.

For each aperture and each set of Coulter Counter settings, part of the particle size distribution was obtained from the 128 channels of data in the MCA output. The first eight channels were eliminated by the lower level discriminator of the MCA. With the average log base, b, of 1.038 from Table II, the range in diameters from channel 9 to 128 was

$$\frac{d_{128}}{d_9} = b^{(128-9)/3} = 4.39 \tag{14}$$

The diameter ratio between channels is only $(1.038)^{1/3} = 1.013$ which is greater resolution than justified by the sizing technique or desired in data presentation. By grouping eight channels of MCA data to compute one point of a size distribution, a diameter ratio of $(1.038)^{8/3} = 1.105$ between points is obtained, which is reasonable considering the spread observed in the microsphere distribution. The calculation of the particle size distribution then becomes

$$n(d_p) = \frac{N}{\Delta d_p} \tag{15}$$

where N is the sum of the counts in eight channels of the MCA

$$N = \sum_{j=i}^{i+7} N_j \tag{16}$$

and Δd_p is the difference between the diameter of the first channel of the next grouping of eight channels and the diameter of the first channel in the group of eight, or

$$\Delta d_p = d_{i+8} - d_i . \tag{17}$$

The particle diameter, d_p, is taken as the geometric mean of the diameters of the eight channels, or

$$d_p = \left[\prod_{j=i}^{i+7} d_j \right]^{1/8} \tag{18}$$

The accuracy of grouping eight channels together in calculating particle size distributions was checked by integrating the distribution over the range of diameters to obtain the total number of counts. Total counts obtained by integration never differed more than 0.1 per cent from the total counts recorded by the MCA indicating the choice of channel groupings did not distort the size distribution function.

Size distributions were not always obtained down to channel nine because some electronic noise was usually present at the lowest channels. Coulter Counter settings of amplification and current were chosen to measure the smallest particles possible, which meant including some electronic noise in the first few channels of the MCA. Blanks of 0.22 μm Millipore filtered artificial seawater were counted to determine the magnitude of electronic noise signals and background particles. For size distribution calculations the beginning channel was chosen such that the particle counts were at least ten times greater than the counts in that channel of the blank solution. Because the electronic noise fell off very rapidly at higher channels, the eight channels that compose the first point of the size distribution had a noise component less than ten per cent.

With an effective diameter range of only 4.39, the measurement of broader distributions requires either multiple settings at one aperture or use of multiple apertures. Multiple apertures are usually preferred because 1) flow rates through the smallest apertures are very slow and only suitable for counting the smallest particles, 2) the number of larger particles is usually low and larger volumes must be sampled which is not practical for the smaller apertures, 3) small apertures break up some aggregates at smaller diameters than larger apertures (16), and 4) because number concentration falls off rapidly with increasing diameter and flow rates through the orifices increase with increasing aperture size, coincidence corrections can be avoided when multiple apertures are used with only a single dilution of the sample. Thus, there are a number of advantages in using multiple apertures in obtaining broad size distributions. In the next section examples of solid and aggregate sizing demonstrate the procedures discussed above and point out some difficulties.

SOLID AND AGGREGATE SIZING EXAMPLES

This section presents examples of size distributions obtained with a Coulter Counter based sizing system. The solid suspension is composed of iron oxide crystals (γFeOOH) prepared by Sung (19). The aggregate suspensions are from particle coagulation experiments conducted in artificial seawater under uniform fluid shear in a rotating cylinder apparatus (11).

Volume distributions for the iron oxide suspension are shown in Figure 2 with ordinate units of particle volume per gram of solid. The distribution has a very sharp peak near 2 μm and only the 30 and 70 μm apertures were used for sizing. Two different settings for the 30 μm aperture gave very good agreement in the region of overlap. Data for the 70 μm aperture did not agree as well, being 30 per cent above the volume distribution measured by the 30 μm aperture for diameters less than the peak. The size distributions obtained indicate internal consistency in the sizing procedure.

The second test for a sizing test is to determine aggregate size distributions using careful sampling procedures to avoid aggregate disruption. Figure 3 contains a plot of volume distributions for one sample from a kaolinite clay in seawater coagulation experiment at a uniform fluid shear rate of $G = 4\ \text{sec}^{-1}$ using 30, 70 and 140 μm apertures. The important feature in these distributions is the lack of agreement in volume distribution between apertures in regions of diameter overlap. The reason for the misalignment was the breakup of larger aggregates in the high fluid shear near the orifice. The oscilloscope on the Model ZBI Coulter Counter displayed signal pulses of particles passing through the orifice. When a large aggregate passed through the orifice, a burst of small signals was displayed on the oscilloscope indicating the aggregate broke up before entering the sensing zone of the orifice. The burst of smaller signals was not all recorded by the MCA because the signals in the burst exceed the data collection rate or the MCA. So, for larger aggregates the counting system recorded only some of the aggregate volume as smaller particles.

In coagulation experiments with montmorillonite clay in artificial seawater, the volume distributions in Figure 4 shows a noticeable difference between aperture alignment at $G = 1/2\ \text{sec}^{-1}$ and at $G = 16\ \text{sec}^{-1}$. At $G = 1/2\ \text{sec}^{-1}$ only the 30 μm aperture data below about 1.3 μm measured the aggregate distributions while larger diameters measured with the 30 μm aperture and all aggregate sizes measured by the other two apertures were dominated by aggregate breakup during counting. The measured distributions at $G = 16\ \text{sec}^{-1}$ had regions of agreement between pairs of apertures and demonstrated the size dependence of breakup during counting with different apertures; small apertures breakup particles during counting at smaller aggregate diameters than larger apertures (16). The difference in alignment among apertures at low and high shear rates indicated there is an increase in aggregate strength at the larger shear rate.

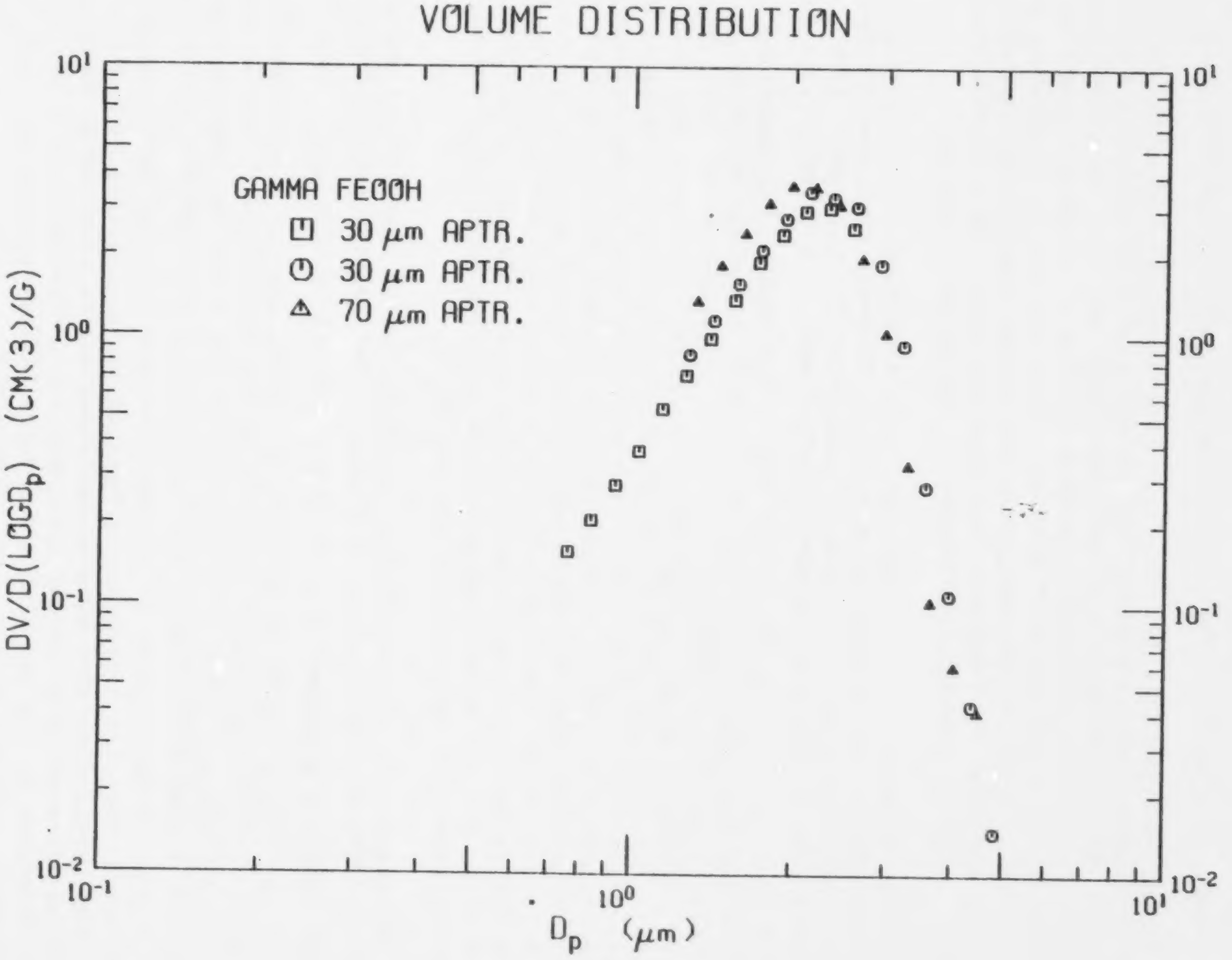

Figure 2. Volume distribution of γ- FeOOH measured with 30 and 70 μm apertures.

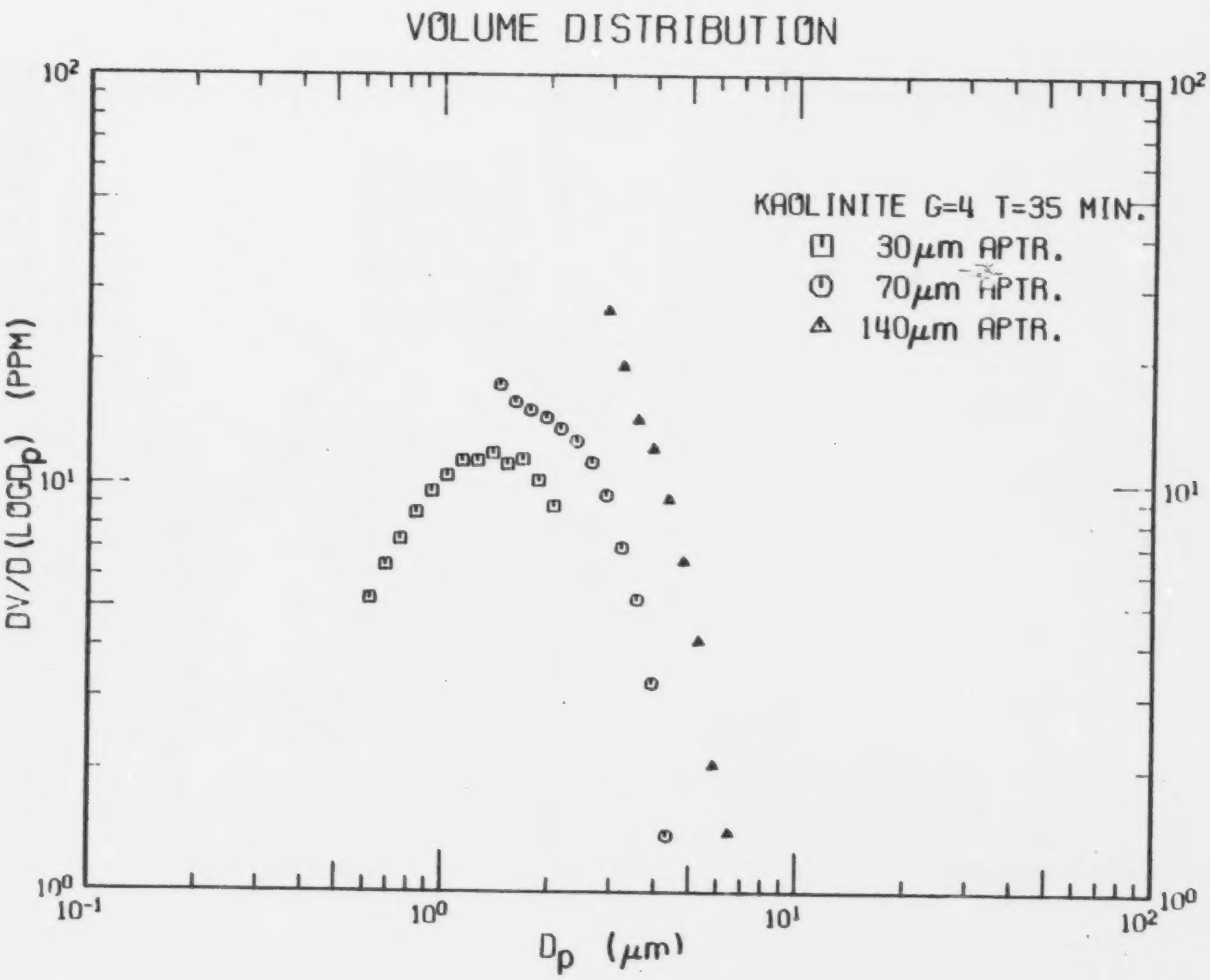

Figure 3. Volume distribution of kaolinite in seawater 35 minutes after initial mixing, observed by 30, 70, and 140 μm apertures.

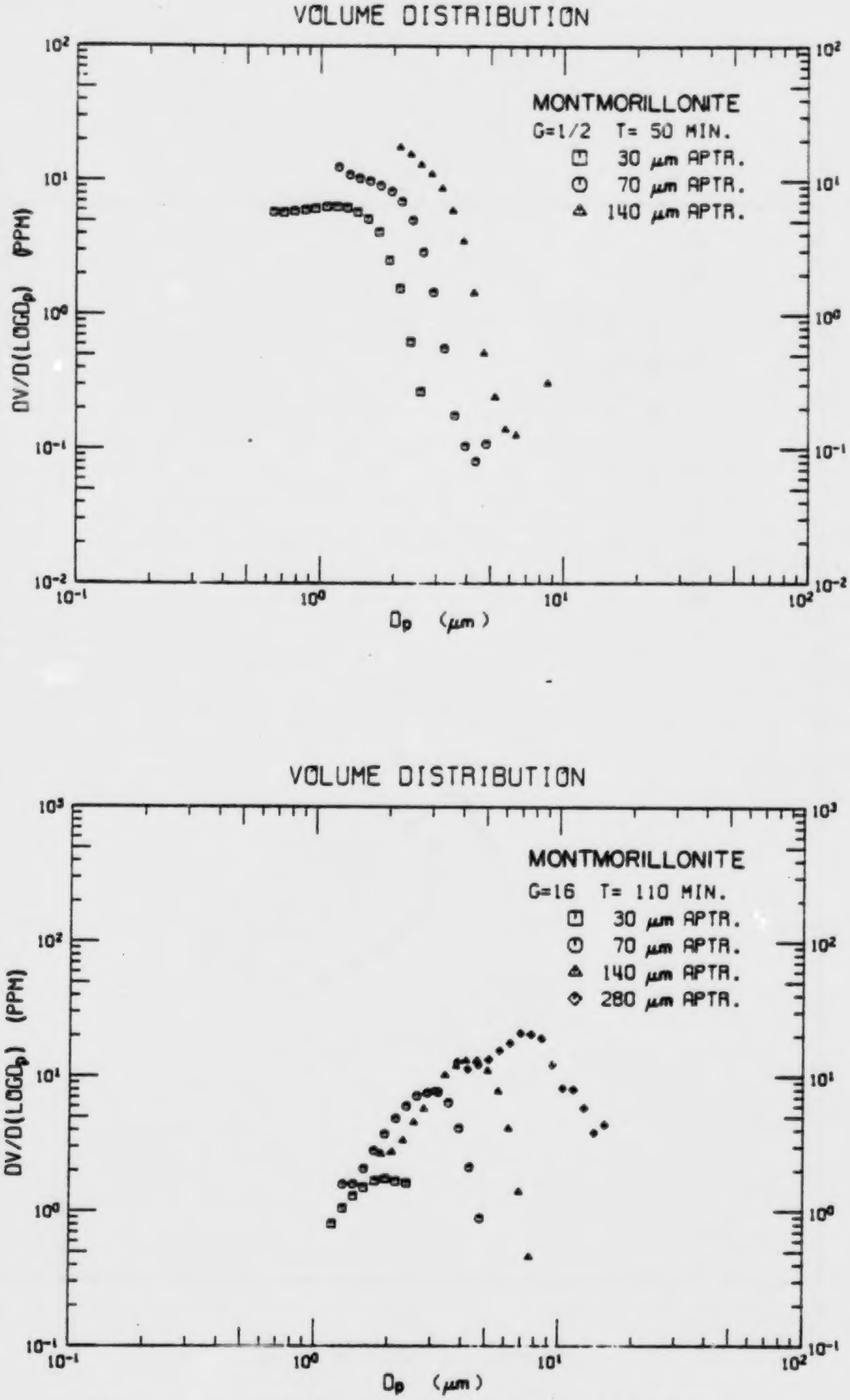

Figure 4. Multiple aperture volume distributions for montmorillonite in seawater at fluid shear rates of ½ sec^{-1} and 16 sec^{-1}.

The above aggregate size distributions were determined by an electrical resistivity sizing instrument which responds only to solid particles within the sensing zone. The data reported are not for the aggregate diameter but for the equivalent spherical diameter of coalesced aggregates having no void spaces. If the same aggregate suspension was sized by a light blockage instrument, the reported diameters would be for the porous aggregates and the calculated size distribution would be different. Treweek and Morgan (4) discuss adjustment of multichannel analyzer output from aggregate suspensions to account for aggregate porosity. Such adjustments can not be applied in general because they are limited to analyzing aggregates composed of monodisperse primary particles. The adjustments also incorporate an empirically determined asymptotic porosity value using a conservation of measured particle volume approach which assumes aggregates do not breakup during counting.

Size distributions of solids suspended in liquids are readily determined with available instruments down to diameters of approximately 0.6 μm. Sizing is more difficult for aggregate suspensions because of the weak, porous sturcture of the aggregates. Future effort will be directed toward improving aggregate sizing procedures by decreasing the flow rate through the sensor which will decrease the shear stresses experienced by the suspended particles.

SUMMARY

This paper has reviewed general procedures for measuring suspended particle size distributions using a number of the available sizing techniques. The principles of particle sensing and continuous particle size distribution measurement were discussed. For rapid and detailed size distribution measurement, electronic signal processing is needed for logarithmic conversion, multichannel analysis, and data storage.

Particle sizing systems must be calibrated with narrowly distributed latex microspheres and the calibration should be checked using a solid suspension with a broad distribution. Once a sizing system is calibrated there is no guarantee that aggregate size distribution can be obtained because of aggregate breakup by the high fluid shear near the sensing zone of particle counters. A Coulter Counter based sizing system was used to demonstrate the methods for calibration and size distribution calculations and the results were shown for sizing one solid suspension and two aggregate suspensions. Particle size distribution measurement is not automatic or easy, rather it requires considerable expense and effort. Such constraints, once known and accepted, will allow a better experimental and theoretical understanding of particle removal during water and wastewater treatment.

REFERENCES

1. Yao, K., M. T. Habibian, and C. R. O'Melia (1971) Water and wastewater filtration: concepts and applications. Environ. Sci. Technol. 5, 1105 - 1112.

2. Spielman, L., and J. A. FitzPatrick (1973) Theory for particle collection under London and gravity forces. J. Colloid Intf. Sci. 42(3), 607 - 623.

3. Sheldon, R. W., and T. R. Parsons (1967) A practical manual on the use of the Coulter Counter in marine research. Coulter Electronics, Toronto.

4. Treweek, G. P., and J. J. Morgan (1977) Size distributions of flocculated particles: application of electronic particle counters. Environ. Sci. Technol. 11(7), 707 - 714.

5. Kavanaugh, M. C., U. Zimmermann, and A. Vagenknecht (1977) Determination of particle size distributions in natural waters, use of Zeiss Micro-Videomat image analyzer. Swiss J. Hydrology 39(1), 86 - 98.

6. Kay, W. (1973) Low angle laser light scattering-particle measurement. J. Colloid Intf. Sci. 44, 384 - 386.

7. Diehl, S. R., D. T. Smith, and M. Sydor (1979) Analysis of suspended solids by single-particle scattering. Applied Optics 18(10), 1653 - 1658.

8. Beard, J. D., II, and T. S. Tanaka (1977) A comparison of particle counting and nephelometry. J. Amer. Water Works Assoc. 69(10), 533 - 538.

9. Tate, C. H., and R. R. Trussell (1978) The use of particle counting in developing plant design criteria. J. Amer. Water Works Assoc. 70(12), 691 - 698.

10. Lawler, D. F. (1979) A particle approach to the thickening process. Ph.D. thesis, The University of North Carolina at Chapel Hill.

11. Hunt, J. R. (1980) Coagulation in continuous particle size distributions; theory and experimental verification. Ph.D. thesis, California Institute of Technology, Pasadena, California.

12. Faisst, W. K. (1980) Characterization of particulates in digested sludge. Advances in Chemistry 189, 259 - 282.

13. Lawler, D. R., C. R. O'Melia, and J. E. Tobiason (1980) Integral water treatment plant design: from particle size to plant performance. Advances in Chemistry 189, 353 - 388.

14. Friedlander, S. K. (1977) Smoke, Dust, and Haze. Fundamentals of Aerosol Behavior. Wiley-Interscience, New York.

15. Bader, H. (1970) The hyperbolic distribution of particle sizes. J. Geophysical Res. 75, 2822 - 2830.

16. Birkner, F. B., and J. J. Morgan (1968) Polymer flocculation kinetics of dilute colloidal suspensions. J. Amer. Water Works Assoc. 60(2), 175 - 191.

17. Cassatt, W. A., Y. T. Yap, W. P. Reed, and S. A. Mills (1976) Results of measurements on fine particle standard reference materials at NBS. Powder Technol. 13, 27 - 31.

18. Venolia, A. W. (1978) Resistive-pulse particle sizing instrument. Analytical Chem. 50(9), 1275 - 1279.

19. Sung, W. (1981) The effect of the γFeOOH (lepidocrocite) surface on the oxygenation kinetics of aqueous manganous manganese and ferrous iron. Ph.D. thesis, California Institute of Technology, Pasadena, California.

Comments on
Particle Size Distribution Dynamics During Coagulation

Charles R. O'Melia
The Johns Hopkins University
Baltimore, Maryland

The objectives of this research project are (1) to establish experimental methodology capable of determining the size distribution of particles in water supplies, wastewaters, and their associated treatment systems, (2) to use these methods in laboratory experiments designed to test current theories of coagulation, and (3) to improve present theories for coagulation by examining aggregate breakup in flocculation. These objectives focus on important areas in coagulation theory and its application to practice.

The paper by Hunt entitled "Measurement of Aqueous Particle Size Distribution" is a valuable contribution and consistent with the objectives and research plan of the project. For many aqueous solutions, it is possible that analytical capabilities are stretching or even surpassing our ability to use the results. This is not so for suspensions. Data are needed about such parameters as particle density, "floc strength", and particle size distributions to interpret field and laboratory observations about the performance of solid-liquid separation processes and to facilitate the application of available theory to practice.

The results presented in this paper provide a good beginning toward improving our use and understanding of particle counters that are based on changes in solution resistivity. It is possible that the suspensions tested to date, viz., silica and clays in seawater, provide a test for particle counting that is more rigorous and significantly different from conditions pertinent to chemical and biological aggregates in water and wastewater treatment. The research program should focus as soon as possible on the measurement of particle size distributions for these chemical and biological flocs.

The second objective of the research, viz., the testing of coagulation theories, cannot be accomplished until the first phase dealing with size measurement is substantially completed. There are models for coagulation, sedimentation, and filtration (e.g., Hunt, 1980; Lawler et al., 1980; Ramaley et al., 1981) that promise significant new insights for these processes and will, in the opinion of this reviewer, permit improvements in efficiency and economies in construction and operation for plants in practice. At present the models have not been adequately tested. When disagreement arises between models or between model predictions and observations, it is not clear which is wrong, theory or measurement. From the accomplishments of this research to date and from evaluation of proposed future studies, help is on the way.

In the opinion of this reviewer, the breakup of aggregates in water and wastewater treatment systems occurs to a significantly greater extent than presently realized. There are no theories to predict aggregate breakup and there are no dependable data to document it unambiguously. The proposed research program to investigate breakup under controlled conditions is an important and timely combination of a problem (breakup) and developing analytical equipment (particle size distribution measurement).

Overall, the research problem is important, the research plan is well conceived, and the research progress is slow, developing adequately, and consistent with the research proposal.

REFERENCES

Hunt, James R., "Predictions of Oceanic Particle Size Distributions from Coagulation and Sedimentation Mechanisms", in Particulates in Water, edited by M.C. Kavanaugh and J.O. Leckie, Advances in Chemistry Series 189, American Chemical Society, Washington, D.C., pp. 243-257 (1980).

Lawler, Desmond R., Charles R. O'Melia, and John E. Tobiason, "Integral Water Treatment Plant Design: From Particle Size to Plant Performance", in Particulates in Water, edited by M.C. Kavanaugh and J.O. Leckie, Advance in Chemistry Series 189, American Chemical Society, Washington, D.C., pp. 353-388 (1980).

Ramaley, Brian L., Desmond F. Lawler, William C. Wright, and Charles R. O'Melia, "Integral Analysis of Water Plant Performance", Proceedings of the American Society of Civil Engineers, Journal of the Environmental Engineering Division, Vol. 107, No. EE3, pp. 547-562 (June, 1981).

ANALYTICAL FOURIER TRANSFORM MASS SPECTROMETRY

Michael L. Gross
Department of Chemistry
University of Nebraska
Lincoln, NE. 68588

Charles L. Wilkins
Department of Chemistry
University of California- Riverside
Riverside, CA. 92521

ABSTRACT

This paper is a progress report on the development of Fourier Transform mass spectrometry (FT-MS) for purposes of chemical analysis. Four general analytical applications will be considered: (1) High resolution measurements, (2) Precise and accurate mass measurement, (3) Chemical ionization spectra, and (4) Gas chromatography/ mass spectrometry. The research goals are to determine the capabilities of FT-MS, to improve on them where possible, to test the instrumentation for analysis of model systems, and finally to apply FT-MS to real analytical problems. The research completed to date has been devoted to the first three goals.

INTRODUCTION

Fourier Transform mass spectrometry was first demonstrated by Comisarow and Marshall (1) at the University of British Columbia. The underlying principle upon which the technique is based is the motion of charged particles in a magnetic field. An ion stored in a uniform magnetic field will undergo circular motion with a frequency which is dependent on the charge-to-mass ratio (z/m) of the particle (equation 1),

$$\omega = zB/m \qquad (1)$$

where ω is the angular frequency and B is the strength of the magnetic field. For a singly charged ion of mass 100 daltons in a magnetic field of 1.0 tesla, the frequency will be about 153,000 cycles per second or 153 kHz.

The circular motion can be excited, and the ion trajectory increased to larger radii by applying an alternating electromagnetic field of the same frequency. The ion absorbs power from the external alternating field.

The resonance was detected in earlier ion cyclotron resonance (icr) spectrometers by measuring the power absorption using a marginal oscillator for excitation of a single mass ion. Mass spectra were obtained by a slow scan of the magnetic field using a constant excitation frequency. A scan from m/z 30 to m/z 300 required 10-20 minutes.

In Fourier Transform mass spectrometry, all ions are put into resonance by a rapid scan of the excitation (about 1 millisecond is required) at a constant magnetic field strength. The excitation is nearly simultaneous for all mass ions compared to the slow scans in ICR spectrometry. The excitation is admitted to the cell on either the front or back plate (called the transmitter plate) of a cubic cell (see Figure 1).

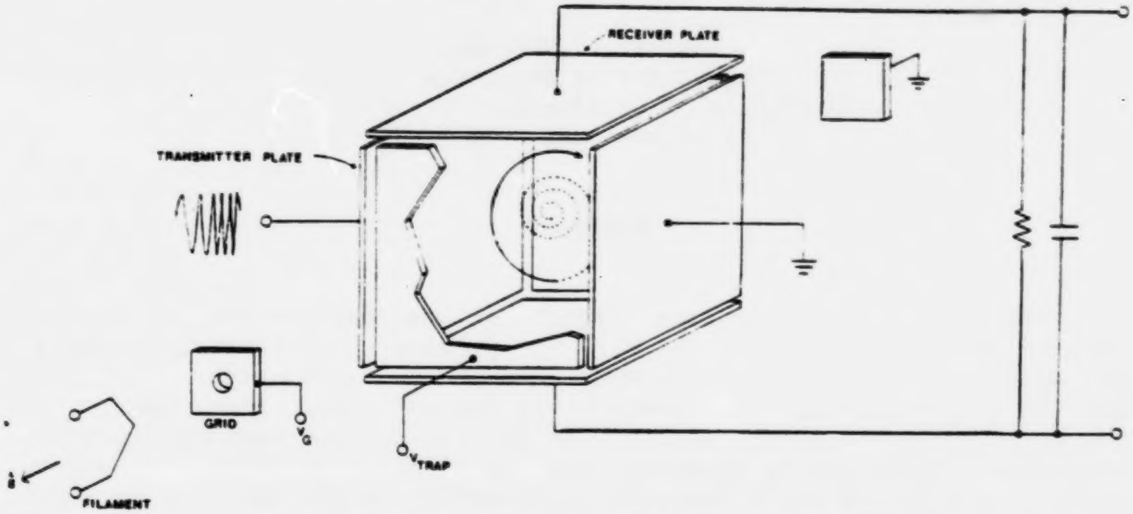

Figure 1. Cubic Analyzer Cell used for FT-MS.

The cell itself is a 2.54 x 2.54 x 2.54cm stainless steel box located in a high vacuum chamber situated between the poles of a 1.2 tesla electromagnet. The magnetic field lines are perpendicular to the plane of the figure. As the ions absorb power during the excitation, their radius of trajectory is increased (depicted by the broken line in Figure 1) until the excitation is completed. At that time, they will remain in the larger radius orbital (depicted by the solid line) until their motion is interrupted by collisions with background gas. Ion loss from the cell is prevented by applying a small (∿1V) voltage on the side plates which is of the same polarity as the ions under study.

Detection of the ions is truly simultaneous and is based on the phenomenon of image currents. The cycloiding ions induce small alternating currents to flow in the circuit consisting of the receiver plates and the shunt resistor and capacitor (see Figure 1). These image currents give rise across the resistor to alternating voltages of the same frequencies as the excited ions. These signals are a composite of all ion frequencies and appear as a transient decay in the time domain as shown in Figure 2. The signal decays because the coherent motion of the ions is disrupted by collisions with background gas as was discussed earlier. A Fourier transformation of the time domain signal gives a frequency domain output which is a mass spectrum (a display of all the frequencies and their amplitudes which compose the time domain ion decay). The spectrum is displayed on the bottom on Figure 2.

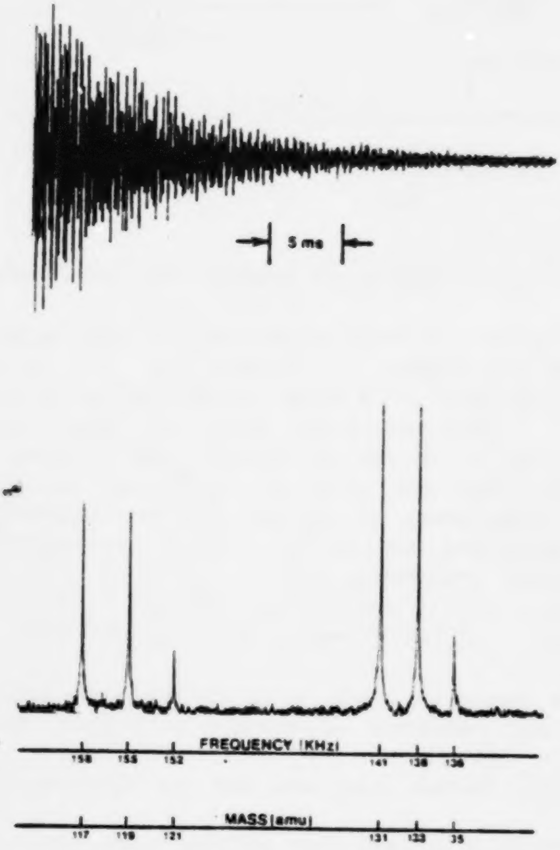

Figure 2. Time domain transient and FT-MS spectrum of 1,1,1,2-tetrachloroethane.

Thus far we have said nothing about ion formation. In the electron impact mode, an electron beam is pulsed on for about 5-10 milliseconds. The electrons enter the cell and ionize a small fraction (say 0-1%) of the background gas (N) according to equation (2).

$$N + e \longrightarrow N^{+} + 2e \qquad (2)$$

Other methods of sample ionization will be discussed later under the topic of Chemical Ionization.

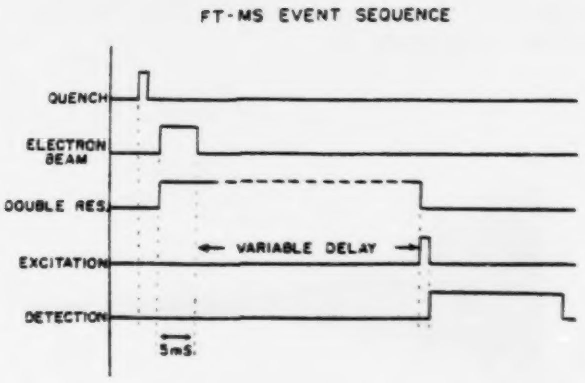

Figure 3. Typical sequence of events for the FT-MS experiment.

The entire sequence of events leading to the acquisition of one mass spectrum is depicted in Figure 3. First, the cell is quenched by biasing one of the trapping plates at a high potential to drive out ions from an earlier experiment. The electron beam is then turned on for 5-10 milliseconds to prepare a new set of sample ions. Often it is desireable to remove certain ions from the cell in order to determine their fate by comparison with an experiment in which they are present. This is done by admitting a high amplitude excitation signal corresponding to the desired mass during the double resonance pulse. After a suitable delay, the ions are excited by turning on the excitation "chirp" (rapidly scanned excitation frequency) for about 1 millisecond. This is followed by turning on the detection circuitry.

If no variable delay is used (ions are excited immediately after their formation), the entire sequence of events will take about 30 milliseconds resulting in a full, low resolution, electron impact mass spectrum. This "fast scanning" would permit the analyst to acquire 33 mass spectra per second.

By using a variable delay, the analyst can observe reactions of ions with background neutral molecules (ion-molecule reactions) in a time-resolved way.

High resolution mass spectra are obtained in a narrow band scan by exciting a single ion and observing its transient decay for a long period of time (100 milliseconds to 5 seconds). (The relationship between transient decay times and mass resolution will be discussed in the following section). This experiment is done in a mixer mode to prevent overloading the computer memory during a long term experiment. In this mode, the ion decay signal is multiplied by a reference of nearly the same frequency. The difference frequency is extracted and digitized at a lower rate than the original frequency.

HIGH MASS RESOLUTION

Using an instrument constructed in our laboratory, we have obtained resolution up to 760,000 for the molecular ion of benzene at m/z 78 (see Figure 4a) (2).

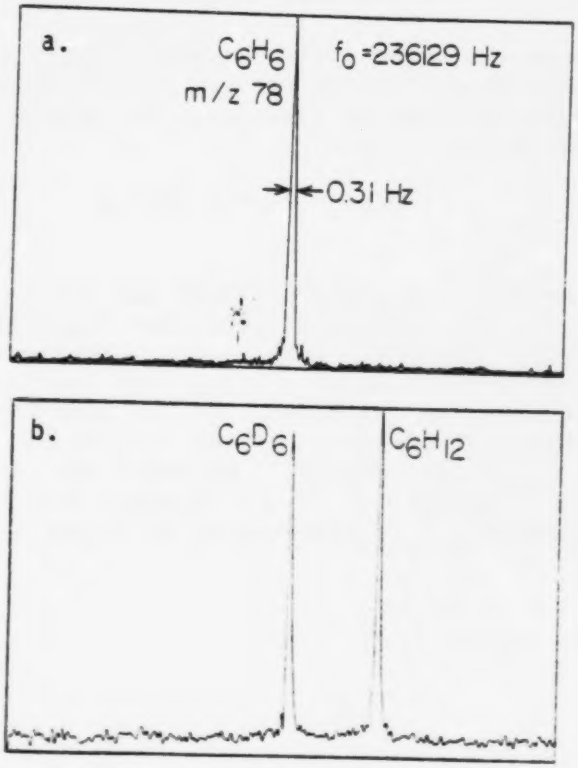

Figure 4. (a) Ultra-high-resolution (not magnitude mode) spectrum of benzene at m/z 78, obtained from a signal with τ of 1.0 s at a magnet field strength of 1.2T. Resolution is 760 000 (FWHH definition). (b) Resolved benzene-d_6/cyclohexane m/z 84 doublet, absorption mode, at 1.2 T. Resolution is 220 000 (FWHH definition).

This result was obtained using a benzene pressure of ca. 5×10^{-9} torr at a magnetic field strength of 1.2T. In a related experiment, the m/z 84 doublet from a mixture of benzene-d_6 and cyclohexane (see Figure 4b) at a total pressure of 2×10^{-8}torr was resolved. Other relevant experimental parameters for the latter measurement are: instantaneous source emission current, 300 nA; beam duration, 5 msec; electron energy, 70 eV; rf level, 24 V p-p applied to the cell; frequency excitation window, 219.920 to 220.060 kHz; rf chirp rate, 2 Hz/microsecond; trap voltage, 0.25 V; quench pulse applied between successive scans, 100 signal averaged (time domain) scans; 1 msec delay between electron beam turn off and excitation scan start. Conditions, with the exception of the frequency window chosen and pressure, were the same for the benzene measurement.

This result stimulated our interest in the relationship between signal-to-noise ratio (S/N) and resolution in the FT-MS experiment. We have shown that it is possible to simultaneously increase mass resolution and S/N, a feature unique to the FT instruments compared to conventional mass spectrometers.

We may examine the relationship between signal-to-noise and resolution by deriving an expression for the latter. The frequency resolution (full-width-at-half-height definition) assuming the entire transient signal is observed, is found to be

$$m/\Delta m = \pi f_0 \tau = zB\tau/2m \qquad (3)$$

for which B is the magnetic field strength and z/m is charge to mass ratio of ions. Therefore, the resolution increases linearly with magnetic field strength and varies inversely with mass. Furthermore, the resolution increases in direct proportion to τ , the time constant for decay. As the value of this parameter is increased, say by lowering the pressure in the analyzer cell, signal-to-noise ratio and resolution increase together if other parameters are held constant. Alternatively stated, the area under the peak remains constant as τ is changed and other parameters are unchanged. This phenomenon is illustrated in Figure 5.

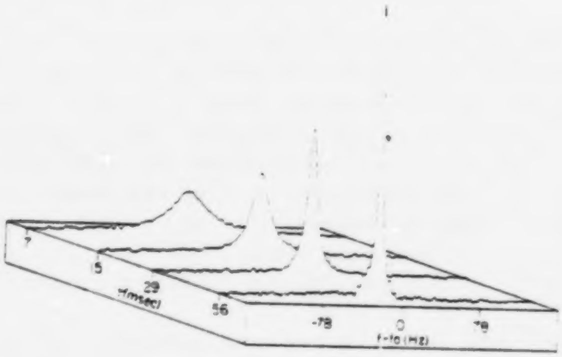

Figure 5. Simultaneous increase in resolution and signal-to-noise ratio with decreasing pressure for benzene at m/z 78. As benzene pressure was varied, electron beam emission current was adjusted to keep the number of ions in the cell constant for each spectrum. Spectra are absorption mode, rather than magnitude mode displays.

The essential trade-off is resolution vs. mass range rather than resolution vs. signal-to-noise, as in other forms of mass spectrometry. The mass range trade-off is inherent in mixer-mode operation of the FT-MS.

We believe the unique relationship between resolution and signal-to-noise in FT-MS will prove important in analytical applications of the method, paticularly in gas chromatographic FT-MS experiments.

PRECISE AND ACCURATE MASS MEASUREMENT

It is well known that the capability to measure exact masses of chemical substances is extremely important for both structure proofs of new compounds and for highly specific trace analysis. These measurements, which can lead to unambiguous assignments of elemental compositions, have been made traditionally using complicated double-focusing mass spectrometers. One of the principal limitations of the high resolution mode is that it is extremely difficult to acquire high resolution data across a wide mass range in short times (e.g. the several second duration of a capillary column gas chromatographic peak) in either a scanning or a peak switch mode. Nonetheless, rapid peak switching to obtain high resolution measurements of ions widely separated on the mass scale would be invaluable in conjunction with high resolution gas chromatographic separation of mixture components.

As a first step, we have made a preliminary investigation of the mass measurement capabilities of Fourier Transform mass spectrometry (3). The result of our study is a practical method for rapidly obtaining exact masses of sufficient accuracy and precision for determination of elemental compositions by FT-MS.

Consideration of equation (1) reveals that a very simple relationship exists between mass and frequency in FT-MS. Unfortunately, that relationship is not sufficiently accurate because it does not take into account the fact that the trapping fields perturb the ion frequencies. We need to measure frequency accurately and then relate frequency to mass in order to make accurate mass measurements. We have derived the necessary relationship for a cubic cell, and the results have been published elsewhere (3). It is sufficient to state here that the calibration equation is of a quadratic form (eq. 4) in which m_1 is the mass of an ion, f_1 is

$$m_1{}^2 f_1{}^2 = a_o - b_o m_1 + c_o m_1{}^2 \qquad (4)$$

its cyclotron frequency, and a_o, b_o, and c_o are calibration constants.

The derived mass calibration procedure was tested against the six major ions in the spectrum of 1,1,1,2-tetrachloroethane, which provides six intense calibration peaks in a useful region of the mass spectrum (see Figure 2). Mass accuracy was evaluated over various mass ranges using the quadratic mass calibration formula.

We find that the parabolic calibration procedure of Equation 4 produces mass measurements of sufficient accuracy and precision to permit elemental composition assignments over a mass range of at least 18 amu, centered at m/e 126. Frequency measurement precision for the six major ions in the spectrum of 1,1,1,2-tetrachloroethane, (standard deviation over ten successive Fourier Transform mass spectra) was typically 0.3 Hz and in no case exceeded 1.5 Hz. The quantity $(m_1 f_1)^2$ was fitted to the parabolic form in Equation 4 and the masses then back-calculated (see Table I for results) using the empirically determined values of a_o, b_o, and c_o. Over an 18 amu range, the parabolic calibration procedure gives mass errors of less than 1 millimass unit.

In practice, we have found the mass accuracy shown in Table I is routinely obtained over a broad range of operating conditions including various values of electron beam emission currents.

TABLE I. TYPICAL RESULTS OF A PARABOLIC MASS CALIBRATION OVER THE MAJOR IONS IN THE MASS SPECTRUM OF 1,1,1,2-TETRACHLOROETHANE

m_i	calculated masses[a]	error[b] amu	error[b] ppm
116.9066	116.9064 ± 0.0003	-0.0002	(1.7)
118.9036	118.9041 ± 0.0003	+0.0005	(4.2)
120.9007	120.8999 ± 0.0008	-0.0008	(6.6)
130.9222	130.9226 ± 0.0004	+0.0004	(3.1)
132.9192	132.9188 ± 0.0004	-0.0004	(3.0)
134.9163	134.9164 ± 0.0006	+0.0001	(0.7)

[a] Average of ten determinations made on ten successive mass spectra. [b] Tolerances shown represent single standard deviations over ten trials

We have also calibrated successfully over a wider mass range extending from m/z 78 to nearly m/z 240. Mass measurement errors were less than 6 ppm for the masses assigned.

It is well known that high mass resolution is not necessarily needed for exact measurements, so long as mass spectral peaks are not composed of multiplets of isobaric ion species. The measurements discussed here were made at mass resolution of ca. 1000 (full width at half height definition). For analytical purposes, it should be possible to perform exact mass measurements on wideband, low resolution ICR mass spectra, then switch to high resolution multiple ion monitoring mode to resolve potential multiplet peaks as a check. Since this operation would involve only frequency switching and pulse width adjustments, it could be performed rapidly and automatically under computer control. We reemphasize that FT-MS is capable of much higher mass resolution than 1000. The use of higher resolving power is expected to further increase the precision, and possibly the accuracy, of mass measurements by FT-MS.

CHEMICAL IONIZATION

Sample ionization can also be accomplished by ion-molecule reactions. The most common mode is proton transfer. The neutral sample molecules are protonated by a reagent ion in a gas-phase acid-base reaction. The advantage of this method of ionization is that molecules which give weak or no molecular ions by electron impact can be protonated to give intense $[M + H]^+$ ions where M is the neutral molecule. The second advantage of chemical ionization is that fragmentation of the $[M + H]^+$ ion can be readily controlled by choosing a "gentle" protonating reagent.

Chemical ionization is now an established method in conventional mass spectrometry and is available on most commercial instruments. It is well known that the sources of these spectrometers must be operated at a relatively high reagent gas pressure (0.1-1.0 torr) and sample partial pressures (10^{-5}-10^{-4} torr) for significant conversion of neutrals into ions. The high pressure is needed to compensate for the short residence time of the ions in the source ($\sim 10^{-4}$ seconds).

Chemical ionization can be conducted using FT-MS at low reagent gas pressure (10^{-6} torr) and even lower sample pressure ($\sim 10^{-8}$ torr) because the ions can be trapped for long periods of time (up to 1 second and more). This low pressure CI should give, in principle, higher sensitivity (lower detection limits) than electron impact because sufficient time can be provided during the variable delay to permit quantitative transfer of ionization from reagent (ionized at higher pressure) to sample (present at lower pressure). This advantage has not been achieved in CI using conventional mass spectometers.

We have recently demonstrated the capabilities of low pressure CI for a wide range of compounds and reagent gases (4). Furthermore, we have described some alternate ways of obtaining CI spectra in the FT-MS mode. Some highlights of that work will be presented here.

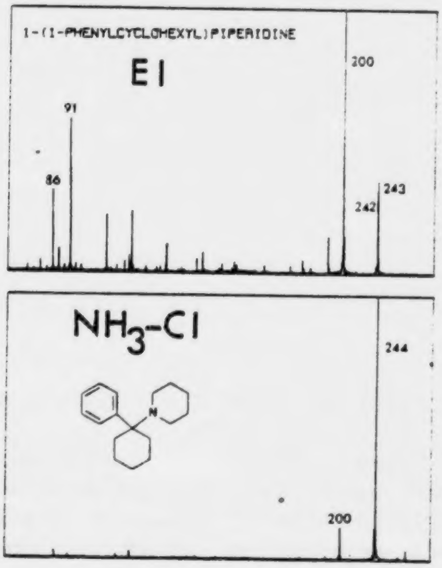

Figure 6. EI and ammonia CI mass spectra of 1-(1-phenylcyclohexyl)piperidine (PCP or "Angel dust") over identical bandwidths.

The first approach for obtaining spectra in the CI mode is to introduce an appropriate delay time between the ionization and excitation, thus allowing ions and neutral molecules to react before mass analysis. The reagent gas is introduced to approximately 10^{-6} torr and the sample can be evaporated from a direct probe. Selection of the delay time is determined by the time required to establish a high concentration of reagent ions. For example, the concentration of the reagent ions CH_5^+ and $C_2H_5^+$ is constant after about 100 milliseconds in methane at 10^{-6} torr. Formation of H_3O^+ in water at 2 x 10^{-6} torr is complete within 10 milliseconds. These reagent ions are now available for proton transfer. A comparison of the EI and CI spectra for the abused drug "Angel Dust" is shown in Figure 6. The CI spectrum originates from protonation of the sample by NH_4^+ to give m/z 244 followed by a minor amount of decomposition of $[M + H]^+$.

In the absence of reagent gas, CI can take place by reaction of the fragment ions of the sample and the sample neutral molecules. We term this method "self CI". This procedure is well suited for molecules containing large hydrocarbon moieties such as fatty acids, fatty acid esters, pheromones, and other long chain aliphatics containing one or more functional groups. The EI spectra of these molecules contain many closed-shell ions which are potential proton transfer reagents. After a suitable delay, the ion current borne by these fragments is transferred to $[M + H]^+$ permitting higher sensitivity detection of the sample using a single ion of high structural significance. An example is given by the self CI spectrum of methyl stearate at 1 x 10^{-7} torr (Figure 7).

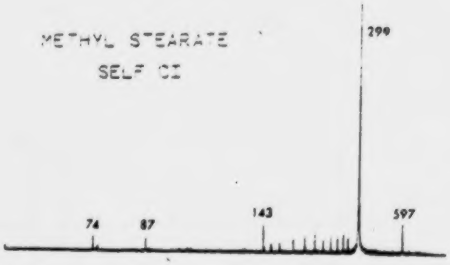

Figure 7. Self-CI spectrum of methyl stearate at 1 x 10^{-7} torr.

A third method is "Quench-Off CI". In this mode, we forego the quench pulse (see Figure 3) and allow ions to accumulate in the cell. The ion concentration grows until a steady state is reached which represents a balance of ion production by electron impact and ion loss by drift from the cell.

The principal advantage of "Quench-Off CI" is the capability to produce spectra at a more rapid rate than the two procedures described above. In some cases, the extent of protonation produced in a quench-off CI experiment using a delay of approximately 10 milliseconds is equivalent to that produced in a quench-on mode using a delay of 200 milliseconds. Thus, data acquisition can be 20 times more rapid in the former mode.

We have also demonstrated that CI spectra can be obtained for negative ions, for radical cation reagent ions, and for deuterium exchange to count exchangeable hydrocarbons (4). The unique double resonance capability of FT-MS permits us to study the mechanisms of formation of the various ions in addition to applying the chemistry for analysis.

GAS CHROMATOGRAPHY/FOURIER-TRANSFORM MASS SPECTROMETRY

A long range goal of our research is to evaluate the feasibility of interfacing a gas chromatograph to a FT-MS for the purpose of obtaining high resolution mass scans of mixture components emerging from a capillary column. We have established a number of secondary goals to be accomplished enroute to this ultimate goal. They include: (a) the interface of a GC to a FT-MS, (b) demonstration of fast scanning to obtain full spectra of components from a capillary column, (c) demonstration of sufficient pumping speed at the cell to permit high resolution measurements over narrow mass ranges, (d) demonstration of sufficient sensitivity for high resolution single ion monitoring for analysis of single components, (e) development of peak switching capability to permit multiple ion monitoring to increase the certainty of identifying specific chemical substances, (f) evaluation of the capability to make precise and accurate mass measurements in a multiple ion monitoring mode, and (g) development of the capacity to obtain full spectra at medium resolving power (5,000-10,000) and to assign accurate masses to the peaks in the spectra of components emerging from a capillary column.

We have recently developed an interface for GC and the FT-MS instruments and have demonstrated that the fast scanning capabilities of the FT-MS are sufficient to obtain full low resolution mass spectra (5).

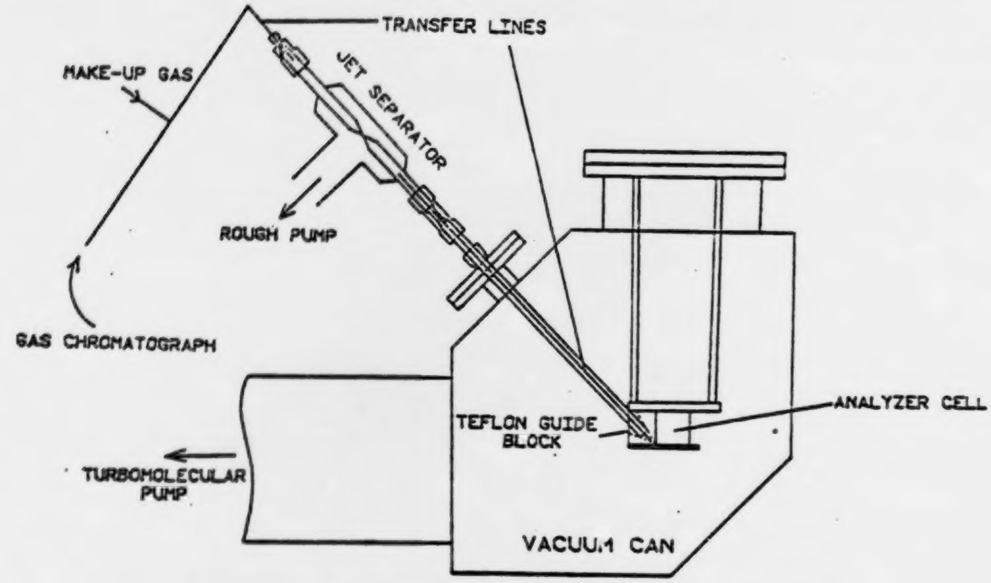

Figure 8. Schematic of cell, vacuum system, and interface for GC/FT-MS.

The FT-MS instrument used for this study was specially designed with a high gas conductance vacuum chamber. This allows the mass analyzer to operate at low pressure, which is necessary for high mass resolution. The forward end of the vacuum chamber, which contains a cubic trapped ion analyzer cell (plate separation 0.0254 m), has a nominally rectangular shape. The width (internal 0.0667 m) is sufficient to permit insertion into the 0.0762 m air gap of a Varian V-7300 0.305 m electromagnet. That volume expands into a 0.152 m i.d. stainless steel tube which is outfitted with a 0.152 m gate valve. The tube terminates at a 500L/second turbomolecular pump which is backed by a fast mechanical pump.

The pumping speed at the cell is 360 L/s which was determined by calculation and verified experimentally by introducing a known flow rate of helium and observing the pressure. A schematic of the vacuum can and separator is given in Figure 8.

The electromagnet is equipped with one pair of 0.305 m cylindrical ring-shim pole caps with iron-cobalt ring for high homogeneity. Its maximum field strength is 1.37 T at the center of the air gap, and it was operated at 1.2 T for these experiments.

The vacuum system is interfaced to a Perkin-Elmer Sigma II gas chromatograph containing an OV101 15.2 m x 0.5 mm SCOT capillary column at 150°C (isothermal). The interface consisted of either a direct coupled transfer line (0.5 mm i.d., 0.6 mm o.d. gas-lined stainless steel obtained from Scientific Glass and Engineering) or a standard glass jet separator coupled to the transfer line. Both were held at 200°C. When the separator was used, 20 mL/minute of make-up helium gas was introduced prior to the jet separator.

Full low resolution spectra were obtained at a rate of 0.5 seconds per spectrum for a 1:1:1 mixture of benzene, toluene, and xylene (see Figure 9). This serves as a demonstration of the fast scanning ability of the combined system.

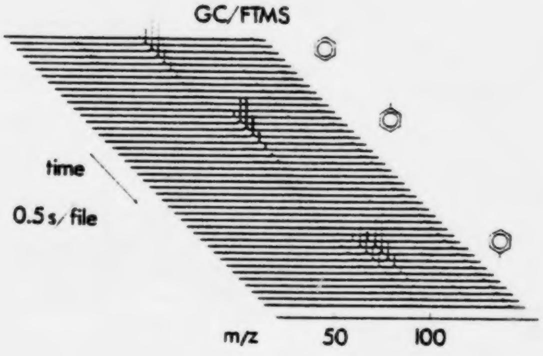

Figure 9. GC-FT/MS spectra of a mixture of equal amounts of benzene, toluene, and xylene. Twenty-five signal averaged scans were taken per file.

The separator design and pumping speed are sufficient to permit high resolution single ion monitoring over narrow mass bands. Using the jet separator, we have been able to observe the m/z 78 (molecular ion of benzene) with a resolution of 23,000 (full width at half height definition). Two components at m/z 106: xylene (m/z 106.0782) and benzaldehyde (m/z 106.0419) were separated easily with a mass resolution of 9,000. This experiment was done as a demonstration of useful resolution by admitting benzaldehyde via a liquid inlet and the xylene via the capillary column.

Since the spectral bandwidth selection in FT-MS involves setting the frequency sweep of an rf sine wave excitation, it should be possible to alter both the size and position of a mass observation window by changing a few computer words. This could be easily done within microseconds under computer control. Switching of this type would allow for acquisition of high-resolution narrow mass range data for two or more widely separated masses during the elution of a single chromatographic peak. This has been demonstrated for a mixture of benzene and bromobenzene. Both molecular ions (m/z 78 and m/z 156) were monitored sequentially at a mass resolution of 20,000 (at m/z 78) at a rate of 3.5 Hertz.

We believe a similar experiment could be done in which full low resolution spectra were acquired in one half cycle and a single ion was monitored at high resolution in the other half cycle. This remains to be demonstrated.

We have made some preliminary measurements of sensitivity by injecting ever decreasing quantities of material onto the GC and using the FT-MS in a single ion monitoring mode. In this way, we have established a detection limit of about 1 nanogram of material (see Figure 10). We anticipate that better detection limits will be achieved by making improvements in the design of the detection circuitry and of the interface of the transfer line to the FT-MS cell. It also may be possible to improve the detection limit by employing new cell designs in lieu of the present cubic one.

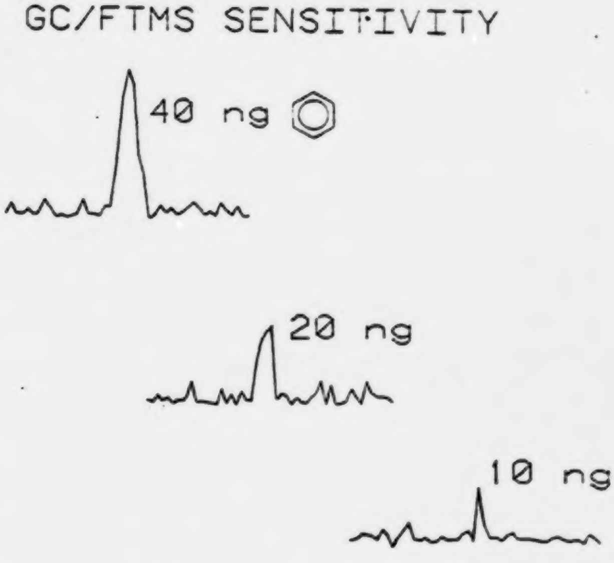

Figure 10. Demonstrated sensitivity for GC/FT-MS using fast pumped system.

In summary, we have verified that high resolution measurements can be made routinely using FT-MS, and that precise and accurate mass measurements are possible using this new form of mass spectrometry. Furthermore, we have demonstrated that a wide variety of chemical ionization options can be used in FT-MS. Finally, the important goal of interfacing an FT-MS with a GC has been satisfied, and the capabilities for multiple ion monitoring at high resolution have been demonstrated. Future work will be directed at improving on these capabilities so that real problems in chemical analysis can be addressed.

References:

(1) M.B. Comisarow and A.G. Marshall, J. Chem. Phys., 64, 110 (1976).

(2) R.L. White, E.B. Ledford, Jr., S. Ghaderi, C.L. Wilkins, and M.L. Gross, Anal. Chem., 52 1525 (1980).

(3) E.B. Ledford, Jr., S. Ghaderi, R.L. White, R.B. Spencer, P.S. Kulkarni, C.L. Wilkins, and M.L. Gross, Anal. Chem., 52, 463 (1980).

(4) S. Ghaderi, P.S. Kulkarni, E.B. Ledford, Jr., C.L. Wilkins, and M.L. Gross, Anal. Chem., 52, 428 (1981).

(5) E.B. Ledford, Jr., R.L. White, S. Ghaderi, C.L. Wilkins, and M.L. Gross, Anal. Chem., 52, 2450 (1980).

Comments on
Application of Fourier Transform Mass Spectrometry to the Analysis of Organic Emission Samples

S.A. Hoenig
Department of Electrical Engineering
University of Arizona
Tucson, Arizona

The authors suggested the use of Fourier Transform Mass Spectrometry (FTMS) to what might be called Ion Trap Mass Spectrometry (ITMS). In ITMS, a sample is volatilized into a closed box and ionized by a beam of electrons. The ions are excited into cyclotron resonance and are detected by the induced voltages as the ions pass a detector plate.

The application of FTMS to this process involves the analysis of signals produced by the moving ions. FTMS is ideally suited for this application. Analysis by any other technique would be very difficult.

The authors have demonstrated that the system works and that high resolution with good sensitivity is quite practical. The proposed application to analysis of small quantities of toxic pollutants looks very good, particularly when a gas chromatograph is used ahead of the mass spectrometer.

I suggest that the authors are doing an excellent job and should continue. They might consider the application of their apparatus to observing the course of a chemical reaction by periodically ionizing and sampling the reacting system.

THE INVESTIGATION AND DEMONSTRATION OF A HYDROPERM MICROFILTRATION SYSTEM FOR THE TREATMENT OF ELECTROPLATING WASTEWATER EFFLUENT

Han-Lieh Liu, Senior Research Scientist
HYDRONAUTICS, Incorporated
7210 Pindell School Road
Laurel, Maryland 20707

INTRODUCTION

This paper presents the on-going study of an EPA co-sponsored research, development and demonstration program for the application of a Hydroperm™ microfiltration system to treat electroplating wastewater. By applying cross-flow filtration principle to the thick-walled porous plastics tubes, Hydroperm microfiltration shows a new method of suspended solids removal from the wastewater. These tubes, whose wall thickness, inside diameter, porosity, and pore-size distribution can all be closely controlled, can be selected for a particular wastewater so as to obtain optimum performance. It should be pointed out that cross-flow microfiltration, which is intended primarily for the removal of suspended solids, is significantly different from membrane ultrafiltration (UF) or hyperfiltration (RO) which remove substances on the molecular level and are primarily for the removal of dissolved solids. They have been, however, used to remove suspended solids in the wastewater in some industries. In UF, higher filtration pressures (~50-150 psi) are used, with even higher pressures (from 600~1,200 psi) for RO, compared with only ~15 psi for Hydroperm microfiltration. Furthermore, UF and RO employ relatively thin membranes, compared with the relatively thick-walled (~1 mm) Hydroperm microfilters. As a result, power requirements as well as both capital and operating costs are higher for membrane systems than for Hydroperm microfiltration.

In this paper, the general description of cross-flow microfiltration will be discussed first. The application study on electroplating wastewater is then followed.

CROSS-FLOW MICROFILTRATION

In the treatment of both domestic and industrial wastewaters, the removal of suspended solids is a required operation which arises under a variety of circumstances. For example, this unit operation is often essential as a pretreatment step prior to undertaking further advanced treatment. Fine-solids removal is also often necessary as a "polishing" step after chemical or biological treatment processes. There are several existing physical treatment processes available for this purpose, such as gravity clarification, multimedia filtration, etc. However, most of these processes have inherent disadvantages in dealing with fine and difficult-to-settle solids.

Two types of filtration processes have been widely used in removing of suspended solids: (1) the through-flow (e.g., multimedia) filter; and (2) cross-flow filtration (e.g., ultrafiltration and reversed osmosis). Although they can remove some of the suspended solids, conventional through-flow filters have the disadvantage of requiring frequent backwashing, since the filtered particles continuously accumulate on, or actually enter, the filtration barrier. Through-flow filtration is, by its very nature, a batch process, with the flux declining when the driving pressure differential across the filtration barrier is held constant.

On the other hand, in cross-flow filtration, the direction of the feed flow is parallel to the filter surface, so that accumulation of the filtered solids on the filter medium can be minimized by the shearing action of the flow. Thus, cross-flow filtration affords the possibility of a quasi-steady state operation with a nearly-constant flux when driving pressure differential is held constant.

The filtration characteristics of Hydroperm tubes combine both the "in-depth" filtration aspects of multimedia filters and the cross-flow filtration aspects of membrane ultrafilters. For example, in a manner similar to multimedia filters, the Hydroperm tubes may allow some of the smaller particles in the waste streams to actually penetrate into their wall matrix. However, it should be noted that the pore structure of the Hydroperm tubes differs from those of membrane ultrafilters in that the pore sizes of the former are of the order of several microns with the "length" of the pores being many times their diameters. The entrapped solids in the wall matrix will not pass through the tube wall because of this long and tortuous path. Chemical solvent can be used to dissolve these entrapped species if necessary. The penetration of these small particles (usually less than microns) is limited to the formation of a dynamic membrane layer on the inner side of the tube in the cross-flow filtration process. The existence of this layer is due to the establishment of the boundary layer of the flow through the tube. It is this layer which can help in preventing further penetration of small particles into the wall matrix. It is also conjectured that this layer behaves like another filter media. Thus, while the tubes are primarily designed for the separation of suspended solids from the feed, they frequently achieve some levels of dissolved solids separation because of this layer.

The characteristics of this membrane vary with the characteristics of the solids in the feed. The thickness of the membrane is controlled by the shear exerted by the circulation flow and the nature of the solids in the feed. In his paper presented at the 1980 Annual Fine Particle Society Meeting, Mr. Tulin proposed a deposition and erosion model to predict the formation of this dynamic membrane layer (1). The cohesiveness of the particles is identified and related to the permeation rate of the tubes. In general, the cohesiveless particles in the feed can yield relatively high permeate flux while cohesion particles form slime like layer and result in lower permeate flux value.

The principle element of the Hydroperm microfiltration system is a thick-walled (~1 mm) hollow tubular filter (6-9 mm I.D.), made of thermoplastic material and containing micron-size pores. These tubes can be made from a variety of extrudable thermoplastics, such as nylon, polyethylene, and polypropylene by a proprietary manufacturing process.

Pore-size distributions of two typical Hydroperm tubes are shown in Figure 1. Tube I has a rather "flat" distribution with the pores ranging in size from 2 microns to 10 microns. On the other hand, Tube II has a "peaked" distribution, with most of the pores being in the 2-micron range. It should be noted that the pore-size distributions shown in Figure 1 are initial values, since the pore-size distribution of the tubes undergoes a change during the filtration process because of the penetration of small particles into the tube wall.

Two views of the pore structure of a typical Hydroperm tube are shown in Figure 2. These photographs were taken with the aid of a Scanning Electron Microscope and are of a transverse section of the tubes. The view in 2a has a magnification factor of two hundred, while that in 2b has a magnification factor of one thousand. The open-cell, reticulated nature of the pore structure can be appreciated from these photographs.

ELECTROPLATING WASTEWATER TREATMENT

The electroplating industry produces a large volume of wastewaters which contain primarily four common toxic heavy metals (i.e., chromium, zinc, copper and nickel), as well as a variety of others such as lead, cadmium, tin, silver, etc. The uniqueness of the plating wastewater required to remove not only the heavy metals, but also the toxicity of the water which is mainly due to the presence of cyanide and hexavalent chromium. The conventional treatment involves the unit operations of chromium reduction, cyanide oxidation, neutralization, clarification and sludge concentration. The conversion of heavy metals into insoluble hydroxides usually results in hydrous and difficult to settle solids. The conventional settling processes is not adequate to achieve good quality effluent and concentrated sludge. The problem is further complicated by plating wastewaters contain compounds that interact with dissolved metals and interfere with their precipitation as metal hydroxides. These compounds, called chelates, combine with the dissolved metal ion to form a complexed ion that is relatively soluble in neutral and slightly alkaline solutions. Alternatives such as sulfide precipitation, waste stream segregation and extreme pH treatments, are studied by many people with some sucess (2).

A two-phase R & D program was granted by EPA Office of Exploratory Research to investigate the feasibility of using Hydroperm microfiltration system to treat plating wastewater after they have been detoxicated. Phase I involves the laboratory Hydroperm filterability studies. Phase II consists of design, construction and field testing a full scale portable unit in a plating shop.

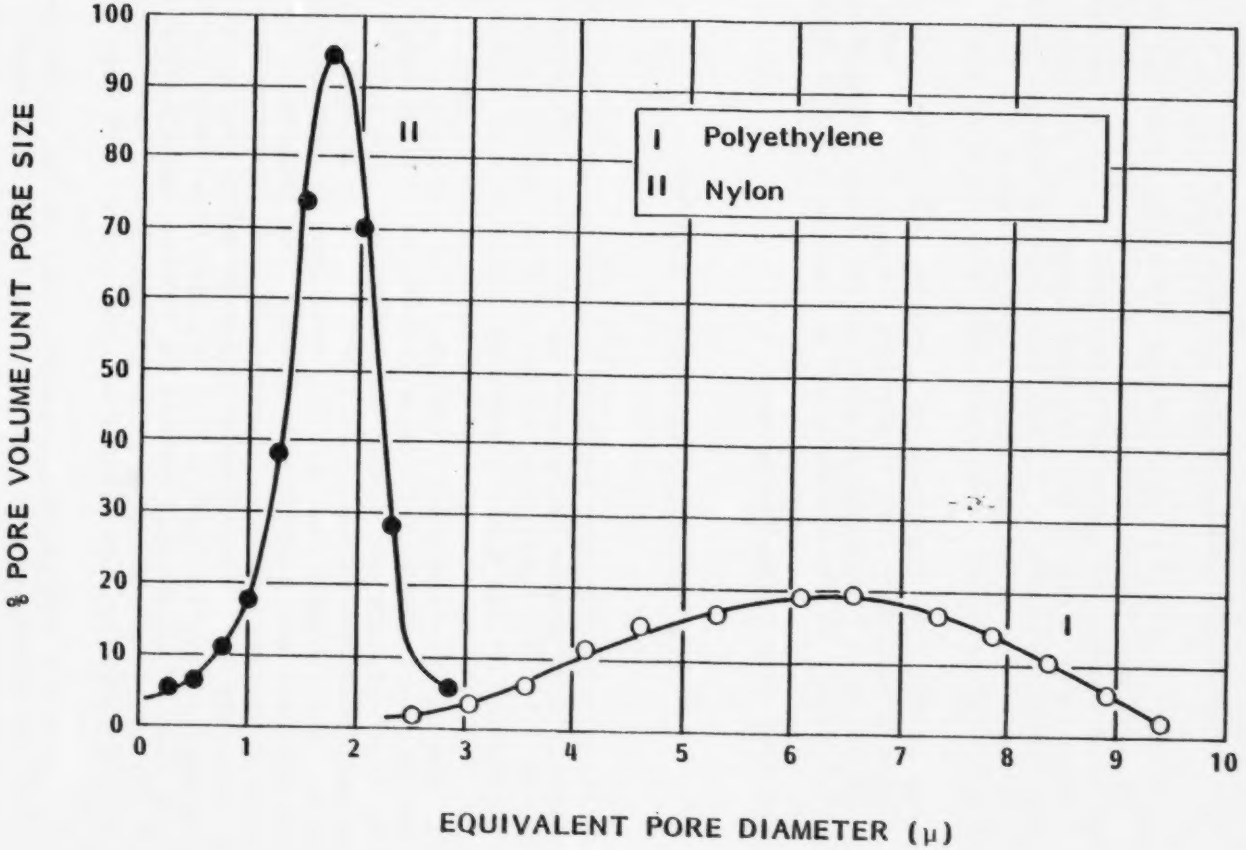

FIGURE 1. TYPICAL PORE SIZE DISTRIBUTION OF HYDROPERM™ TUBE.

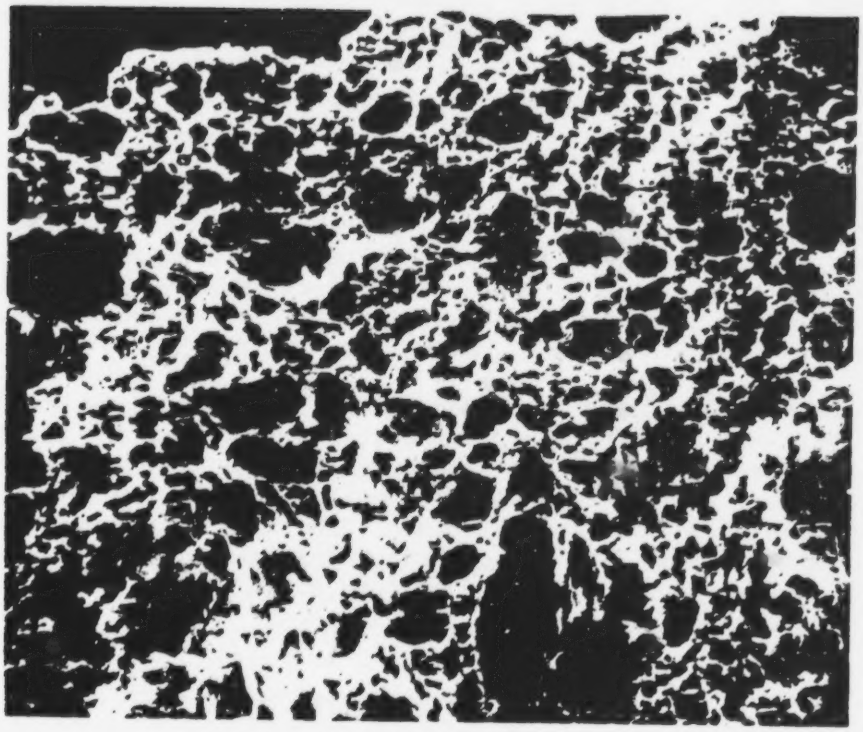

S.E.M. 200X

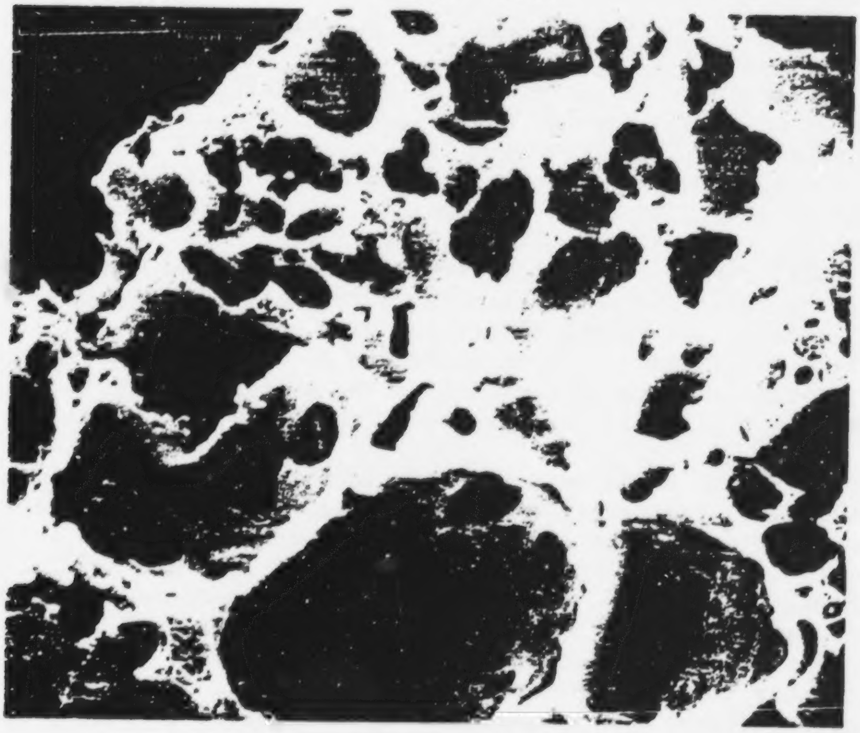

S.E.M. 1000X

FIGURE 2. ELECTRON MICROPHOTOGRAPHS OF HYDROPERM™ TUBE PORE STRUCTURE - TRANSVERSE SECTION.

PHASE I LABORATORY STUDY

Wastewater samples from three different shops were received for the phase I evaluation. It consisted of jar tests and Hydroperm filtration tests. The test variables included different precipitants and flocculants used in the industry. The precipitants under investigation are the slaked lime and caustic. The flocculants under study are Ferric sulfate, alum and polymer. In the jar test, the particle formation and its settling characteristics are evaluated. The filterability of these particle laden wastewater is then examined through the Hydroperm test apparatus. The results of this series of evaluation tests also finalized the optimum tube characteristics for the field module tests.

The laboratory results indicated that all three wastewater sources can be effectively treated with Hydroperm microfiltration process. The flux values of these wastewater depended upon the chemical used in the various conventional treatment steps. A flux value over 200 gal/ft^2-day can be demonstrated. The permeate quality are quite good, Table 1. The high copper concentration in the permeate for sample 1 is conjecturated that excessive carbonate and incomplete cyanide destruction may cause to form copper complexes which will not precipitate from the solutions.

PHASE II - FIELD DEMONSTRATION STUDY

A full scale demonstration unit was designed and constructed. There are four modules arranged in series and in parallel on this unit. Each module has 25 ft^2 filtration surface area and is 5-ft tall, 4-in. in diameter. The demonstration unit thus has 100 ft^2 filtration surface area. This self-contained unit is skid mounted with dimension of 6' x 6' x 8.5' and is equiped with main circulation pump, permeate transfer pump, temporary permeate holding tank, clean solution tank, and various control valves. The demonstration site was selected at the Craftsman Plating and Tinning Corporation in Chicago. Presently, CP&T treats their wastewater with conventional processes: cyanide destruction by chlorine; neutralization with caustic; suspended solids removal through clarifier; and sludge thickening with centrifuge. The flow diagram for the plant wastewater is shown in Figure 3. As shown in the figure, Hydroperm system is operated parallel to the existing clarifier system. A direct comparison of these two systems is thus readily available.

The preliminary field data was very encouraging. Table II shows some typical analytical laboratory analyses. As shown in the laboratory analyses, the permeate quality is not sensitive to the amount of metals in the wastewater so long as they are in suspended form. If they are in dissolved form, due to improper pH control, cyanide destruction procedures or both, the quality of permeate may vary. The unit is now under an eight-week long term test with actual daily plating wastewater. No attempts were made to alter the present plant wastewater treatment procedures or chemicals. It should be pointed out, however, higher fluxes can be expected with different treatment chemicals.

TABLE I. LABORATORY ANALYSES ON METALS IN THE PLATING WASTEWATER EFFLUENTS (PHASE I STUDY)

Samples*		TS	SS	Cr	Cu	Zn	Cyanide	
1.	Feed	1860	616	15.4	57.3	32	12	
	Permeate	1320	8	<0.01	36.4	0.38	11	
		TS	SS	Cd	Cu	Pb	Sb	
2.	Feed	4100	721	170	12.5	0.10	0.8	
	Permeate	2860	16	0.3	0.11	<0.01	<0.1	
		TS	SS	Cr	Cd	Cu	Ni	Zn
3.	Feed	5940	4010	90	11.5	3.85	120	800
	Permeate	2250	2	<0.01	0.06	0.42	2.16	1.44

*Note: 1. Alexandria Metal Finisher; 2. Craftsman Plating and Tinning; and 3. Chrome-Rite

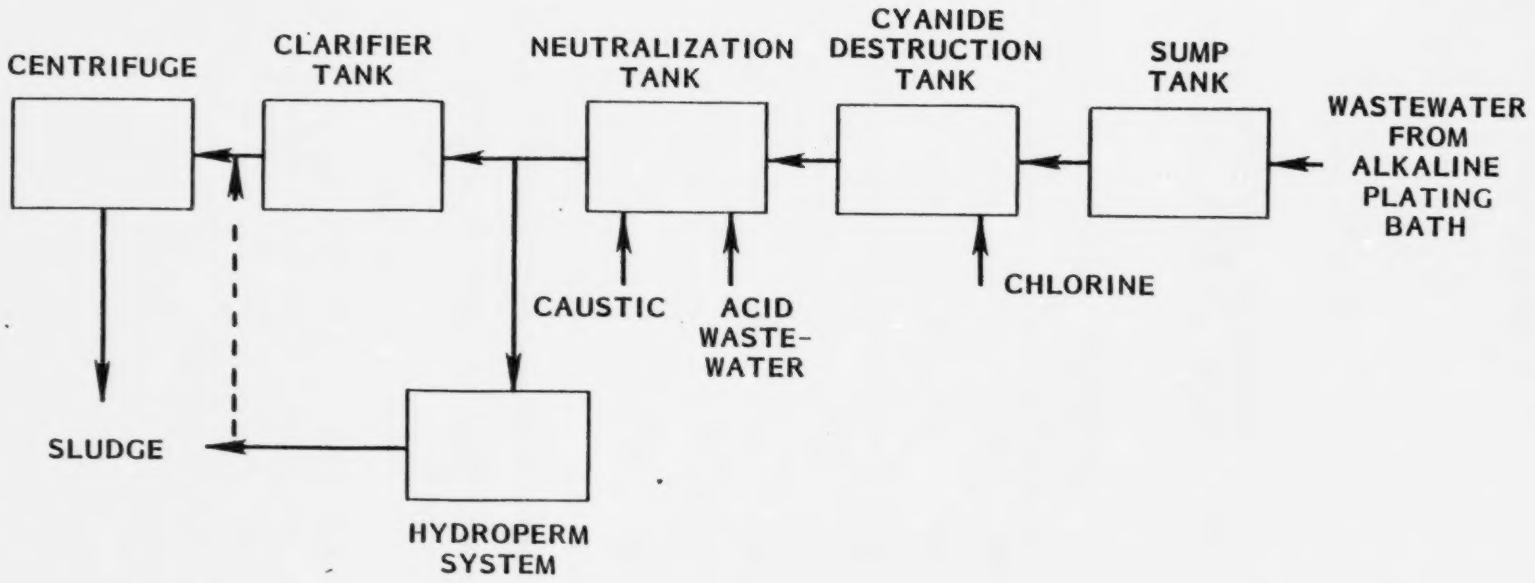
CENTRIFUGE
CLARIFIER TANK
NEUTRALIZATION TANK
CYANIDE DESTRUCTION TANK
SUMP TANK
WASTEWATER FROM ALKALINE PLATING BATH
CHLORINE
CAUSTIC
ACID WASTE-WATER
SLUDGE
HYDROPERM SYSTEM

FIGURE 3. WASTEWATER TREATMENT FLOW DIAGRAM.

TABLE II. LABORATORY ANALYSES ON METALS
(PHASE II FIELD STUDY)

DATE	SAMPLES	PH	TS	SS	Cd	Cu	Zn
5-28	Feed	11.29	4960	408	44	1.5	7.6
	Permeate	11.25	4580	6	0.1	0.1	<0.1
6-1	Feed	10.28	12020	5940	1200	22	190
	Permeate	10.30	5090	6	0.2	<0.1	<0.1
	Sludge	9.91	31450	25280	7000	106	720
6-8	Feed	7.55	10890	8480	380	33	57
	Permeate	7.82	2620	<0.1	0.9	0.3	<0.1

CONCLUSION

Hydroperm cross-flow microfiltration is an effective new technology for the treatment of electroplating wastewater. The laboratory study of this two-phase R & D program proves the feasibility of this new technology application. Reasonably high flux and good effluent quality have been demonstrated. The second phase of study for field demonstration is underway. Preliminary results show the good permeate quality can be easily achieved regardless the metal concentration in the feed. The flux value is, however, dependent upon the chemical used in the wastewater treatment process. A direct comparison of the economics of this system with the conventional clarifier will be made at the end of this R & D program.

ACKNOWLEDGEMENTS

The author wishes to acknowledge the financial support partially provided by the U.S. Environmental Protection Agency. Valuable assistance from the following agencies are also sincerely appreciated: American Electroplating Society; Alexandria Metal Finisher, Virginia; Craftsman Plating and Tinning Corporation, Illinois; and Chrome-Rite Corporation, Illinois.

REFERENCES

1. Tulin, M. P.
   Cross-flow Filtration - Paper presented at Fine Particle Society Fall Meeting. September 16-18 1980, University of Maryland.

2. EPA Summary Report
   Control and Treatment Technology for the Metal Finishing Industry - Sulfide Precipitation,Technology Transfer EPA 625/8-80-003, April 1980.

Comments on
The Investigation and Demonstration of a Hydroperm Microfiltration System for the Treatment of Electroplating Wastewater Effluent

E. Robert Baumann
Iowa State University
Ames, Iowa

The Hydroperm microfiltration system uses the principle of cross-flow filtration with thick-walled plastic tubes to treat wastewaters to:

(a) remove virtually all suspended solids
(b) produce a sludge containing a minimum of water, and
(c) produce a filtered product water for reuse.

The author's company received an EPA Grant to demonstrate the applicability of the microfiltration system to the treatment of electroplating wastewater effluent. The paper presented was intended to be a progress report describing the research completed to date.

The Hydroperm microfiltration system uses 6-9 mm I.D. tubes and a pressure differential of about 15 psi to provide continuous removal of suspended solids from wastewater. The research-demonstration proposal proposed a 2-phase program to:

1. Evaluate the treatibility of electroplating wastewater after neutralization for removal of Cu, Zn, Cr, Cd, and Ni. The lab studies proposed would be used to optimize the tube material, pore structure, chemical precipitants, and the operating conditions (flow or flux, recycle rate, operating pressure).
2. Using the lab results, build and operate a field unit for several electroplating wastewater treatment systems.

In phase 1, jar tests were to be used to select precipitants (caustic, lime, soda ash) and coagulants (alum, ferric sulfate, ferric chloride, polymer) in which type of chemical, its concentration, and pH were controlled. Effectiveness was to be evaluated using particle size distribution (Coulter counter) and turbidity studies (108 tests). Then, single tube tests were to be made in the laboratory using a pressure differential of 15 psi, a flow velocity of 4-7 ft/sec, and ambient temperature using both nylon and polyethylene tubes (65% porosity). Runs of 24 hours would be made with and without chemicals evaluating removal of SS and metals, operating flux, and the sludge dewatering properties of the concentrated SS. No mention was made of evaluating the SS characteristics (i.e., concentration) on the operating flux and pressure. A total of 21 test runs were proposed.

In phase 2, a pilot plant was to be placed in continuous operation to provide data for making a mass balance:

Flow in and out
Flux history as feed SS change
Quality of feed
Quality of permeate

No mention is made of determining the percent feed conversion to permeate or of determining progressive changes in the water content or dewatering characteristics of the sludge produced.

The application of Hydroperm microfiltration systems to electroplating wastewater treatment would seem to require information for design on:

1. What is the quantitative effect of the concentration of SS in the feed on filter efficiency as recycle increases the SS level in the feed? The phase 1 single loop tests proposed keeps the permeate and feed continuously mixed together, so that the results are for a single constant SS pass through the treatment unit.

2. The field results using microfiltration must be compared with the performance of the plant existing treatment unit to indicate both operating problems and economics.

It must be recognized that the progress report presented today is merely a progress report. All of the phase 1 tests are apparently completed, but little data or data evaluation of this phase were reported. The data from phase 1 presented included some pilot plant data on the metals in the feed and permeate in three electroplating plant wastes which indicate removal of the metals desired. The only phase 2 data from a plant-scale run presented three days of data showing significant concentration of metals in the recycle (removal from the permeate). No engineering or design data were included. The data in Table II in the paper indicate some (6/1 data) material balance problems because the SS in the sludge increased about 4.2 times, the Cd by 5.8 times, the Cu by 4.8 times, and the Zn by only 3.8 times. The paper used 7 pages to describe the product under test and only about 4 pages to describe the laboratory results to date. This reviewer will look forward with interest to the technical report of the study results.

WET OXIDATION OF THE WASTE WATER FROM COAL GASIFICATION INSTALLATIONS

O. J. Hahn, J. C. Carter and O. W. Stewart
Department of Mechanical Engineering
University of Kentucky
Lexington, KY 40506

ABSTRACT

The objective of the research program is to demonstrate with the University of Kentucky half ton per day moving bed gasifier and small laboratory apparata that wet-oxidation of organic and inorganic material in the waste waters from gasifiers is technically feasible and economically attractive.

The primary waste waters are produced in the first quenching and scrubbing of the exit gas from the gasifier. Moving or fixed bed gasifiers produce more tar and oils than fluidized or entrained systems. The organic material in the waste waters is converted to carbon dioxide and water with air or pure oxygen at elevated temperatures and pressure. The initial tests were conducted with simple organic compounds to determine reaction parameters. However, it is not known which compound in the waste waters is rate determining. Thus, the moving bed coal gasifier was readied for test and waste water production. Instrumentation for the determination of interfering gases such as H_2S, NH_3, etc. was aquired and calibrated. The data acquisition system and the HP1000-F Series Computer was made operational.

Initial data should be available by the end of July 1981.

INTRODUCTION

In many coal gasifying systems water (1) is used to wash and condense the oils and tars(2) in the product gas after it leaves the gasifier. Washing the product gas is necessary in commercial gasifiers in order to protect the environment and to prevent fouling of the equipment designed to remove H_2S from the product gas(3). It is also necessary in research gasifiers to measure the oil, tar, dust and gas which are removed from the product gas in order to analyze the gasifier performance. In most gasifiers the water is in contact with the product gas and thus material is transferred from the gas to the water. The water which is referred to as scrub water may flow through the gasifier once, or it may be recycled. In either case, it is desirable to continuously remove from this scrub water those materials (oil, tar, dust and gas) classified as pollutants which the water has received from the product gas. It is frequently not only desirable but mandatory to reduce the amount of pollutants released to the environment.

The amount of tar and oil produced in a gasification unit varies greatly dependent on the outlet pressure, temperature and residence time at that temperature before quenching (i.e., size of the system load on the system and free space above the gasifier). Under optimum conditions 4% of the weight of bituminous coals appears as tar; under the worst conditions this can increase 22%. The water from the scrubber should not be dumped without excessive cleaning due to the phenolic compounds. If the scrub water is recycled, some cleaning is required to prevent plugging of the system by an accumulation of inorganic or organic compounds. In most gasifiers it is envisioned to return the tar to the gasifier. If the tar contains little water at the METC Process (2) it can be returned directly. Otherwise a separation or treatment step are necessary. This still results in water treatment requirements.

There are many ways in which the scrub water from the gasifier can be cleaned. One of which is a system in which the phenomena of wet-oxidation is used. This phenomena known variously as wet-oxidation, wet-combustion, and wet-air oxidation has been used extensively for waste disposal when the waste is in the form of a slurry such as the scrub water from a paper mill or sewage sludge.

The process of oxidation is one of converting undesirable chemical species to species which are neither harmful nor otherwise objectionable. Most frequently it is neither necessary nor practical to carry the oxidation process to absolute completion. The toxic phenol molecule, for example, can be quantitatively oxidized to carbon dioxide and water with a strong oxidizing agent. Depending on the oxidant and the oxidizing conditions, compounds of much lower toxicity and less objectionable characteristics are formed as intermediate oxidation products. The further oxidation of these compounds, if not absolutely required, is often not justifiable from an economic point of view. Also, the reaction times for complete oxidation (if no catalysts are used) are often so long as to render sufficient detention facilities impractical. For these reasons, it is realistic to define chemical oxidation in water and wastewater treatment as a method for selective modification of objectionable and/or toxic substances. These substances include:

1. Organic substances (for example, Mn^{2+}, Fe^{2-}, CN^-, SO_3^{2-});
2. Organic substances (for example, phenols, amines, humic acids, other taste, odor, or color-producing or toxic compounds, bacteria, and algae).

This research will determine to what extent it is feasible to oxidize the organic and inorganic substances in scrub water. The oxidation will be done by means of the wet-oxidation phenomena with and without catalysts. The wet-oxidation phenomena functions best at high temperatures and corresponding saturation pressures.

Therefore, when a gasifier is operating at pressures and temperatures less than those required for the satisfactory functioning of the wet-oxidizer, it is necessary to increase the pressure of the scrub water to that required in the wet-oxidizer.

The concept of a wet-oxidation system for cleaning scrub water from a coal gasifier installation is shown schematically on Figure 1.

OBJECTIVE

The objective of the proposed research program is to demonstrate with the University of Kentucky coal gasifier and small laboratory apparata that the wet-oxidation of organic and inorganic material in the scrub water from the gasifier is technically feasible and economically attractive, to determine the kinetic parameters controlling the process, and to find possible catalysts to accelerate the reaction.

PRINCIPLES OF WET-OXIDATION

Wet-oxidation refers to the aqueous phase oxidation of dissolved or suspended organic substances at elevated temperatures and pressures. This is accomplished by heating the solution or slurry to an appropriate temperature in a closed vessel into which compressed air is admitted. Oxygen in the air reacts with the organic material in the solution or slurry. The terms "wet-oxidation", "wet-air oxidation (WAO)" and "wet-combustion" are used interchangeably to describe this process.

The WAO reaction proceeds towards completion at relatively low temperatures, 350F (177C) to 650F (343C) (3, 5). Pressure is maintained at a level high enough to prevent excessive evaporation, generally 300 psi (2.07 MPa) to 3000 psi (20.7 MPa).

Wet-oxidation takes place through a family of related oxidation and hydrolysis reactions which leads to a range of intermediate products. Catalyst addition results in increased oxidation and decreased hydrolysis (6). High molecular weight compounds are converted to lower molecular weight compounds. Final WAO products from organic compounds are carbon dioxide and water.

The oxidation of inorganic compounds is also important. Most multivalent metallic cations are converted to the highest oxidation state possible, and appear as dissolved compounds or as insoluble hydroxides or oxides. All sulfur forms are oxidized to sulfates which are retained in the product liquor or slurry. Organic nitrogen is converted almost exclusively to ammonia. This can be removed by a small stripping tower, or its generation can be suppressed by catalysts (6). SOx and NOx concentrations are negligible in the gaseous effluent from a WAO process.

THE OXIDATION PROCESS

The research work in wet-oxidation has emphasized the disposal of waste such as sewage sludge (7-25) and paper mill effluents. Zimpro Corporation of Rothschild, Wisconsin has been marketing these systems. Wet-oxidation has been investigated extensively as a waste disposal method for space (8, 15, 16, 20) and ship (10, 11, 12, 18, 19, 21) use. Wet-oxidation has also been proposed for the oxidation of low-grade fuels such as coal washing wastes (4).

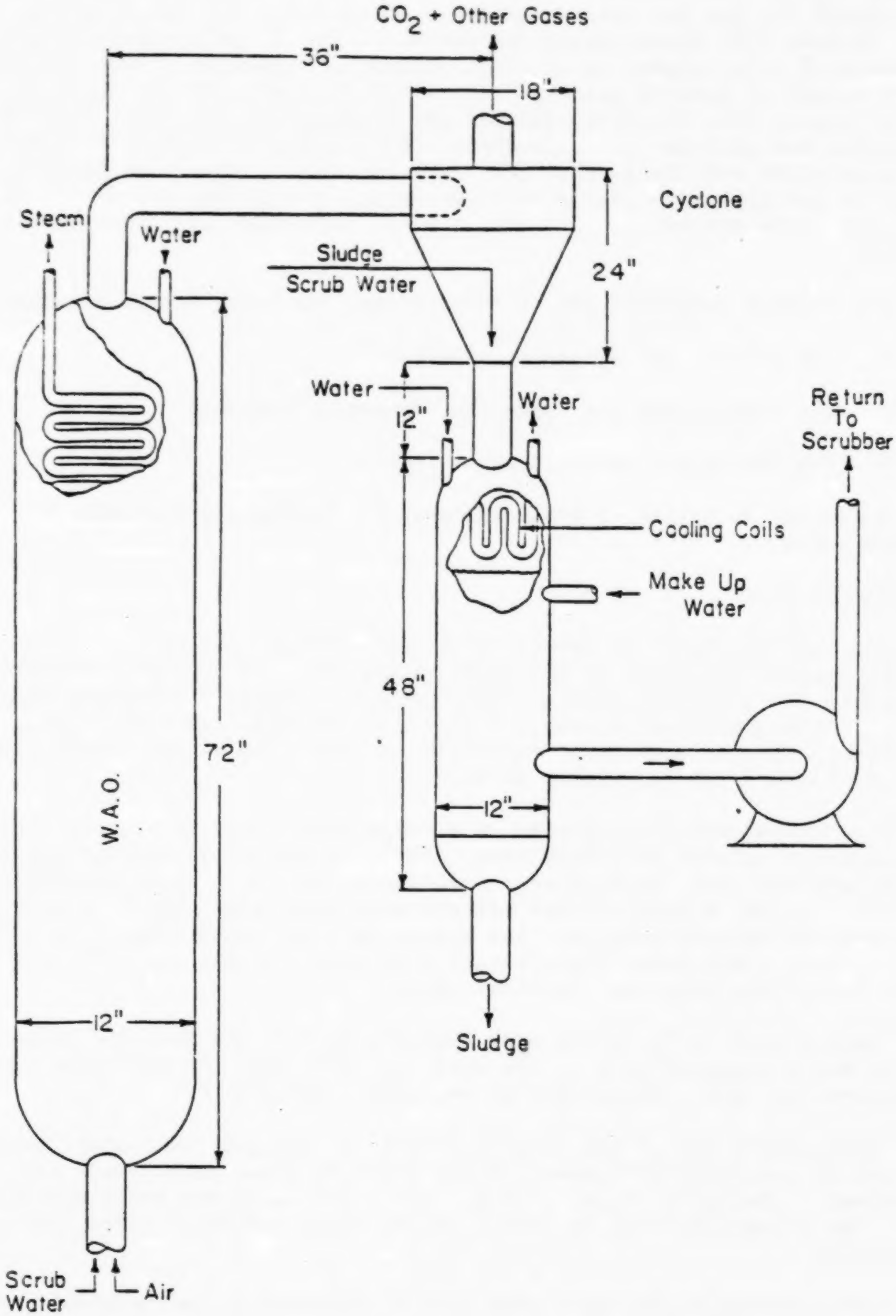
CO2 + Other Gases
36"
18"
Cyclone
Steam
Water
Sludge
Scrub Water
24"
Water
12"
Water
Return
To
Scrubber
Cooling Coils
Make Up
Water
48"
72"
W.A.O.
12"
12"
Sludge
Scrub
Water
Air

Figure 1. Conceptual Wet-Oxidizer Installation at a Gasifier

A literature review of oxidation at high pressures in aqueous solutions by Weygant (26) in 1969 uncovered essentially no theoretical studies of the process except for the patented processes by Toland (27, 28) and Zimmerman (29, 30). Weygant (26) investigated the wet-oxidation of twenty-three organic compounds at temperatures up to 250°C without any catalysts. Converstion ranged from zero to hundred percent. The work by Katzer (31) and Fishbeck, et al. (6) showed that catalyst addition can increase the oxidation from 70 to 99 percent and decrease the hydrolysis reaction under less severe conditions (of temperature and pressure). This suggests that it should be possible to clean the gasifier scrub water in a catalytic wet-oxidizer for recycling and avoid the formation of ammonia, acetic acid, andydrides and other hydrolysis products.

The primary variables for cleanup of gasifier scrub waters are then;

1. the organic and inorganic materials
2. the temperature (and thus the saturation pressure)
3. the catalysts for increased oxidation.

It is the objective to evaluate these parameters and determine the conversion rates.

PROGRESS TO DATE

The existing half ton per day coal gasification unit was modified to permit the easier collection of the waste waters from two venturi scrubbers and to monitor the process conditions more closely. Figure 2 shows the schematic layout of the gasification unit. A test run was completed. Additional modification to the gas monitoring equipment are near completion. Waste water runs are planned for the middle of July.

A batch wet-oxidation system as shown schematically in Figure 3 consisting mainly of a liter autoclave (max. 1000°F at 5000 psig) and various analysis systems has been constructed. Preliminary runs with known compounds were started. It was decided to make several runs with waste waters to find the rate determining compounds and then concentrate the model compound studies on them. Actual waste water from venturi scrubbers contains dust (ash and coal), heavy tars, light oils and dissolved gases.

Considerable difficulties were encountered with the analysis techniques due to the plugging effects of the dust (ash and coal) and the heavy tars. Procedures are under development to overcome these problems.

Considerable effort was made to expand the gas analysis capability both for the wet-oxidation off-gases and the gasifier trace gases which will become dissolved in the waste water. Table 1 lists the gases and their analysis method. An attempt was made to secure two analysis methods for each gas wherever possible.

The organics in the water will also be analyzed by two methods, one; an

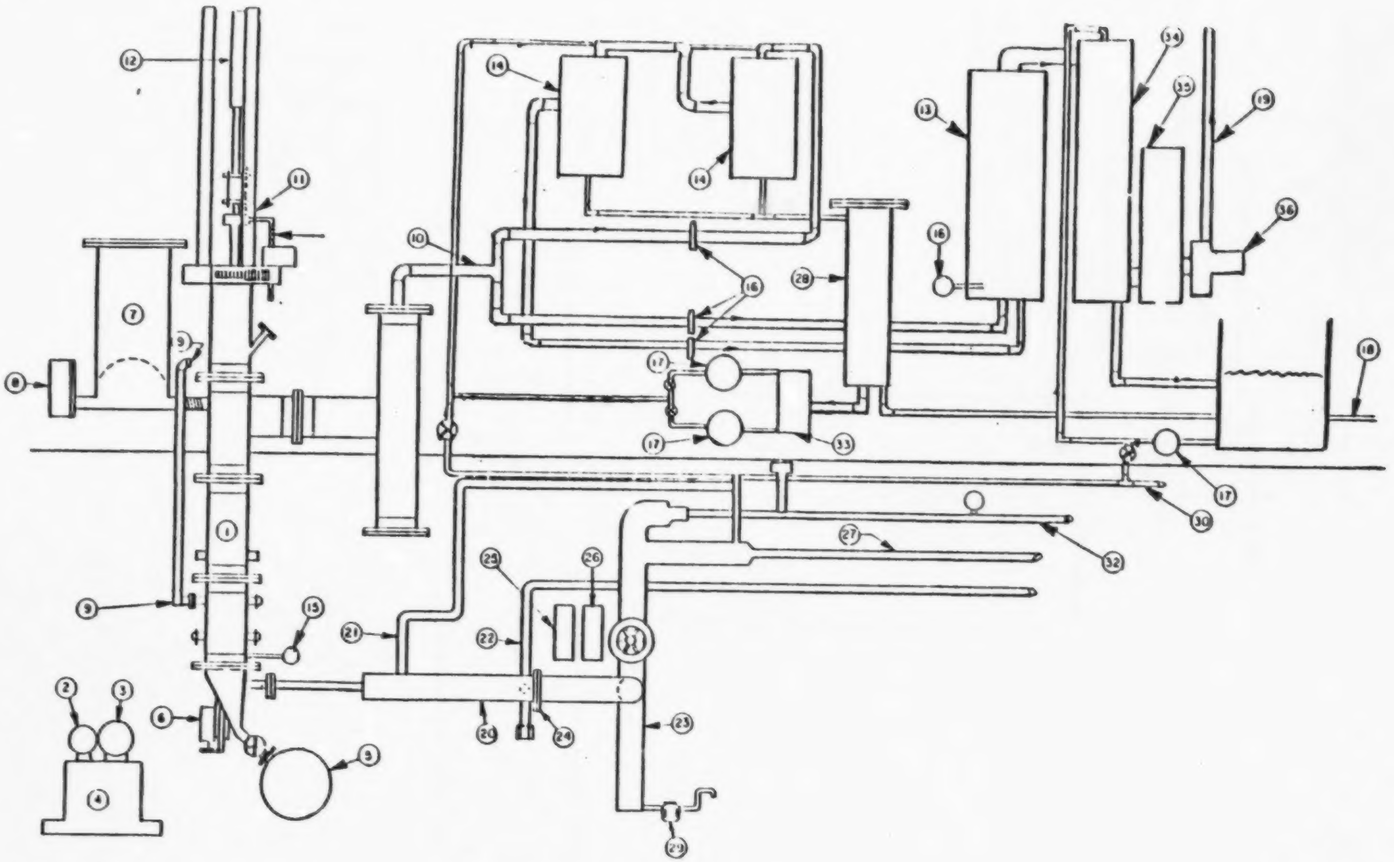

1 GASIFIER
2 FILTER ELEMENT
3 HYDRAULIC PUMP & MOTOR
4 RESERVOIR
5 ASH HOPPER
6 ASH GRATE GEAR HOUSING
7 COAL HOPPER
8 COAL AUGER GEAR SYSTEM
9 RUPTURE DISK
10 3" PIPE

11 AGITATOR
12 HYDRAULIC RAM
13 BAFFLED BURNER
14 VENTURI SCRUBBER & SEPAR.
15 LIGHT OFF BURNER
16 ORIFICE FLOW METERS
17 WATER PUMP & MOTOR
18 DRAIN PIPE TO STORAGE
19 STACK
20 HEAT EXCHANGER

21 3/4" STEAM LINE
22 3/4" CONDENSATE LINE
23 2 1/2" AIR & STEAM LINE
24 AIR ORIFICE METER
25 DIFFERENTIAL MANOMETER
26 PRESSURE MANOMETER
27 STEAM LINE (INLET)
28 TAR SEPAR. & WATERFILTER
29 STEAM TRAP

30 WATER LINE
31 POSITION CONTROL
32 AIR LINE (INLET)
33 FLOW METER & FILTER
34 EXHAUST SCRUBBER
35 MOISTURE SEPAR.
36 EXHAUST FAN
37 DUST SEPARATOR

Figure 2. Gasification Facility.

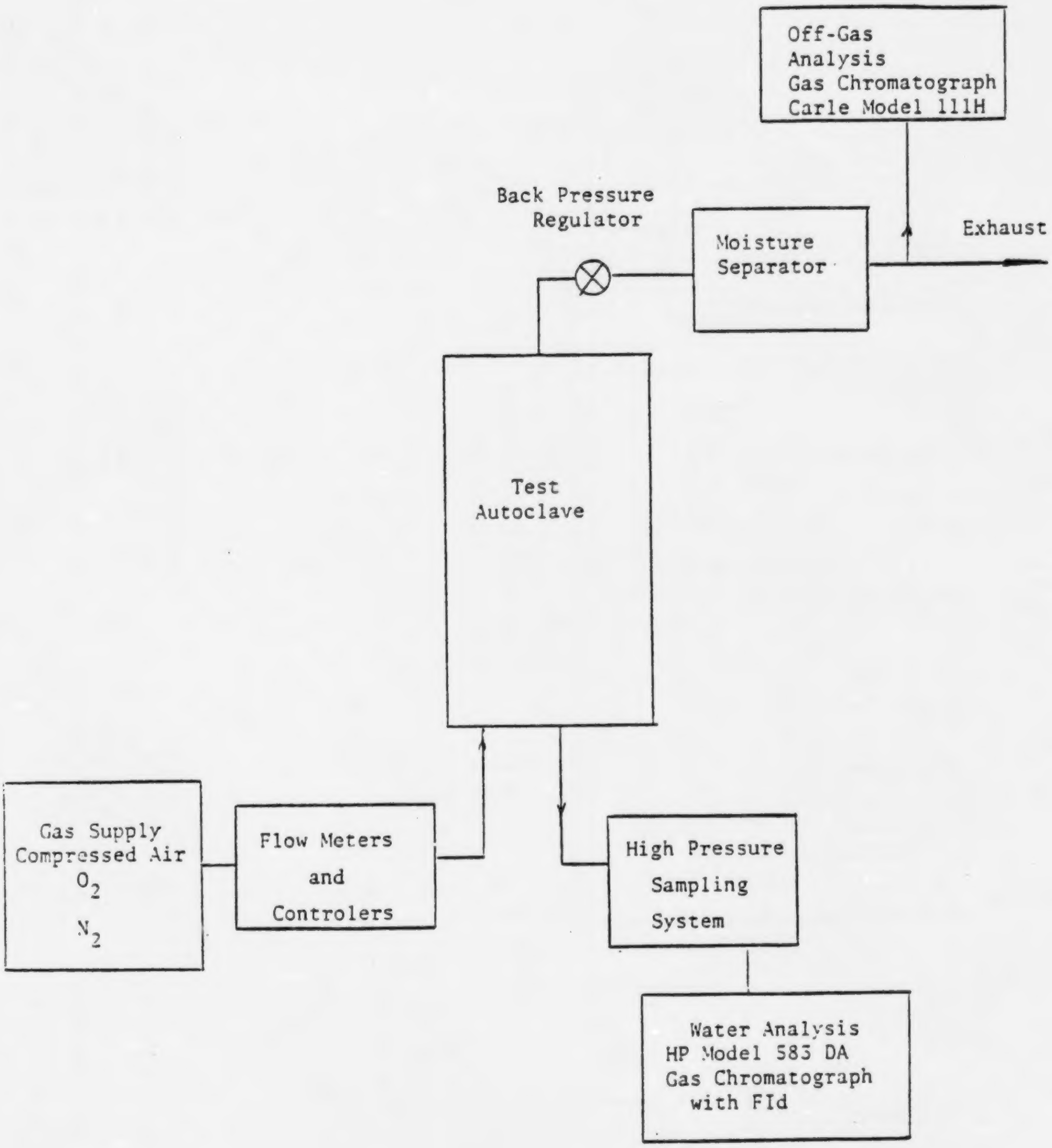
Off-Gas
Analysis
Gas Chromatograph
Carle Model 111H
Back Pressure
Regulator
Moisture
Separator
Exhaust
Test
Autoclave
Gas Supply
Compressed Air
O_2
N_2
Flow Meters
and
Controlers
High Pressure
Sampling
System
Water Analysis
HP Model 583 DA
Gas Chromatograph
with FId

Figure 3. Batch Reactor for Wet-Oxidation.

TABLE 1. GAS ANALYSIS METHODS

	Instruments			
Gases	Infrared Spectrometer*	Ion or Gas Sensitive Electrodes	Gas Chromatograph**	O_2*** Analyzer
H_2S		yes same as (.003)++	---	
COS	yes (0.2)+	yes	---	
CS_2	yes (.5)+	yes	---	
HCN	yes (.4)+	yes (.02)+	---	
NH_3	yes (.2)+	---	yes	
CH_4	yes (.2)+	---	yes	
CO_2	yes (.2)+	---	yes	
CO	yes (.2)+	---	yes	
H_2	---	---	yes	
O_2	---	---	---	yes
N_2 ****	---	---	---	
NO_x	yes (.07-2)+	---	---	

*Beckman Microlab 600 Computing Spectrometer

**Carle Gas Chromatograph Model 111H and Model 111

***Beckman Oxygen Meter Model OH-11EA

****N_2 is determined by difference.

+Minimum detectable concentration, ppm

++Minimum detectable concentration, ppm for all 3 combined

HP Model 5830A gaschromatograph with FI detectors, the other a liquid chromatograph separation on a Beckman column (run with two Constametric II Lab Data Control pumps) and analysis in an infrared spectrometer.

Filtering of the dust (ash and coal) and getting the heavy tars into solution has delayed some of the analysis methods and data.

An HP 1000 Model F Computer was brought on line with extensive data acquisition and control equipment. Programs for data reduction of the IR and GC data are under development.

CONCLUSIONS

The instrumentation and equipment for the study of wet-oxidation of waste from coal conversion plants is in place. Analysis problems due to dust (ash and coal) and heavy tar should be overcome allowing data acquisition by the end of July 1981.

REFERENCES

1. Von Gratkowski, H.W., "Kohlevergasung", Ullmanns Encyklopaedie der technischen Chemie, Third Ed., 1958, pp. 360-483.

2. ...., Low-Btu/Fixed Bed Gasification Program, Morgantown Energy Technology Center, Briefing Document Based on TRW Contract No. DE-AT21-78MC 08496, January 1980.

3. Vasan, S., Peabody Engineering System Co., Private Communications, November, 1976.

4. Pradt, Louis A., Wet Oxidation Boiler-Incenerator Paper Presented at the Annual Kentucky Coal Conference, University of Kentucky, May 2, 1958.

5. Fishbeck, A.G., Anshus, B.E., and Katzer, J.R., "A Design and Economic Evaluation of Wet-Air and Catalytic Oxidation of Sewage Sludge", PB-245-266/2ST (May 1974).

6. Jebens, H.J. and Johnson, R.D., "Water and Waste Water Reclamation in a 21st Century Space Colony", ASME Paper No. 77-ENAS-47 for Meeting, July 11-16, 1977.

7. Jagow, R.B., "Design Fabrication and Testing of a Spacecraft Wet Oxidation System Including Trash Pulverization Studies", ASMW Paper, No. 76-ENAS- 5 for Meeting, July 12-15, 1976.

8. Groves, D., "Wet Oxidation Processing Equipment for Shipboard Usage", Naval Engr. J. 86, 5, 57059 (1974).

9. Fassell, W.M., and Gridges, D.W., "Parctec System for Treatment of Shipboard Waste", Mar. Technol., 11, 3, 297-303, (1976).

10. Schatzberg, Paul, Jackson, D.F., and Kelley, C.M., "Experimental Investigation of the Wet Oxidation Destruction of Shipboard Waste Streams", ASME Paper 74-ENAS-5 for Meeting, July 29 - August 1 (1974).

11. Jagow, R.B., "Investigation of the Feasibility of Using Wet Oxidation to Process Dilute Sewage Onboard a Coast Guard Vessel", ASME Paper 74-ENAS-4 Meeting, July 29 - August 1 (1974).

12. Jagow, R.B., "Development of a Spacecraft Wet Oxidation Waste Processing System", ASME Paper 72-ENAV-3 for Meeting, August 14-16 (1972).

13. Jagow, R.B., Jaffe, R.J., Rynewicz, Jr., and Saunders, "Selection of Materials for Wet Oxidation Waste Treatment Equipment", Space Shuttle Materials, Volume 3, NST Conf., October 5-7, 1971, Soc. Aerosp. Mat. and Process Engr., 1971, p. 507.

14. Jagow, R.B., Jaffe, R.J., and Saunders, C.G., "Processing of Human Wastes by Wet Oxidation for Manned Spacecraft", ASME Paper 70-Av/SpT-1 for meeting, June 21-29 (1970).

15. Weitzmann, A.L., "Development and Testing of a Wet Oxidation Waste Processing System", NASA Report No. NASA-CR-151324 (March 31, 1977).

16. Sommers, L.E., and Curtis, E.H., "Effect of Wet-Air Oxidation on the Oxidation Composition of Sewage Sludges", PB-257-841/8ST (1976).

17. Bridges, D.W., and Fassell, W.M., "Pilot-Plant Demonstration of Wet-Oxidation for Treatment of Shipboard Waste Waters", AD-A028-812/6ST (1974).

18. Jagow, R.B., "A Study to Evaluate the Feasibility of Wet Oxidation for Shipboard Waste Water Treatment Application", AD-A022-854/4ST (1975).

19. ...., Lockheed Missiles and Space Co., "Design, Fabrication and Testing of a Wet Oxidation Waste Processing System", N75-28721/9ST (1975).

20. Schnatzberg, P., Jackson, D.F., and Kelley, C.M., "Experimental Investigation of the Wet Oxidation Destruction of Shipboard Waste Streams", AD-787-061/1SL (1974).

21. Koubek, E., "Hydrogen Peroxide Treatment of Effluent Resulting from Shipboard Pollution Abatement", AD-777-096 (1973).

22. ...., National Materials Adviosry Board, Wash., D.C., "Materials for Wet Oxidation Processing Equipment (Shipboard)", AD-771-745/7 (1973).

23. Rowell, C.F., "Some Technical and Economic Concerns Relating to Shipboard Pollution Abatement", AD-755-540 (1972).

24. Jagow, R.B., "Design and Development of a Prototype Wet Oxidation System for the Reclamation of Water and Disposition of Waste Residues Onboard Space Vehicles", N72-33115.

25. Weygandt, J.C., "High Pressure Oxidation of Organic Compounds in Aqueous Solutions", Ph.D. Dissertation, Kent State University, 1969.

26. Toland, W.G., Jr., U.S. Pat. 2,587,666 (1952), cited by Weygandt.

27. Toland, W.G., Jr., U.S. Pat. 2695313 (1954), cited by Weygandt.

28. Zimmerman, F.J., U.S. Pat. 2824058 (1958).

29. Zimmerman, F.J., U.S. Pat. 2903425 (1959).

30. Katzer, James R., "Solubilization and Wet Oxidation of Suspended and Dissolved Organics", PB-247-106/8ST (1975).

31. De Maio, D., and Naglieri, A., "Catalyst Selection and Evaluation", Chem. Engineering, July 1958.

Comments on
Wet Oxidation of the Waste Water from Coal Gasification Installations

Rolf T. Skrinde
Olympic Associates Co.
Seattle, Washington

INTRODUCTION

The project title is "Wet Oxidation of Waste Water from Coal Gasification Installations", and the Principal Investigator is Dr. O.J. Hahn of the University of Kentucky. The project period is 11/15/80 - 11/14/82, and total project budget $245,275.

The waste water being subjected to wet oxidation is produced at an existing pilot scale coal gasifier at the University of Kentucky. This gasifier has a scrubber system in which the organic pollutants accumulate to a concentration of approximately 5,000 mg/l of which 50% are phenols or phenolic compounds.

PROJECT OBJECTIVES

In the initial stage of research, a series of catalysts will be evaluated to improve wet oxidation efficiencies. In addition, reaction parameters such as temperature, pressure, air/oxygen ratios, and retention times will be investigated in small laboratory autoclave systems which simulate a batch operated wet oxidation process. Later a test loop will be installed in the gasifier system which will be equivalent to continuous flow wet oxidation. This will be operated to confirm reaction parameters and investigate buildup of trace elements in the treated and recirculated waste water. The final phase will consist of data evaluation in a model to predict wet oxidation operation and applicability to larger systems.

PROGRESS TO DATE

Since the project was initiated on November 15, 1980, the primary effort to date has been the construction and start-up of the wet oxidation apparatus. Literature review was essentially complete prior to project start-up.

The existing 1,000 lb. per day coal gasification unit has been modified to permit easier collection of waste waters for use in the research program, and initial waste water runs are planned for July 1981.

A batch wet oxidation system has been constructed and tested on simulated waste waters containing known organic compounds. Organics are analyzed by gas and liquid chromatography and by infrared spectrophotometry. Programs for use of a computer for data acquisition and reduction of IR and GC data are being developed.

SUMMARY COMMENTS

In the eight months since project initiation, the progress appears to be normal. Several months are always required for acquisition, installation, and testing the apparatus to be used. This portion of the work has probably proceeded as well as could be expected.

Distinguishing features of this program, as compared with previous uses of wet oxidation for treatment of organics in waste waters, are the very short retention times to be investigated and the use of catalysts. The well known Zimpro process was typically operated using a one-hour retention time, no catalysts, and achieved essentially 100% oxidation of phenols and phenolic compounds. Recent EPA Pollution Control Guidance Documents contain information on thirty-minute retention periods, which achieved approximately 80% destruction of COD and phenolic compounds. The investigators on this project will use three to five minutes of retention time and will evaluate various catalysts. If substantial oxidation with such short retention periods can be achieved, this will be a significant development in lowering the cost of wet oxidation as a treatment process for coal gasification and liquefaction waste waters.

Based upon the qualifications of the investigators and the ideal location of the project at an existing gasifier, the probability of substantial achievement is anticipated. A primary concern of this reviewer, however, is that the opportunity may be missed to obtain the most useful data possible with respect to wet oxidation as a treatment method. The effluent stream after wet oxidation should be very carefully analyzed not only for the specific organic materials remaining, but also for their susceptibility to biodegradation as a final treatment step.

Wet oxidation has great potential for treatment of non-biodegradable organics not only in that there may be complete oxidation of some components, but an equally valuable use could be in modification of refractory compounds to render them biodegradable. Thus, while the wet oxidation process has appeared to be costly and difficult to apply in past sewage sludge treatment facilities because of the requirements for high operating pressures and temperatures, such operating conditions are routine in coal gasification and liquefaction plants. Reducing the retention time as proposed in this research could more than offset the high costs by the resulting use of smaller reaction vessels. Reduced loadings and modifications of refractive compounds brought about by wet oxidation could also result in substantial cost savings in downstream treatment processes. The use of the Phenolsolvan or other pretreatment processes ahead of biological treatment could be eliminated, and efficient biological treatment of those wastes which are discharged rather than recycled could be achieved.

Although the original proposal does not include biological treatability studies on wet oxidation effluents, the research would be greatly enhanced by incorporating such studies into the program.

THEORY FOR PENETRATION IN A PULSE-JET CLEANED FABRIC FILTER

David Leith, Michael J. Ellenbecker,
and Melvin W. First

Harvard School of Public Health
Department of Environmental Health Sciences
665 Huntington Avenue
Boston, MA 02115

INTRODUCTION

In spite of many attempts to model penetration through fabric filters(2-5), there is presently no satisfactory way to predict dust penetration through a pulse-jet cleaned fabric filter. This is not because of insufficient interest in the problem. Pulse-jet filters have captured a substantial portion of the fabric filter market(1), and the efficiency with which they operate is of strong interest to regulatory officials, to industrial users who must meet emission regulations, and to equipment manufacturers who supply these filters with a performance guarantee.

Performance characteristics which must be considered when modeling penetration include: (1) particle collection by clean fibers in a new fabric, (2) particle collection by the dust deposit accumulated on and in these fabrics, and (3) retention of this dust so it does not seep through the fabric during the rather violent cleaning cycle.

PENETRATION STRAIGHT THROUGH A CLEAN FABRIC

Particle collection by isolated, clean cylinders or fibers has been well studied, and adaptation of single fiber collection models into models for particle penetration through an array of clean fibers are well known(6). Fraser and Foley(4) have made use of this work to describe penetration through a clean woven fabric and Hampl and Rimberg(2) have adapted clean fiber bed theory to a study of particle penetration through clean felt of the kind used in pulse-jet cleaned filters. The latter found that penetration of 0.35 to 1.1 μm particles through clean, new industrial felts ranged from 20 to 70% at typical pulse-jet filtration velocities, penetrations that are much higher than the 1% or less generally found for intermittently cleaned industrial filters using fabrics well conditioned with dust(7-9). Although agreement is excellent between penetration theory and data for clean, new felt fabrics(2), the performance of new felt in the laboratory is clearly different from that of a well conditioned felt when used in an industrial pulse-jet filter.

PENETRATION STRAIGHT THROUGH A DUST DEPOSIT

The accumulation of dust in and on a fabric can affect dust collection in several ways. At low dust accumulation, before a continuous dust deposit forms on the fabric surface, dust particles collect on previously collected particles adhering to the fibers, as well as on the fibers themselves. Because of the greater collection efficiency of the deposited dust particles for collecting additional particles, the apparent efficiency of individual fibers increases as dust collects upon them so that fabrics conditioned with dust have lower penetration than bed(6) or fabric(3,4) composed of new, clean fibers. Fraser and Foley(4) modeled the effect of dust accumulating on woven fabrics by assuming the effect equivalent to a reduction of fiber diameter.

At high dust holdings, when the dust deposit is continuous and uniform on the fabric surface, the deposit acts as a filter cake and efficiency improves further. Cooper and Hampl(3) studied dust penetration straight through a well-developed dust deposit using an entirely theoretical model under the assumptions that impaction, interception (sieving), and diffusion are the important particle collection mechanisms. They determined that essentially no particles larger than 1 μm or so should pass through the dust deposit unless pinholes are present in it. Although models for penetration straight through a dust deposit are not as well developed as those for penetration straight through a clean fiber bed or a clean fabric, theory suggests that a continuous, unflawed deposit should collect virtually all particles from the aerosol passing through it. Theory predicts that penetration straight through a deposit should decrease with increasing particle diameter and increasing filtration velocity(3) for particle diameters larger than a few tenths micrometer.

Although penetration data must be carefully examined with reference to the conditions under which the tests were made, tests on new, clean felts by Hampl and Rimberg(2) show the decrease in penetration with increasing particle diameter and filtration velocity predicted by straight-through theory and bench-scale experiments by Afify and Mohamed(10) and by Hall(11) show that penetration through an uncleaned felt becomes very low when a substantial dust deposit builds up on it. These conclusions generally confirm the Fraser-Foley(4) and Cooper-Hampl(3) theories that virtually no dust penetrates an established dust deposit. However, experiments on uncleaned fabrics are not relevant to the effects of seepage caused by filter cleaning.

PENETRATION BY SEEPAGE

Seepage penetration is defined as a process whereby collected particles later pass through the filter, i.e., seepage is a failure to retain collected dust rather than a failure of collection. In pulse-jet cleaned filters, most seepage is thought to occur when the conditioned fabric strikes its supporting cage at the end of a cleaning pulse(12). Rapid deceleration of the residual dust deposit causes some particles or agglomerates to separate from the support (fabric fibers or other dust particles). As normal filtration flow resumes, some of these particles or agglomerates are swept through the fabric and into the cleaned gas stream.

Seepage penetration is likely to increase whenever the separation force between the collected dust and its substrate increases. For example, large particles or agglomerates with considerable inertia are likely to break loose more easily than small particles when the fabric strikes its supporting cage smartly at the end of a cleaning pulse. It is reasoned that high filtration velocity, which drives the fabric back onto its cage at a faster rate, causes it to hit with greater impact, and thereby aggravates seepage. In contrast, straight-through penetration theory predicts penetration should decrease with increasing particle size and with increasing filtration velocity(2-4) for particles larger than a few tenths micrometer in size. This is opposite to the trends expected from seepage.

PENETRATION MODEL

A reasonable model to describe dust penetration through a pulse-jet-cleaned filter should consider both straight-through penetration and seepage penetration. The rate at which dust passes through the filter can be expressed in terms of outlet mass flux, the mass of dust that penetrates per unit fabric area per unit time:

$$N = N_{st} + N_{se} \qquad (1)$$

in which N represents the total outlet mass flux, N_{st} is the outlet flux due to straight-through penetration, and N_{se} is the flux due to seepage.

The total straight-through flux, for particles of all sizes, will depend on penetration for particles of each size in the inlet aerosol:

$$N_{st} = v\,c_i \int_0^1 P_{st}\,dG \qquad (2)$$

in which v is superficial filtration velocity, c_i is the overall mass concentration for particles approaching the filter, P_{st} is the fraction of particles of a particular size that pass straight through the filter, and dG is the mass fraction of all incoming particles which are of that size.

If the relationship between particle diameter and straight-through flux is needed, then relationships among particle diameter, straight-through penetration, and inlet dust size distribution must be known. However, if an overall value for straight-through flux is sufficient, the overall mass fraction of the inlet dust that passes straight through the filter, $\overline{P_{st}}$, can be used in place of the integral in Equation (2).

As discussed above, dust that seeps through a pulse-jet-cleaned fabric may be comprised essentially of dust driven through the fabric when the fabric strikes its supporting cage as a cleaning pulse ends and filtration resumes. Deceleration of the dust held by the fabric as it strikes the cage may cause a separation force sufficient to free some dust which normal filtration air can then sweep through into the cleaned gas stream. If so, then seepage flux will be:

$$N_{se} = \frac{w}{t} \int_0^1 \varepsilon \, dH \qquad (3)$$

in which w is the mass areal density of the total dust deposit on the fabric as it strikes its cage, t is the time interval between cleaning pulses, ε is the fraction of particles or agglomerates of a particular size in the dust deposit that is separated from the dust deposit as the fabric strikes the cage, and dH is the mass fraction of all particles or agglomerates in the dust deposit that are of that particular size.

If the relationship between particle diameter and outlet flux is required, the relationships among ε, dH, and particle or agglomerate size must be known. If an overall mass outlet flux is sufficient, an overall mass-weighted average for ε can be used, $\bar{\varepsilon}$, in place of the integral in Equation (3). Insufficient data are presently available to allow evaluation of the integral in Equation (3) and in the following discussion $\bar{\varepsilon}$ will be used.

The overall mass fraction of dust separated from a conditioned fabric, $\bar{\varepsilon}$, can be related(14) to the applied area-specific force causing the separation, F_s/A. The exact relationship between fraction of dust separated and separation force applied is not known, and is presently under investigation at this laboratory. Pending the outcome of this work it will be assumed that these variables are proportional:

$$\bar{\varepsilon} = \frac{k^* F_s}{A} \qquad (4)$$

Impulse-momentum considerations say that the area-specific separation force applied, F_s/A, times the time over which this force acts, t^*, will equal the momentum of the area-specific dust deposit as it begins deceleration upon striking the cage:

$$\frac{F_s t^*}{A} = w\,v \qquad (5)$$

Substitution of Equations (4) and (5) into Equation (3) yields:

$$N_{se} = \frac{k^* w^2 v}{t^* t} = \frac{k w^2 v}{t} \qquad (6)$$

in which the unknown proportionality constant, k*, and the time necessary to stop the fabric as it strikes its cage, t*, are combined in a new constant, k, which should depend on the dust separation and retention characteristics of the fabric and fabric elasticity.

Equations (2) and (6) can be substituted into Equation (1) to give an expression for overall outlet flux through the pulse-jet cleaned filter:

$$N = c_i v \overline{P_{st}} + k \frac{w^2 v}{t}. \tag{7}$$

EXPECTED TRENDS IN OUTLET FLUX

Equation (7) predicts the effects of changes in filter operation on overall outlet flux, N. First, consider the case in which straight-through penetration is much more important than seepage; that is, the first term on the right side of Equation (7) is considerably larger than the second:

$$N \doteq c_i v \overline{P_{st}} \tag{8}$$

In this instance, Equation (8) shows that decreases in inlet dust concentration, c_i, should cause a decrease in outlet flux. However, Dennis(9) has determined from field and laboratory studies(7,15) that the mass emission rate or flux from a fabric filter is essentially constant despite changes in inlet concentration.

Straight-through theory predicts that factors which decrease overall penetration, $\overline{P_{st}}$, such as increasing diameter for particles larger than a few tenths micrometer, or increasing dust deposit areal density, should also decrease outlet flux. However, Leith and First(8) determined that large particles penetrate a pulse-jet filter as readily as small particles, at variance with this prediction. Data(16,17) discussed later in this section of the report indicate that more dust penetrates if the dust deposit areal density increases, also at variance with this prediction.

The effect of increased filtration velocity on straight-through outlet flux is unclear. Equation (8) suggests that outlet flux should increase with velocity, v, if all else remains constant; however, increased velocity should also decrease penetration, $\overline{P_{st}}$, for particles collected by impaction so that the net effect of velocity changes on outlet flux is uncertain. In summary, straight-through penetration theory predicts trends generally at variance with those determined experimentally for changes in pulse-jet filter operating conditions such as inlet dust concentration, particle diameter, and areal density of the dust deposit.

Next, consider the case in which seepage is much more important than straight-through penetration, that is, the second term on the right side of Equation (7) is considerably larger than the first:

$$N \doteq k \frac{w^2 v}{t} \tag{9}$$

Equation (9) predicts that outlet flux should decrease with decreases in the areal density of the dust deposit, w, in marked contrast to straight-through theory, but in agreement with experimental data reported by Ellenbecker(6) and by Leith et al.(17). Equation (9) also indicates that decreases in filtration velocity should decrease outlet mass flux, in agreement with several experimental studies(8,18-20) using pilot scale and full scale pulse-jet filters. Dennis(9), Hall(11), and Löffler(13) have shown that outlet dust concentration from a pulse-jet cleaned filter increases substantially but momentarily, immediately after cleaning. Modifications to the cleaning pulse which ease the cleaned bag back to its supporting cage gently so that it hits with less impact have been shown to decrease penetration compared to that found with normal pulse-jet cleaning(21). These results are expected if seepage associated with pulse-jet cleaning causes penetration.

Leith and First(10) measured the relative amounts of straight-through flux and seepage flux for fly ash penetrating a pulse-jet filter using untreated but conditioned polyester bags at superficial filtration velocities from 50 to 150 m/s. Outlet flux was very low for the straight-through mechanism under all conditions, but the seepage mechanism increased with increasing filtration velocity. In general, the conclusion was reached that seepage accounted for essentially all the dust that passed through the pulse-jet filter and was particularly important at high filtration velocities.

Although Equation (9) is presently inadequate to describe the dependence of outlet flux on particle diameter, this relationship can be incorporated into the equation when information adequate to allow integration of Equation (9) becomes available. It should be clear that penetration by particle size will be greatly influenced by filtration velocity, dust loading, pulse pressure, etc. In summary, penetration trends predicted by seepage theory seem generally to agree with trends observed in experiments conducted over a range of pulse-jet filter operating conditions. These trends require precise quantification to make possible a fully comprehensive mathematical model of a pulse-jet cleaned filter. These tests are presently under way at this laboratory.

COMPARISON OF MODEL WITH DATA

If seepage alone accounts for nearly all the dust penetration from a pulse-jet cleaned fabric filter, Equation (9) predicts that a log-log plot of outlet dust flux versus the group w^2v/t should yield a straight line with a slope of unity and an intercept at log(k). Data(16,17) adequate to check this prediction are summarized in Tables (1) and (2). Bags made from untreated polyester felt and Gore-tex felt were tested in a three-bag pulse-jet filter at superficial filtration velocities from 50 to 150 mm/s. Outlet dust concentrations were measured, and total outlet flux calculated. The areal density of the dust on the bags was measured by weighing the bags and subtracting the weight of the clean new fabric. The interval between cleaning pulses was 60 s per bag in each test.

Figure (1) is a log-log plot of outlet dust flux, N, against w^2v/t. The data for both bag types scatter about lines with a unit slope as Equation (9) indicates will occur when outlet flux caused by straight-through penetration is negligible and seepage is caused by deceleration of the bag as it hits the supporting cage. A least squares fit for Equation (9) to the data shown in Figure (1) gives values of $k = 0.0077$ m·s/kg for untreated polyester fabric with coefficient of determination, $r^2 = 0.92$, and $k = 0.034$ m·s/kg for the

TABLE 1. PENETRATION DATA: PULSE-JET CLEANED FILTERS(16,17)

Fabric	N, $kg/m^2 \cdot s$	v, m/s	w, kg/m^2	t,s	w^2v/t, $kg^2/m^3 \cdot s^2$
Gore-tex	3.47×10^{-7}	0.05	0.108	60	9.63×10^{-6}
"	6.30×10^{-7}	0.05	0.149	60	1.84×10^{-5}
"	6.90×10^{-7}	0.05	0.157	60	2.05×10^{-5}
"	3.38×10^{-7}	0.05	0.119	60	1.18×10^{-5}
"	2.58×10^{-6}	0.10	0.222	60	8.21×10^{-5}
"	3.73×10^{-6}	0.10	0.215	60	7.71×10^{-5}
"	1.31×10^{-6}	0.10	0.142	60	3.35×10^{-5}
"	1.55×10^{-6}	0.10	0.195	60	6.31×10^{-5}
Polyester	7.76×10^{-7}	0.05	0.384	60	1.23×10^{-4}
"	9.77×10^{-7}	0.05	0.420	60	1.47×10^{-4}
"	8.64×10^{-7}	0.05	0.349	60	1.01×10^{-4}
"	1.11×10^{-6}	0.075	0.423	60	2.23×10^{-4}
"	1.35×10^{-6}	0.075	0.546	60	3.72×10^{-4}
"	1.13×10^{-6}	0.075	0.348	60	1.51×10^{-4}
"	1.62×10^{-6}	0.10	0.402	60	2.69×10^{-4}
"	3.42×10^{-6}	0.10	0.501	60	4.19×10^{-4}
"	1.83×10^{-6}	0.10	0.372	60	2.30×10^{-4}
"	2.81×10^{-6}	0.125	0.338	60	2.37×10^{-4}
"	2.44×10^{-6}	0.125	0.331	60	2.28×10^{-4}
"	2.74×10^{-6}	0.125	0.441	60	4.04×10^{-4}
"	1.55×10^{-5}	0.15	0.658	60	1.08×10^{-3}
"	1.37×10^{-5}	0.15	0.700	60	1.23×10^{-3}

TABLE 2. OPERATING CONDITIONS: PULSE-JET-CLEANED FILTERS(16,17)

Pulses	
Frequency	once each 60 seconds to each bag
Pressure	690 kPa
Dust	
Type	fly ash precipitated from coal-fired utility boiler
Count median diameter	0.30 μm
Geometric standard deviation	2.7
Feed rate per unit bag area	$3.1 \times 10^{-3} kg/m^2 \cdot s$
Bags	
Number	3
Size	114 mm diameter and 2.44 m long
Construction	Polyester: no surface treatment Gore-tex: ptfe laminate over polyester felt
Weight	Polyester: 0.54 kg/m^2 Gore-tex: 0.46 kg/m^2
Permeability	Polyester: 29 cfm/ft^2 at ½ inch of water Gore-tex: 13 cfm/ft^3 at ½ inch of water

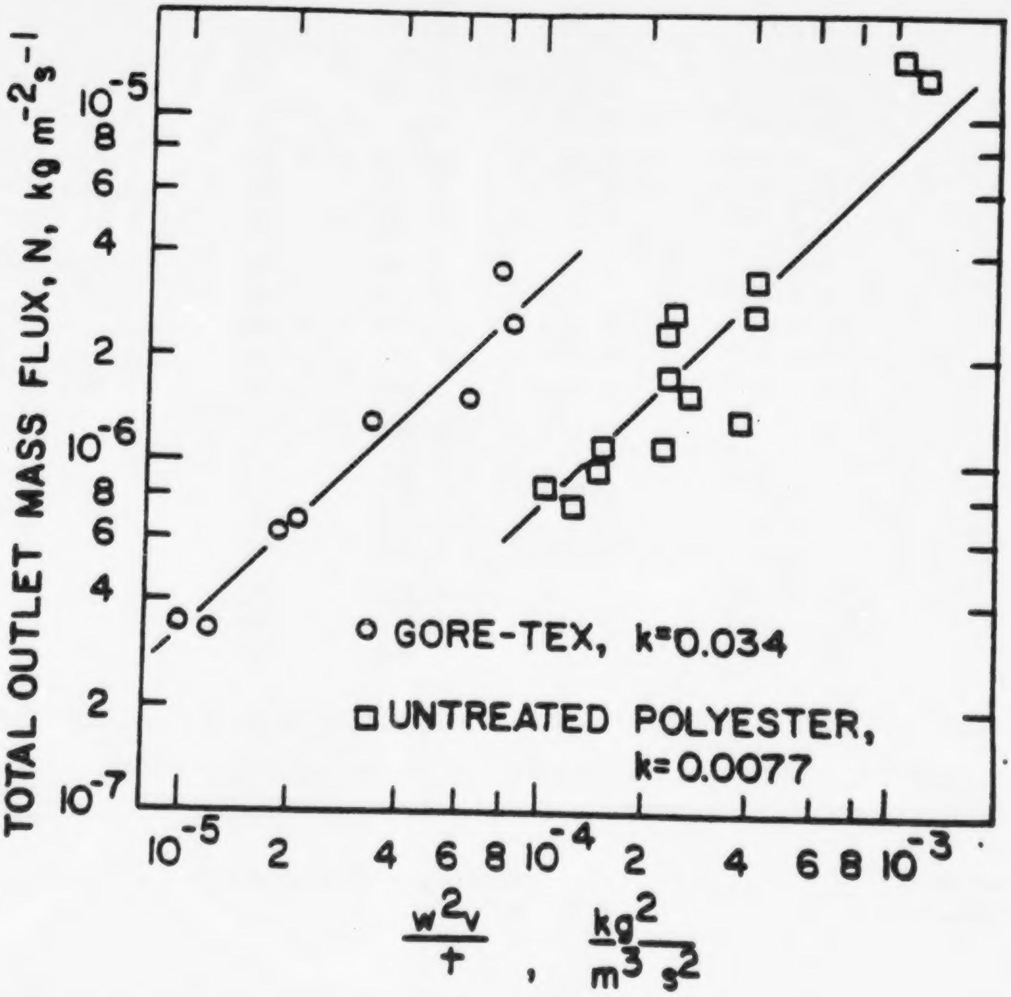

Figure 1. Total outlet mass flux, N, versus w^2v/t, for bags made from Gore-tex and untreated polyester felt.

Gore-tex fabric with $r^2 = 0.96$. The higher value for constant k found for Gore-tex fabric should not necessarily be interpreted to mean that penetration in an operating filter will be higher using Gore-tex fabric, as this fabric retains less dust. Although Equation (9) shows that outlet flux increases with increasing k, it decreases with the square of areal dust density, w. Inter-fabric comparisons require knowledge of both factors.

Figure (2) is a plot of outlet flux determined by Equation (9) using these k values against experimental measurements of outlet flux. It shows that, in general, Equation (9) predicts filter outlet flux reasonably well over a relatively broad range of filtration velocities and dust areal densities, and for fabrics of two kinds.

DISCUSSION

To predict outlet mass flux using Equation (9), values are needed for filtration velocity, v, time between cleaning pulses, t, constant, k, and areal density of the dust deposit, w. Although velocity and time between cleaning pulses are ordinarily known, the other two parameters might not be known. At present the only way to determine constant k is to evaluate data as done in Figure (1). Our data to the present indicate that constant k depends on fabric type, although it is likely to depend as well on the characteristics of the dust collected, pulse pressure, filtration velocity, and other parameters.

The areal density of the dust deposit on the fabric is also likely to be unknown. The magnitude and distribution of the dust deposit on an operating nonwoven bag can be measured with difficulty(22). A procedure for calculating the areal density of the dust deposit on a pulse-jet cleaned filter has recently been developed as part of a theoretical model for pressure drop(14). This procedure, however, requires other information concerning the resistance of the fabric and the specific resistance of the dust deposit which may not be available. Regrettably, it is not presently possible to use Equation (9) to predict quantitatively the outlet flux from a pulse-jet-cleaned fabric filter; further work is necessary.

However, the model is useful to predict the direction of outlet flux to changes in pulse-jet filter operating variables. Equation (9) shows that outlet flux increases with increasing filtration velocity. Increased pulse pressure should decrease the areal dust density, w; if so, outlet flux should also decrease although sufficient dust must remain on the filter to assure good collection of incoming dust. Equation (9) suggests that increasing t, the time between pulses to each bag, should decrease emissions, but this might also increase the areal density, w, of the dust deposit on the bag. An increase in areal density should increase emissions so that the net effect of pulse interval on outlet flux is unclear. Changes to the size distribution of the dust, to the relative humidity or temperature of the gas stream, or to the electrostatic properties of the dust or fabric may all affect constant k; the relationships between these variables and this constant are presently unknown.

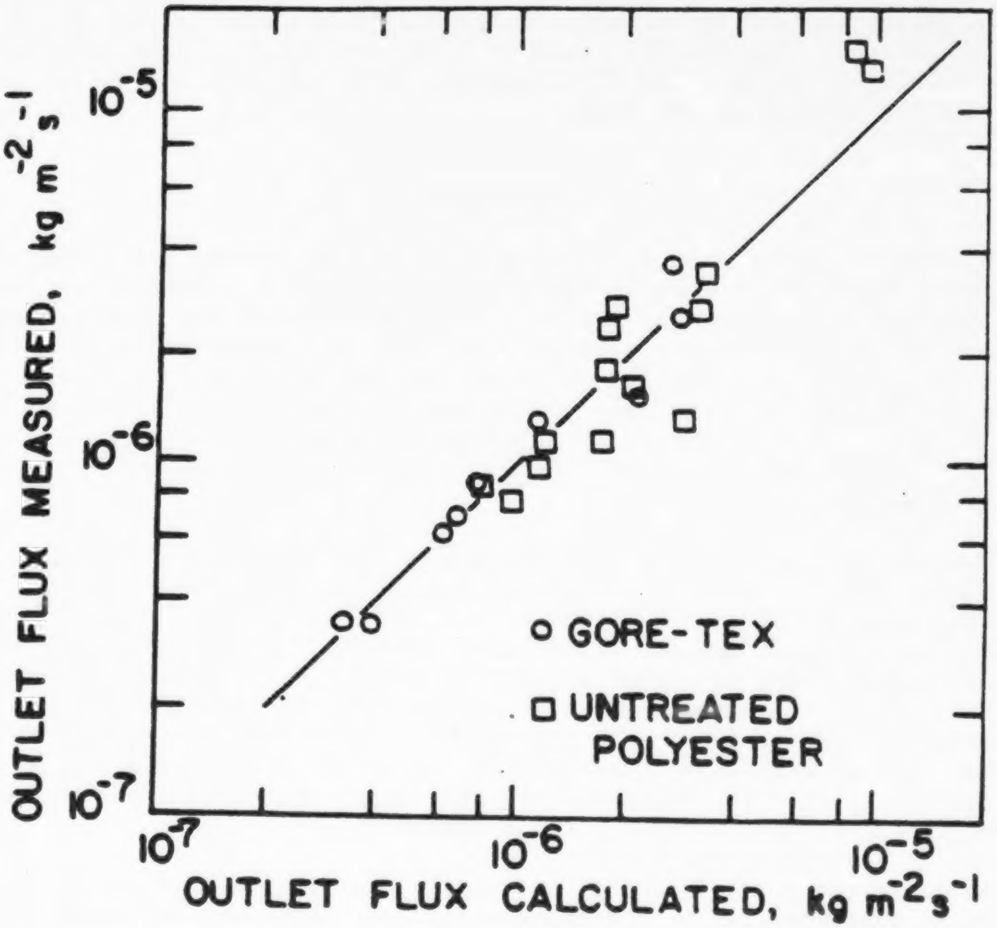

Figure 2. Total outlet mass flux measured versus total outlet mass flux predicted using Equation 9 with k = 0.034 m·s/kg and k = 0.0077 □·s/kg for Gore-tex and untreated polyester bags, respectively.

SUMMARY

Dust can pass straight through a pulse-jet-cleaned fabric filter, and can also pass through by seepage. A model is presented which describes penetration by each of these processes. Comparison of the model with data shows that outlet mass flux from operating filters can be accounted for by seepage alone. Although insufficient information is presently available to use the model for penetration prediction on an absolute scale, these conclusions suggest that additional research on developing a penetration model should emphasize seepage of collected particles through the filter rather than the process of particle collection itself. Furthermore, these results suggest the trends in outlet flux that should occur with changes in operating variables such as filtration velocity, pulse pressure, and fabric type.

The utility of the present model lies in its ability to interpret penetration characteristics of pulse-jet-cleaned filters that previously could not be explained effectively. The agreement found between data and model predictions for outlet flux over a range of filtration velocities, areal dust densities, and for two different fabrics lends strong support to the validity of the assumptions used in the model's derivation. These results strongly suggest that penetration models which do not consider seepage as an important penetration mechanism are seriously flawed. Furthermore, these results indicate that penetration models intended to describe the fractional efficiency characteristics of a pulse-jet-cleaned filter must consider the agglomeration characteristics and particle size-dependent release characteristics of the fabric and dust deposit, rather than relationships between particle size and straight-through penetration alone. These results suggest which future research is likely to be productive, and which is not.

NOMENCLATURE

c_i	dust inlet concentration, kg/m^3
dG	mass fraction of particles of a particular size in the inlet dust, dimensionless
dH	mass fraction of particles or agglomerates of a particular size in the dust deposit, dimensionless
F_s/A	area-specific force acting to separate the dust deposit from its substrate, N/m^2
k	constant, see Equation 6, $m \cdot s/kg$
k^*	constant, see Equation 4, m^2/N
N	total outlet mass flux, $kg/m^2 \cdot s$
N_{st}	outlet mass flux due to straight-through penetration, $kg/m^2 \cdot s$
N_{se}	outlet mass flux due to seepage penetration, $kg/m^2 \cdot s$
P_{st}	fraction of particles of a particular size that pass straight through the filter, dimensionless
$\overline{P_{st}}$	mass fraction of the inlet dust that passes straight through the filter, dimensionless
t	time between cleaning pulses, s
t^*	time during which dust deposit decelerates, s
v	superficial filtration velocity, m/s

w	areal density of dust deposit on and in fabric, kg/m^2
ε	fraction of particles or agglomerates of a particular size in the dust deposit that are separated from the dust deposit, dimensionless
$\bar{\varepsilon}$	mass fraction of the dust deposit that is separated from the dust deposit, dimensionless

REFERENCES

1. Frey, R.E. Types of Fabric Installations. J. Air Poll. Control Assoc., 24:1148, 1974.

2. Hampl, V. and D. Rimberg. Aerosol Penetration of Felt Filter Media. Presented at Annual Conference of Gesellschaft fur Aerosol-Forschung E.V. (Association for Aerosol Research), Bad Soden, Germany, Oct. 16, 1974.

3. Cooper, D.W. and V. Hampl. Fabric Filter Performance Model. In: Conference on Particulate Collection Problems in Converting to Low Sulfur Coals. EPA-600/7-76-016, NTIS, Springfield, Virginia, 1976. pp. 149-185.

4. Fraser, M.D. and G.J. Foley. A Predictive Performance Model for Fabric Filter Systems. 1. Intermittently Cleaned Single Compartment Systems. Paper 74-99 presented at 67th Annual Meeting of the Air Poll. Control Assoc., Denver, Colorado, 1974.

5. Dennis, R., R.W. Cass, D.W. Cooper, R.K. Hall, V. Hampl, H.A. Klemm, J.E. Langley and R.W. Stern. Filtration Model for Coal Fly Ash with Glass Fabrics. EPA-600/7-77-084, NTIS, Springfield, Virginia, 1977.

6. Davies, C.N. Air Filtration. Academic Press, New York, 1973.

7. Dennis, R. and J. Wilder. Fabric Filter Cleaning Studies. EPA-650/2-75-009, NTIS, Springfield, Virginia, 1975.

8. Leith, D. and M.W. First. Performance of a Pulse-Jet Filter at High Filtration Velocity. 1. Particle Collection. J. Air Poll. Control Assoc., 27:534, 1977.

9. Dennis, R. Collection Efficiency as a Function of Particle Size, Shape, and Density: Theory and Experience. J. Air Poll. Control Assoc., 24: 1156, 1974.

10. Afify, E.M. and M.H. Mohamed. Collection of Efficiency and Pressure Drop of Needle Punched Filters. J. of Engineering for Industry, 98:675, 1976.

11. Hall, R.F. Getting the Best Results from Needlefelts in Dust Filtration. Filtr. and Sep., 14:350, 1977.

12. Leith, D. and M.W. First. Performance of a Pulse-Jet Filter at High Filtration Velocity III. Penetration by Fault Processes. J. Air Poll. Control Assoc., 27:754, 1977.

13. Löffler, F. Separation Efficiency and Pressure Loss of Filter Materials of Different Structure, at Differing Conditions. Staub, Reinhalt. Luft., 30(12):27, 1970.

14. Leith, D. and M.J. Ellenbecker. Theory for Pressure Drop in a Pulse-Jet Fabric Filter. Atmospheric Environment, 14:845, 1980.

15. Dennis, R., G.A. Johnson, M.W. First, and L. Silverman. How Dust Collectors Perform. Chem. Eng., 59:196, 1952.

16. Ellenbecker, M.J. Pressure Drop in a Pulse-Jet Fabric Filter. Sc.D. Thesis, Harvard School of Public Health, Boston, 1979.

17. Leith, D., M.J. Ellenbecker, M.W. First, J.M. Price, A. Martin, and D.W. Gibson. Performance of a High Velocity Pulse-Jet Filter II. EPA-600/7-80-042, Research Triangle Park, North Carolina, 1980.

18. Billings, C.E., M.W. First, R. Dennis, and L. Silverman. Laboratory Performance of Fabric Dust and Fume Collectors. AEC Report No. NYO-1590 (revised), 1961.

19. McKenna, J.D., J.C. Mycock, and W.O. Lipscomb. Performance and Cost Comparisons Between Fabric Filters and Alternate Particulate Control Techniques. J. Air Poll. Control Assoc., 24:1144, 1974.

20. Mohamed, M.H., E.M. Afify, and J.W. Vogler. Needle Punched Fabrics in Filtration. Paper presented at Technical Symposium - Nonwoven Product Technology, International Nonwovens and Disposables Association, Washington, D.C., 1974.

21. Leith, D., M.W. First, and D.D. Gibson. Effect of Modified Cleaning Pulses on Pulse-Jet Filter Performance. Filtr. and Sep., 15:393, 1978.

22. Ellenbecker, M.J. and D. Leith. Dust Deposit Profiles in a High Velocity Pulse-Jet Fabric Filter. J. Air Poll. Control Assoc., 29:1236, 1979.

Comments on
Pulse-Jet Fabric Filter Performance

Richard B. Engdahl
Battelle Columbus Laboratories
Columbus, Ohio

This paper is a preliminary report on EPA grant-supported research which is being done on the fundamentals of pulse-jet filtration. In the grant application the following results were expected:

1. Knowledge of particle size released, and models for the mechanisms of release,
2. Knowledge of factors affecting energy consumption.
3. Operational conditions which will optimize cost of operation versus efficiency of capture.

The work described here does not give any of these answers, but it does show good promise of leading toward such definite results.

The careful attention that is being given in this research to all of the factors affecting seepage of particles through the filter medium should lead eventually to actions and practices which will boost the practical efficiency of a device which already has a characteristically high efficiency. Also, it is to be hoped that if this research finds some sources of needless pressure loss in this type of filtration, some means can be devised to eliminate or minimize such losses and thus lead to energy conservation.

The models that are proposed and that have been partially tested appear to provide a better understanding of filter performance which, it is hoped, will show ways to quantify the effects of the important design factors involved.

When the author is farther along in his research, I hope that he can include in each future publication a table showing just what all this means in practical terms. That is, in terms of actual practical numbers, what is the effect of each of the important variables on the performance of typical real-world filters. Such a tabulation will make it easier for engineers to appreciate and to apply the results for practical filter design.

INTEGRATED SWINE WASTE MANAGEMENT SYSTEM FOR POLLUTION CONTROL AND ENERGY AND FOOD PRODUCTION

P. Y. Yang
Department of Agricultural Engineering
University of Hawaii
Honolulu, Hawaii 96822

INTRODUCTION

Anaerobic lagoon has been used as the main swine waste disposal system in Hawaii for years. The operation of anaerobic lagoons system has the following disadvantages: no by-products (such as methane, cell protein) recovery; possible contamination of ground water; large land area; odor problems; accumulation of solids or sludge in the lagoon; and weed growth. Among the existing treatment alternatives for improving the above listed disadvantages, an integrated system combining an effective anaerobic digester (less reactor volume) and a mixed-aerobic microorganism and algae (algal biomass) raceway system is proposed and shown in Figure 1. This system offers the following advantages: a small land requirement; possible biogas collection (fuel use); protein recovery; further removal of soluble chemical oxygen demand (COD), nitrogen, and phosphorous; and environmental acceptability. Two biological reactors, namely, anaerobic digester and algae-bacteria raceway, play an important role in the overall operational performance of the system. Thus, the appropriate design and operational criteria for these two biological reactors are required for the successful operation of a completely integrated swine waste management system.

ANAEROBIC DIGESTION PROCESS

Laboratory bench scale and pilot scale studies of anaerobic digestion of swine wastes in Hawaii have been reported (1, 2, 3, 4).

PROCESS KINETIC (BATCH)

Kinetic studies of methane fermentation by using soluble substrate have been conducted previously by Pearson (5), Pretorius (6), Lawrence and McCarty (7), Ghosh and Pohland (8). The relationship between substrate utilization

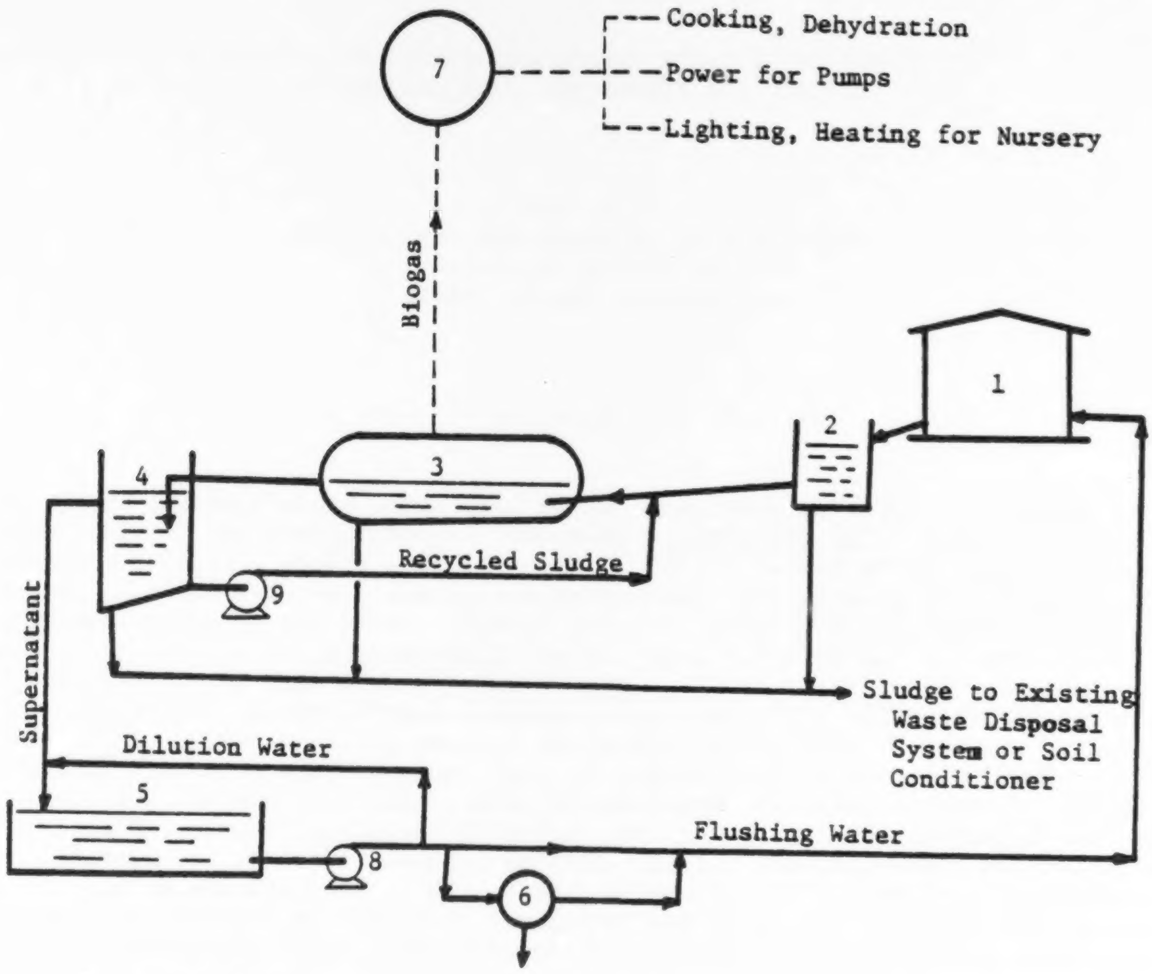
7
Cooking, Dehydration
Power for Pumps
Lighting, Heating for Nursery
Biogas
1
2
4
3
Recycled Sludge
9
Supernatant
Sludge to Existing Waste Disposal System or Soil Conditioner
Dilution Water
5
Flushing Water
8
6

1. Swine House
2. Rectangular Pit
3. Rubber Digester
4. Sedimentation Pit
5. Raceway System
6. Centrifuge or Air Flotation
7. Biogas Holder
8. Flushing Water Transfer Pump
9. Recycled Cell Transfer Pump

Figure 1. Flow diagram of swine waste management system.

and microbial growth can be easily established as shown in the equation developed by Monod (9). However, the use of these models is questionable for the prediction of semi-solid or concentrated agricultural and/or industrial wastewater anaerobic fermentation. Modification of the "Monod" model by using SRT (Solid Retention Time) or HRT (Hydraulic Retention Time) related to substrate stabilization and biogas production was studied and used for predicting and controlling purposes (10, 11). In order to simplify the model, a study was initiated and developed by using direct measurement of total gas production instead of measurement of biological solid content to relate to the total (soluble and insoluble) biodegradable substrate contained in the poultry waste (12). In our previous study (4), this relationship was further investigated as applied to the anaerobic fermentation of swine waste with and without addition of algal biomass since the proposed swine waste management system (Figure 1) includes "algal biomass water" for flushing the pigpens. The result indicates that the gas production is related to the substrate concentration measured as Total Volatile Solids (TVS). Also, two phases of gas production occurring in the methane fermentation of swine waste with and without addition of algal biomass. Therefore, two sets of biological kinetic constants were suggested for the methane fermentation of swine waste with and without addition of algal biomass. Gas yield (the amount of gas produced per TVS removed) and quality of methane content will not be affected by adding 10 percent TVS of algal biomass in the anaerobic digestion of swine waste.

PROCESS PERFORMANCE (SEMI-CONTINUOUS FLOW)

In order to reduce the reactor volume or decrease the hydraulic retention time for the anaerobic fermentation process, a sludge-recycle-system (3) was applied and investigated in both anaerobic digesters of 0.2 m^3 (laboratory scale) and 20 m^3 (field scale). For the anaerobic digester of 0.2 m^3 the operational criteria are listed as follows:

- Loading rate, 2.0 to 3.0 grams of TVS (Total Volatile Solids) per liter of liquid volume per day
- Feeding rate, three times a week
- Ratio of flow rate of recycled sludge to influent flow rate, 0.25
- Ratio of TVS of recycled sludge to TVS of effluent, 3.0 to 3.5
- Overall hydraulic retention time, 6 days

The anaerobic digester resembling a flexible bag 20 m^3 (5,284 gal) was installed and operated at Oshiro's Hog Farm on Oahu, Hawaii. This reactor is shaped like a sausage with a 2 m (6.5-foot) diameter and 6.5 m (21.3-foot) length. The material consists of red-mud plastic and has been called "Rubber or RMP Digester" because of its unique structure, material and shape. The "RMP" digester before and after installation as shown in Figures 2 and 3 features a 20-cm (8-inch) diameter input pipe on one end with two similarly sized effluent pipes on the opposite end. The lower effluent pipe drains the bottom sludge, while the second effluent pipe (located just below the center of the end wall) drains supernatant to a sedimentation pit. Biogas is

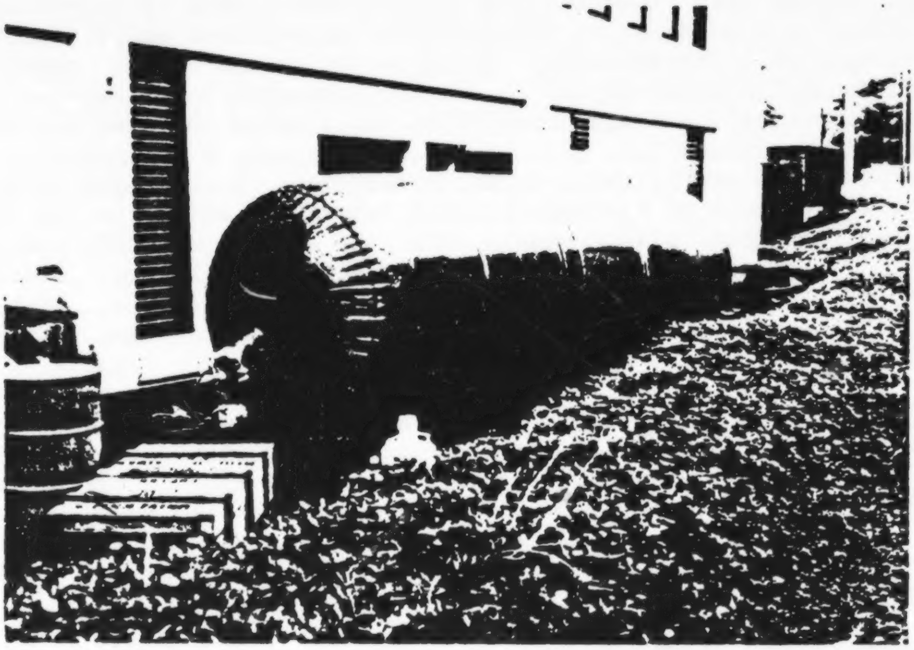

Figure 2. "RMP" digester before installation (20 m^3).

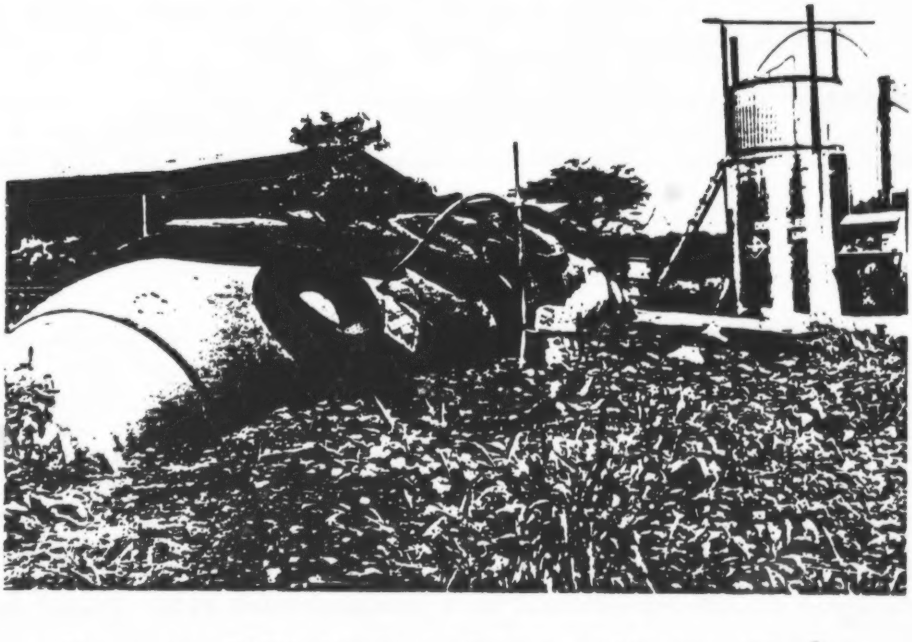

Figure 3. "RMP" digester after installation (20 m^3).

withdrawn from a hose fitted to the upper body. This "rubber" digester has advantages, such as, easy installation, simple operation, low cost and attached gas storage. Operational criteria for this anaerobic digester are listed as follows:

- Loading rate, 1.5 to 3.5 grams of TVS per liter of liquid volume per day
- Liquid volume, 15 m^3
- Feeding rate, twice a week
- Ratio of flow rate of recycled sludge to influent flow rate, 0.2 to 0.26
- Ratio of TVS of recycled sludge to TVS of effluent, 0.5 to 2.5
- Overall hydraulic retention time, 10 days

The gas production rate and gas yield values of 0.2 m^3 are 1.4 liters of gas produced per liter of liquid volume per day and 1.6 liters of gas produced per gram of TVS removed, respectively. Comparing the values to the system without sludge recycle reported previously (1), the system with sludge recycling has slightly higher values. Also, what is more significant is that the system with sludge recycle requires only half of the hydraulic retention time to achieve nearly the same gas production rate. Thus, the reactor volume can be reduced to one-half that of the system without sludge recycling in treating the same quantity of manure per day.

Results of the laboratory study by application of sludge recycling was extended to a field anaerobic digester (20 m^3). Operational criteria were similar to the laboratory scale unit except the overall hydraulic retention time was maintained at 10 days and the ratio of TVS of recycled sludge of TVS of effluent TVS was varied from 0.5 to 2.5. This is because of some difficulties involved in using the appropriate settling tank for maintaining the higher concentration of TVS for recycling in the field. However, as production rate and gas yield value are above 1.0 liter of gas produced per liter of liquid volume per day and 2.0 liters of gas produced per gram of TVS removed between day 60 and 100. After 100 days of operation, they are 0.4 and 1.0, respectively. The methane component in both periods of operation was maintained at about 65 percent of the total gas produced. The occurrence, during the same period, of lower values of gas production rate and gas yield value may be related to the ratio of TVS in the recycling sludge and effluent. Before day 60, the ratio was maintained in the range of 1.0 to 2.5. After day 60, it was difficult to maintain the ratio above 1.0. The higher sludge recycle ratio is expected to provide a higher gas production rate and gas yield value. This is because of decreasing the food to microorganism ratio by increasing the sludge recycle ratio. Therefore, the improvement of better settling or effective separation of solid and liquid for the digested effluent is another area of study which should be further investigated. This will definitely improve the digestion process by the application of sludge recycling. Under sludge recycling condition, both values of gas production rate and gas yield using overall hydraulic retention time of 10 days are higher than the system without sludge recycling (2). Further study on the design and operational criteria of sludge recycling concentration and the minimum hydraulic retention time for anaerobic digestion process of swine waste are still in progress.

ADVANCED AEROBIC TREATMENT PROCESS

Generally, the anaerobic digested effluent still contains high concentration of soluble NH_4-N and COD. The effluent collected from the 20 m^3 anaerobic digester installed at Oshiro's Hog Farm contains 2,000 to 3,000 mg/liter and 10,000 to 24,000 mg/liter of soluble NH_4-N and COD, respectively. This can be considered as an additional water pollution potential if it is released to the existing or receiving water body without further treatment. Therefore, a combined micro-algae and bacteria raceway system to receive the anaerobically digested effluent is proposed. This is expected to:

- Remove (biologically) excess soluble nitrogen and phosphorus and COD
- Enrich the cell protein production by harvesting the algae and bacteria cells
- Purify the anaerobically digested effluent water for reuse
- Serve as a system for aquaculture operation, and crop or vegetable growing if desired

The basic growth kinetic study of mixed micro-algae-bacteria was reported (4). It was concluded that the overall growth pattern of mixed micro-algae-bacteria is similar to the bacteria growth kinetics by using NH_4-N as the growth limiting nutrient. Also, inhibition (decrease of specific growth rate of mixed algae-bacteria) will occur when NH_4-N concentration is above 80 mg/liter. Based on this basic information, a pilot-scale-raceway (3.62 m^3) was developed and operated for 6 months by using the semi-continuous (4.5 months) and continuous (1.5 months) flow operation. The NH_4-N loading rate was maintained at 0.025 gram NH_4-N per liter of liquid volume per day. The removal of soluble NH_4-N and COD was above 96 percent and 87 percent, respectively. The NH_4-N concentrations remained under 80 mg/liter which is the critical value for developing the inhibition effect for the growth rate of algal biomass as indicated in the previous report (4). The soluble COD concentrations were under 1,000 mg/liter (i.e., soluble BOD_5 concentrations were under 300 mg/liter). The suspended solid concentration was maintained in the range of 600 to 900 mg/liter. The crude protein content in the suspended solid was determined occasionally and ranged between 48 to 56 percent. The dissolved oxygen in the system was maintained above 1.0 mg/liter through oxygen input by surface aeration of the rotor (6 rpm), compressed air (air flow rate = 0.55 liter of air per liter of liquid volume per hour) and algal-metabolic generation of oxygen. The compressed air can be eliminated if an appropriate rotor were designed for improvement of oxygen transfer efficiency and optimal growth of algae were maintained.

The effluent produced from the present raceway system can be discharged to the existing domestic sewer system for further treatment if it is available and convenient. If not, the effluent can be further developed for possible use in an aquaculture system or separation of solid (for animal feed or organic fertilizer), and liquid (for reuse of water for the flushing of pigpen). Improvement of solid and liquid separation is in progress now.

A pilot scale involving the integrated swine waste management system is under construction at the Waialee Experiment Station (WES). Hawaii Institute of Tropical Agriculture and Human Resources. The results generated from this integrated system will provide the necessary information to develop an improved and stable swine waste management system for pollution control and energy and animal feed production. Also, mathematical modelling and economic analysis of the system can be developed.

Preliminary study on the anaerobic digestion of swine waste and algae-bacteria processing of anaerobically digested wastewater indicates that an integrated swine waste management system incorporating these two biological reactors for pollution control, energy and animal feed production is technically feasible (3). This system is especially relevant for the location where land, fuel and feed are costly.

ACKNOWLEDGMENTS

This work was partly supported by a research grant from the U. S. Environmental Protection Agency, Hawaii's Governor's Agriculture Coordinating Committee, and Hawaii Institute of Tropical Agriculture and Human Resources. Messrs. Sheiko and David Oshiro generously provided the place for installation and operation of the 20 m^3 anaerobic digester.

REFERENCES

1. Yang, P.Y., Huang, C.J., and Gitlin, H.M., Enhanced Energy Production and Water Reuse for Swine Operation in Hawaii. Presented at the Summer Meeting of ASAE and CSAE, Winnipeg, Canada, 1979.

2. Yang, P.Y., Huang, C.J., Gitlin, H.M., and Hugh, W.I., Low Cost, On Site and Effective Waste Management System for 2000-pig Farm in Hawaii. Presented at the International Symposium on Biogas, Microalgae and Livestock Wastes, Taipei, Taiwan, 1980.

3. Yang, P.Y., Nagano, S.Y., Lin, J.K., and Wong, Y.T., Integrated Swine Waste Management System - A Preliminary Study. Presented at the 36th Annual Purdue Industrial Waste Conference, West Lafayette, Indiana, 1981.

4. Yang, P.Y., and Huang, C.J., Anaerobic and Micro-Algal Process Kinetics for Swine Wastes. In press, Journal of the Environmental Engineering Division, ASCE, 1981.

5. Pearson, E.A., Kinetics of Biological Treatment. In: Advances in Water Quality Improvement; E.F. Gloyna and W.W. Eckenfelder, Jr., (ed.), University of Texas, Austin, 1968, pp. 381-384.

6. Pretorius, W.A., Anaerobic Digestion III, Kinetics of Anaerobic Fermentation. Water Research, Vol. 3, 1969, pp. 545-558.

7. Lawrence, A.W., and McCarty, P.L., A Unified Basis for Biological Treatment Design and Operation. Jour. Sanitary Eng. Div., ASCE, Vol. 96, 1970, pp. 757-778.

8. Ghosh, S., and Pohland, F.G., Kinetics of Substrate Assimilation and Production Formation in Anaerobic Digestion. Jour. Water Poll. Control Fed., Vol. 46, 1974, pp. 748-759.

9. Monod, J., The Growth of Bacterial Cultures. Ann. Rev. Microbiol., Vol. 3, 1949, pp. 371-394.

10. Morris, G.R., Jewell, W.J., and Loehr, R.C., Anaerobic Fermentation of Animal Wastes: A Kinetic Design Evaluation. Proc., Industrial Waste Conf., Purdue Univ., Lafayette, Indiana, Vol. 32, 1977, pp. 689-700.

11. Chen, Y.R., and Hashimoto, A.G., Kinetics of Methane Fermentation. Biotech. and Bioeng. Symp., Vol. 8, 1978, pp. 269-282.

12. Yang, P.Y., and Chen, K.K., Anaerobic Digestion of Poultry Wastes With and Without Acid Hydrolysis Pretreatment. Proc., Cornell Agr. Waste Mgmt. Conf., Syracuse, New York, 1977, pp. 423-435.

Comments on
Integrated Swine Waste Management System for Pollution Control and Energy and Food Production

Richard I. Dick
Cornell University
Ithaca, New York

INTRODUCTION

The swine waste management problem is intriguing. The wastewater contains high concentrations of potential contaminants, and the wastewater volume is comparatively low. Also, the identification of workable solutions requires consideration of the nature of the industry. That is, simple and economical solutions have merit.

PROCESS SELECTION

Fortunately, the wastewater is readily biodegradable. The anaerobic digestion process being explored by the principal investigator for this concentrated biodegradable waste is an obvious choice.

Professor Yang's finding that separation and recycle of suspended solids improved anaerobic digestion performance is the expected result. The treatment scheme used is the anaerobic contact process developed by Fullen (1953) and Schroepfer, et al. (1955). The applicability of this variation of the anaerobic digestion process in this instance seems questionable, however, because of the desirability of a simple treatment facility. Separation of solids from anaerobically digested material is troublesome, and the process requires an additional pump and operating attention.

Because an economical and simple digestion facility is sought, the merit of digester volume reduction through solids separation and recycle needs to be closely examined. A larger (but, still, low-cost) digester could be used in lieu of the anaerobic contact process to achieve comparable results. Jewell, et al. (1981) has used simple plug-flow reactors in anaerobic digestion of dairy cattle wastes with good success. Their digesters are built with flexible liner material; the lower portion of the reactor is earthen-supported and the upper portion inflates with digester gas.

While it may seem heretic to question the desirability of algal biomass production, the aerobic phase of the proposed treatment scheme adds complications and expense. Professor Yang suggests that the output from the aerobic treatment process would be valuable as a fertilizer, but it should be noted that the nitrogen content would probably be lower than that of the anaerobic digester discharge because of ammonia stripping from the aerated basin. It is not clear why a satisfactorily stabilized sludge directly from the anaerobic digester could not be applied to agricultural land, eliminating the need for the aerobic phase. Similarly, the justification of aerobic treatment to produce biomass to serve as the source for additional methane from the anaerobic digester seems tenuous inasmuch as Professor Yang indicates that the algal biomass will represent only about 10 percent of the volatile solids fed to the anaerobic digester. It seems doubtful that the increased gas production would justify the inclusion of aerobic treatment facilities with associated costs and operational difficulties (note that the separation of algal cells from treated wastewater is not a simple matter). Based on results from the research, it would be desirable to ascertain whether or not aerobic treatment is justified except where required to achieve a high quality effluent.

DATA COLLECTION AND ANALYSIS

It is recognized that the data presented in the paper are from the author's previous work—not from work conducted under the current EPA grant. However, to achieve the objective of developing design and operation criteria for integrated swine management facilities, changes in data collection and evaluation procedures will be necessary.

Professor Yang used the hydraulic residence time and the recycle rate to specify anaerobic digester design and operating conditions. These parameters do not provide an adequate description of conditions. The appropriate parameter is the mean cell residence time which is established by the inventory of solids in the anaerobic system and the rate at which they are removed. The mean cell residence time can readily be determined, but not from the operation data reported.

Similarly, data that will permit rigorous analysis of performance must be obtained if results are to be used to develop design and operational criteria in accordance with the project proposal. Complete mass balances (on suspended solids, volatile suspended solids, chemical oxygen demand, nitrogen, and other parameters) are needed to assess performance, and additional operational parameters (such as alkalinity, volatile acids, pH, etc.) must be observed. Similarly, in order to assess results it is necessary to have an evaluation of the ultimate biodegradability of the raw waste. (Note that Chandler, et al. (1980) reported that wastewater from piggeries exhibited a higher degree of biodegradability than most common residues.)

OPTIMIZED DESIGN

While it is proposed to develop design criteria for integrated systems of swine waste management, the objective of the treatment system is not clear. What is the basis for optimization in design and operation of such a facility? Is gas production to be maximized? Is the degree of stabilization to be maximized? Is gas production per unit of expenditure to be maximized? Is cost to meet some effluent quality requirement to be minimized? It would seem necessary to identify an objective to determine appropriate design and operating conditions.

SUMMARY

In summary, if the goal of developing design and operating criteria for swine wastewater management systems is to be achieved, appropriate data collection and analysis procedures must be used. If solids separation and recycle is practiced in the anaerobic digester, then the data required to determine the mean cell residence time should be collected. Studies of the biodegradability of the waste would be desirable to enable assessment of results. Complete mass balances on the treatment systems are needed to meet project objectives and appropriate operational data should be collected.

To meet the goal of developing design and operational criteria, it will be necessary to specify the objectives of the treatment process. It is hoped that the project results (including information on operational stability and convenience) will be combined with economic data in order to assess the relative merit of process configurations. The writer suspects that the complications imposed by use of the anaerobic contact process may not be warranted for simple swine waste management systems (that is, a larger digester of low-cost construction may be preferable to a smaller one with solids separation and recycle) and that the use of aerobic treatment may not be justifiable in the system unless it is required to meet effluent quality (that is, use of aerobic treatment simply for biomass production may be unjustified).

REFERENCES

Chandler, J.A., W.M. Jewell, G.M. Gossett, P.J. Van Soest, and J.B. Robertson, "Predicting Methane Fermentation Biodegradability", Biotechnology and Bioengineering Symposium No. 10, 93-107 (1980).

Fullen, W.S., "Anaerobic Digestion of Packing Plant Waste", Sewage and Industrial Wastes, 25, 576-585 (1953).

Jewell, W.M., R.M. Kabrick, S. Dell'Orto, K.J. Fanfoni, and R.J. Cummings, "Earthen-Supported Plug Flow Reactor for Dairy Applications", paper presented at Methane Technology for Agriculture Conference, Cornell University, Ithaca, New York (1981).

Schroepfer, G.J., W.J. Fullen, A.S. Johnson, N.R. Ziemke, and J.J. Anderson, "The Anaerobic Contact Process as Applied to Packinghouse Wastes", Sewage and Industrial Wastes, 27, 460-486 (1955).

THE REMOVAL OF HEAVY METALS BY ACTIVATED CARBON PROCESS FROM WATER AND WASTEWATER

I. SOME PRELIMINARY OBSERVATIONS

C. P. Huang, M. O. Corapcioglu,
D. W. Blankenship, A. E. Boomhower, P. L. K. Fu
Department of Civil Engineering
University of Delaware, Newark, Delaware 19711

INTRODUCTION

Heavy metals are hazards to almost all living systems. Most of the commonly occurring heavy metals in the environment, such as lead(II), mercury(II), cadmium(II), nickel(II), chromium(VI), and silver(I), are biologically non-essential and non-beneficial, and have a high pollution potential (1). Much has been reported on the occurrence, the distribution, and the adverse effects of heavy metals in the environment; it is clear that the elimination or removal of heavy metals from water and wastewater is extremely important for the protection of public health.

Many processes have been suggested for removing heavy metals from the aqueous system (2). These include chemical precipitation, ion exchange, membrane separation, liquid extraction, foam separation, and adsorption processes. While no single process may be superior to the other, it appears that a technically effective process is not always economically feasible and vice versa. Chemical precipitation by neutralization, for example, is probably by far the most popular technique for heavy metal removal due to its relatively low cost and simplicity of operation. However, the presence of organic and inorganic substances capable of forming metal complexes can render this process ineffective. Furthermore, the extra post-precipitation effort in precipitate-water separation that is always needed for total industrial wastewater treatment can be very costly. The search for a process that will be subject to application over a wide range of conditions appears to be a worthy undertaking in light of the increasing heavy metal pollution problems. The objective of this research was to investigate the activated carbon process as an alternative to other treatment schemes for metal-containing water and wastewater.

Activated carbon, since its introduction in 1900 by Ostrejko, has been used mostly as an adsorbent for the removal of organic substances (3). The use of activated carbon for inorganic removal is a relatively recent endeavor. A recent review of inorganic removal by activated carbon processes by Huang revealed that most of the research effort on the subject matter was made by foreign researchers such as the Russians, the Japanese, and the Europeans. In the United States, the research effort on pollutant removal by activated carbon has been overwhelmingly concentrated on organic substances, due partly to the lack of understanding of the surface chemistry of activated carbon and the chemistry of heavy metals in water and wastewater.

Many factors can affect the heavy metal removal capacity of activated carbon. Notably, the surface properties of activated carbon and the physical-chemical characteristics of heavy metal-containing solutions are the two most important gross parameters. Since the chemical speciation of metal ions and the development of surface charge depend on the pH values of the system, pH was chosen as a master variable in the present study to examine the effect of activated carbon type on the removal of five heavy metals, namely cadmium(II), zinc(II), lead(II), mercury(II), and arsenate(V). The presence of organic substances on the removal of heavy metal was also investigated.

AQUEOUS HEAVY METAL CHEMISTRY

Important information pertinent to the mode of chemical interactions between heavy metals and hydrous solids such as activated carbon is the speciation of aqueous metal ions. In the absence of complex formation agents, except hydroxyl ions which are intrinsic to the deprotonation reaction of water molecules, divalent metal ions can exist in aqueous solution as the barest cations, e.g., M^{2+}, or as metal-hydroxo species, e.g., $M(OH)_x{}^{2-x}$. Many hydrolysis reactions of multivalent metal ions have been thoroughly studied and reported in the literature (5). The following expression is generally applicable to describing the hydrolysis reaction with the formation of hydroxo species

$$M^{2+} + xH_2O = M(OH)_x{}^{2-x} + xH^+ \ ; \quad {}^*K_x \tag{1}$$

where, $^*K_x$ is the equilibrium hydrolysis constant. Table 1 lists the $^*K_x$ values for the metals studied (6). As a result of the hydrolysis reactions, the amount of total metal, M(II), should include the $M(OH)_x{}^{2-x}$ species, i.e.,

$$M(II) = \sum_{x=o}^{n} M(OH)_x{}^{2-x} \tag{2}$$

or

$$M(II) = [M^{2+}] + \sum_{x=1}^{n} {}^*K_x[M^{2+}]/[H^+]^x \tag{3}$$

The first term on the right-hand side of Equation (3) is referred to as the free metal ion which is generally hydrated. The number of coordinated water molecules associated with each free metal ion is a function of the relative ionic radius of the free metal ion and the water molecule. Accordingly, the fraction of the various metal species, $\alpha_{M(OH)_x}{}^{2-x}$, can be expressed by the following expression:

$$\alpha_{M(OH)_x}{}^{2-x} = \frac{[M(OH)_x{}^{2-x}]}{M(II)} \tag{4}$$

$$= \frac{[M(OH)_x^{x-2}]}{\sum_{x=o}^{n} [M(OH)_x^{2-x}]} \qquad (4a)$$

$$= \frac{*K_x/[H^+]^x}{1 + \sum_{x=1}^{n} *K_x/[H^+]^x} \qquad (4b)$$

TABLE 1. EQUILIBRIUM CONSTANTS FOR METAL HYDROLYSIS (6)

Equilibrium	Log Constant (25°C, I=0)
$Hg^{2+} + H_2O \rightleftharpoons Hg(OH)^+ + H^+ ; *K_1$	- 3.4
$Hg^{2+} + 2H_2O \rightleftharpoons Hg(OH)_2 + 2H^+ ; *K_2$	- 6.2
$Hg^{2+} + 3H_2O \rightleftharpoons Hg(OH)_3^- + 3H^+ ; *K_3$	-21.1
$Pb^{2+} + H_2O \rightleftharpoons Pb(OH)^+ + H^+ ; *K_1$	- 7.7
$Pb^{2+} + 2H_2O \rightleftharpoons Pb(OH)_2 + 2H^+ ; *K_2$	-17.1
$Pb^{2+} + 3H_2O \rightleftharpoons Pb(OH)_3^- + 3H^+ ; *K_3$	-28.1
$Zn^{2+} + H_2O \rightleftharpoons Zn(OH)^+ + H^+ ; *K_1$	- 9.0
$Zn^{2+} + 2H_2O \rightleftharpoons Zn(OH)_2 + 2H^+ ; *K_2$	-16.9
$Zn^{2+} + 3H_2O \rightleftharpoons Zn(OH)_3^- + 3H^+ ; *K_3$	-28.4
$Zn^{2+} + 4H_2O \rightleftharpoons Zn(OH)_4^- + 4H^+ ; *K_4$	-41.2
$Cd^{2+} + H_2O \rightleftharpoons Cd(OH)^+ + H^+ ; *K_1$	-10.1
$Cd^{2+} + 2H_2O \rightleftharpoons Cd(OH)_2 + 2H^+ ; *K_2$	-20.3
$Cd^{2+} + 3H_2O \rightleftharpoons Cd(OH)_3^- + 3H^+ ; *K_3$	-31.7
$Cd^{2+} + 4H_2O \rightleftharpoons Cd(OH)_4^{2-} + 4H^+ ; *K_4$	-44.0
$H_3AsO_4 \rightleftharpoons H_2AsO_4^- + H^+ ; K_{a1}$	- 2.24
$H_2AsO_4 \rightleftharpoons HAsO_4^{2-} + H^+ ; K_{a2}$	- 6.96
$HAsO_4 \rightleftharpoons AsO_4^{3-} + H^+ ; K_{a3}$	-11.50

Results of chemical speciation of the metals studied are shown in Figure 1. From Figure 1, it is seen that, in the absence of complex-formation and chemical precipitation, the pH region within which free metal ions are the major species is < 2, < 4, < 7, and < 8, respectively for Hg^{2+}, Pb^{2+}, Zn^{2+}, and Cd^{2+}. In other words, the acidity of the free metal ions follow the order $Hg^{2+} > Pb^{2+} > Zn^{2+} > Cd^{2+}$. Furthermore, the only metal monohydroxo species that is present in significant quantity is $Pb(OH)^+$ ($9 < pH < 10$); whereas, $M(OH)_2(aq)$ is the major species for Zn(II), Hg(II) and Cd(II) over the pH range studied herein.

The aqueous chemistry of arsenic is not as straightforward as the above heavy metals since it can exist in water at two stable oxidation states, namely As(V) and As(III). Arsenite is a weak monoprotic base; whereas, arsenate is a weak triprotic base. Since arsenite behavior is rather inert toward most adsorbents, research effort only emphasized arsenate. The speciation of arsenate is accomplished by the following expressions

$$\alpha_{H_3AsO_4} = \frac{[H^+]^3}{D} \tag{5a}$$

$$\alpha_{H_2AsO_4^-} = \frac{[H^+]^2 \cdot K_{a1}}{D} \tag{5b}$$

$$\alpha_{HAsO_4^{2-}} = \frac{[H^+] \cdot K_{a2} \cdot K_{a1}}{D} \tag{5c}$$

$$\alpha_{AsO_4^{3-}} = \frac{K_{a3} \cdot K_{a2} \cdot K_{a1}}{D}\, . \tag{5d}$$

Where $D = K_{a1}K_{a2}K_{a3} + K_{a1}K_{a2}[H^+] + K_{a1}[H^+]^2 + [H^+]^3$; K_{a1}, K_{a2}, K_{a3} are the acidity constants for the consecutive deprotonation reactions

$$H_3AsO_4 \rightleftharpoons H^+ + H_2AsO_4^- \tag{6a}$$

$$H_2AsO_4^- \rightleftharpoons H^+ + HAsO_4^{2-} \tag{6b}$$

$$HAsO_4^{2-} \rightleftharpoons H^+ + AsO_4^{3-} \tag{6c}$$

Figure 1 shows the distribution of various As(V) species as a function of pH. It indicates that within the pH of interest, i.e., $3 < pH < 10$, the major As(V) species are $H_2AsO_4^-$ and $HAsO_4^{2-}$.

MATERIALS AND METHODS

ACTIVATED CARBON

A total of 14 different brands of activated carbon provided by three major national activated carbon manufacturers were used in this study. They

TABLE 2. TYPICAL PHYSICAL-CHEMICAL PROPERTIES OF ACTIVATED CARBON $^{(a)}$

Manufacturer	Carbon Type	Iodine Number (mg/g)	Surface Area		Total Pore Volume (cm^3/g)	Average Diameter (mm)	Ash %	Water Soluble %	pH$_{zpc}$ (this lab)
			N$_2$ BET	(m^2/g) (b)					
CALGON P.O. Box 1346 Pittsburgh, PA 15230	Filtrasorb								
	100	> 850	850- 950	950	--	--	4.3$^{(b)}$	--	6.5$^{(c)}$
	200	> 850	850- 900	925	--	--	3.6$^{(b)}$	--	--
	300	> 900	950-1050	900	--	1.5-1.7	11.1$^{(b)}$	0.5	
	400	>1000	950-1050	1100	--	0.9-1.1	5.1$^{(b)}$	0.5	7.0$^{(b)}$
ICI Wilmington, DE 19897	Darco G-60	--	--	--	--	--	1.4	0.3	--
	KB	--	1500	--	1.5	--	2.6	1.5	--
	S-51	--	650	600	1.0	--	19.2	1.5	--
	T-70	900	1000-1100	--	0.9	--	< 6.0$^{(a)}$	--	--
	Hydro Darco								
	3000	550	550- 650	550	1.0	1.4-1.6	21.0	--	5.5$^{(c)}$
	C	--	550	--	--	--	28.2	5.5	--
WESTVACO Covington, VA 24426	Nuchar SA	> 800	1400-1800	700$^{(b)}$	--	--	5.3	3-4	3.7$^{(b)}$
	SN	> 800	1400-1800	1400$^{(b)}$	--	--	5.0	3-4	4.2$^{(b)}$
	WVG	>1050	>1100	900	--	0.90-1.20	6.1	--	--
	WVL	> 950	>1000	1250	--	1.4-1.7	7.0	--	7.5$^{(c)}$
	WVW	> 850	> 910	925	--	--	4.8	--	--

(a) Provided by manufacturers unless indicated.

(b) This laboratory

(c) Singer, P. C. (7)

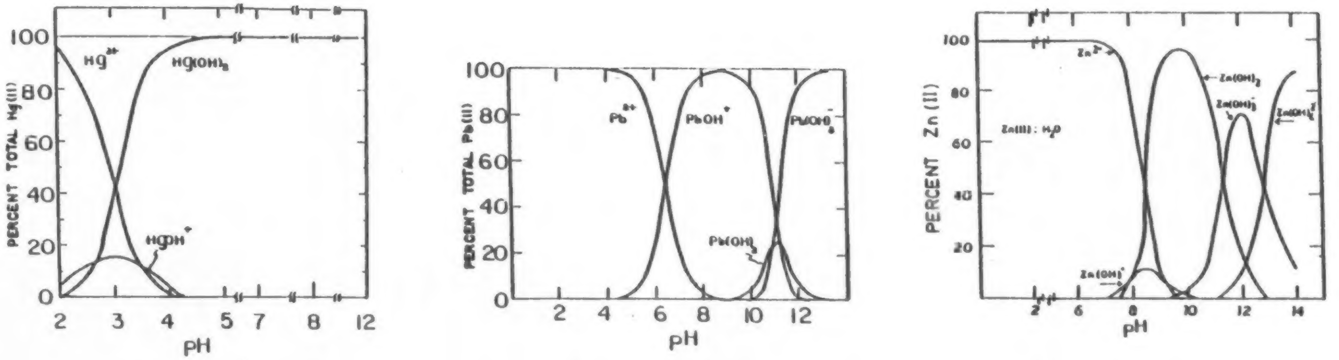

Figure 1a

Figure 1b

Figure 1c

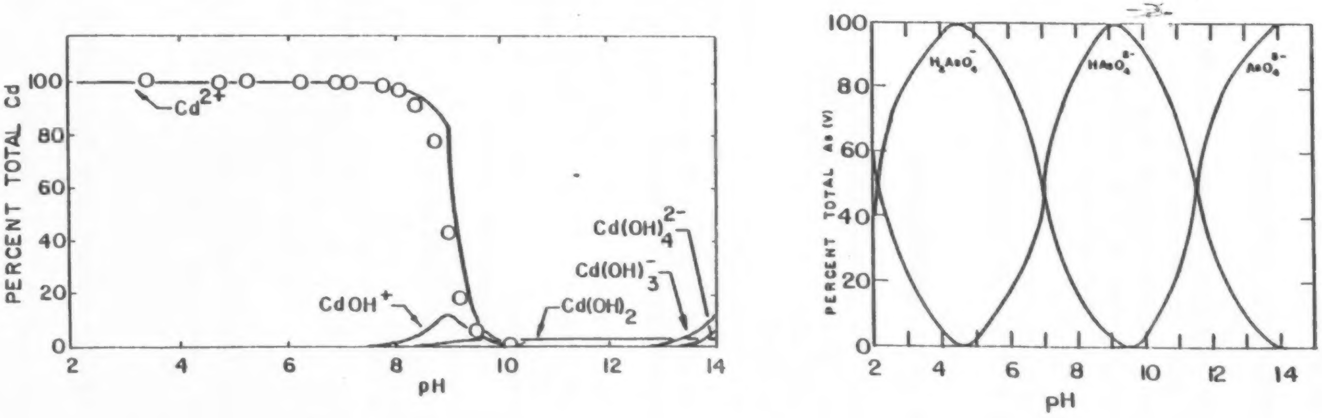

Figure 1d

Figure 1e

Figure 1. Chemical speciation of heavy metals studied: (a) Mercury(II), (b) Lead(II), (c) Zinc(II), (d) Cadmium(II), and (e) Arsenic(V). All solutions are prepared with metal perchlorate except Cadmium (II) which is a synthetic cadmium plating solution which composition was given by Huang and Smith (8).

are Filtrasorb 100, Filtrasorb 200, Filtrasorb 300, Filtrasorb 400 (manufactured by Calgon Co.), Nuchar SN, Nuchar SA, Nuchar WV-W, Nuchar WV-L, Nuchar WV-G (manufactured by Westvaco Co.), Darco-KB, Darco-HDC, Darco G-60, Darco S-51, and Darco HD 3000 (manufactured by ICI Americas, Inc.) Table 2 gives the typical physical-chemical properties of the activated carbons used in this study. All activated carbons were used as received unless noted in the experimental section.

CADMIUM(II) ADSORPTION EXPERIMENTS

A synthetic cadmium plating wastewater prepared as $Cd(BF_4)_2$ solution was used (8). In this study the activated carbon was first hydrated in distilled water for 5 days before adding the stock chemical solutions to give an overall 10^{-4} M of $Cd(BF_4)_2$ and 10^{-2} M of $NaClO_4$. All samples were pH adjusted using NaOH and $HClO_4$ and then shaken on a mechanical shaker for 72 ± 4 hours. At the end of this mixing period, the final pH value was recorded, the sample filtered and the filtrate was analyzed for residual Cd(II) concentration with a Jarrell-Ash 810 Atomic Absorption Spectrophotometer at a primary wavelength of 2288 Å.

MERCURY(II) REMOVAL EXPERIMENTS

All activated carbons used were first washed three times in distilled-deionized water then dried to constant weight in a 105° C oven. The carbon was then equilibriated in 0.025 M $NaClO_4$ solution for at least one week prior to use for hydration reaction to occur. The stock mercury solution was prepared by adding approximately 0.1 g of HgO powder to 1 ℓ of 0.025 M $NaClO_4$. The resulting suspension was stirred overnight and then filtered (Gelman membrane filter 0.45 μm) yielding a saturated Hg(II) solution of *ca* 2×10^{-4} M Hg(II) verified later by Hg(II) standards.

Removal experiments were conducted in closed 125 mℓ LPE bottles (Nalgene). To begin the experiment, 50 mℓ of Hg(II) stock solution was added to 50 mℓ of the stock carbon suspension. Adjustment of pH was accomplished using standard reagent grade $HClO_4$ and freshly prepared NaOH solution. The bottles were placed in a plexiglass chamber with constant flow-through prepurified N_2-gas to minimize the effect of CO_2 on pH. Mixing was provided by a reciprocating shaker (Eberbach Model 6000) at 150 excursions per minute. At the end of the reaction period, 24 ± 2 hours, the activated carbon particles were separated from the suspension by centrifugation and/or filtration. The residual concentration of Hg(II) was determined by the cold-vapor technique at a wavelength of 2537 Å with a Jarrell-Ash Atomic Absorption Spectrophotometer (9).

To account for possible Hg(II) removal by reduction and volatilization, the cold-vapor apparatus was modified to monitor the quantities of Hg(g) released upon the addition of activated carbon under various pre-selected pH conditions.

ZINC(II) AND PB(II) ADSORPTION EXPERIMENTS

A given amount (1 g) of activated carbon was mixed with given volume of stock $Zn(ClO_4)_2$ or $Pb(ClO_4)_2$ solution and $NaClO_4$ to give an overall metal concentration of 10^{-4} M or 5×10^{-9} M. Ionic strength was 5×10^{-2} M (as $NaClO_4$) and the carbon dose was 10 g/ℓ. The pH values of the samples were adjusted with $HClO_4$ and/or NaOH to cover the range of 2.5 to 11. The samples were constantly mixed with a reciprocating shaker for 24 hours. At the end of this preselected time period, the pH values were measured and recorded; the activated carbon particles were separated from the suspension by filtration with 0.45 μm membrane filters. The amounts of Zn(II) or Pb(II) removed were determined by measuring the residual concentration of Zn(II) or Pb(II) with an Atomic Absorption Spectrophotometer (Jarrell-Ash Model 810) at 2139 Å and 2170 Å for Zn(II) and Pb(II), respectively.

ARSENATE REMOVAL EXPERIMENTS

The activated carbon at a quantity of 20 gm was prewashed with 10 mℓ of 1 M NaOH for 24 hours followed by three consecutive washings with 1 ℓ distilled water each time for three hours. The washed carbon was then dried in an oven at 103° C overnight then cooled in a temperature before use. Samples were prepared by adding a given amount of activated carbon to 125 mℓ plastic bottles containing given amount of stock arsenate and $NaClO_4$ solutions to yield an overall arsenate concentration of 10^{-4} M and ionic strength of 10^{-2} M as $NaClO_4$. The samples were adjusted to various initial pH values with NaOH and $HClO_4$, then shaken constantly in a mechanical shaker for 24 hours. At the end of this time period, after recording the final pH value, three 10 mℓ identical samples, with carbon particles separated by filtration, were taken for chemical analyses.

To the first subsample (#1) was added 1 mℓ of an oxidizing agent, KIO_3 (5×10^{-2} M), and one drop of 1 M HCl to oxidize arsenite As(III) to arsenate As(V) for total arsenic analysis; 2 mℓ of a reducing agent, metabisulfite-thiosulfate was added to the second subsample (#2) for background phosphate analysis; and to the third subsample (#3) was added a blue color developing agent, a mixture of ammonium molybdate, sulfuric acid, ascorbic acid and potassium antimony tartrate to obtain the concentration of phosphate and arsenate together. The absorbance was measured with a UV-visible Spectrophotometer, Hitachi-Perkin Elmer at 8650 Å (10). The amount of arsenate removed by reduction is determined by taking the difference in concentration between the first and the third subsamples.

The amount of arsenate adsorbed is obtained from the total initial arsenate, the amount of arsenite, and the amount of arsenate remaining in solution. The last quantity was taken from the difference in concentration between subsamples #3 and #2.

RESULTS

The rate of metal adsorption on activated carbon is rather fast as exemplified by Hg(II) (Figure 2). The equilibrium adsorption was attained over a time period of a few hours. The results shown in Figure 2 were for a powdered activated carbon, with a surface area mainly of external origin. It is speculated that the reaction rate for powdered activated carbon should

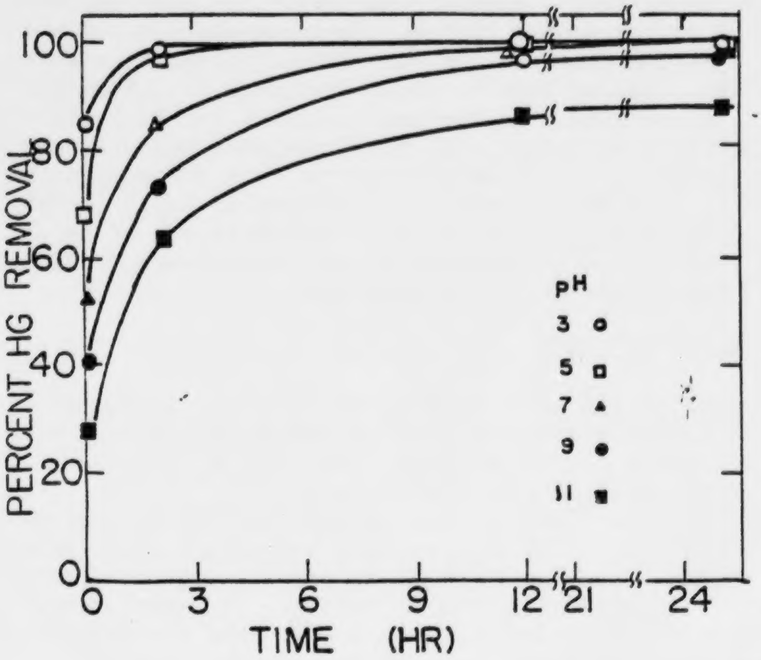

Figure 2. The rate of Hg(II) removal by activated carbon. The experimental conditions were 10^{-5} M $Hg(ClO_4)_2$, 1 g/ℓ Nuchar SA and 0.025 M $NaClO_4$ as ionic strength.

be faster than for granular activated carbon, since diffusional resistance could be much greater with the granular activated carbon where surface sites are largely contributed by internal micropores. However, the results reported by Huang and Ostovic (11), and Huang and Smith (8) did not show much difference in the rate of Cd(II) removal by granular activated carbon. The results reported herein were obtained from adsorption experiments carried out at least for a time period of 24 hours and longer and can therefore be considered as equilibrium data.

The adsorption characteristics of Cd(II) by various brands of activated carbon are illustrated in Figure 3. The results show that the magnitude of Cd(II) adsorption increases with pH to reach a maximum value. This adsorption behavior is, in general, similar to other adsorption systems of heavy metals and solid oxides or hydroxides (12,13). At a specific pH value, depending upon carbon type, an abrupt increase of Cd(II) adsorption was observed. This implies that the particular activated carbon can have greater Cd(II) removal capacity in the acidic region if the pH of abrupt adsorption, pH_{abr} , is low. Among the various types of activated carbon tested, Nuchar SA and SN appear to have the smallest pH_{abr} at *ca* 3; Darco HDC has a pH_{abr} of 7; whereas all other activated carbons have a pH_{abr} ranging between 8 and 8.5. The results also show that regardless of activated carbon type, a 100% Cd(II) removal can be accomplished, at least under the experimental conditions observed. From Figure 3, it is also seen that chemical precipitation may play a significant role in Cd(II) removal at pH > 8.5, although it is not possible to differentiate these two removal mechanisms, i.e., adsorption and precipitation, with the present experimental procedure.

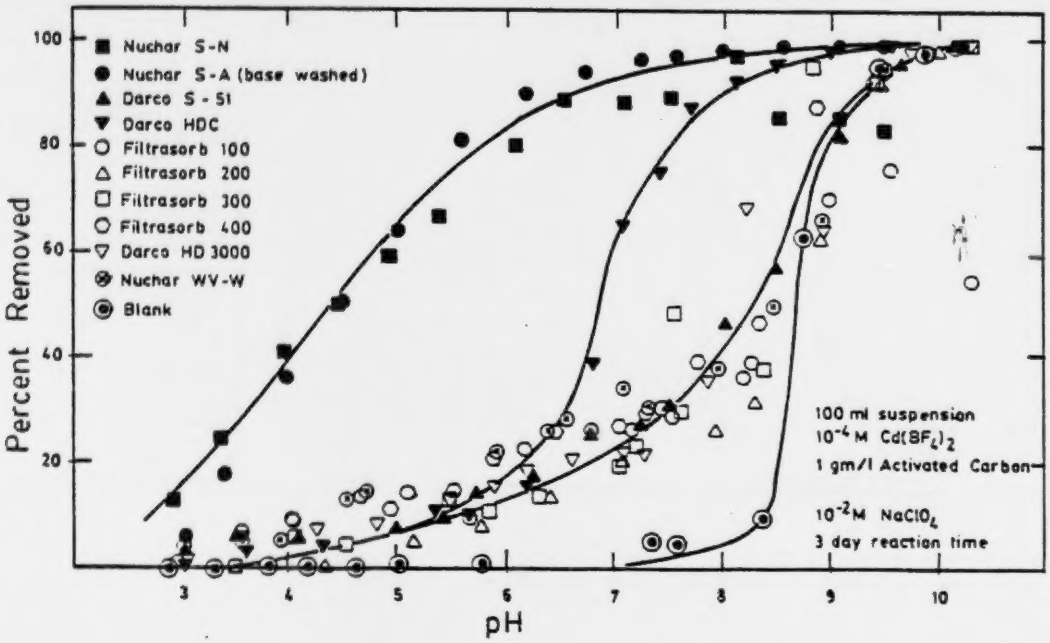

Figure 3. Effect of carbon type on Cd(II) removal.

The adsorption behavior of Zn(II) by activated carbon is shown in Figure 4. The results indicate that Zn(II) removal depends more on carbon type than Cd(II), as almost each activated carbon has its own discrete absorption curve. However, the overall adsorption pattern remains unchanged, i.e., the amount of Zn(II) adsorption increased with increasing pH and abruptly increases at a specific pH value; the extent of Zn(II) adsorption remains at a maximum in the mid-pH region then decreases somewhat with increasing pH. The values of pH_{abr} are Nuchar SN << 2, Nuchar SA < 3, Darco KB < 3.5, Filtrasorb ∿ 4, Nuchar WV-W, Darco S ∿ 5.0 and Darco HDC ∿ 5.5. The results also indicate that the removal of Zn(II) is mostly accomplished by adsorption reaction rather than chemical precipitation.

Figure 5 shows the removal of Pb(II) by the various types of activated carbon. The results show extremely good performance by all activated carbons in Pb(II) removal. Furthermore, the major mechanism responsible for Pb(II) removal is adsorption rather than chemical precipitation. The results again demonstrate that Nuchar SA and Nuchar SN, although appearing most effective in Pb(II) removal in the acidic region, become somewhat less capable in comparison with other activated carbon at pH > 6 due partly to their highly negatively charged surfaces.

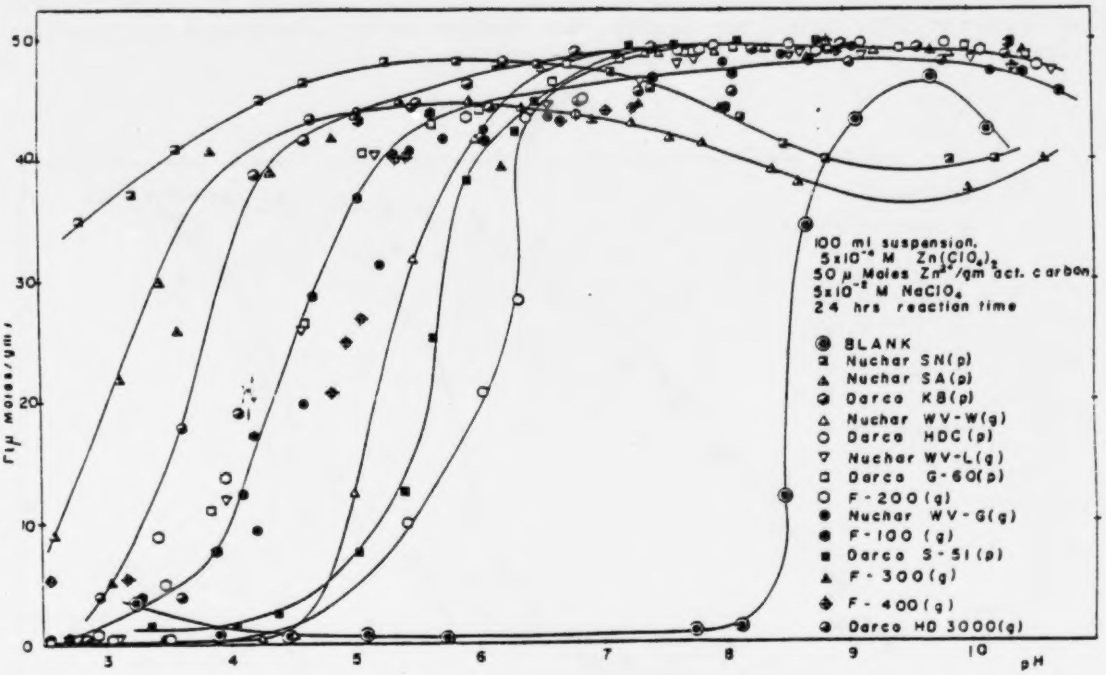

Figure 4. Effect of carbon type on Zn(II) removal.

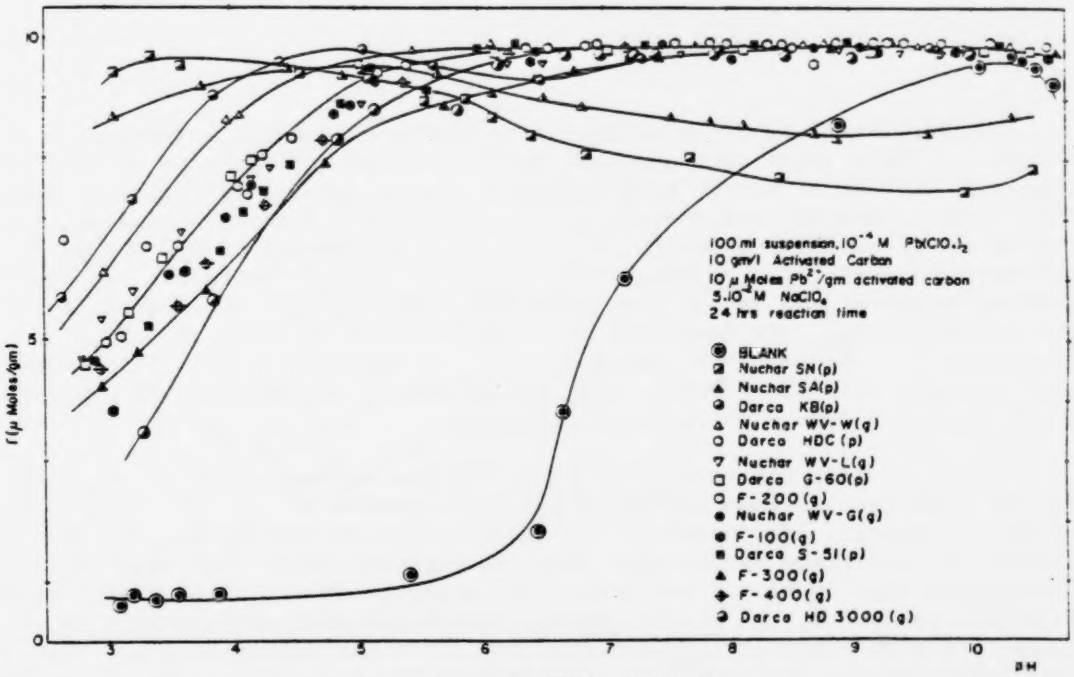

Figure 5. Effect of carbon type on Pb(II) removal.

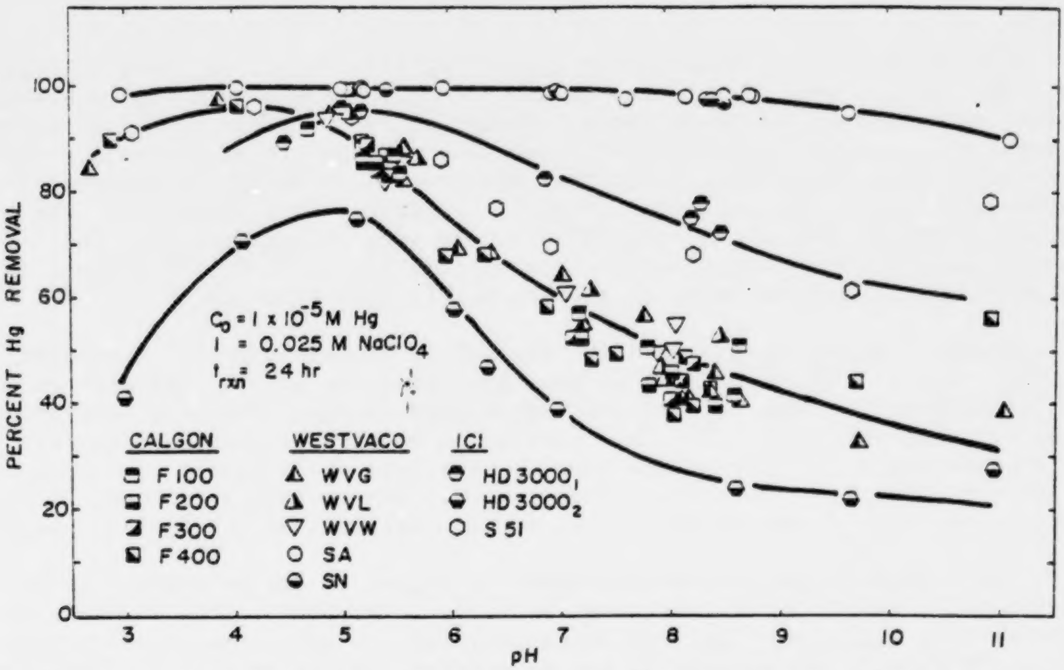

Figure 6a. The effect of carbon type on Hg(II) removal: (a) Total removal.

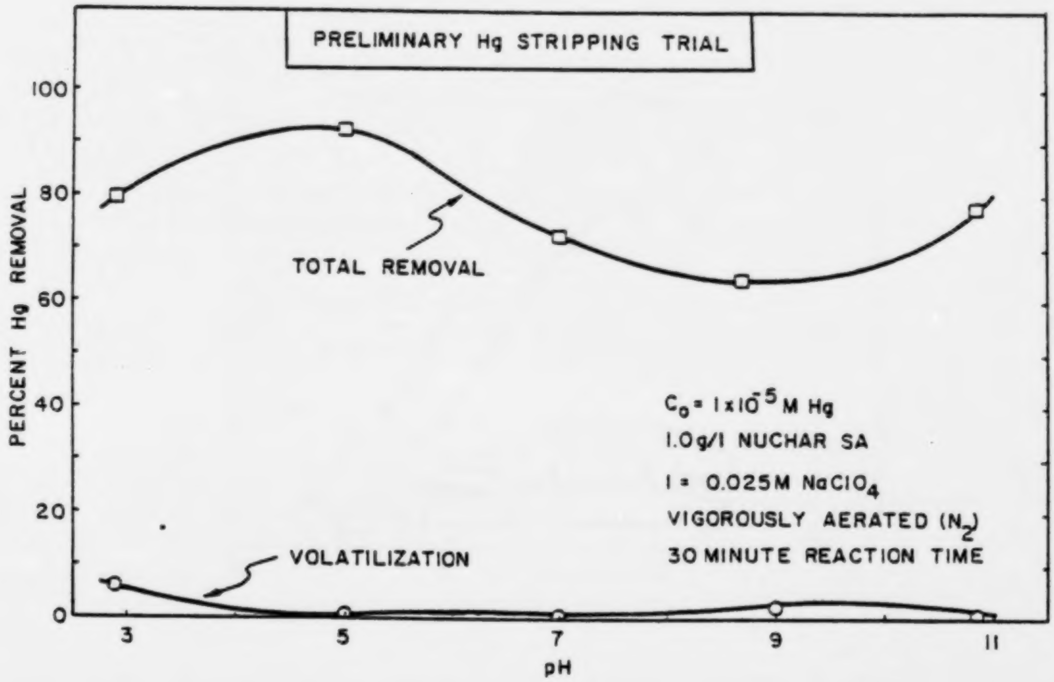

Figure 6b. The effect of carbon type on Hg(II) removal: (b) Volatilization.

The effect of activated carbon type on Hg(II) removal is shown by Figure 6a. The results show that Nuchar SA and Nuchar SN have a very high percentage Hg(II) removal over a wide pH range. Except at pH *ca* 4, the extent of Hg(II) removal by all other brands of activated carbon decreases significantly with increasing pH. It was speculated that the removal of Hg(II) by activated carbon may result from reduction of Hg(II) to Hg(g), volatilization. The extent of Hg(II) removal by volatilization is seen from Figure 6b. The results show that the contribution from volatilization in Hg(II) removal is rather insignificant at least at a total Hg(II) concentration of 10^{-5} M.

Figure 7 gives results on As(V) removal by various types of activated carbon. Since As(V) is present in solution mainly as anions, the adsorption curves differ from those of cationic metal ions in that a maximum adsorption peak was observed at pH 4.5. This adsorption pattern is exactly identical to the adsorption of most anions such as phosphate and silicate on oxides and hydroxides (14,15). The results clearly show that activated carbons which have a low pH_{zpc} , such as Nuchar SA, do not have much As(V) removal capacity.

The results on As(V) removal, shown in Figure 7, can be attributed to adsorption rather than the reduction of As(V) to As(III). This evidence was derived from laboratory analyses which involved the use of an oxidizing agent, KIO_3. If As(III) was present in the supernatant as the result of a reduction

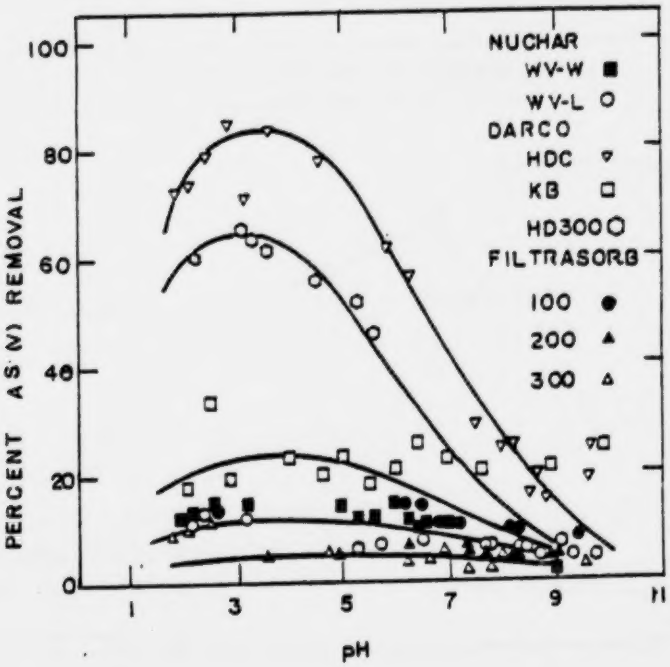

Figure 7. Effect of carbon type on As(V) removal. Experimental conditions were 10^{-4} M Na_3AsO_4 and 5 g/ℓ of activated carbon except Darco HDC and KB, in which system Na_3AsO_4 and carbon dose were 5×10^{-5} M and 1 g/ℓ, respectively. The ionic strength was 10^{-2} M as $NaClO_4$.

reaction, it will be detected after being oxidized to As(V) with KIO_3. Under all circumstances, there was no detectable amount of As(III) in the supernatant. The results shown in Figure 7 also demonstrate that the extent of As(V) removal becomes insignificant at pH > 10.

DISCUSSION

EFFECT OF PH

Similar to other solid adsorbents, the removal of heavy metals by activated carbons is markedly affected by the pH value of the system. This can be attributed to the fact that the speciation of heavy metals and the development of surface charge on activated carbon are pH-dependent phenomena. The results shown above clearly indicate the importance of pH-control on heavy metal removal. As the system pH changes, the distribution of metal species and the surface charge vary accordingly. The effect of pH on heavy metal adsorption at the solid-liquid interface can be best appreciated by realizing the mechanism of ionic adsorption. According to Grahame (16), the adsorption density of a species, Γ_i, is described by the following expression,

$$\Gamma_i = 2C_i r_i \exp(-\Delta G_i^{ads}/RT) \tag{7}$$

where C_i, r_i, and ΔG_i^{ads} stand for the equilibrium concentration, size and free energy of adsorption, respectively. The total adsorption quantity, Γ_t, for a specific heavy metal is therefore the sum of component adsorption density, Γ_i, i.e.

$$\Gamma_t = \sum_{i=1}^{n} \Gamma_i \tag{8}$$

According to Parks (17), the free energy of adsorption can be generally subdivided into several components of free energy term

$$\Delta G_i^{ads} = \Delta G_i^{elect} + \Delta G_i^{cov} + \Delta G_i^{hydo} + \Delta G_i^{hyda} + \Delta G_i^{vw} + \Delta G_i^{hyph} \tag{9a}$$

Where ΔG_i^{elect}, ΔG_i^{cov}, ΔG_i^{hydo}, ΔG_i^{hyda}, ΔG_k^{vw}, and ΔG_i^{hyph} represent free energy change due to electrostatic interaction, formation of covalent bonding, hydrogen bonding, hydration, van der Waals, and hydrophobicity. Quantitatively, it is difficult to differentiate between these component energy terms. A simpler version of this equation is

$$\Delta G_i^{ads} = \Delta G_i^{elect} + \Delta G_i^{hyda} + \Delta G_i^{chem} \tag{9b}$$

in that all energy terms related to the formation of chemical bondings such as covalent, hydrogen, van der Waals and hydrophobicity are represented by ΔG_i^{chem} the free energy change of specific chemical interactions. The term ΔG_i^{hyda} has a definite positive value indicating an hindrance to adsorption.

However, due to the hydrophobic nature of activated carbon and the large size of the metal ions used in this work, the contribution from ΔG_i^{hyda} is relatively insignificant (18).

It is further noticed that the amount of heavy metal removed decreases greatly in highly acidic pH regions, a phenomenon described by Maattman et al. as "ion exclusion effect" by which the strongest acid, hydronium ion (H_3O^+) becomes "tightly" associated with the solid surface at extremely low pH values (19).

The pH values at which the metal ions becomes excluded from the surface depends also on the acidity of the metal ions. For example Hg^{2+}, the strongest acid among the four metal ions studied, when in contact with an acidic activated carbon, such as Nuchar SA, the pH value of ionic exclusion is < 3; whereas, Cd^{2+}, the weakest acid of all, is excluded at a pH of *ca* from 5 to 6 with Nuchar SA. From an engineering point of view, the importance of pH on heavy metal removal by activated carbon and other adsorbents in general is obvious.

EFFECT OF CARBON TYPE

In connection with this pH effect, the results presented above clearly show the effect of activated carbon type on heavy metal removal. Several physical-chemical properties of activated carbon can be readily recognized as essential to inorganics removal; namely, surface acidity, surface area and surface morphology. Owing to the generally porous nature of most activated carbon, the surface acidity of activated carbon becomes the sole important parameter. While a thorough laboratory determination of the surface acidity of activated carbon is yet to be accomplished, Huang and Ostovic had reported the surface acidity of three activated carbons, namely Filtrasorb 400, Nuchar C-190-N and Nuchar 722 (11). The surface acidity, according to Huang and Ostovic, is qualitatively related to the pH_{zpc}. The stronger the acidity, measured in terms of the free energy change from surface deprotonation reactions, the lower the pH_{zpc}. The results shown in Figure 8 give the surface charge or electrophoretic mobility of various activated carbons as a function of pH. As indicated in Figure 8, the activated carbon surface is positively charged at $pH < pH_{zpc}$. The nature of surface charge is of primary importance in heavy metal removal.

From the information presented in Figure 1 on the chemical speciation of metal ions, except As(V), and in Figure 8 on the nature of surface charge, it becomes clear that the major metal species removed are free metals, i.e., M^{2+} ions and mono-hydroxo species, i.e., MOH^+ if present at significant quantities. For example, the removal of Cd(II) by Nuchar SA (or SN) is more pronounced at pH 6 (or < 6) than all other activated carbons because at pH 6, the surface of Nuchar SA (or SN) is negatively charged, whereas the surface charge of the rest of the activated carbons is either neutral or positive. Furthermore, the Cd^{2+} ion is the major Cd(II) species at pH 6, therefore creating a favorable electrostatic condition for Cd^{2+} adsorption. This reaction scheme is generally valid for other metals, namely Pb(II), Zn(II), and Hg(II). In the case of Pb(II), it is plausible to suggest that the good removal at pH 6 by all activated carbons may be caused by adsorption of the $Pb(OH)^+$ species present in major quantities at pH > 4.

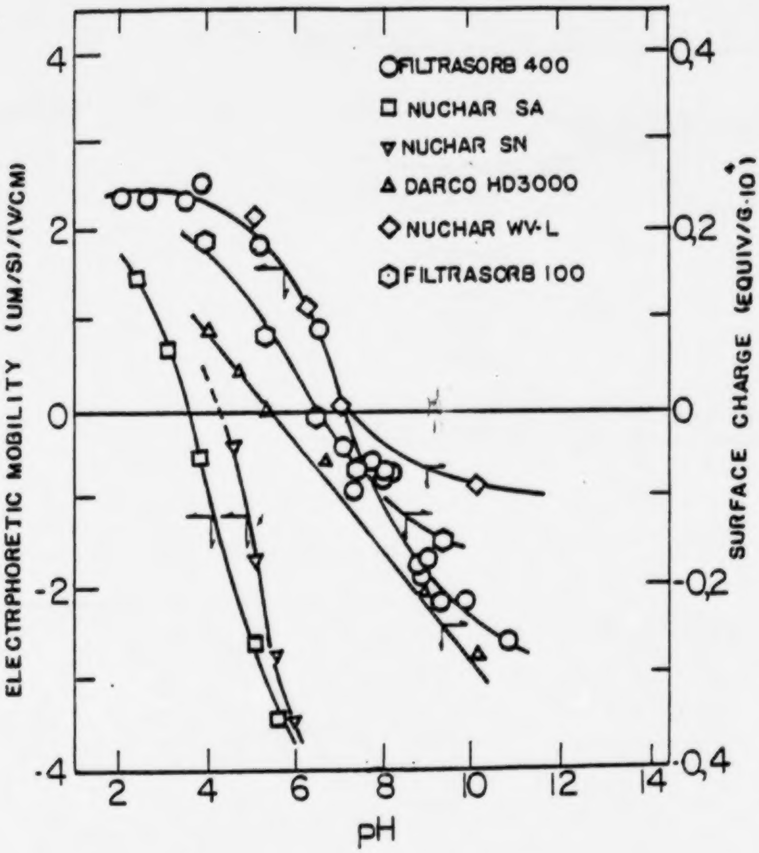

Figure 8. The surface charge of activated carbon as a function of pH. The data on Darco HD 3000, Nuchar WV-L, and Filtrasorb 100 were taken from Singer (7).

In the case of arsenate, since the major species are $H_2AsO_4^-$ and $HAsO_4^{2-}$ over the pH range where significant As(V) removal occurs, the major removal mechanism can also be attributed to interaction between these anionic As(V) species and the positively charged activated carbon surface. This explains why acidic activated carbon such as Nuchar SA does not have good As(V) removal capacity; instead, the basic activated carbons such as the Darco series exhibit significant As(V) removal capacity. Within the context of electrostatic interaction, it is clear that when the activated carbons are highly negatively charged, electrostatic repulsion starts to dictate the adsorption picture thereby decreasing the adsorption density.

However, electrostatic interaction alone can not give a total account for the amount of heavy metal adsorbed. The results also show finite and significant amounts of metal adsorption at the pH_{zpc} and $pH > pH_{zpc}$ for cationic heavy metals and $pH < pH_{zpc}$ for arsenate. This observation can only be attributed to specific chemical adsorption.

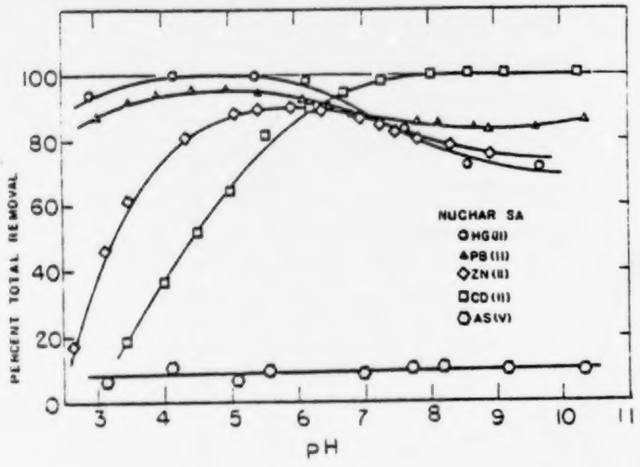

Figure 9a. Nuchar SA

Figure 9b. Darco HD 3000

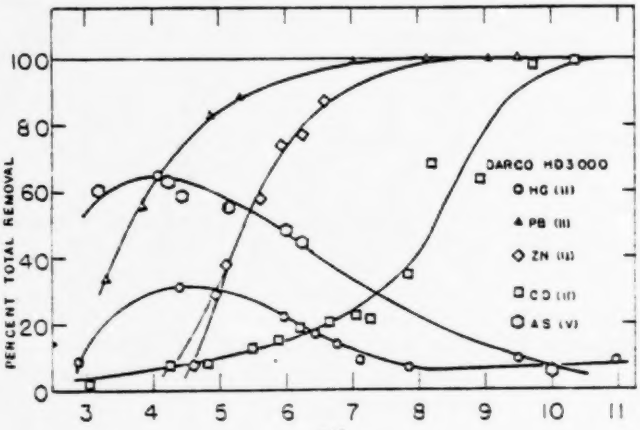

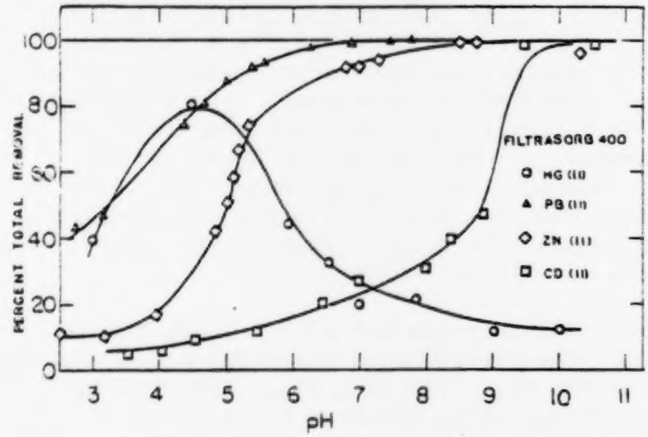

Figure 9c. Filtrasorb 400

Figure 9. Effect of metal type on heavy metal removal. Data were taken from Figure 3 through Figure 7.

Further evaluation of the heavy metal adsorption characteristics is presented in Figure 9. For an acidic activated carbon such as Nuchar SA (Figure 9a), its metal removal capacity appears in favor of the acidic metal ions at pH less than *ca* 6.5, i.e., acidic condition. The extent of metal removal follows an order: Hg(II) > Pb(II) > Zn(II) > Cd(II) at pH < 6.5; whereas the order of metal removal is reversed at pH > 6.5. Since arsenate is a weak base, the extent of As(V) removal by an acidic activated carbon is poor. However, this sharp reversal in metal removability at a specific pH value becomes rather obscure when the acidity of the activated carbon becomes weakened (higher pH_{zpc}). The results clearly demonstrate the importance of the acidity of both the activated carbon and the metal ions on the extent of metal removal. For an activated carbon with strong acidity and in the acidic region, the extent of heavy metal removal increases with the acidity of the metal ions; the order decreases when an alkaline environment is encountered. For an activated carbon with weak acidity, the extent of heavy metal removal is better with metal ions of weak acidity and in the alkaline pH region.

EFFECT OF COMPLEX FORMATION

The formation of metal complexes can alter the distribution of metal species and thereby affect the extent of heavy metal removal. Figure 10 shows that the amount of Cd(II) removal is enhanced in the presence of tryptophan. The enhancement in Cd(II) adsorption can be primarily attributed to the bridging effect provided by the tryptophan. Since organics such as tryptophan are generally adsorbable by activated carbon, the adsorbed tryptophan species, by forming complexes with Cd^{2+} improves Cd(II) adsorption. It is noted that the

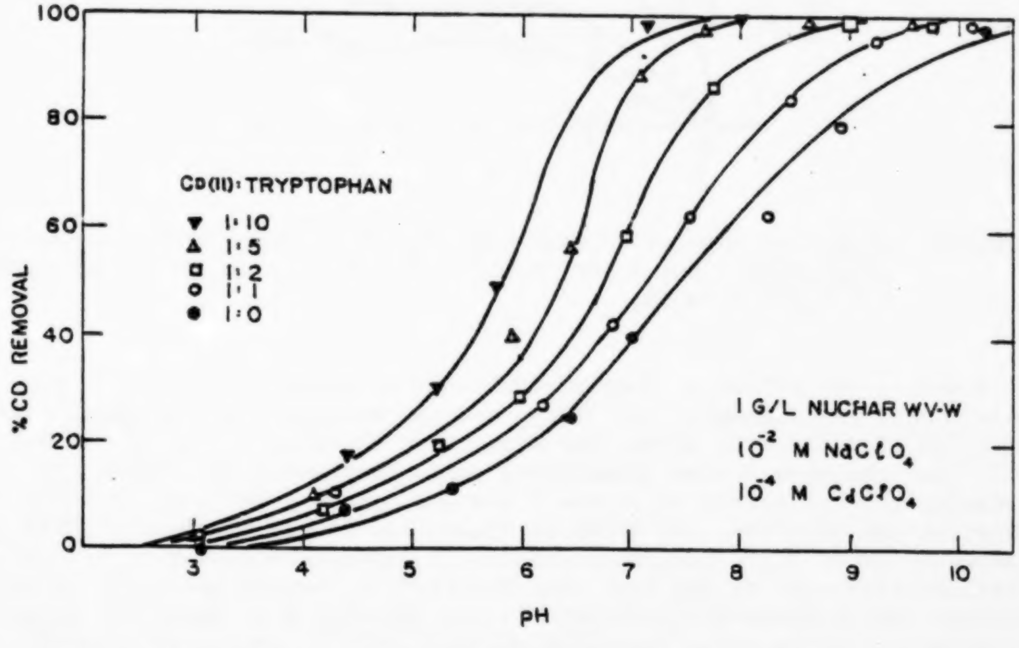

Figure 10. Effect of complex formation on Cd(II) removal.

cadmium-tryptophan complex is a bidentated neutral molecule, CdA_2. The marked increase in Cd(II) adsorption by the presence of tryptophan is also a result of the combined effect of electrostatic interaction and specific chemical adsorption.

However, the chemical nature of the metal complexes also has a significant effect on the adsorption of metal ion per se. This is demonstrated by results shown in Figure 11. The extent of complex formation between Cu(II) and each of the amino acids is essentially identical, as measured by their stability constants. However, under otherwise similar conditions, the extent of Cu(II) adsorption in the presence of various types of amino acid is quite different. Elliott and Huang attributed this observation to the hydrophobicity of the adsorbates (13). Since the hydrophobicity of the amino acids decreases in the order: phenylalanine (Phe) > leucine (Leu) > valine (Val) > alanine (Ala) > glycine (Gly). Phenylalanine is adsorbed most by the activated carbon, thereby yielding the largest extent of Cu(II) adsorption.

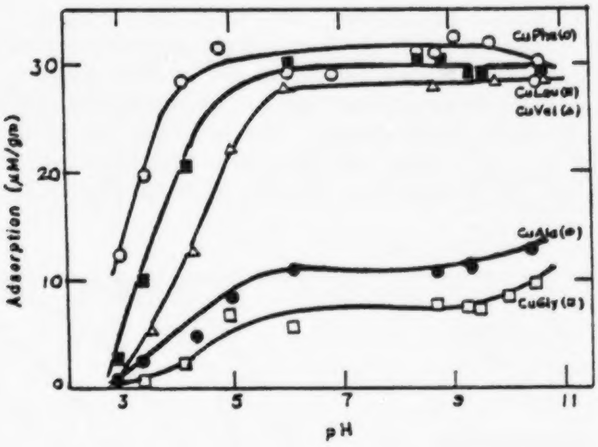

Figure 11. Effect of complex formation on Cu(II) removal. Experimental conditions: $Cu_T = 10^{-4}$ M, $L_T = 10^{-3}$ M, 2.5 g/ℓ Filtrasorb 400, I = 0.025 M $NaClO_4$.

However, the effect of complex formation on metal adsorption is not always one of enhancement. The charge and the structure of the metal complexes can significantly affect the adsorption characteristics of the metal ions. When chelates (three dimensional metal complexes) are formed, by increasing the concentration of the chelating agent, a decrease in heavy metal adsorption was observed. As shown in Figure 12, in the presence of EDTA (a tetraprotic acid, H_4Y), the extent of Zn(II) removal decreases. This can be partially attributed to the fact that the (ZnY^{2-}) complex has an octahedral structure and is anionic. When both Zn(II) and EDTA are present at exact stoichiometric ratio, i.e., 1:1, the anionic (ZnY^{2-}) complex is somewhat repelled from the counter-charged activated carbon surface. Since EDTA is adsorbable by the activated carbon, a further increase in EDTA concentration can only reduce the available Zn(II) adsorption sites.

Figure 12 gives the effect of EDTA on Zn(II) adsorption by Nuchar SA and Filtrasorb 400. When present at 1:10 stoichiometric ratio, the Zn(II) removal capacity remains unchanged at pH values greater than which the activated carbon surface is negatively charged. When EDTA was present at an amount 5 times that of Zn(II), the amount of Zn(II) adsorbed was greatly reduced except at pH < 3 for Nuchar SA. This observation again is in agreement with the contention that electrostatic and specific chemical reactions play an important role on the adsorption characteristics of complexed heavy metals.

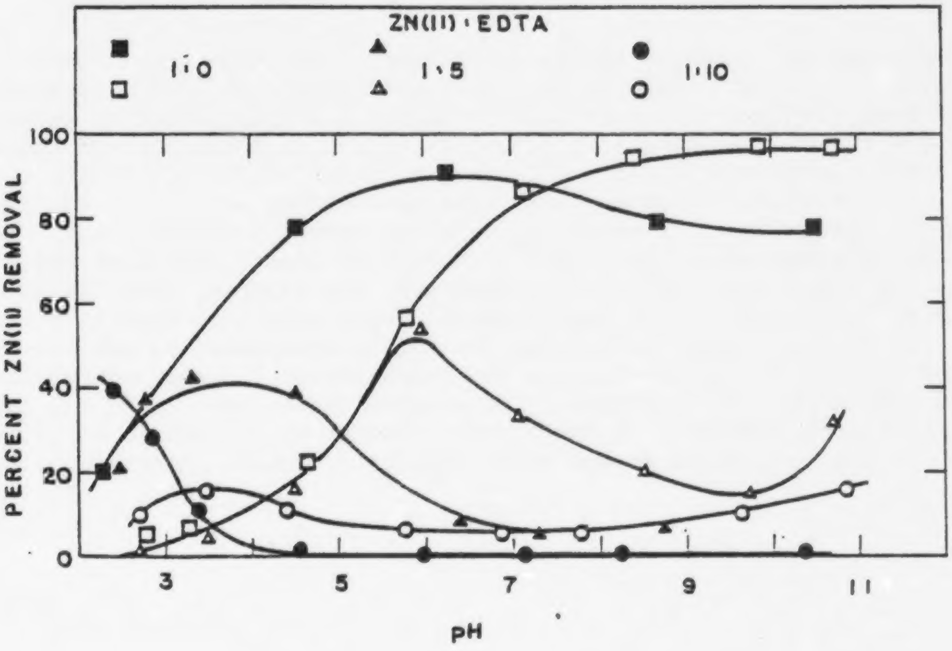

Figure 12. Effect of complex formation on Zn(II) removal. Experimental conditions: 100 mℓ suspension 0.87 x 10^{-5} M $Zn(ClO_4)_2$, 10 g/ℓ Filtrasorb (open data points) or Nuchar SA (solid data points).

SUMMARY

In dealing with heavy metal removal from water and wastewater by adsorption on activated carbon, it is imperative to understand the chemistry of the water and the wastewater and the surface chemistry of the activated carbon. The results shown in this report clearly indicate the importance of solution chemistry and the surface acidity of activated carbon on the extent of heavy metal removal. A careful selection of the activated carbon, and properly monitored pH values will assure a high percentage of heavy metal removal. Among the heavy metals studied, namely, Hg(II), Pb(II), Zn(II), and Cd(II), it was observed that acidic activated carbons such as Nuchar SA and SN were among the most effective especially in the acidic to neutral pH region for metal removal. However, in the alkaline region, although chemical precipitation may start to play its role, the effect of carbon type became less important, high percentage removal was always accomplished by all carbons. For anionic arsenate, basic activated carbons are most effective.

Preliminary results also indicate that electrostatic interactions between free metal ions, M^{2+}, and to a certain extent MOH^+ species, anionic or arsenate ions and activated carbon surface is the major removal mechanism. However, specific chemical interactions with the formation of specific chemical bonds or hydrophobicity also play an important role in heavy metal removal.

When complex formation agents are present, the heavy metal removal characteristics of activated carbon are significantly modified. Preliminary results show that the structure and the charge characteristics of metal complexes are two of the important parameters affecting adsorption of complexed metal ions. Since most organic ligands are rather adsorbable by the activated carbon, if the metal complexes have three-dimensional structure, the presence of organic substances will hinder heavy metal removal; however, their presence will promote heavy metal adsorption if planar or linear complexes are formed. The various copper (II)-amino acid complexes, for example, have different effects on Cu(II) adsorption regardless of their identical stability constants and similar linear structure; the Cu(II)-phenylalanine was the most adsorbed whereas Cu(II)-glycine was the least adsorbed, since phenylalanine is more hydrophobic than glycine. The results demonstrate again the importance of solution chemistry on heavy metal removal by adsorption on activated carbon surface in particular and other physical-chemical processes in general.

REFERENCES

1. Beliles, R. P., "Metals," Chapter 18 in *Toxicology* (Eds., L. J. Casarett and J. Doull), MacMillan Publishing Co., Inc., New York, pp. 454-502, 1975.

2. Sabadell, J. E., *Traces of Heavy Metals in Water: Removal Processes and Monitoring*, Center for Environmental Studies and the Water Resources Program, Princeton University, EPA-902/2-74-001, 342 pp.

3. Ostrejko, R., British Patents 14224 (1900); 18040 (1900); German Patent 136792 (1901), cited by Hassler, J. W. in *Activated Carbon*, Chemical Publishing Co., New York, 1963.

4. Huang, C. P., "Chemical Interactions Between Inorganics and Activated Carbon," Chapter 8 in *Carbon Adsorption Handbook* (Eds., P. N. Cheremisinoff and F. Ellerbush), Ann Arbor Science Publishers, Inc., Ann Arbor, Michigan, 1978.

5. Stumm, W. and Morgan, J. J., *Aquatic Chemistry* (2nd edition), John Wiley, New York, NY, 1981.

6. Smith, R. M. and Martell, A. E., *Critical Stability Constants*, Plenum Press, New York, NY, *Vol. 4*, 1976.

7. Singer, P. C., "Activated Carbon for the Removal of Trace Metals from Aqueous Solutions," Chapter 21 in *Ion Exchange for Pollution Control*, Vol. II (Eds., C. Calmon and H. Gold), CRC Press, Inc., Boca Raton, FL, pp 195-201, 1978.

8. Huang, C. P. and Smith, E. H., "Removal of Cd(II) from Plating Wastewater by An Activated Carbon Process," Chapter 17 in *Chemistry of Water Reuse* (Ed., W. J. Cooper), Ann Arbor Science Publishers, Inc., Ann Arbor, MI., p. 355, 1981.

9. Kopp, J. F., Longbottom, M. C. and Lobring, L. B., "Cold Vapor Method for Determing Mercury," *J. Am. Water Works Assoc.*, *64(1)*, 20, 1972.

10. Strickland, J. D. H. and Parsons, T. R., *A Practical Handbook of Seawater Analysis*, Fisheries Research Board of Canada, Bulletin 167, Ottawa, 1972.

11. Huang, C. P. and Ostovic, F. B., "The Removal of Cadmium(II) from Dilute Aqueous Solution by Activated Carbon Adsorption," *J. Environ. Eng. Div., A.S.C.E. 104 (EES)*, 1978.

12. Elliott, H. A. and Huang, C. P., "The Adsorption Characteristics of Cu(II) in the Presence of Chelating Agents," *J. Colloid & Interface Sci.*, *70(1)*, 29, 1979.

13. Elliott, H. A. and Huang, C. P., "Adsorption of Some Copper(II)-Amino Acid Complexes at the Solid-Solution Interface Effect of Liquid and surface Hydrophobicity," *Environ. Sci. & Technol.*, 14(1), 87, 1980.

14. Huang, C. P., "Adsorption of Phosphate at the Hydrous γ-Al_2O_3-Electrolyte Interface," *J. Colloid & Interface Sci.*, *53(2)*, 178, 1975.

15. Huang, C. P., "The Removal of Aqueous Silica from Dilute Aqueous Solution," *Earth and Planetary Series Lectures*, *27*, 265, 1975.

16. Grahame, D. C., "The Electrical Double Layer and the Theory of Electrocapillarity," *Chem. Rev.*, *41*, 441, 1954.

17. Parks, G. A., "Adsorption in the Marine Environment," in Chemical Oceanography, (2nd edition), Vol. 1 (Eds., J. P. Riley and G. Skirrow), Academic Press, London, 1975.

18. James, R. O. and Healy, T. W., "Adsorption of Hydrolyzable Metal Ions at the Oxide-Water Interface. III. A Thermodynamic Model of Adsorption," J. Colloid & Interface Sci., 40, 65, 1972.

19. Maattman, R. W., Rubingh, D. N., Mellema, B. J., Bass, G. R., and Hoekstra, P. M., "The Exclusion of Ions from the Region Near the Surface of Activated Carbon," J. Colloid & Interface Sci., 31, 95, 1969.

Comments on
The Removal of Heavy Metals by Activated Carbon Process from Water and Wastewater:
I. Some Preliminary Observations

Walter J. Weber
Environmental and Water Resources Engineering
The University of Michigan
Ann Arbor, Michigan

Activated carbon is used extensively for the adsorption of trace organic substances from waters and wastewaters. The suitability of this material for such applications is based on its relatively low cost vis-a-vis alternative processes, its general applicability to a broad range of organic substances, and the fact that it can be regenerated and reused. Activated carbon is also capable of adsorbing a number of inorganic species from aqueous solution, particularly heavy metals. Applications of carbon for this purpose have been limited, however, primarily because lower cost alternative treatment schemes such as chemical precipitation and/or selective ion exchange usually provide high quality effluents and often provide for effective metal recovery. There is little current evidence to suggest that the use of activated carbon will offer serious competition to such alternatives on the basis of cost alone.

With these considerations in mind, the present work must be evaluated in light of two fundamental questions. First, does the work have the potential to address important theoretical questions concerning activated carbon adsorption or heavy metal chemistry? Second, does the work have practical implications that will either suggest possible benefits from the use of activated carbon for heavy metal removal that outweigh the inherent cost disadvantages with respect to alternative processes, or that will define avenues for process optimization that will eliminate or reverse cost differentials?

To date the research has demonstrated that five heavy metals are removed from solution more extensively by activated carbon over most pH ranges than by precipitation in systems containing no carbon. Removals have been observed to vary significantly with the specific heavy metal, the type of activated carbon used, the pH of the system, and the presence of organic ligands. Efforts have been made to elucidate mechanisms responsible for observed removals, and this constitutes the major theoretical thrust of the research.

An apparent correlation between removal and surface acidity appears to be the most promising result to date. A word of caution is in order with respect to extrapolation of this observed correlation to a mechanistic explanation. It is difficult, if not impossible, to distinguish between adsorption and precipitation onto the carbon surface, and it is possible that the increased removals observed in the presence of activated carbon can be attributed to the abundance of nucleation sites provided by the carbon surfaces. In this context the large surface areas (as reflected by the N_2 BET values) of the most acidic carbons could explain the larger capacities of these adsorbents. This is not suggested as a more likely explanation than that advanced by the authors, but rather as an exemplary indication that further study of the several differences among activated carbons is required for insight into adsorption mechanisms.

Additional questions of a theoretical nature necessarily arise as adsorption mechanisms are investigated. It may not be possible to completely delineate specific adsorptive interactions, but adsorption reactions can be experimentally evaluated in ways that help elucidate these phenomena. The traditional adsorption isotherm is a valuable means for characterizing solid-liquid interactions as the relationship between the concentration of adsorbing species in the two phases is described over a range of values. This relationship can quantify the intensity or energy of adsorption as well as the capacity of the adsorbent for uptake of a specific metal. Desorption experiments are useful in that they provide quantitative information on the reversibility of the reaction. Finally, kinetic studies provide yet another perspective on such reactions as well as being essential for verification of assumptions of equilibrium in other experiments. It is suggested that a thorough review of the literature pertaining to adsorption methodologies be undertaken with the goal of application to the present study in mind.

The better understanding of process phenomena and effects to be gained from more rigorous experimental design is not only of interest with respect to delineation of adsorption mechanisms, but can also be useful in process applications. The practicality of using activated carbon for removal of heavy metals from aqueous solution will be determined by such factors as the capacity of the adsorbent and the reversibility of the reaction. Since adsorption technologies enter the arena of heavy metal removal processes at an initial cost disadvantage, efficient design and operation based on a thorough understanding of the physical-chemical processes or observable effects operative in the system are essential.

This research has not, as yet, addressed many practical questions that will ultimately determine the value of activated carbon for treatment of waters and wastes containing heavy metals. It is suggested that the following points be given consideration in the future direction of the project:

- Adsorption isotherms should be conducted over wide ranges of concentration of both metals and carbons. These data should give indication of the concentration sensitivities and operative capacities of different carbons under different conditions, should define the practical limits of the process, and should provide valuable theoretical insights with respect to process energetics.
- Kinetic studies should be conducted to verify the assumptions of equilibria and to assess the practicality of designing treatment facilities using this process.
- Desorption studies may provide important mechanistic information as well as an estimation of displacement hysteresis effects on the performance of adsorption systems under changing influent conditions and concentrations.
- The possibility of regeneration should be studied. Since any regeneration scheme will likely involve chemical treatment of the spent carbon, undesirable effects on carbon surfaces and matrices should be considered.
- Metal adsorption from solutions containing complex mixtures of uncharacterized organics typical of many wastes and all natural waters should be evaluated.

While a thorough investigation of all points raised above is beyond the scope of such a project, at least a preliminary evaluation of each is in order. The authors have shown that heavy metals are removed from solution in laboratory tests with activated carbon and suggest that this is a viable treatment technology. A more definitive and quantitative estimate of the capabilities and limitations of the process is needed to substantiate such a conclusion. With this information the direction of future research and applications can be better determined.

HETEROGENEOUS CATALYTIC OXIDATION OF MODEL CHLORINATED HYDROCARBONS

Michael P. Manning
Department of Chemical Engineering
Massachusetts Institute of Technology
Cambridge, Massachusetts 02139

ABSTRACT

Improved processes for the total oxidation of a diverse range of organic by-products and wastes generated in the chemical industry are necessary for the continuing co-existence of a profitable chemical industry and a safe, unpolluted environment. To this end, we have examined methods for establishing the feasibility and important engineering parameters in the heterogeneous catalytic oxidation of such organic materials. Given the diverse chemical, physical, and stoichiometric composition of these wastes, our efforts have concentrated on the oxidation of model chlorinated hydrocarbons. The use of model compounds allows the systematic investigation of the independent variable parameters such as bond type and order (paraffin, olefin, aromatic, etc.), degree of halogen substitution, and synergistic mixing effects for each of the catalysts.

At present, we have completed an extensive investigation of the experimental chromatographic procedures necessary to separate the expected reactants and products of an experimental catalytic reactor, have performed some preliminary oxidation and materials compatibility experiments on one catalyst area. A summary of the results in all three of these efforts and the implications for our continuing research are presented.

CHROMATOGRAPHIC SEPARATION

In order to analyse the performance of any chemical reactor, one must first be able to sample the feed and product streams. Thus, our first efforts have been devoted to the separation and quantification of the major components expected in these streams. These components include HCl, Cl_2, N_2, O_2, CO_2, H_2O and chlorinated methanes, ethylenes, and benzenes. In addition, separation of potential catalyst poisons such as SO_2, NO_x and other combustion products not routinely expected such as phosgene is also desirable. Their analysis is, of necessity, difficult to perform due to the number and variety of components to be determined. The reactive nature of some of the components requires selection modification, and utilization of inert, corrosion-resistant materials in the sampling and flow lines. Unfortunately, no single column exists which would separate all these species. Therefore, we tested multiple columns for separating various fractions of the mixture and developed a valve switching sequence to allow quantitation of all components from a single sample injection. The use of a single injection is required for an accurate material balance in that there are no key components which appear equally well separated on columns used to separate the various fractions of the feed and product mixtures, as will become more apparent later.

Testing of the various packing materials was performed following a standard procedure. A column containing one of the packing materials shown in Table 1, was mounted in the oven of a Hewlett Packard 5730A Gas Chromatograph. The column was conditioned by heating the column overnight in flowing carrier gas at a temperature near the manufacturer's recommended maximum operating temperature. Samples of the various components were then injected manually into the heated injection port of the chromatograph and the retention times measured. Injections of mixtures were used to check the resolution of components with similar retention times.

A summary of the results obtained in the experiments with these columns is best presented by discussing the classes of compounds and packing materials in sequence.

ATMOSPHERIC FIXED GASES

The separation of O_2, N_2, CO, CH_4 is readily accomplished on a column containing molecular sieve 5Å. Unfortunately these zeolithic packing materials are rapidly deactivated on contact with water or CO_2. The chlorinated organic compounds are so strongly adsorbed that the sorption may be considered irreversible.

CHLORINATED ORGANICS

Many packing materials containing specially selected liquid phases have been shown extremely powerful in separating very difficult chlorocarbon mixtures, e.g., the entire range of PCB isomers. Unfortunately these selective liquid phases are very sensitive to water and often oxygen. Thus, they are not useful in the present separation. We have, however, found that the series of Halocarbon oils are quite suitable as liquid phases in separating the chlorinated methanes and ethylenes and are compatible with water and oxygen at temperatures up to 200°C. These liquid phases are normally supported on teflon packing material to minimize support interactions (1).

COMBUSTION PRODUCTS

The most difficult part of the entire separation scheme was separation of the combustion products H_2O, CO_2, HCl, and Cl_2. The difficulty arose from both the lack of compatibility of many packing materials with these constituents as mentioned in the other separations and because most packing materials will not separate these species. A search of the voluminous literature did not identify a single study in which H_2O, HCl, and Cl_2 have

TABLE 1. ANALYTICAL COLUMNS TESTED FOR SEPARATING SELECTED CONSTITUENTS

Column	Length (m)	Diameter (mm)	Packing Material (mesh size)(support)	Liquid Phase
A	3.00	3.2	40/60 Chromosorb T	7% OV -17
B	3.66	3.2	60/80 Carbopak B	10% H_3PO_4
C	1.83	3.2	80/100 Poropak Q-HF*	--
D	1.83	3.2	80/100 Poropak R	--
E	1.83	3.2	80/100 Poropak Q	--
F	3.05	3.2	80/100 Poropak Q-HF*	5% Halocarbon 700
G	3.05	6.4	40/60 Chromosorb T	--
H	3.05	6.4	40/60 Chromosorb T	0.1% Halocarbon 40
I	6.10	3.2	40/60 Chromosorb T	7% Halocarbon 40
J	2.00	3.2	80/100 Poropak N	--
K	1.83	3.2	100/120 Molecular Sieve 5A	--
L	6.10	3.2	40/60 Chromosorb T	16.7% Halocarbon 40
M	6.00	3.2	40/60 Chromosorb T	10.0% Halocarbon 14-25
N	4.27	3.2	40/60 Chromosorb T	16.7% Kel-F Wax
O	3.05	3.2	80/100 Tenax-GC	--

*Poropak Q-HF indicates Poropak Q packing which has been treated with HF to saturate residual vinyl groups in the polymer packing and reduce tailing as discussed by Hertl and Neumann (1971).

Note: All columns in teflon or teflon-lined tubing.

been separated chromatographically. As solid polymeric packings without liquid phases have been shown to be superior in reducing tailing and other analysis problems in samples containing water (2), we examined several of the Poropak series packings and a new high temperature packing, Tenax-GC. Only the Tenax-GC packing was able to resolve a mixture containing HCl, Cl_2, and H_2O. The Poropak packing materials which are basically a family of vinyl polymers exhibited two problems. The first problem is that packing materials contain some unreacted vinyl groups as reported previously. Hertl and Neumann (3) have shown that these residual groups can be removed by pretreatment with HF. Early experiments with HCl and Cl_2 injections on Poropak showed that a similar pretreatment procedure allowed detection of small concentrations (1% or less) of HCl or Cl_2 in N_2 which was impossible on untreated packing material. Presumably, the HCl or Cl_2 in the samples reacted with the packing just as the HF did during the pretreatment procedure. However, even after the pretreatment, the Poropak packings did not resolve HCl from Cl_2 but would separate HCl/Cl_2 as a single peak from water.

ANALYSIS PROCEDURE

Sample chromatographs from each of the three separate separations are shown in figures 1, 2, and 3. For separations shown, all columns were operated isothermally at 80°C with a carrier gas flow of 15 ml/min. Retention times for the various components are shown in Table 2. As is evident in the figures, all component peaks are well resolved. The overall procedure is being automated as shown in figure 4. The use of two bypass valves and compensating restrictors will allow the separation of a single injection into the three groups as discussed previously. The total analysis time for a sample containing all of the chloromethanes will be about 15 minutes. Some additional temperature programming will be required to minimize the analysis time for the chlorobenzenes.

EXPERIMENTAL APPARATUS

An experimental apparatus to measure the heterogeneous catalytic oxidation of chlorocarbons has been constructed. The earliest version of the apparatus is portrayed schematically in Figure 5. Commercially pure gases in standard cylinders are connected via two stage regulators and flow controllers to a single gas inlet line. For chlorocarbons which are normally liquids at ambient conditions a glass saturator is placed in parallel with the nitrogen line and a portion of the nitrogen is bubbled through the liquid and over a column of glass beads wetted with liquid. The glass saturator is immersed in a constant temperature bath to maintain the liquid temperature and thus adjust the vapor pressure of the component. By setting the bath temperature and nitrogen flow rate, any desired concentration of the chlorocarbon in the feed stream can be obtained.

The mixed feed stream then flows to two split tube furnaces placed in series. The first furnace functions as a preheater to bring the reactant

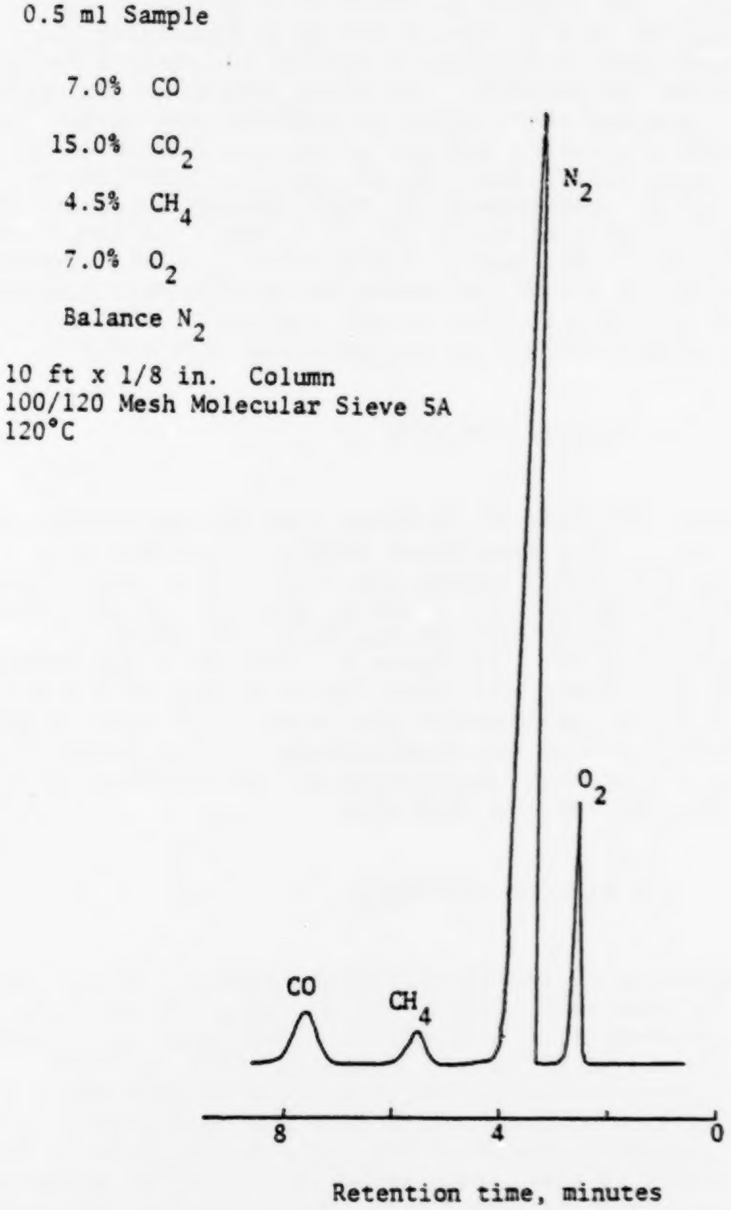

0.5 ml Sample

7.0% CO

15.0% CO_2

4.5% CH_4

7.0% O_2

Balance N_2

10 ft x 1/8 in. Column
100/120 Mesh Molecular Sieve 5A
120°C

Figure 1. Separation of Atmospheric Gases on Molecular Sieve.

0.2 µl Liquid Sample
20 ft x 1/8 in. column
16.7% Halocarbon 40 on 40/60 mesh Chromosorb T
80°C

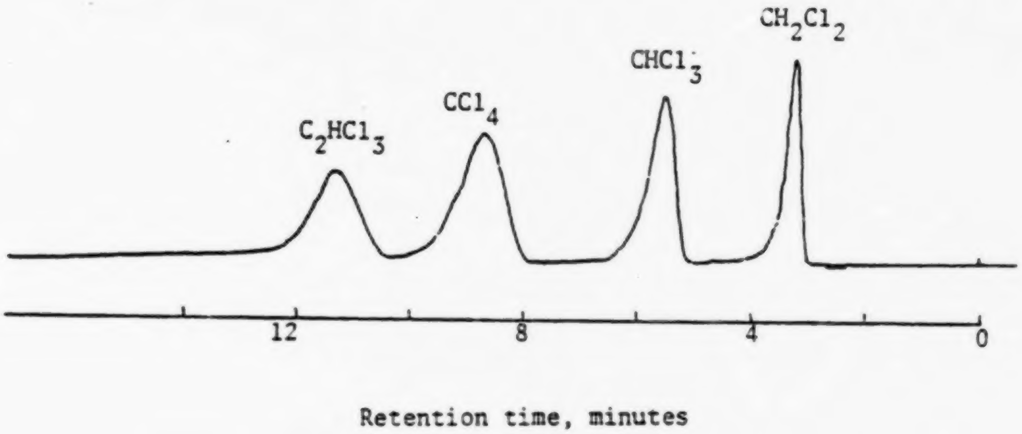

Figure 2. Separation of Chlorinated Hydrocarbons.

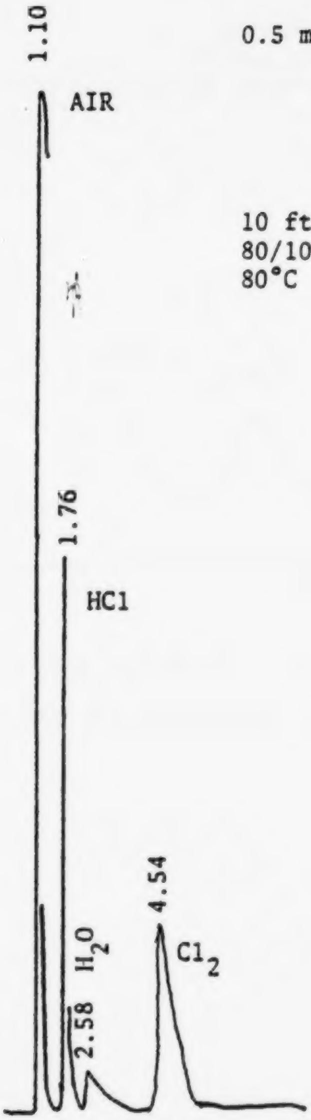

0.5 ml Gas Sample

59% Air
20% HCl
20% Cl_2
2% H_2O

10 ft x 1/8 in. Column
80/100 mesh Tenax-GC
80°C

Figure 3. Separation of HCl, H_2O and Cl_2 on Tenax-GC.

TABLE 2. RETENTION TIMES* FOR SELECTED COMPOUNDS AT NEAR OPTIMUM CONDITIONS

	Column Identification		
	L	O	K
Oven Temperature (°C)	80	80	80
H_2	1.48	1.05	1.08
O_2	1.48	1.05	0.78
CH_4	1.48	1.05	1.87
CO	1.48	1.05	2.33
CO_2	1.48	1.19	--
HCl	1.57	1.76	--
Cl_2	2.01	4.54	--
H_2O	1.90	2.56	--
CH_2Cl_2	3.57	--	--
$CHCl_3$	5.98	--	--
CCl_4	9.48	--	--
C_2HCl_3	11.40	--	--
Carrier flow (ml/min)	15	15	56

*Retention times in minutes

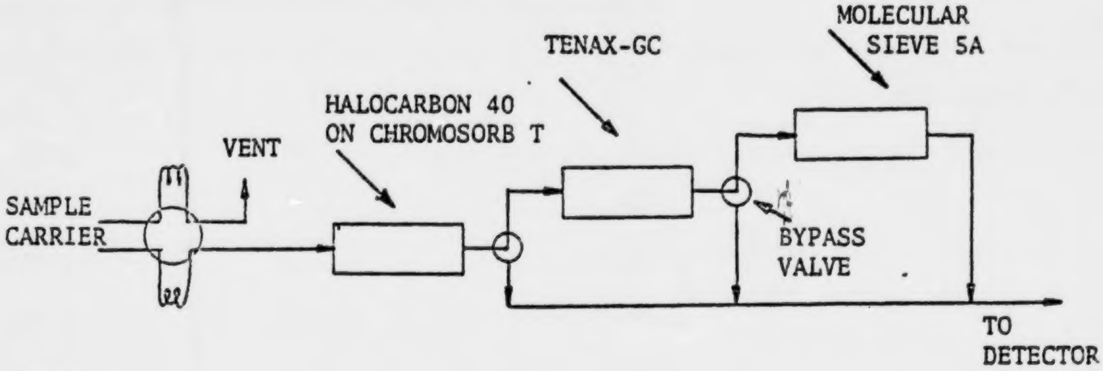
MOLECULAR SIEVE 5A
TENAX-GC
HALOCARBON 40 ON CHROMOSORB T
VENT
SAMPLE
CARRIER
BYPASS VALVE
TO DETECTOR

Figure 4. Column and Bypass Valve Arrangement for Automated Separation.

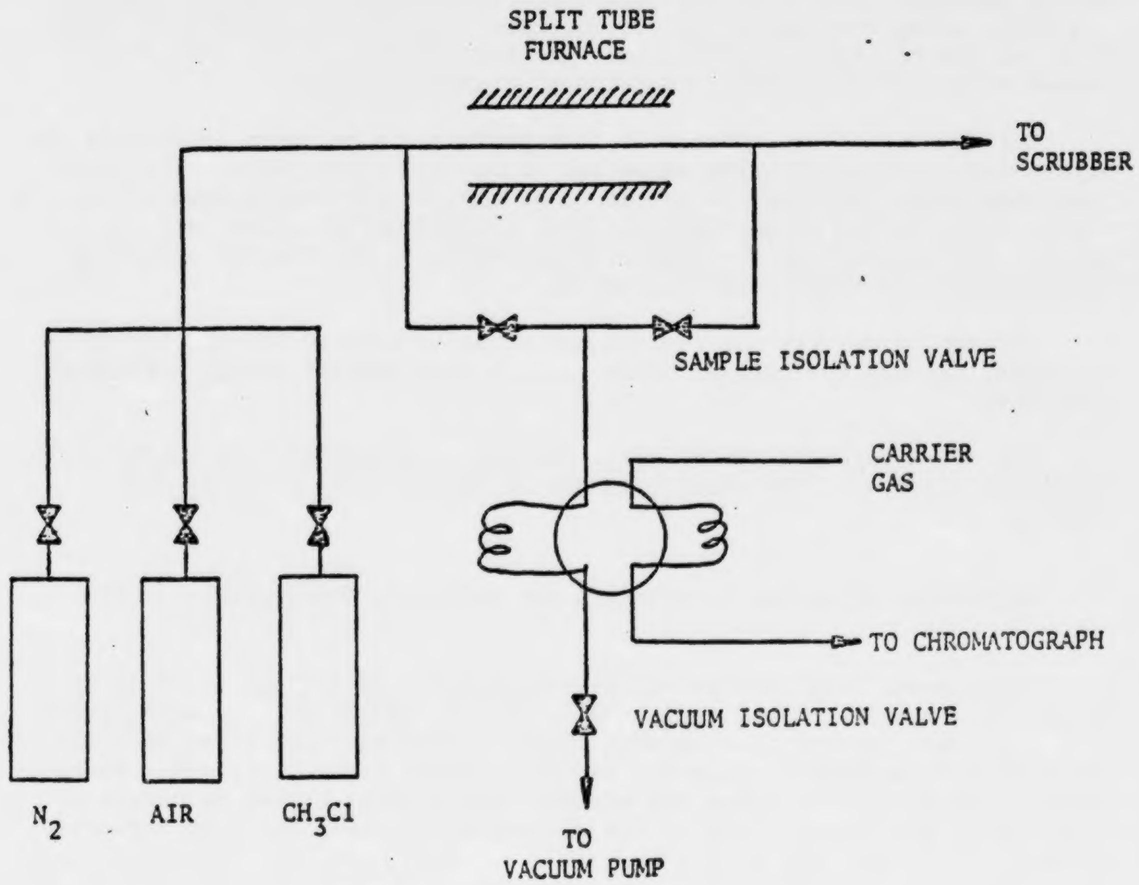
SPLIT TUBE
FURNACE
TO
SCRUBBER
SAMPLE ISOLATION VALVE
CARRIER
GAS
TO CHROMATOGRAPH
VACUUM ISOLATION VALVE
TO
VACUUM PUMP
N2
AIR
CH3Cl

Figure 5. Reactor Experimental Flowsheet.

gases up to the desired temperature. The second furnace is used to maintain the desired reaction temperature. The reactor is a glass-lined stainless steel tube, 4 mm I.D. The preheater portion of this tube is packed with zeolites to enhance heat transport to the flowing gases. The reactor portion of the catalyst tube is fitted into a solid aluminum cylinder to eliminate hot spots along the reactor wall. The tube is normally packed with about 2 cm^3 of sieved catalyst particles. The last section of the tube is also packed with zeolite to hold the catalyst charge in place.

Gas samples of the reactor feed or product can be taken by opening the appropriate sample isolation valve and vacuum isolation valve. The vacuum pump then draws gas from the reactor tube through the sample loop of the gas sample valve in the chromatograph. When the vacuum isolation valve is closed, the pressure in the sample loop returns to the reactor operating pressure and the sample may be injected.

Exhaust gases from the reactor are normally bubbled through caustic to remove halogen and halogen acids and are then vented through a chemical fume hood.

The first catalyst tested was a commercial supported V_2O_5 sulfuric acid oxidation catalyst. The specifications of the catalyst are listed in Table 3.

PRELIMINARY OXIDATION EXPERIMENTS AND MATERIALS COMPATIBILITY TESTS

Experiments were carried out at temperatures of 360 and 412°C using inlet concentrations of 5% (mole) CH_3Cl in air. CH_3Cl and air were passed over the fresh catalyst for several hours before data was taken to allow the reaction and catalyst activity to reach steady state. At both temperatures, a comparison of inlet and effluent gas streams showed no change in composition and no new peaks in the chromatogram - indicating no conversion of CH_3Cl.

The catalyst was removed from the reactor and repacked with fresh catalyst. Results were repeatable and disappointing - no conversion of CH_3Cl was observed. Visual inspection of the used catalyst showed a pronounced color change: the yellow-brown fresh catalyst had turned blue-green after exposure to CH_3Cl. By slicing the catalyst, it was possible to determine that the blue-green catalyst was different from the color of the pellet interior, which resembled the color of fresh catalyst. Some chlorine had been incorporated into the catalyst as was shown by a standard silver precipitation of chloride ion from a catalyst sample washing.

As the catalyst change was initially hypothesized to be due to chlorine incorporation/poisoning, we ran other experiments in which proposed catalysts and sample pieces of materials of construction were placed in the reactor tube and exposed to 1/2 % of HCl and Cl_2 in air at 440°C. In this experiment, none of the catalysts underwent any visual changes including the V_2O_5 oxidation catalyst. In a similar experiment, alumina, cordierite -

TABLE 3. SPECIFICATION OF SUPPORTED V_2O_5 CATALYST, UNITED CATALYST TYPE C116-2-01

Chemical composition (wt %)	
V_2O_5	7.25 - 8.25
K_2O	9.0 - 10.75
Na	0.5 - 1.5
SiO_2	55 - 60
S	6.25 or greater
Bulk Density	45±5 lb/ft^3
BET Surface Area	1.0 - 5.0 m^2/g
Pore Volume (mercury porosimetry)	0.30 - 0.50 cc/g
Average Pore Diameter	0.5 microns
Particle Size (as purchased)	3/16" x 5/16"
Particle Size (as used in reactor)	425 - 850 microns

a monolith support material, nickel, Hastalloy C, and Inconel were all found to appear unchanged while both type 304 and type 316 showed obvious signs of gas phase corrosion.

DISCUSSION OF RESULTS

The present results are initially quite contradictory to the results of Kageyama (4). Kageyama prepared his catalyst by impregnating α alumina with an aqueous solution of pentavalent V_2O_5 in oxalic acid and calcining in air. The catalyst gave prolonged decomposition of both methyl chloride (12% conversion) and ethylene (15% conversion) at 400°C with a space velocity of 40,000 hr^{-1}. The differences can be understood, however, in terms of a combination of the rather complex behavior of molten salt catalysts and supported liquid phase catalysts. These areas have been recently reviewed by Kenney (5) and Villadsen and Livbjerg (6). In both reviews, the status of the fundamental understanding of the sulfuric acid oxidation catalyst is discussed. Although some advances have been made, the nature of the catalytic phase(s) is (are) not well understood. Basically it is accepted that most of the vanadium and potassium present form a single liquid phase of unspecified composition. Tandy (7) examined the equilibria of these melts with SO_2-O_2-SO_3 in the range 380 to 600°C. He concluded that above 440°C the liquid melt contains a vanadium compound dissolved in $K_2S_2O_7$. By gravimetric techniques, Tandy concluded that the vanadium compound at low temperatures was probably tetravalent $VOSO_4$ in a liquid melt where the potassium to vanadium ratio was 2.5 as in most commercial catalysts. The distribution of vanadium between noncatalytic tetravalent and catalytic pentavalent states was shown to change abruptly in the range 400-440°C with essentially all tetravalent vanadium at 400°C. Sulfur dioxide was also shown to be sufficiently reducing to carry out this reduction.

Glueck and Kenney (8) proposed a three step mechanism for the oxidation of SO_2 to SO_3 with two catalytic tetravalent vanadium species $V_2O_4 \cdot SO_3$ and $(VOSO_4^-)_2$. A reanalysis of some of Tandy's data was shown to be consistent with their proposed vanadyl sulfate dimer. However, they humbly reported that considerably more data would be required to distinguish between the many alternative mechanisms.

It would appear that in our experiments one experimentally consistent conclusion would be that the initial yellow pentavalent vanadium species had been reduced to an apparently non-catalytic tetravalent species. In this process, the methyl chloride would be oxidized and the catalyst melt reduced. A blue green color would be consistent with a large tetravalent $VOSO_4$ (blue) with minor amounts of pentavalent V_2O_5 (yellow). Moreover, the temperature range of our experiments, 360-412°C, would appear to be too low to activate an alkali sulfate promoted catalyst, but not necessarily for an oxalate/vanadate catalyst such as that used by Kayegama.

This last point raises further questions: given the rather complicated phase relationship of the chemical species comprising the catalyst, how can one expect to formulate a widely applicable toxic waste oxidation catalyst.

The rather stringent compositional requirements arising from the complex inorganic phase diagrams of the salt melts requires that inorganic substances not be included in the waste to be oxidized. This obviously requires that such supported liquid phase catalysts not be used in a primary combustor stage. In addition, it must be recognized that the equations governing the operation of the catalyst may have unconventional nonlinearities associated with the expected phase changes or regions of catalyst stability. On behalf of such catalysts, however, one must note that operation in large concentrations (10%) of such notorious catalyst poisons as SO_2 are possible. Obviously, much work remains and the costs and benefits have yet to be weighed.

CONCLUSIONS

(1) A gas chromatographic analysis procedure for the quantification of feed and product streams of a chlorohydrocarbon oxidation reactor has been developed.

(2) Tenax-GC is capable of separating HCl, Cl_2, and H_2O among other species - a separation not previously reported.

(3) A commercial promoted V_2O_5 oxidation catalyst has been found to be inactive for the oxidation of methyl chloride below 420°C. This inactivity is most probably due to the temperature involved rather than halogen poisoning.

REFERENCES

1. J.J. Kirkland, "Flourine-Containing Polymers as Solid Supports in Gas Chromatography", Anal. Chem., 35, 2003 (1963).
2. O.L. Hollis and W.V. Hughes, J. Gas Chromatog., 4, 235 (1966).
3. W. Hertl and M.G. Neumann, "Active Surface Sites and Deactivation of Chromosorb 102", J. Chromatog., 60, 319 (1971).
4. Y. Kageyama, "Method of Decomposing Halohydrocarbons", U.S. Patent 3,972,979 to Mitsubishi Chemical Industries, August 3, 1976.
5. C.N. Kenney, "Molten Salt Catalysis of Gas Reactions", Catal. Rev. - Sci. Eng., 11, 197 (1975).
6. J. Villadsen and H. Livbjerg, "Supported Liquid-Phase Catalysts", Catal. Rev. - Sci. Eng., 17, 203 (1978).
7. G.H. Tandy, "The Role of Alkali Sulfates in Vanadium Catalysts for Sulphur Dioxide Oxidation", J. Appl. Chem., 6, 68 (1956).
8. A.R. Glueck and C.N. Kenney, "The Oxidation of Sulfur Dioxide Over Molten Salts", Chem. Eng. Sci., 23, 1257 (1968).

Comments on Heterogeneous Catalytic Oxidation of Model Chlorinated Hydrocarbons

H. William Prengle, Jr.
University of Houston
Houston, Texas

At the outset one notes that this work involves gas-solid heterogeneous catalytic oxidation reactions, and has some very interesting possibilities for application to combined thermal and catalytic incineration.

The principal investigator and his coworkers are only about seven months into the work; their effort has been primarily devoted to setting up the experimental equipment and working out the analytical methods to track the molecular species.

The original proposal states the objectives of the project to be three-fold:

1) to measure the kinetics of heterogeneous oxidation of three sets of model compounds on three catalysts, supported V_2O_5, Cr_2O_3, and an oxyhydrochlorination catalyst;

2) to correlate the measured rates and determine rate expressions for the oxidation of chlorinated paraffins, olefins, and aromatic compounds as a function of temperature and reactant concentrations; and

3) to assess the effect of nitrogen and sulfur as potential catalyst poisons by measuring the rates of catalytic oxidation in the presence of SO_2 and NO_2.

At this point, I would like to comment on the possible future application of the results of the project.

You are all aware of the fact that as a result of certain industrial manufacturing operations—chemical manufacturing, refining operations, hardware manufacture, etc.—certain toxic and hazardous substances are produced. In some instances these materials can be chemically reprocessed (reduced, oxidized, or decomposed) for further use, but in numerous instances must be disposed, and incineration (combustion oxidation) is a prime candidate process. For substantial quantities of material this method is already being used, recovering the energy value of the waste in the process.

The obvious question arises: where do we stand on a general solution to incineration of toxic and hazardous wastes? Much work is being done on combustion research, a major thrust of which is to improve combustion efficiencies as a means to greater energy utilization and conservation. Surveys conducted in 1973-74 indicated that process heaters and combustors in the process industries averaged approximately 70% combustion efficiency, representing a substantial potential for energy conservation. Hence a drive was started to get combustion efficiencies up to the 90% range, and I'm pleased to report that new process heaters-combustors are being routinely installed with 92% combustion efficiency, by a combination of 1) air preheat with stack gas, 2) susbstantial reduction in excess air, 3) improved burners, and 4) improved instrumentation and control.

How does all this relate on the project we have just heard about? Obviously, one cannot simply combust all candidate toxic waste materials--thermally the oxidation may not be complete and undesirable products may be produced. Hence a combined thermal and catalytic combustion unit is indicated. However, today we cannot design such a unit with a high degree of reliability.

Having come from industry, petroleum refining, and chemical manufacture, into academia, I can project what a chemical plant manager would like to accomplish the task. We might call it an energy optimized toxic waste incinerator, and visualize it as shown in the accompanying figure. Liquid waste plus fuel is mixed with preheated air at the burner inlet and then combusted, releasing heat to a process fluid in the radiant and convection sections of the furnace, the process fluid being used to recover the energy. The combustion gases leaving the top of the furnace flow through the catalytic oxidation unit where molecular species are oxidized to lowest oxidation states. In this step the temperature would rise slightly because of additional oxidation. The exit gases flow through duct work into the air preheater, and thence, after heat exchange through a scrubber (if required), and finally out the stack. Depending on the pressure drop through the system, an inlet blower and an induced draft blower (existing technology) would be necessary.

Finally, in conclusion many of us eagerly await the results of the work of Manning and coworkers so that we can design a catalytic oxidation unit and evaluate its economics. We are particularly interested in:

1) the mechanisms and kinetics of the oxidation;
2) the catalysts, their site mechanisms, and whether there is significant thermal (free radical mechanisms) effects in the gas phase; and

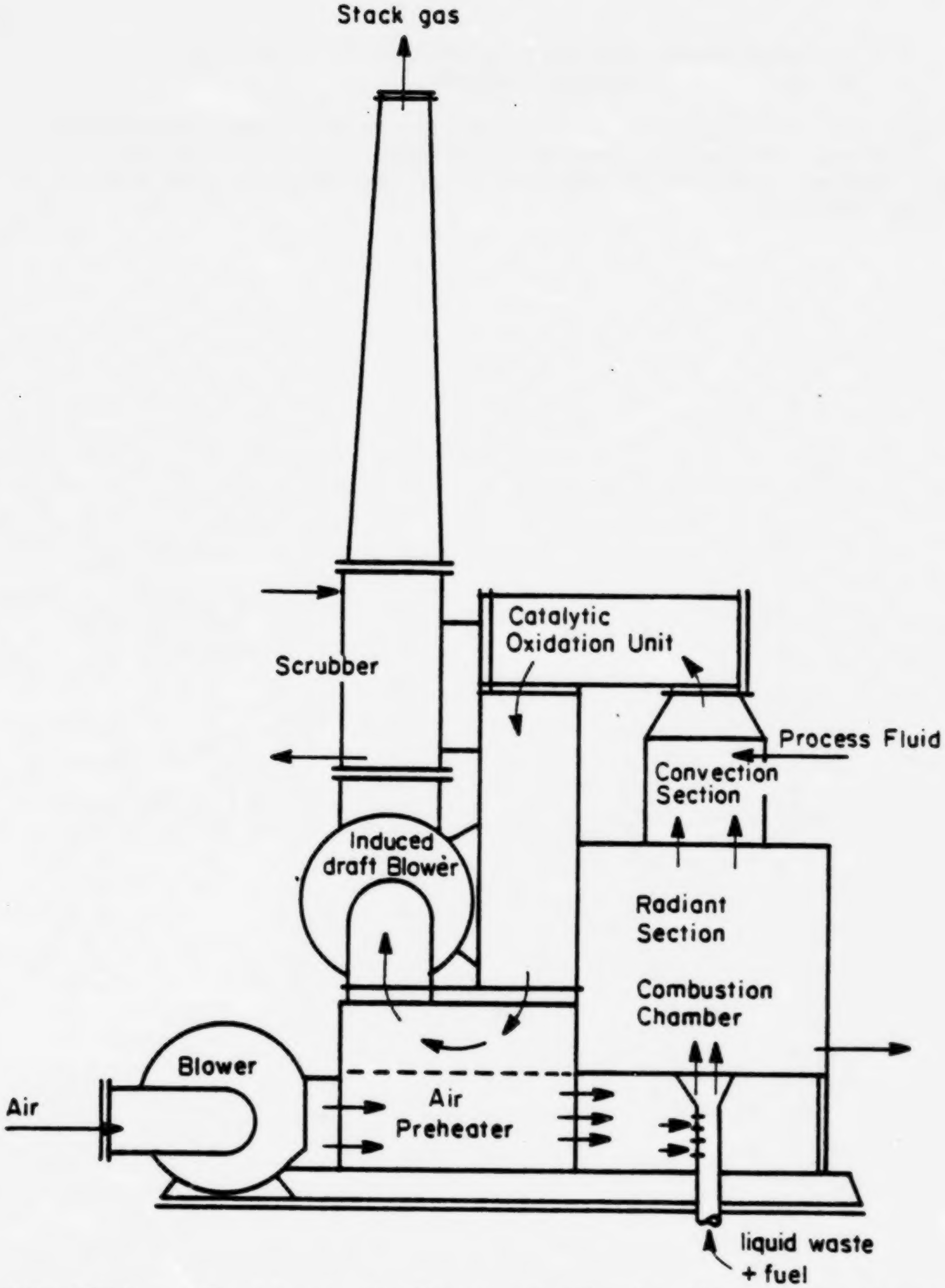
Stack gas
Catalytic
Oxidation Unit
Scrubber
Process Fluid
Convection
Section
Induced
draft Blower
Radiant
Section
Combustion
Chamber
Blower
Air
Air
Preheater
liquid waste
+ fuel

FIGURE - Energy Optimized Toxic Waste Incinerator

3) the temperatures and space velocities for conversion of the critical molecular species.

The fact that the catalyst changed color, in the preliminary experiments indicates that its chemical composition changed. Of course, a highly stable catalyst requiring no regeneration (or perhaps only once a year) would be desirable.

COMBUSTION OF CHLORINATED HYDROCARBONS

Selim M. Senkan*, Ashwani K. Gupta, John M. Robinson and Horacio Valeiras
Department of Chemical Engineering
and the Energy Laboratory
Massachusetts Institute of Technology
Cambridge, Massachusetts 02139

ABSTRACT

Controlled combustion/incineration of chlorinated hydrocarbons (CHC) under elevated temperature conditions is an attractive and environmentally sound option for implementing the disposal of chemical wastes containing CHC compounds. An understanding of the fundamental properties involved in the high temperature CHC oxidative processes is a prerequisite for the successful design and operation of reliable incinerators.

This paper presents some fundamental combustion characteristics of a number of CHC compounds in premixed methane/air flames at various flame stoichiometry under atmospheric conditions. Sooting limits and burning velocities of a variety of CHC compounds presented here have been determined using a flat flame and a Bunsen burner respectively.

A brief review of the experimental apparatus and methods employed herein is also presented.

INTRODUCTION

Chlorinated hydrocarbons (CHC) are among the most important compounds that are used by a large variety of industries. Significant quantities are produced by the chemical industry either as the primary product or as an intermediate. Consequently a proportional fraction of the CHC compounds are generated as wastes. Because many chlorinated hydrocarbons possess acute and chronic toxicity, stability, and accumulation in tissues they pose a potential threat to human health and the environment unless they are properly managed.

---

*To whom correspondence should be sent

Although there are a number of methods available for the disposal of hazardous wastes, direct controlled incineration at elevated temperatures appears to be an attractive method of treatment for the ultimate disposal of chlorinated hydrocarbons. Incineration/combustion, in spite of the high costs associated with it, is attractive because it can be applied essentially for the direct destruction of all combustible hazardous wastes including the chlorinated hydrocarbons, with the exception of wastes contaminated by volatile inorganics. In addition, combustion reduces the volume of the wastes significantly, thus decreasing the potential dangers associated with time storage and transportation of such toxic wastes. The incineration plants can be associated with the integral part of the waste generating plants or they can be a part of a central treatment/disposal facility.

The present day level understanding of the combustion principles of CHC compounds is at a very primitive level and is inadequate for the optimum design and operation of reliable incinerators. The overall objective of this study is, therefore, to obtain an insight into the fundamental combustion properties of various CHC flames having low heating values (high chlorine contents) with as little as possible (and possibly without) auxiliary fuel.

In this communication both burning velocities and carbon formation limits of various individual chlorinated methanes, ethanes, ethylenes, and chlorobenzene in mixtures with methane and air at various stoichiometry are presented. The utilization of methane as auxiliary fuel is necessary in order to generate self-sustaining stable flames, especially for compounds with chlorine contents in excess of 60-70 wt. %. Methane not only increases the heat of combustion of the mixture but also provides the necessary hydrogen for HCl formation for some of the CHC compounds. The presence of sufficient hydrogen is necessary in order to prevent chlorine formation, because of the difficulties involved in removing Cl_2 from stack gases.

Laminar burning velocity is one of the most important physiochemical properties of a combustible mixture. It is the velocity at which the flame front travels relative to the unburnt mixture and provides an insight into the overall rate of combustion. For one dimensional systems burning velocity corresponds to the eigenvalue of the flame equations. However, in spite of its definitional simplicity, measuring the burning velocity of a combustible mixture is far from being trivial. A large number of excellent reviews have been published over the years on this subject discussing the many different approaches to acquire burning velocity data; the most recent ones being by Andrews and Bradley (1), and Rallis and Garforth (2). Although there is still a lack of consensus as to the most appropriate technique, the method adopted here utilized direct flame photography of the Bunsen cone for obtaining the burning velocity data. The Bunsen cone method was chosen because of a) simple experimental set-up, b) rapid data acquisition and c) data of comparable quality with the other more sophisticated techniques.

The experimental data on the burning velocities of various chlorinated hydrocarbons in the open literature have been limited to very few compounds. However, it is now well established that the flame velocities of CHC compounds are considerably lower than that of the corresponding hydrocarbons without any chlorine. Garner et al. (3) examined the inhibitory effects of chlorinated methanes on the burning velocities of propane/air mixtures when present in quantities less than 1 mole percent. They concluded that the order of effectiveness in reducing burning velocity was $HCl < CH_3Cl < CH_2Cl_2 < CHCl_2 < CCl_4$. Morrison and Scheller (4) reported the amount of various chlorinated methanes needed to reduce the burning velocity of stoichiometric n-hexane-air mixtures by 30%. They reported inhibition effectiveness in an order almost similar to that of Garner et al. (3).

The formation and emission of soot from practical combustion systems is of great importance as it results in poor combustion conditions and loss of combustion efficiency, as well as the production of potentially toxic pollutants. However, under certain applications, the presence of soot in a furnace is beneficial for enhancing flame radiation and hence the efficiency of heat transfer from the flame. The soot is usually characterized by the volume fraction C (Cm^3 soot/cm^3), the number density N(1/cm^3) and the average size of the particles, d (A). For spherical particles $C = \pi/6 \cdot Nd^3$ so that a system can be characterized with a knowledge of any two variables. A number of techniques have been utilized in the past to study the formation and emission of soot from flames. Non-intrusive optical methods are attractive for probing sooting flames which can provide useful information not only for soot size and concentration but also particle growth by surface condensation or coagulation in the early stages of the flame (5,6). The optical properties of the soot are required for the evaluation of results. In this paper, however, the sooting limits were determined visually through the onset (or suppression) of yellow luminosity in CHC flames. Again many papers are available in the literature that address hydrocarbon fuels; the corresponding data from CHC flames are very scarce. One of the earliest systematic studies using conventional hydrocarbon fuels is by Street and Thomas (7), where they also reported that halogenated compounds increased the amount of air required to inhibit soot formation in their experiments.

Garner et al. (3), examined the promoting effects of adding chlorinated methanes on the soot formation rates of n-heptane/air and methylcyclohexane/air diffusion flames. They concluded that the order of effectiveness of the additives in increasing sooting rates was $CH_2Cl_2 < CHCl_3 < CCl_4$. This again indicates that as the proportion of chlorine in the additive molecule increases so does the soot promoting character of the compound when molar quantities are utilized. Scully and Davies (8), compared the soot yields from a variety of aromatic hydrocarbons as well as chlorobenzene flames under partially premixed conditions. The soot yield from chlorobenzene was found to be the highest. This was attributed to the relative ease of formation of the phenyl radicals and their subsequent polymerization. Soot formation limits of various hydrocarbons, as well as some CHC compounds under well stirred conditions were reported by Wright (9). He concluded that the effects of mixing on the carbon formation-limits was relatively small, the difference being of order 10-20% between well stirred and plug flow conditions. Therefore it appears that sooting limits are relatively insensitive to burner configuration.

EXPERIMENTAL APPARATUS

Laminar flame burning velocities were determined using a quartz Bunsen burner with an internal diameter of 1.0 centimeters. Liquid chlorinated hydrocarbons (all of which were with at least 99.9% purity) were injected into the metered and heated air/methane mixtures with a Sage Instruments Model 341A syringe pump as shown in Figure 1. The gases used were of 99.9% purity and were metered through Matheson R4700 series flow meters. When the desired flow rates were set, and a stable, laminar flame was obtained, flame photographs were taken with a 35 mm Olympus OM-I camera against the dark background using high speed black and white film. Flame front areas were then determined from the enlarged photographs of the Bunsen cone using the cone-angle method and consequently have been used to determine the burning velocities (1,2).

Soot formation limits were determined using a recently constructed 5 cm diameter flat flame burner system as shown in Figure 2. By shielding the flame zone with inert gas (nitrogen), the equivalence ratio of the mixture can be kept uniform in the flame by minimizing the entrainment of air from the outside. For the operation of the burner first the air/methane flow rate was established using the critical-orifice flow regulators. These gases were then sent to a heater. Using the pressurized delivery system as shown in Fig. 2, the liquid chlorinated hydrocarbons were injected into the preheated gases. The combustibe mixture was then carried through a mixing chamber and finally into the burner assembly all of which had also been heated to about the same temperature. The burner had a porous, sintered metal flame holder with a heating coil inside, through which water at 80° C, controlled thermostatically, passed continuously. Thus the premixed gases had been kept at a temperature in the range of 75-80° C prior to ignition throughout all the experiments. This appears to be an acceptable temperature regulation because carbon formation limits are not a strong function of preignition temperature (9).

EXPERIMENTAL RESULTS

Burning velocity (u_b), which is the velocity at which unburned gases move through the combustion wave in the direction normal to the wave surface, is an important fundamental property of a mixture. The burning velocity can be related to combustion reaction rates via the following expression which can be obtained through physiochemical reasonings (10):

$$u_b \sim (\alpha \cdot RR)^{0.5} \qquad (1)$$

where α is the thermal diffusivity of the mixture, and RR is the apparent combustion rate, the temperature dependency of which can be given by the following Arrhenius expression:

$$RR \sim k_o \exp\,[-E/RT_f] \qquad (2)$$

where k_o is the pre-exponential factor, E the activation energy, and T_f the flame temperature. It is clear then that a knowledge of flame velocities is desirable not because it is a fundamental property of the mixture,

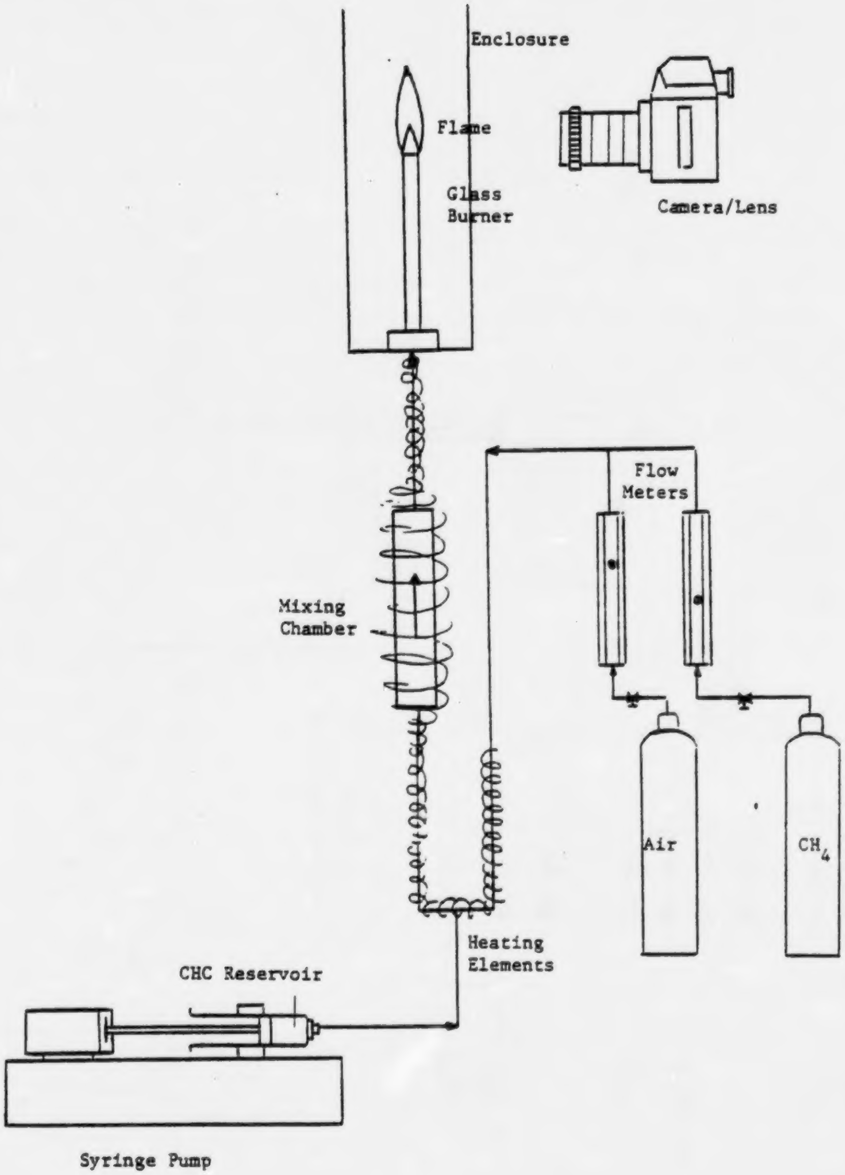
Enclosure
Flame
Glass Burner
Camera/Lens
Flow Meters
Mixing Chamber
Air
CH$_4$
Heating Elements
CHC Reservoir
Syringe Pump

Figure 1. Experimental Set-up for the Burning Velocity Determination

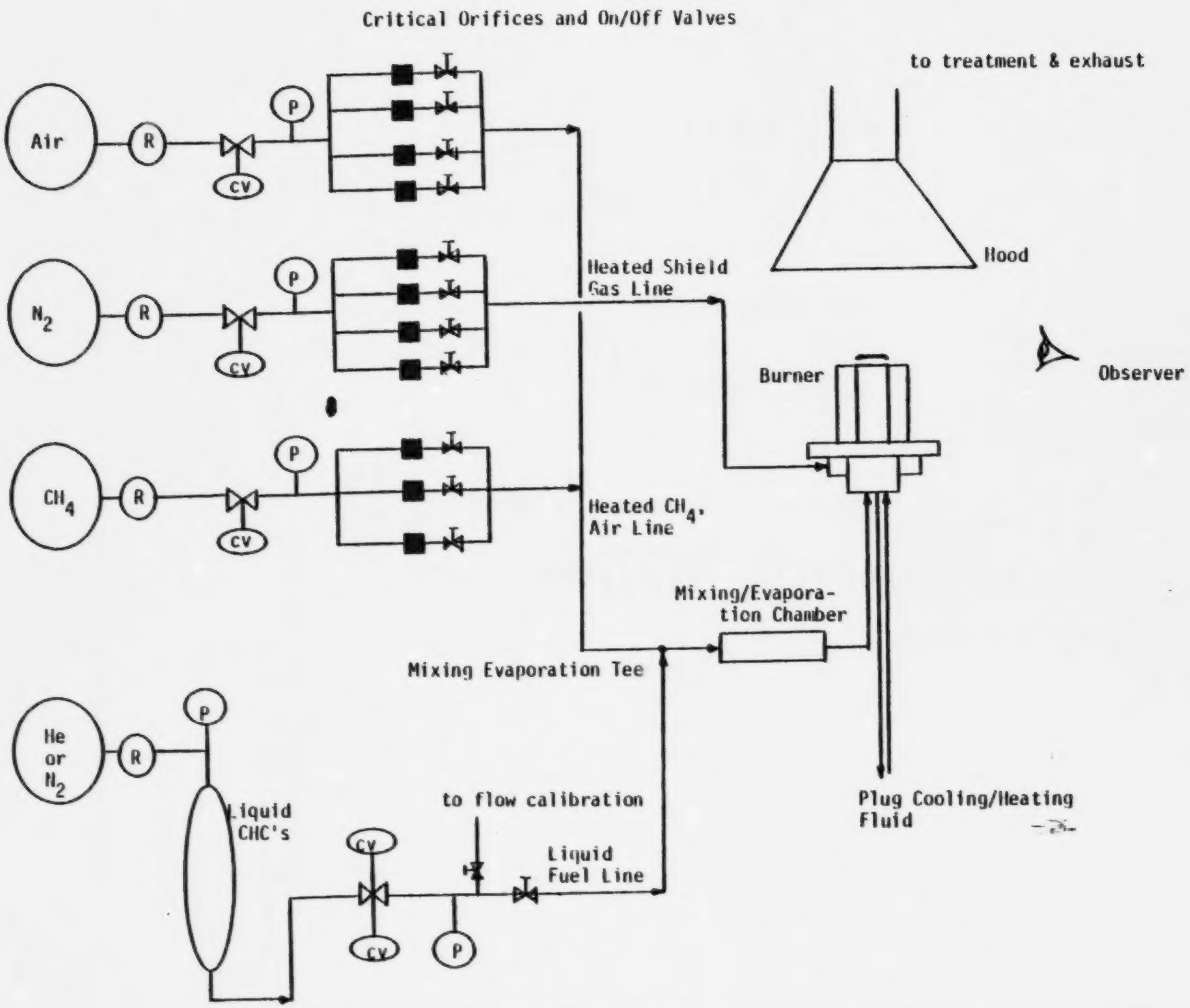
Critical Orifices and On/Off Valves
to treatment & exhaust
Air
R
CV
P
N2
CH4
Heated Shield Gas Line
Hood
Observer
Burner
Heated CH4, Air Line
Mixing/Evaporation Chamber
Mixing Evaporation Tee
He or N2
Liquid CHC's
to flow calibration
Liquid Fuel Line
Plug Cooling/Heating Fluid

Figure 2. A Schematic diagram of the flat-flame burner and the auxilliary equipment

but it also gives an insight to the rates of reaction which are important in the design and operation of practical combustors.

The burning velocities were determined by dividing the premixed gas flowrates by the flame front area which was determined photographically using the cone-angle method. According to this method the flame area (A_f) is approximated by an exact cone with an apex angle β as obtained directly from the pictures. Thus the flame area can be related to the cross-sectional area of the flame holder (A_o) by:

$$\sin \beta = \frac{A_o}{A_f} \quad . \qquad (3)$$

If the average unburnt gas velocity (u_o) is determined at the tube mouth, the burning velocity can then be calculated directly by the relationship:

$$u_b = u_o \sin \beta \quad . \qquad (4)$$

Although the above equation (4) is very easy to use, it is an oversimplification of a more complex picture as the actual flame area is not uniform. However, experiments with methane indicated that this method of analysis would be suitable if an accuracy of 10-20% is desired.

Figures 3 and 4 show how burning velocities of chlorinated methanes in methane/air mixtures vary with the equivalence ratio of the overall mixture (defined as the ratio of the fuel/oxygen ratio to the stoichiometric fuel/oxygen ratio, and the stoichiometric oxygen requirement is defined as the amount O_2 needed to convert all the carbon to CO_2 and the hydrogen left over from the amount needed for HCl formation, to H_2O) with chlorinated methane/methane ratio as the parameter. This stoichiometry is shown below for the general chlorinated hydrocarbons (CH_xCl_y):

$$CH_xCl_y + \left(1 + \frac{x-y}{4}\right) O_2 \rightarrow CO_2 + y\,HCl + \left(\frac{x-y}{2}\right) H_2O \qquad (5)$$

The above relationship reveals that if y > x the use of auxillary fuel is necessary in order to prevent Cl_2 formation. For the case when mixtures of CHC and methane flames are examined the resulting stoichiometric relationship becomes:

$$CH_xCl_y + \frac{1}{R} CH_4 + \left(\frac{2}{R} + 1 + \frac{x-y}{4}\right) O_2 \rightarrow \left(1 + \frac{1}{R}\right) CO_2 + yHCl + \left(\frac{2}{R} + \frac{x-y}{2}\right) H_2O \qquad (6)$$

where R represents the molar CHC-to-methane ratio.

An inspection of Figures 3 and 4 shows that all mixtures manifest the expected inverted U-shape behavior when u_b is plotted against the mixture equivalence ratio, (10). As the CHC/methane ratio is decreased, the curves shift upwards towards the $u_b - \phi$ curve of the methane-air mixture showing the decreasing inhibitory effects of the CHC compounds. From these results it can be concluded that CHC compounds have substantially lower flame velocities than those of the corresponding non-chlorinated hydrocarbons. This

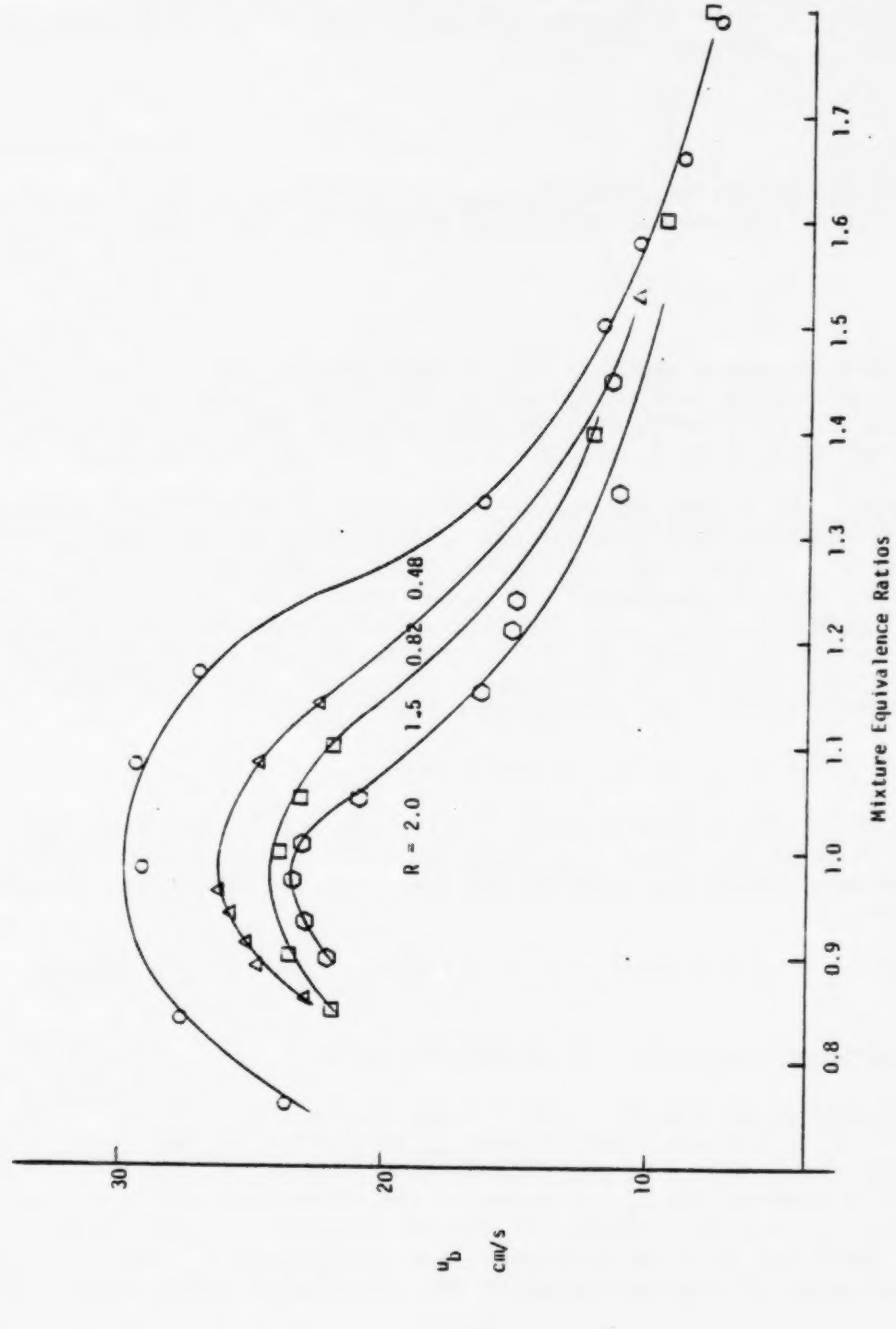

Figure 3. Flame Velocities of CH_3Cl-CH_4-Air Mixtures (T_o=79°C)

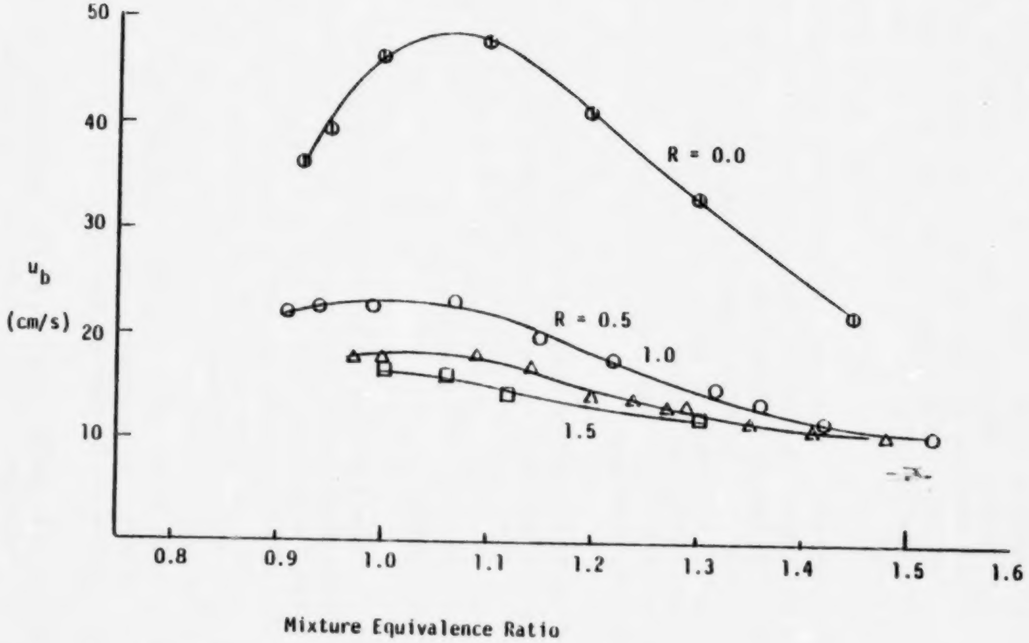

Figure 4. Flame Velocities of CH_2Cl_2-CH_4-Air Mixture (T_o=80°C).

indicates that the rates of combustion of CHC compounds are slower, thus they would need longer residence times and/or higher temperatures for complete combustion.

SOOT FORMATION LIMITS

Soot formation limits were determined visually, and they were identified as the combustible mixture equivalence ratio at which the carbon luminosity was just initiated or suppressed. This is commonly used by researchers and there is significant amount of data available in literature obtained by this method (7,9). The results reported here are in terms of equivalence ratios rather than O/C ratios because of the correlative characteristics of the former approach. For interested readers the limits of soot formation both in terms of critical equivalence ratios and critical O/C ratios are available in another publication (11).

Generally in premixed flames soot formation is not expected if the total oxygen is sufficient to convert the carbon to carbon monoxide. This, however, is an equilibrium consideration. In actual flames, the individual rates of soot formation and burnout times, freezing out of equilibria, etc., must all be considered in order to explain the observed phenomenon. Indeed, in many systems soot formation occurs more readily than might have been expected and varies with fuel type, residence time, temperature and chemical composition of the environment.

In the experimental results presented here, external air entrainment to the flame was minimized by shielding the flame with nitrogen gas. The effects of selective diffusion of species which are responsible for the formation of polyhedral or cellular flames are not considered. However, from the scatter of the data these appear to be of secondary importance in influencing sooting limits.

Figures 5 to 8 show how the onset of carbon formation limits are influenced by the CHC/methane ratio for the various chlorinated hydrocarbons investigated. It can be noticed that the lower the CHC to methane ratio, the higher is the critical equivalence ratios at which carbon formation occurs. This is expected because methane does not produce carbon within its limits of combustion in air, thus one observes a blowout before soot formation can be detected. The influence of CHC compounds in promoting soot formation can also be readily seen from these figures. Indeed, the higher the chlorine content of the parent CHC compound, the more pronounced is this effect, an observation also noted by Garner et al. (3).

Another important parameter that must be considered in examining these figures is the hydrogen/chlorine ratio of the system. If this ratio is less than unity, molecular chlorine will be formed in the combustion products, a situation which is frequently undesirable because of the difficulties involved in Cl_2 removal from stack gases. In most simple terms the possibility of Cl_2 formation can be explored using the following Deacon reaction:

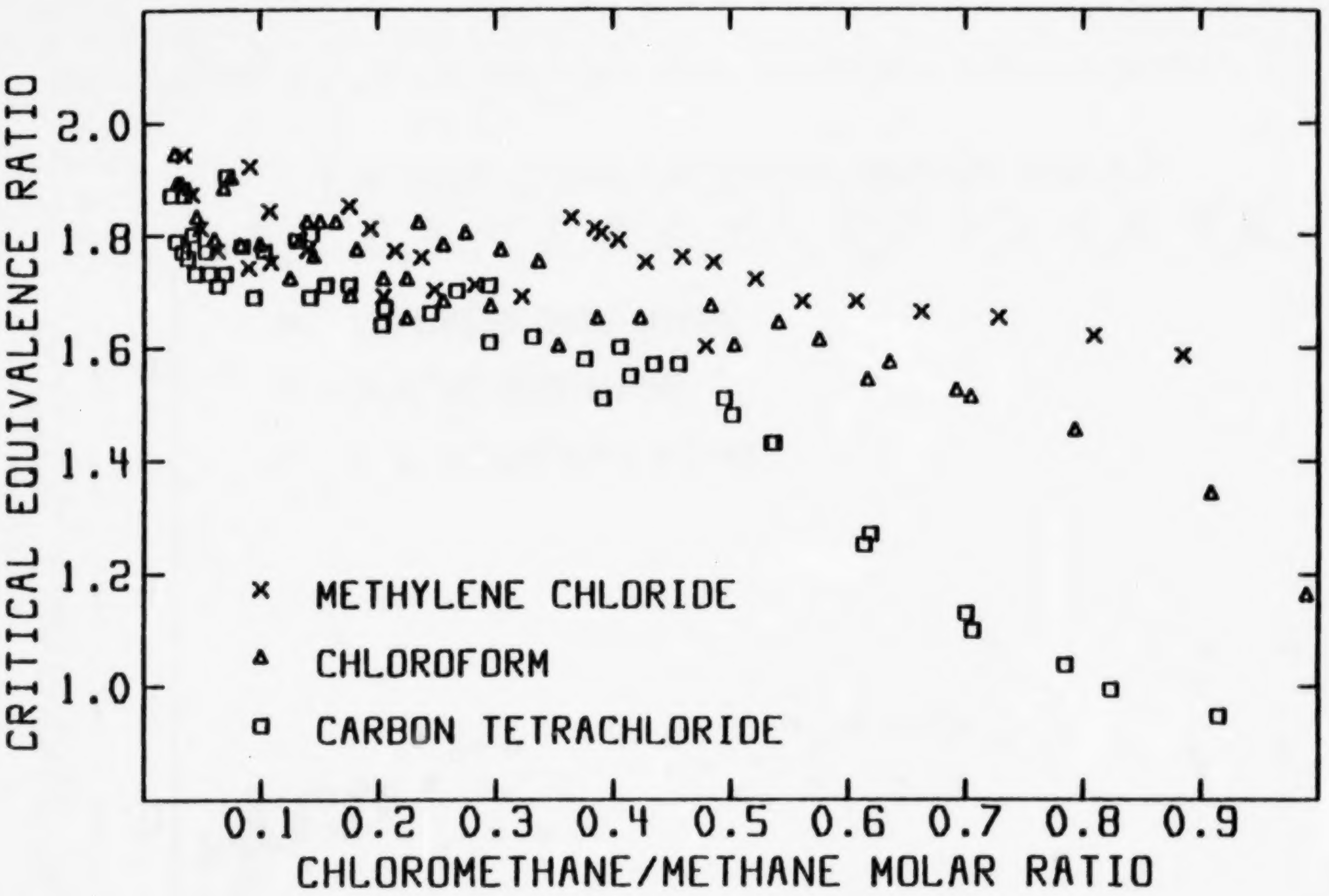

Figure 5. Critical Equivalence Ratios for Chloromethane-Methane-Air Systems.

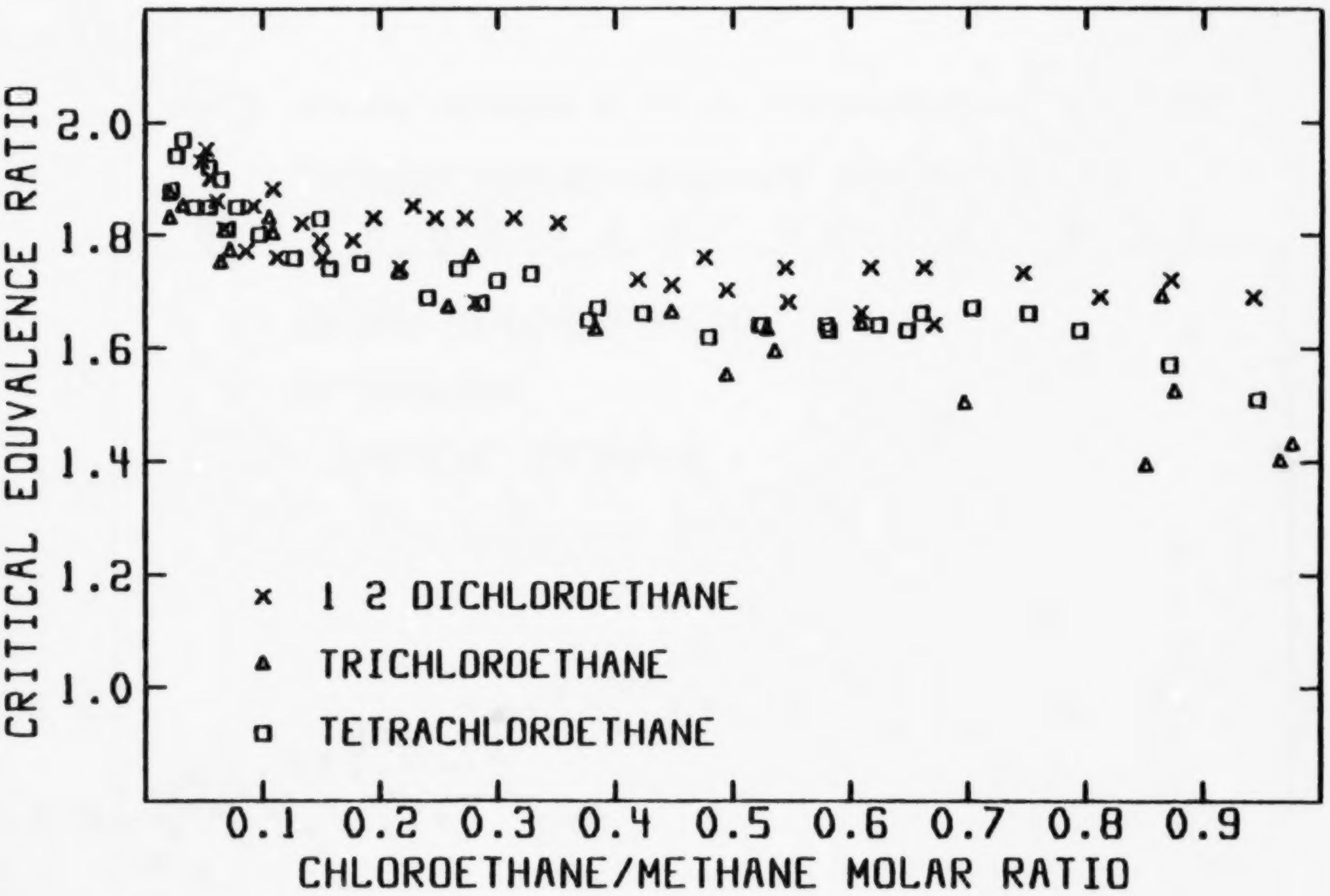

Figure 6. Critical Equivalence Ratios for Chloroethane - Methane-Air Systems.

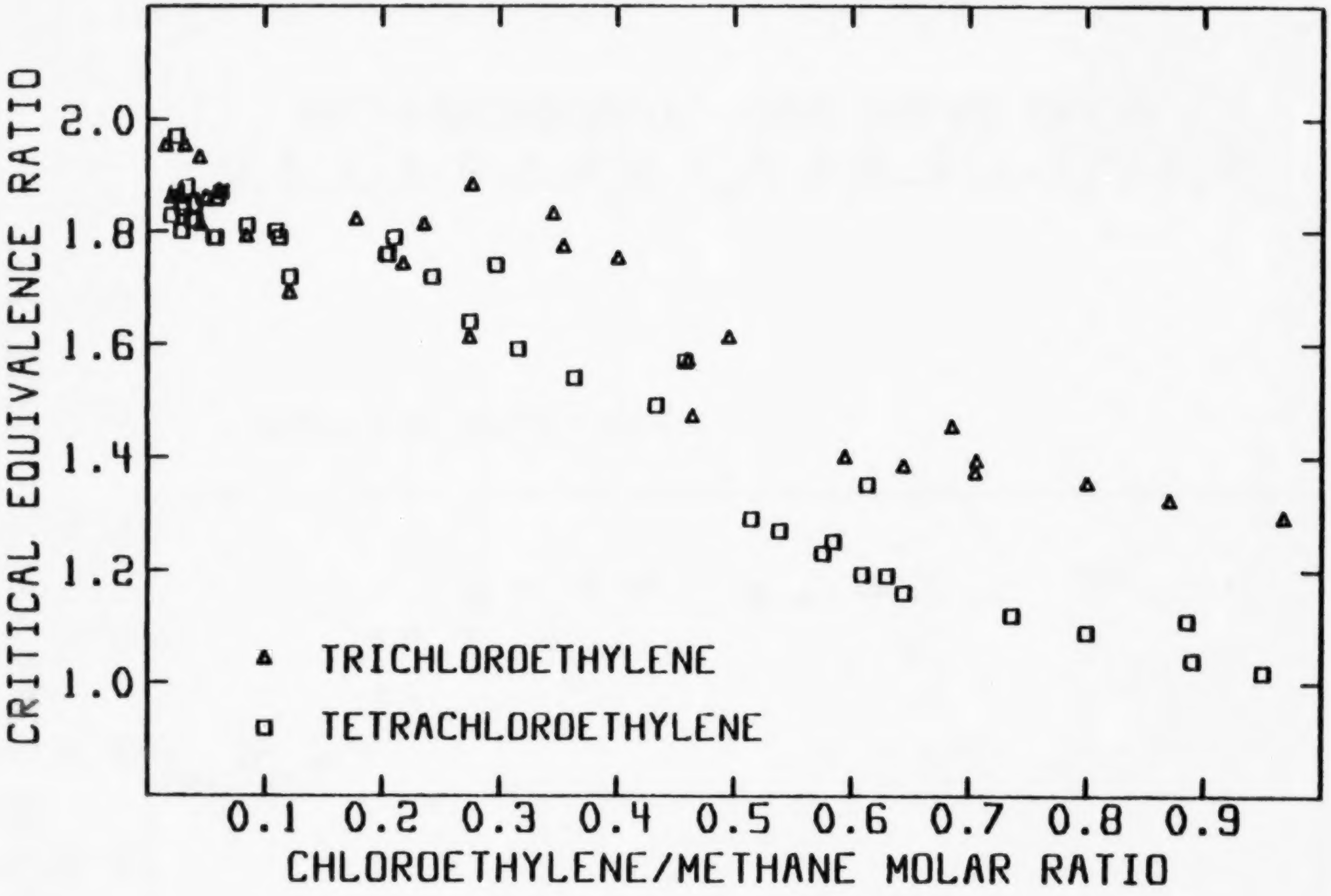

Figure 7. Critical Equivalence Ratios for Chloroethylene-Methane-Air Systems.

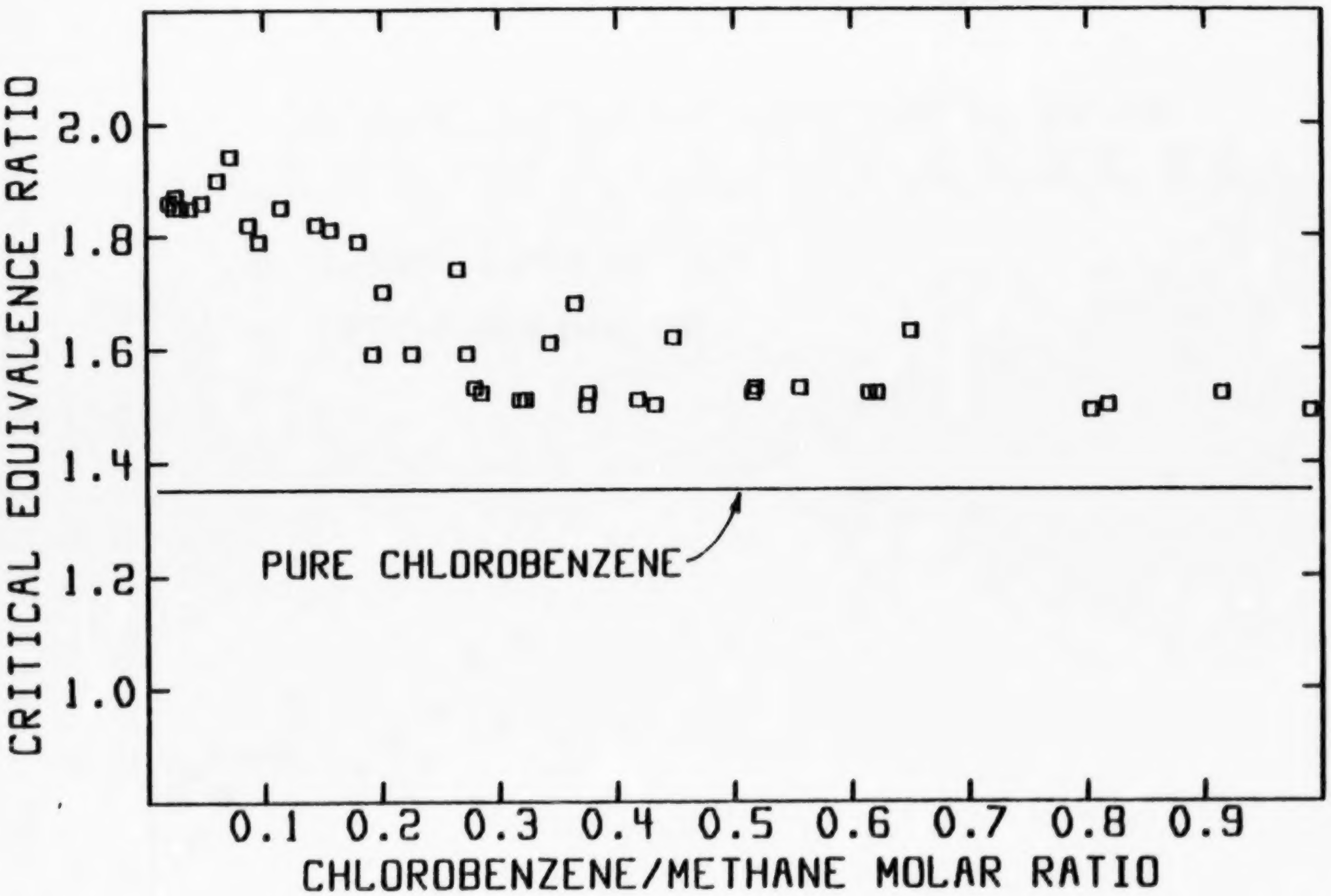

Figure 8. Critical Equivalence Ratios for Chlorobenzene-Methane-Air Systems.

$$2HCl + 1/2\ O_2 = Cl_2 + H_2O \qquad (7)$$

The carbon formation limits presented in these figures reflect the effects of chemical composition and heat transfer. Many data points were taken under conditions of the same chemical composition but different flow rates in order to ascertain the influence (if any) of the extent of cooling by the flame holder. An examination of the data revealed that these effects were of secondary importance in establishing the carbon formation limits.

CONCLUDING REMARKS

Experimental data on the laminar burning velocity of chlorinated methanes in methane-air mixture flames have shown that the burning velocity decreases significantly with increase in chlorine content according to

$$(CCl_4 < CHCl_3) < CH_2Cl_2 < CH_3Cl < CH_4.$$

The onset of soot formation are influenced by the CHC/methane ratio. The lower the CHC/methane ratio, the higher is the combined equivalence ratio at which the formation of soot begins to occur. The formation of soot in chlorinated hydrocarbons is more favored than the corresponding non-chlorinated compounds.

Therefore, both the low combustion rates and increased soot formation propensities of chlorinated hydrocarbons must be considered in the design and operation of practical incinerators.

ACKNOWLEDGEMENTS

This research was sponsored by funds from the United States Environmental Protection Agency, Grant No. R808314010, and the Massachusetts Institute of Technology.

REFERENCES

1. Andrews, G.E., and Bradley, D., "Determination of Burning Velocities: A Critical Review," Combustion and Flame, 18, 133 (1972).
2. Rallis, C.J., and Garforth, A.M., "The Determination of Laminar Burning Velocity," Prog. Energy Combust. Sci., 6, 303 (1980).
3. Garner, F.H., Long, R., Graham, A.J., and Badakshan, A., "The Effect of Certain Halogenated Methanes on Premixed and Diffusion Flames," 6th Symposium (Int'l) on Combustion, p. 802, The Combustion Institute, 1956.
4. Morrison, M.E., and Scheller, K. "The Effect of Burning Velocity Inhibitors on the Ignition of Hydrocarbon-Oxygen-Nitrogen Mixtures," Combus-

tion and Flame, 18, 3 (1972).

5. Wagner, H.G., "Soot Formation in Combustion," 17th Symposium (Int'l) on Combustion, p. 3. The Combustion Institute, 1979.

6. Mok, L., B.S. Thesis, MIT, May, 1980.

7. Street, T.C. and Thomas, A., "Soot Formation in Premixed Flames," Fuel, 34, 4 (1955).

8. Scully, D.B., and Davies, R.A., "Carbon Formation from Aromatic Hydrocarbons," Combustion and Flame, 9, 185 (1965).

9. Wright, F.J., "The Formation of Carbon Under Well-Stirred Conditions," 12 Symposium (Int'l) on Combustion, p. 867, The Combustion Institute, 1969.

10. Glassman, I., "Combustion," Academic Press, New York, 1977.

11. Senkan, S.M., Gupta, A.K., and Robinson, J.M., "Soot Formation Limits of Chlorinated Hydrocarbon-Methane-Air Premixed Flames," Combust. and Flame (to be published).

Comments on Thermal Destruction Kinetics of Chlorinated Hydrocarbons

Richard Chaddock
President, Environmental Management, Inc.
Port Orange, Florida

The objective as specified in the original proposal is to conduct premixed flame studies directed towards developing an understanding of the kinetics of thermal destruction of three classes of chlorinated hydrocarbons (CHC): chloromethanes, chloroethylenes, and chlorobenzenes. Experiments will be conducted using two burner systems: a flat-flame burner, and a Bunsen burner. CHC destruction rates will be studied as a function of changing Cl content of the CHC compound, temperature, excess air, and auxiliary fuel (CH_4) use. Single CHC compounds as well as their mixtures will be investigated. In parallel with the experimental work, theoretical studies will also be undertaken to model the flame structures.

The project, when completed, will provide a better understanding of the combustion processes involved in CHC oxidation. By acquiring such fundamental data, it will establish a basis from which various parameters for incinerator design, such as dwell time-temperature relationships, equivalence ratios, etc., can be set more scientifically.

The research investigation is in a very early phase and only preliminary experiments have been made. However, the work is directed toward achieving the objectives outlined above. The experimental program is well designed to obtain the data discussed in the proposal. The quality of the work appears excellent and it is difficult to find fault with the research studies made to date.

It is recommended that appropriate stack gas analyses be made to check on the combustion efficiency of the materials being burned.

THE EFFECT OF AERATION BASIN CONFIGURATION ON ACTIVATED SLUDGE BULKING AT LOW ORGANIC LOADING

Sang-Eun Lee*, Ben L. Koopman**, David Jenkins* and Ronald F. Lewis***

*Sanitary Engineering Research Laboratory, University of California Berkeley,
Richmond Field Station,
Richmond CA 94804
**Dept. of Environmental Engineering,
University of Florida, Gainesville,
Florida 33012
***Wastewater Research Division,
Municipal Environmental Research Laboratory USEPA,
Cincinnati OH 45268

ABSTRACT

Continuous-flow laboratory-scale activated sludge units were operated on domestic sewage at low F/M. In CSTR units at the F/M range of 0.05-0.25 g COD removed/g TMLVSS, day bulking did not occur with a weak (BOD_5 = 139 mg/L) sewage feed and TMLSS = 1.5 g/L. Supplementation of sewage by blending with raw sludge produced a stronger sewage (BOD_5 = 315 mg/L) which caused TMLSS to increase to 3.5 g/L. Bulking occurred in CSTR, 2, 4, 8, and 16 compartment units. An aeration basin with initial compartment 1/32nd of aeration basin volume prevented but did not cure bulking. An aeration basin with initial compartments 1/74th of aeration basin volume, prevented and cured bulking. Anoxia in an aeration basin with two initial compartments each 1/64th of the total aeration basin volume did not aid in curing bulking. The SVI of sludges at low F/M (0.3-0.35 g COD removed/g TMLVSS, day) and high TMLSS (3.5 g/L) is related to conditions in the initial compartment rather than those in the remainder of the aeration basin. Initial compartment soluble COD, first-compartment F/M, and initial compartment size are important; floc loading, dispersion number and total number of aeration basin compartments are not important.

INTRODUCTION

Filamentous activated sludge bulking is caused by the presence of large amounts (greater than 10 km/gSS) of various types of filamentous organisms extending from the activated sludge floc (Sezgin et al, 1978 (1) Palm, et al, 1980 (2)). Bulking has many causes; the types of filamentous organisms present can be useful in indicating the cause of bulking. Strom and Jenkins (1979)(3), using the key of Eikelboom (1975) (4) have found Sphaerotilus natans and Types 1701, 021N and 1863 to be characteristic of plants with aeration basin dissolved oxygen (DO) too low for the applied organic load (F/M); Microthrix parvicella and Types 0041, 0092 0581 and 1851 were associated with plants having low F/M. The remedy for low DO sludge bulking is to increase aeration basin oxygenation capacity or lower the F/M and is guided in principle by the work of Palm, et al (1980) (2) which established a relationship between F/M and minimum DO to prevent (or cure) S. natans bulking.

Direct remedy of low F/M bulking usually is not possible because low F/M may be required for nitrification, by designer preference, or because of lower than anticipated wastewater flows. Previous work (Chudoba et al, 1973a (5), 1973b (6), 1974 (7); Heide and Pasveer, 1974 (8), Rensink, 1974 (9), Houtmeyers, 1978 (10); Tomlinson and Chambers, 1976 (11), 1978 (12)), suggests that the growth of filamentous organisms at low F/M is suppressed in systems that either have a low degree of longitudinal mixing ("plug flow") or are provided with a short detention time initial compartment where sewage feed and return activated sludge are mixed. The mechanism of filamentous organism suppression is not clear. Suggestions include: lower filamentous organism growth rate compared to floc formers at high substrate levels (Chudoba et al, 1973b (6)); inability of filamentous organisms to store substrate for later use in growth (Houtmeyers, 1978 (10); Rensink, et al, 1977 (13)) and lower substrate utilization rate of filamentous organisms compared to floc formers (Houtmeyers, 1978 (10)). Eikelboom (1981) (14) recently has used the term "biosorption" to lump all of these factors together with physical incorporation of particulate and soluble substrates into the floc. He proposes that filamentous organism growth in activated sludges with high "biosorption capacity" can be suppressed by use of high initial "floc loading" values (mg COD/g MLVSS).

The work reported in this paper was directed towards a further understanding and definition of the effect of aeration basin configuration on activated sludge settling at low F/M values. The data of Palm et al (1980) (2) were used as a guide to set F/M and aeration basin DO concentrations to prevent low DO bulking.

MATERIALS AND METHODS

Experiments were laboratory-scale using systems with acrylic plastic aeration basins of total volumes that ranged from 10.5 L (for the completely mixed (CSTR) units) to up to approx. 80 L for various compartmentalized reactor units. Mixing was by paddles to produce a mean velocity gradient of 85 $\sec^{-1}$ exclusive of aeration. Total mixing intensity was increased by a maximum of 10 percent over that provided by stirring alone when house air was used for aeration; it was unchanged relative to stirring alone when pure oxygen was used for aeration. Air for aeration was cotton-filtered and water-saturated. Oxygen was supplied from cylinders through two-stage regulators and was water-saturated. Both were dispersed by porous diffusers. DO in the CSTR control units and in up to 5 of the initial compartments of the other aeration basin configurations was controlled by a feedback system consisting of a galvanic oxygen electrode, DO analyzer, and a recorder-controller that operated a solenoid valve on the air or O_2 supply line. A control range of approx. -0 mg/L and +1.0 mg/L relative to the desired minimum DO concentration was

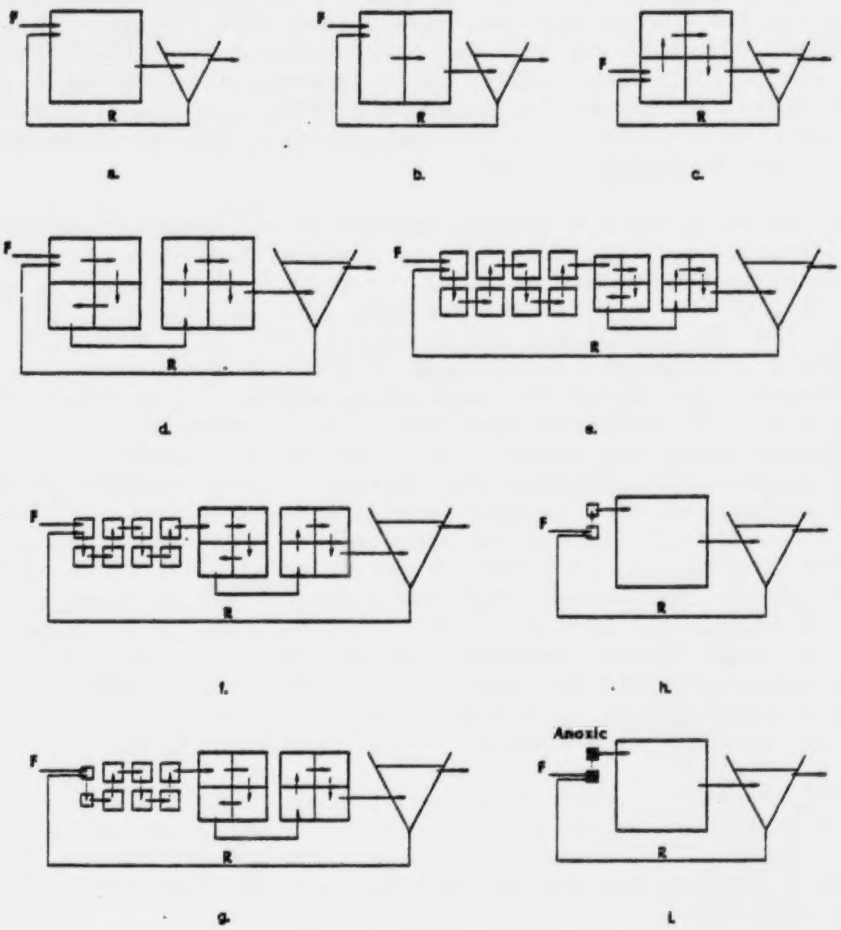

Figure 1. Aeration basin configurations used. Values of V_T/V_i are given in ( ).

a. CSTR system (1); for CSTR control, 10.5 L aeration basin; for 1 compartment system, 40-L aeration basin.

b. 40-L aeration basin, 2 compartments (2).

c. 40-L aeration basin, 4 compartments (4).

d. 80-L aeration basin, 8 compartments (8).

e. 56-L aeration basin, 16 equal-size compartments (16).

f. 58-L aeration basin, 16 compartments (32); first 8 are equal to each 1/32nd of total aeration basin volume and the next 8 are equally sized.

g. 58-L aeration basin, 16 compartments (74); first two are equal to each 1/74th, and the next 6 are equal to each 1/32nd of total aeration basin volume and the last 8 are equally sized.

h. 42-L aeration basin, 3 compartments (64); first two are equal to each 1/64th and the following one compartment is equal to 62/64th of total aeration basin volume.

i. 42-L aeration basin, 3 compartments (64); same as i, but two initial compartments are anoxic.

achieved. Air was supplied at a rate of 0.25 L/min to non-DO controlled compartments in 8 and 16-compartment configurations.

Secondary clarifiers were inverted erlenmeyer flasks with their bottoms cut off and in some cases with an acrylic plastic cylinder attached. Clarifier capacities were varied according to aeration basin capacity as follows: 2.4L for 10.5L aeration basin, 6L for 40L aeration basin, 10.5L for 56-58L aeration basins, and 9.3-10.5L for 80L aeration basin.

Bronze or nichrome wires bent to conform to the conical portion of the inner clarifier walls and rotated at 1 rpm, were used to aid thickened sludge flow to the recycle lines. Both influent sewage and return sludge were dosed into the aeration basin with peristaltic pumps. The ratio of return sludge (RAS) flowrate to influent flowrate was 1.0. Sludge was wasted directly from the aeration basin. Systems were operated at ambient temperature which varied between 18-24°C.

Systems were characterized by V_T/V_i ratio (V_T = total aeration basin volume, V_i = volume of initial aeration basin compartment) and by dispersion number, determined from Rhodamine B slug addition tracer studies on the aeration basin only with no secondary clarifier or RAS stream. Effluent was sampled at 15 min. intervals (approx. 3.5% of average hydraulic detention time). From the tracer curve, Dispersion Number, D/uL, was calculated from the following equation using the Newton-Raphson iteration technique:

$$\sigma^2 = 2(D/uL) - 2(D/uL)^2[1 - \exp(-uL/D)] \qquad (1)$$

Where σ^2 = determined value of variance (second moment of residence time distribution) (Van der Laan, 1958 (15); Levenspiel, 1962 (16)).

ANALYTICAL METHODS

BOD_5, TSS and VSS were by Standard Methods (1975)(17); COD was by Standard Methods (1975)(17) with a 1 hr. reflux time that was shown to yield values 98-100% of those using a 2 hr. reflux time; soluble COD was on Whatman GF/C filtered samples; NH_3-N was by the Solorzano method (Solorzano, 1969 (18)). nitrite/nitrate nitrogen was by copper-cadmium reduction (EPA, 1974 (19))and total Kjeldahl nitrogen was by digestion-distillation (EPA, 1974 (19)). F/M was calculated as:

$$F/M = \frac{\text{Total COD in (g/day) - Soluble COD out (g/day)}}{\text{TMLVSS (g)}}$$

Where COD in = COD of feed
COD out = COD of effluent
TMLVSS = aeration basin VSS, g + clarifier VSS, g

Clarifier VSS was performed on the mixed contents of the clarifier.

Filamentous organisms were characterized by the key of Eikelboom (1975)(4).

RESULTS

Five series of experiments were conducted. In the first series CSTR aeration basins (Figure 1a) were operated at several steady states in the F/M range 0.05-0.25 g COD removed/g TMLVSS, day. Experiments commenced with non-bulking sludge. At F/M values tested the CSTR did not produce a bulking sludge (Figure 2); neither was bulking sludge produced when the settled sewage feed was made stale (septic) by storage at room temperature for 2.5 days (Figure 2). Tomlinson and Chambers (1978)(20) had suggested that stale sewage could promote filamentous organism growth. In these experiments, the rather weak Richmond settled sewage was the feed stock. (BOD_5 = 139 mg/L, COD = 300 mg/L, TSS = 75 mg/L). Because of the weak feed, TMLSS levels were in the range 1.0-1.7 g/L.

Previous work on bulking at low F/M (Chudoba et al, 1973a (5), 1973b (6); Tomlinson et al, 1976 (11), 1978 (12)) was conducted with stronger influent wastes and thus higher MLSS concentrations resulted for an equivalent F/M. Also, Houtmeyers (1978)(10) observed that a continuously-fed, one-compartment activated sludge system produced bulking sludge at MLSS=4 g/L but not when MLSS was 1 g/L. Because of this, the strength of the Richmond settled sewage was increased by blending it with raw sludge settled from the same sewage in the SERL pilot plant primary clarifier. Blending was as follows: mix settled sewage with 15% by volume raw sludge for 1.5 hr; settle 30-45 min; mix supernatant and settled sewage in approx. equal volumes. A comparative analysis of Richmond settled sewage and the supplemented feed (Table 1) shows that while BOD_5 increased from 139 to 315 mg/L and COD increased from 300 to 750 mg/L, the BOD_5/COD ratio and the soluble fractions of BOD_5 and COD were similar. All other experiments were conducted with supplemented sewage.

The second series of experiments was conducted largely at F/M 0.15-0.20 g COD removed/g TMLVSS, day and TMLSS 3.0-3.5 g/L. Two parallel CSTR aeration basin systems were operated (Figure 1a), one receiving stale supplemented sewage and the other being fed with fresh supplemented sewage. Starting with a non-bulking sludge (SVI $\leq$ 100 mL/g, bulking (SVI $\geq$ 150 mL/g) occurred after 35 days in both systems when TMLSS concentration reached 3.0 g/L (Figure 3). Thereafter the two activated sludge systems were operated on fresh supplemented sewage feed. Following the demonstration that fresh supplemented sewage feed produced bulking, the first activated sludge system was designated as a CSTR control. The second unit was operated at steady-state with an aeration basin divided progressively into 2, 4, 8, then 16 equal-sized compartments. Sewage feed and RAS always entered the first compartment. As Figure 3 shows, compartmentalization to 16 equal-sized compartments did not improve sludge settleability over the control CSTR.

The third series of experiments employed a CSTR control (Figure 1a) and a 16 equal-sized compartment aeration basin (Figure 1e). Both units were operated at steady-state F/M values in the ranges 0.15-0.20, 0.20-0.25, 0.35-0.45, 0.5-0.6, 0.6-0.8, 0.9-1.15 and 1.15-1.4 g COD removed/g TMLVSS,day.

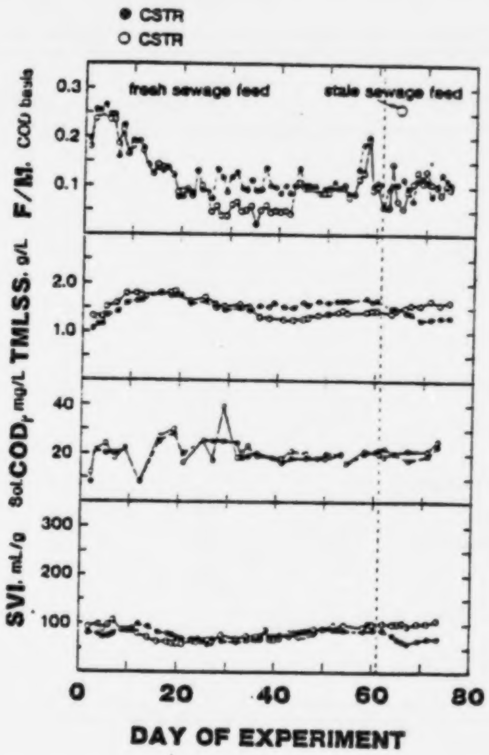

Figure 2. Experimental Data: First series of experiments. Starting with a non-bulking sludge, bulking does not occur in a CSTR (TMLSS = 1.5 g/L), F/M in range 0.05-0.25 g COD removed/g TMLVSS, day, using either fresh or stale unsupplemented Richmond settled sewage feed.

For the F/M values, 0.15-0.20, 0.20-0.25, 0.35-0.45 and 0.5-0.6 the activated sludge initially was bulking (Figure 4); for the F/M values, 0.6-0.8, 0.9-1.15 and 1.15-1.4 the control and 16-compartment unit were started with non-bulking sludge from a laboratory batch system. Figure 4 shows that while sludge in the 16-compartment unit bulked somewhat later than that in the CSTR control, bulking was not prevented at any of these F/M ranges by aeration basins with 16 equal-size compartments. At the lower F/M values it was concluded that bulking could not be cured by use of a 16 equally-sized compartment aeration basin.

Because the use of a 16 equal-size compartment reactor did not prevent or cure bulking at any of the F/M values tested in the third series of experiments, it was decided to return to an F/M value of 0.3 g COD removed/g TMLVSS, day, and examine the effect of utilizing initial reactor compartments smaller than 1/16th of the total reactor volume. The first 8 compartments were reduced in size to the desired fraction of the total aeration basin volume;

TABLE 1. TYPICAL COMPOSITION OF RICHMOND SETTLED AND SUPPLEMENTED SEWAGE

Component	Settled[a]	Supplemented[a]
COD		
Total, mg/L	300	750
Particulate, %	52	48
Soluble, %	48	52
BOD_5		
Total, mg/L	139	315
Total COD/BOD_5	2.2	2.4
Kjeldahl Nitrogen		
Total, mg/L	38	46
Particulate, %	14	25
Soluble, %	86	75
Suspended Solids		
Total, mg/L	75	173
Volatile, %	67	67

[a] $NaHCO_3$ (approx. 400 mg/L) was added to the sewage feed to provide buffer capacity. This maintained aeration basin pH in the range 6.5-7 in the presence of complete nitrification.

the last 8 compartments were sized so that the total reactor volume was 56-58 L. This type of system is referred to as a "selector" configuration. At all times a CSTR control was run in parallel. All units were operated at F/M 0.3 g COD removed/g TMLVSS, day, TMLSS = 3.0-3.5 g/L and with fresh supplemented settled sewage feed.

A selector configuration of 8 reactors each 1/32nd of the total basin volume (Figure 1f), prevented bulking while the CSTR control bulked (Figure 5, Days 0 to 26). At this point (Day 26) the test unit aeration basin was changed back to 16 equal-sized compartments (Figure 1e), and the control CSTR unit was restarted with non-bulking sludge. Again the CSTR bulked. The unit with 16 equal-size compartments also bulked, but less rapidly than the CSTR control (see Figure 5, Days 27 to 58).

The system with 16 equal-size aeration basin compartments (Figure 1e) was returned to a selector configuration with the first 8 compartments, each 1/32nd of the total reactor volume (Figure 1f). This selector configuration, which had previously prevented the bulking of a non-bulking sludge did not cure an already-bulking sludge. The SVI of the selector unit and control unit fluctuated widely, but were similar to each other (Figure 5, Days 59-101).

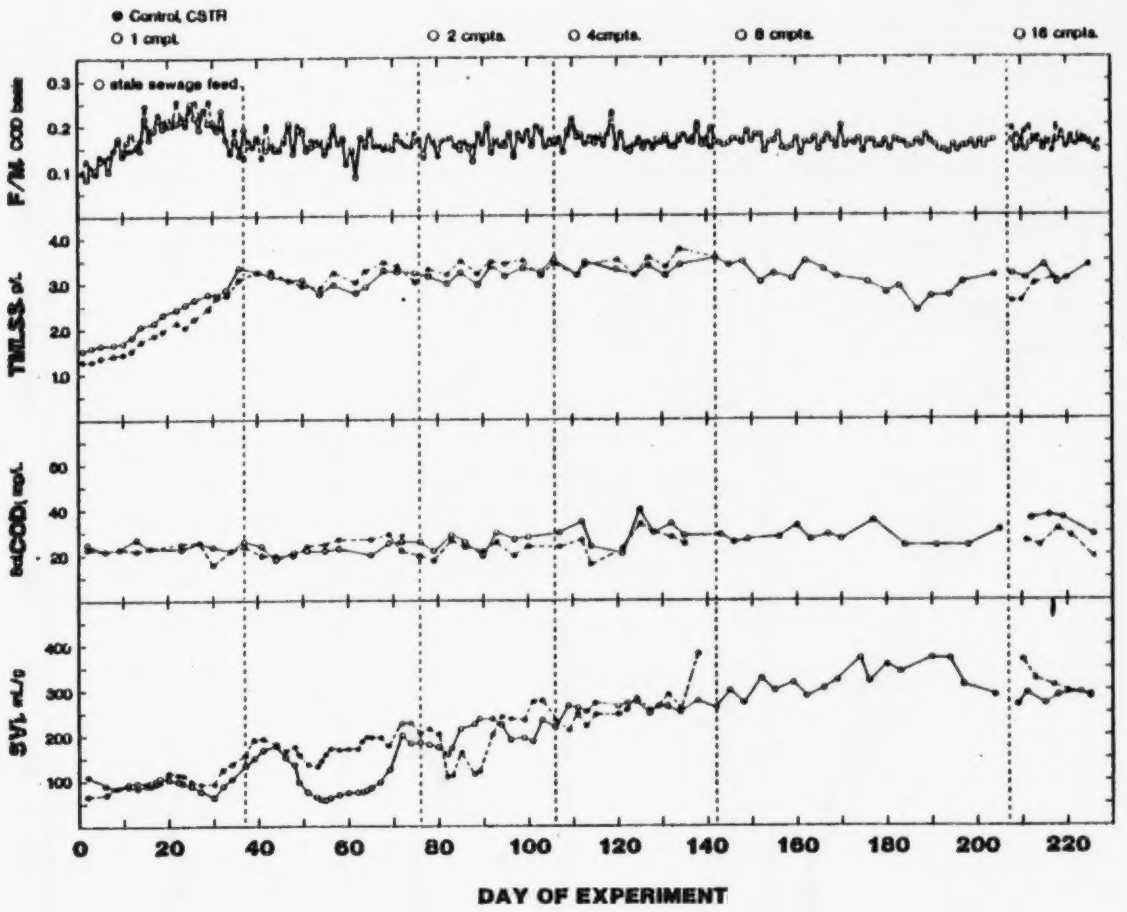

Figure 3. Experimental data; second series of experiments. Starting with a non-bulking sludge and either fresh or stale supplemented sewage feed, bulking occurred at TMLSS = 3-3.5 g/L, F/M = 0.15-0.20 g COD removed/g TMLVSS, day. Compartmentalization of aeration basin successively into 2, 4, 8 and 16 equal size compartments operated with RAS and sewage both entering the first compartment did not dure the bulking.

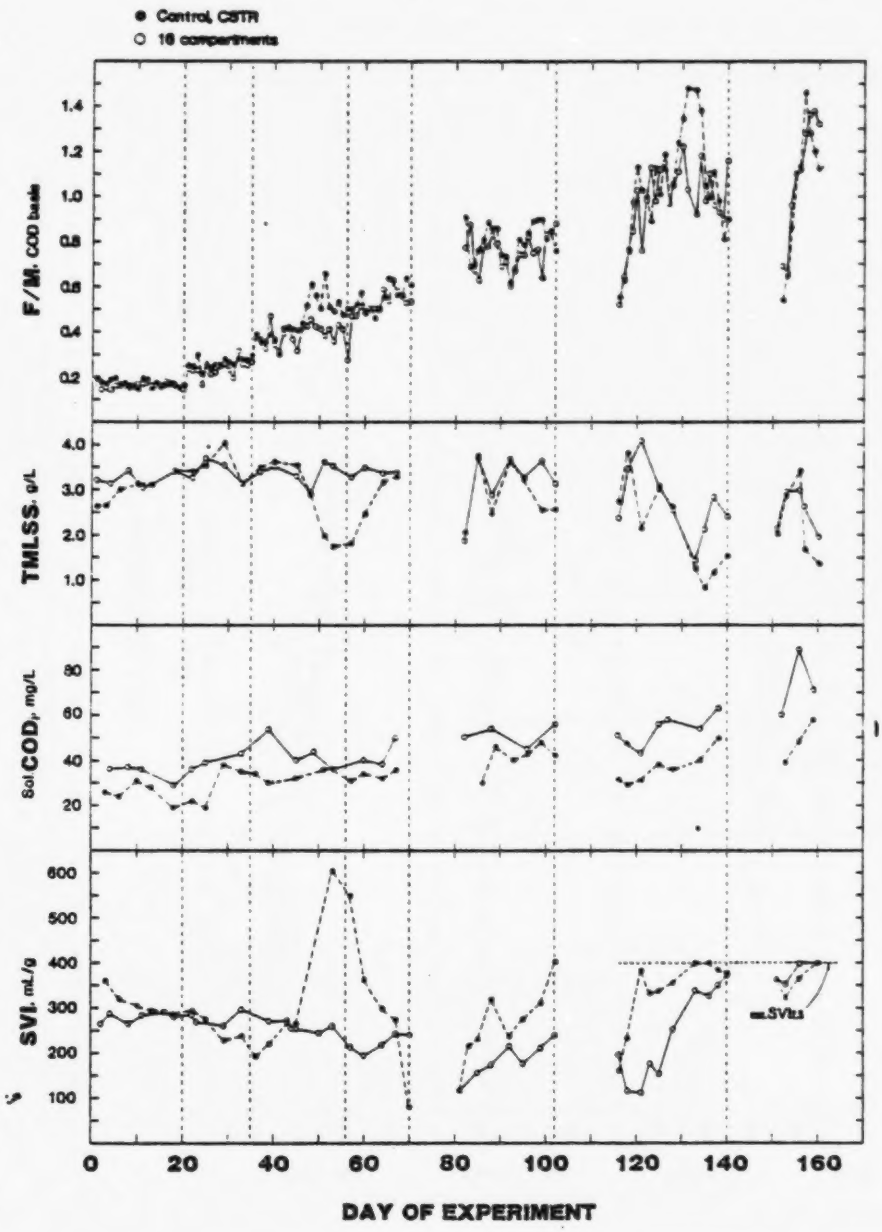

Figure 4. Experimental data; third series of experiments. With a 16 equal-size compartment aeration basin, and RAS and sewage fed to the 1st compartment, F/M was raised progressively from, 0.15-0.20 to 0.2-0.25, 0.35-0.45, 0.5-0.6, 0.6-0.8, 0.9-1.15, 1.15-1.4 (all g COD removed/g TMLVSS, day). Bulking either was not cured or not prevented at all F/M values tested.

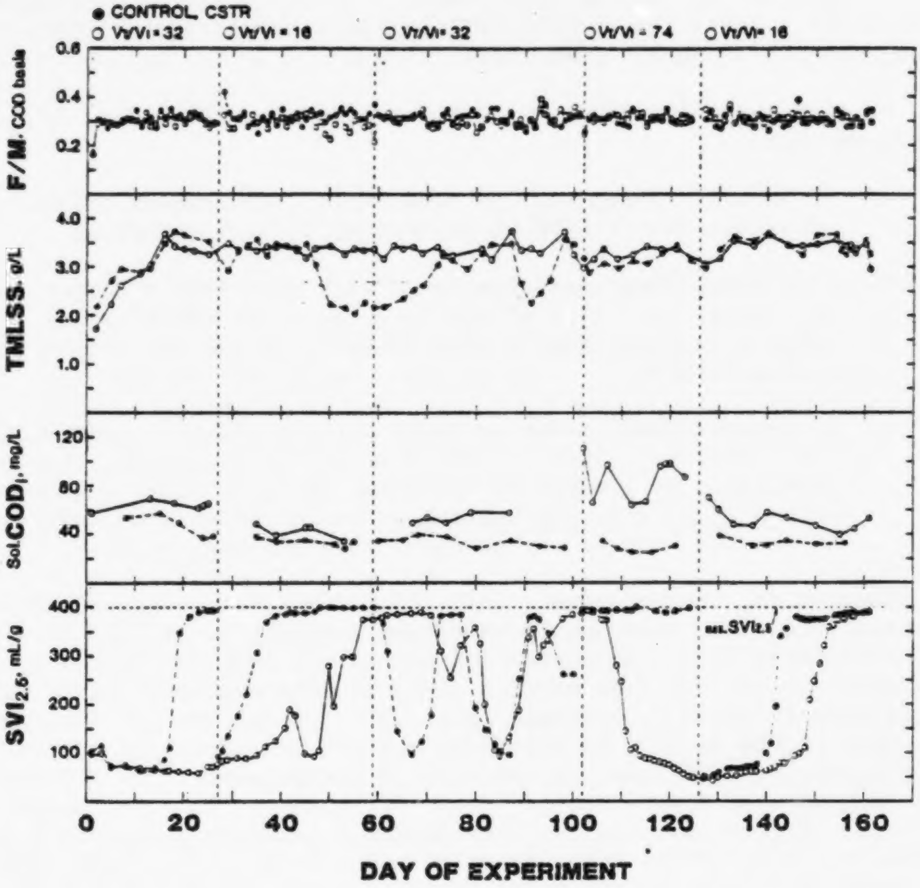

Figure 5. Experimental data: Fourth series of experiments. The first eight compartments were converted to selector units. (V_T = total aeration basin volume; V_i = volume of initial compartment).

At this point it was planned to change the selector configuration so that the first 2 compartments were 1/64th of the total aeration basin volume, the following 6 compartments were 1/32nd of the total aeration basin volume, and the last 8 compartments were equally-sized to give a total aeration basin volume of 56-58L (Figure 1g). However, a measurement error resulted in the first 2 compartments being 1/74th of the total aeration basin volume. Starting with a bulking sludge, this selector configuration rapidly reduced SVI while CSTR continued to bulk (at maximum SVI). (Figure 5, Days 102 to 124)

The unit with the selector configuration containing non-bulking sludge was changed to a 16 equal-size compartment aeration basin (Figure 1e);

the control CSTR was restarted with non-bulking sludge. Both units bulked (Figure 5, Days 127 to 161) as previously at this configuration (Figure 5, Days 27 to 58). Again the control CSTR bulked somewhat more rapidly than the unit with the 16 equal-sized compartments.

At this stage for F/M = 0.3 g COD removed/g TMLVSS, day, it had been deduced that:

a. An aeration basin with 16 equal-size compartments offered little advantage over a CSTR in preventing or curing bulking.

b. A 16-compartment aeration basin with its first 8 compartments each equal to 1/32nd of the total aeration basin volume would prevent bulking (when a CSTR bulked) but was not effective in curing bulking.

c. A 16-compartment aeration basin with its first 2 compartments each equal to 1/74th (at the time of the experiment this was thought to be 1/64th) of the total aeration basin volume would both prevent and cure bulking while an equivalently operated CSTR would bulk or not be cured from bulking.

Because the 16-compartment unit, with 2 initial compartments equal to 1/74th of the total aeration basin volume (thought to be 1/64th at the time) was successful in both preventing and curing bulking, it was decided to determine whether the same results could be obtained when the 2 initial selectors were followed by a single large CSTR (rather than 14 further compartments). Also it was decided to determine whether any advantage existed in creating anoxia (no-aeration) in the first 2 compartments. To achieve these goals 3 reactor trains were set up in the fifth series of experiments: a control CSTR (Figure 1a), and two 3-compartment reactors each with 2 initial compartments 1/64th of the total aeration basin volume and a third with a volume equal to 62/64th of the total aeration basin volume (Figure 1h and 1i). In one of the 3 compartment units the 2 initial selector compartments were aerated with oxygen (DO = 4.5 mg/L); in the other, the 2 initial selector compartments were covered and stirred. The freeboard volume was purged with N_2 gas.

Figure 6 shows that the unit with two 1/64th volume aerated selectors reduced the SVI slowly and erratically to final values of 173 mL/g (at 2.5 g TSS/L) and 150 mL/g (at 1.5 g TSS/L). The final SVI value in the CSTR control and the unit with two 1/64th volume anoxic selectors was the maximum value possible (i.e. 400 mL/g at 2.5 g TSS/L and 667 mL/g at 1.5 g TSS/L). While the final SVI value in the aerated selector would still classify this sludge as a bulking sludge, these values were significantly lower than in either the control or anoxic selector systems. Table 2 summarizes average operating data and initial and final SVI values for all experiments that employed selector configurations.

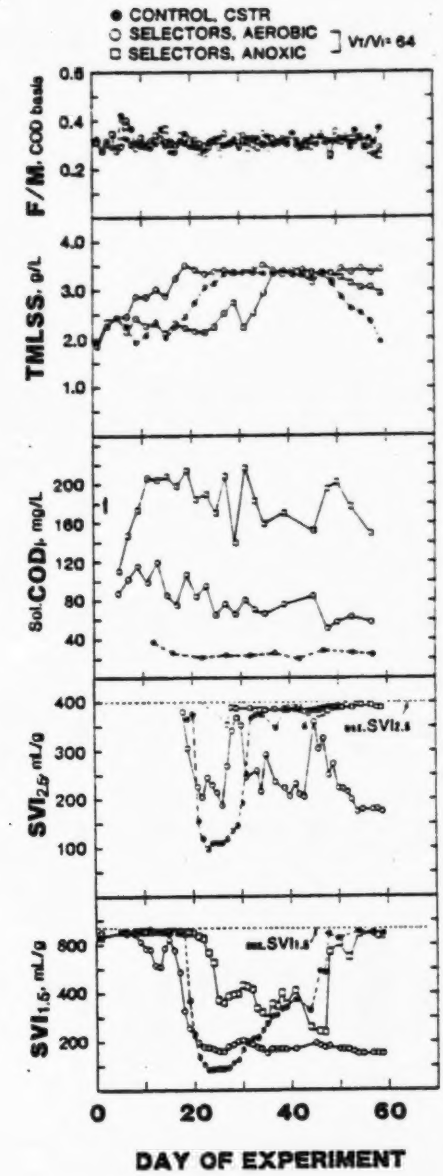

Figure 6. Experimental data; fifth series of experiments. Reactor configuration was two initial compartments each 1/64th of total reactor volume followed by a single compartment to bring total aeration basin volume to 42 L.

TABLE 2. OPERATING DATA SUMMARY FOR EXPERIMENTS EMPLOYING SELECTOR CONFIGURATIONS

Parameters	Units	Control CSTR	16 Compartment aeration basin					Two selectors + CSTR (Aerobic)	(Anaerobic)
V_T/V_1		1.0	32	16	32	74	16	64	64
Operation period	day	216	26	33	42	23	35	56	56
F/M	$\frac{\text{g COD removed}}{\text{g TMLVSS, day}}$	0.31	0.31	0.30	0.30	0.31	0.31	0.31	0.31
TMLSS	g/L	3.0	3.2	3.4	3.4	3.3	3.4	3.2	2.7
Average hydraulic Detention time	hr	19	17	18	19	20	21	21	.22
MCRT	day	15	14	15	14	12	13	12	14
Sewage strength	mg COD/L	720	620	660	720	745	790	830	830
$SVI_{2.5}$									
Initial	mL/g	96	98	78	373	389	46	400*	400*
Final	mL/g	400*	70	373	376	50	387	173	392
Initial Compartment F/M	$\frac{\text{g COD removed}}{\text{g MLVSS, day}}$	0.32	9.0	5.0	8.0	22.0	5.0	21.0	20.0
Soluble COD	mg/L	33	63	43	53	87	48	75	183

*Maximum SVI value at 2.5 gSS/L

DISCUSSION

Bulking at low F/M did not occur when CSTR activated sludge systems were operated for 75 days with unsupplemented (weak) Richmond settled sewage feed. With this feed, aeration basin TMLSS values were in the range 1.0-1.7 g/L and F/M was varied between 0.05-0.25 g COD removed/g TMLVSS, day; both fresh and stale settled sewage were fed. As soon as the TMLSS levels were raised to 3.0-3.5 g/L by feeding stronger sewage (supplemented with raw sludge) the CSTR units bulked. It would therefore appear that low F/M bulking is a phenomenon associated with strong (or raw) sewage feed and/or high MLSS levels. Further work is needed to separate the effects of these two parameters.

The effect of reactor compartmentalization on sludge settling is depicted in Figure 7. This plot is of the final SVI of systems that were started with bulking sludge. The plot shows that as the value of V_T/V_i increases above approx. 40, the final SVI decreases rapidly. It would appear that for this system to produce a sludge with an SVI of below 100 mL/g, at least 2 initial reactors with volumes of 1/70th-1/80th or less of the total reactor volume are required. Previous workers (Chudoba et al, 1973a (5), 1973b (6); Rensink et al, 1977 (13); Tomlinson and Chambers, 1978 (12))have suggested a relationship exists (at low F/M) between SVI and the degree of longitudinal mixing; others (Tomlinson and Chambers, 1976 (11), 1978 (12), Eikelboom, 1981 (14); Houtmeyers 1978 (10))have proposed that it is the presence of an initial high substrate level, where RAS and influent waste mix, that is important. It is argued that it is not important whether this is achieved by a reactor with a low degree of logitudinal mixing(i.e. many small compartments in series) or by one or more small reactors (initial mixing zones) followed by a larger completely mixed basin. The data presented here support the latter view since a plot of final SVI vs the reciprocal of the dispersion number (uL/D) (Figure 8) does not produce the consistent relationship found in the plot of V_T/V_i and final SVI (Figure 7). Some workers (Chudoba, 1973a (5), 1973b (6), Rensink et al, 1977 (13))have suggested that the COD gradient along a compartmentalized aeration basin is an important factor in controlling low F/M bulking. Others (Eikelboom 1981 (14); Tomlinson, 1976 (11))have argued that it is the conditions (e.g. floc loading and soluble COD concentration) in the initial mixing zone that are important. Figure 9 relates the final SVI to soluble COD concentration in the first compartment. It shows the same consistent relationship as that between final SVI and V_T/V_i. Figure 10 shows that apart from differences in the soluble COD concentration in the initial compartment the soluble COD gradients throughout all of the systems examined were virtually identical. These data again support the view that initial compartment conditions are more important than changes in conditions throughout the reactor. Figure 11 is a plot of the final SVI vs F/M in the initial aeration basin compartment. Figure 12 shows the relationship between final SVI and the floc loading(Eikelboom,

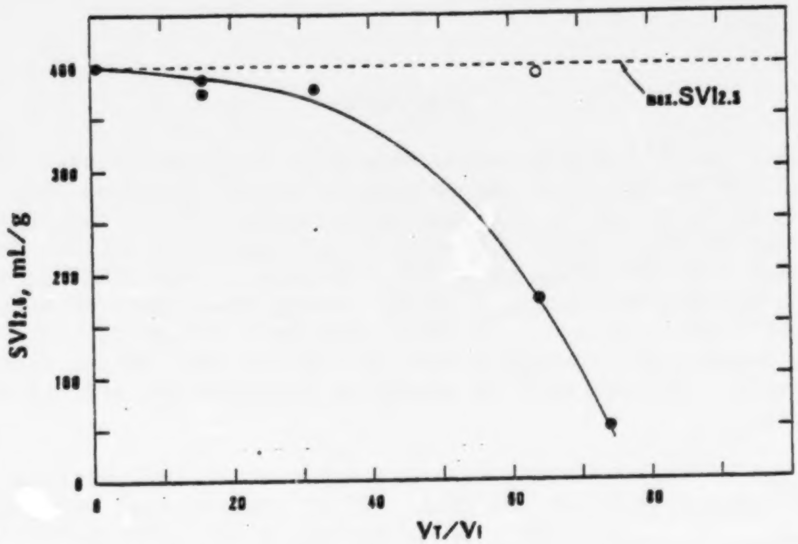

Figure 7. Relationship of final SVI (measured at 2.5 g TSS/L) to relative size of initial aeration basin compartment. (V_T = total aeration basin volume; V_i = volume of initial compartment; ●, for aerated initial compartments; ○, for anoxic initial compartments).

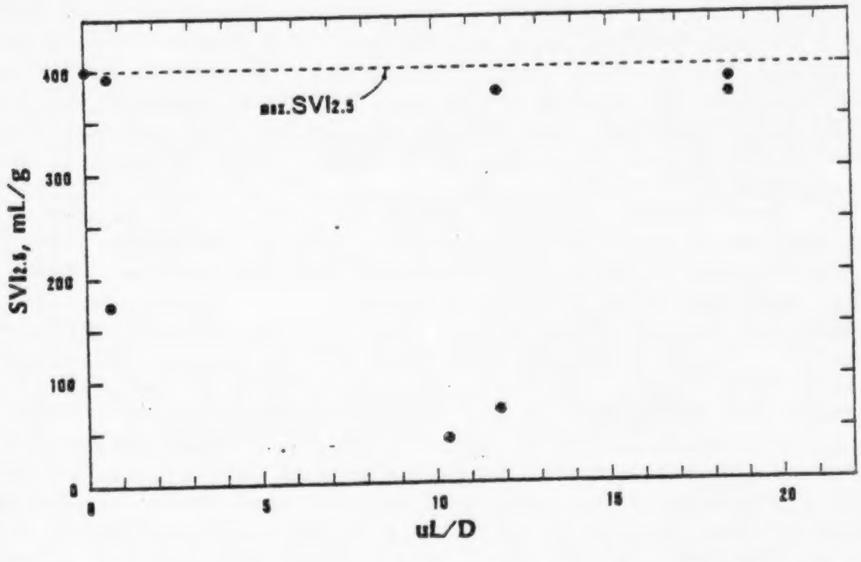

Figure 8. Relationship of final SVI (measured at 2.5 g TSS/L) to reciprocal of Dispersion number (uL/D) for aeration basin alone (no RAS flow or secondary clarifier included).

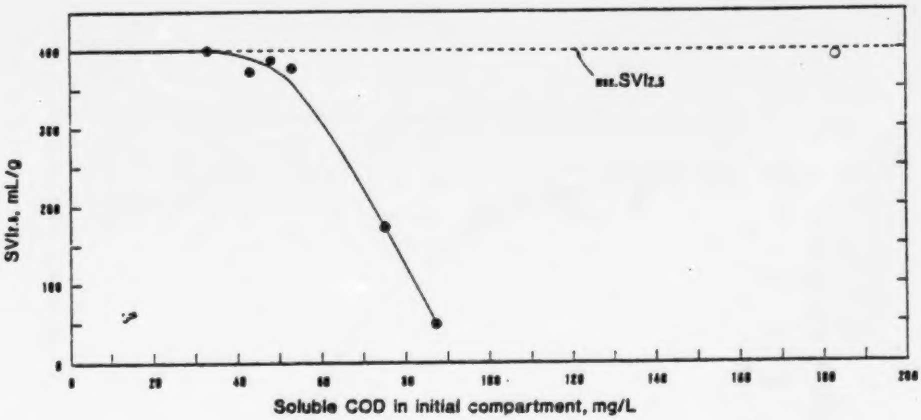

Figure 9. Relationship between SVI (measured at 2.5 g TSS/L) and soluble COD concentration in initial aeration basin compartment (●, aerated initial compartments; ○ anoxic initial compartments).

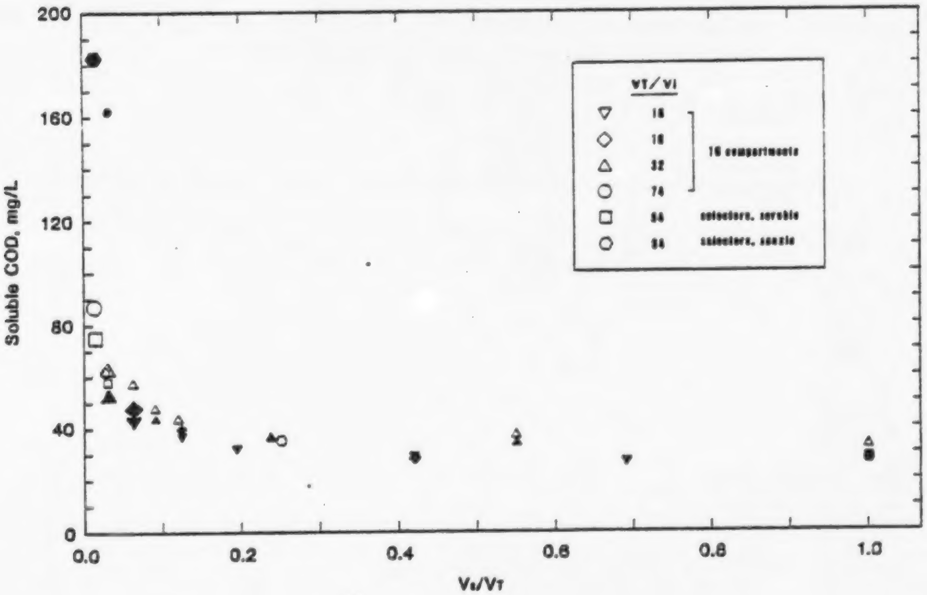

Figure 10. Soluble COD gradient throughout compartmentalized aeration basins. V_s/V_T is the fraction of the total aeration basin volume at the point of measurement. Solid points are systems that bulked; open points are systems that did not bulk. The large symbols are the soluble COD values in the initial compartment.

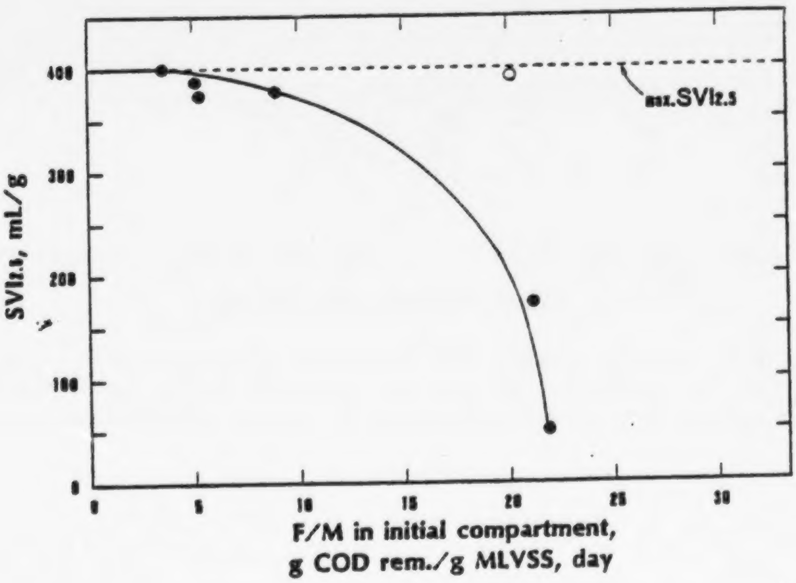

Figure 11. Relationship between SVI (measured at 2.5 g TSS/L) and F/M in initial aeration basin compartment.

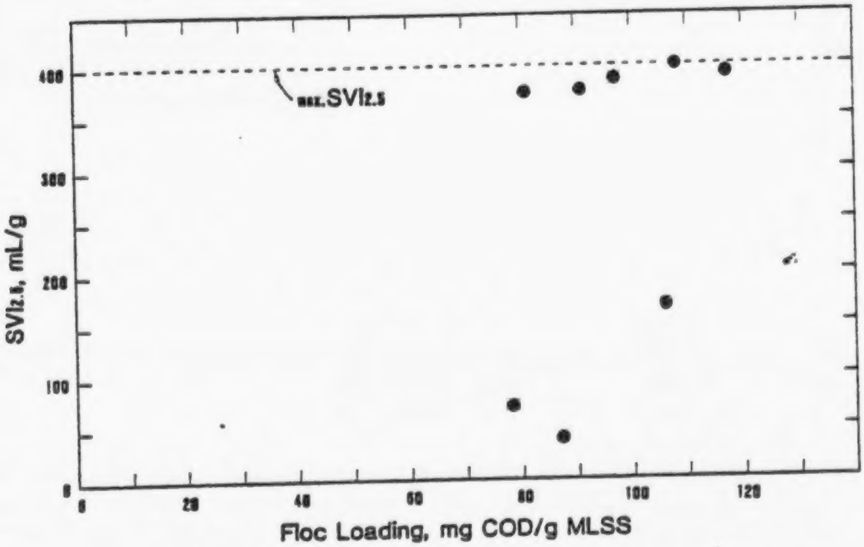

Figure 12. Relationship of SVI (measured at 2.5 g TSS/L)to floc loading (Eikelboom, 1981)(14).

1981)(14). While there is a consistent relationship between SVI and initial compartment F/M (similar to that between SVI and initial compartment size and soluble COD concentration) no such relationship exists between final SVI and floc loadings.

In the fifth series of experiments the following 3 reactors were run:

a. Two initial oxygenated compartments each 1/64th of the total aeration basin volume followed by one compartment 62/64ths of the total aeration basin volume.

b. Same as a. but with both initial compartments stirred and anoxic,

c. CSTR aeration basin.

Systems b. and c. behaved equivalently (Figure 6) and had final $SVI_{2.5}$ at the maximum value of 400 mL/g; system a. final SVI was 173 mL/g. These results and the plots in Figures 7, 9, 10, 11 indicate that anoxia in the initial mixing zone was detrimental to the curing of bulking. Some literature sources (Heide and Pasveer, 1974 (8); Tomlinson and Chambers, 1973 (12); White and Tomlinson, 1978 (21)) have suggested that the initial anoxic zones where RAS and sewage mix successfully prevent and cure bulking at low F/M. Eikelboom (1981)(14) recommends that the initial mixing zone be aerated both for mixing and because "biosorption" proceeds more rapidly than in anoxic basins; our data support this recommendation. Since the mixing conditions in our anoxic and aerated initial reactors were identical, we conclude that the effect of aeration was biochemical rather than physical.

All experiments were conducted with a constant recycle ratio (RAS flow influent flow) of 1.0. Tracer studies indicated, as expected, that recycle increased longitudinal mixing (increased dispersion number) (Table 3). Recycle dilutes soluble COD concentrations in the initial reactor; the recycle ratio determines the contact time between sludge and influent in the first reactor and influences the floc loading in the first reactor. Eikelboom (1981)(14) states that decreasing the recycle rate increases "biosorption" but decreases initial compartment COD removal. He suggests that there exists an optimum recycle rate corresponding to an optimum floc loading that produces optimum "biosorption". The influence of these factors was not addressed in this research because the recycle rate was constant. However, since the recycle ratio was maintained at the rather high value of 1.0, it can be concluded that the limiting sizes of the initial compartments found to be effective in curing bulking at low F/M are conservative, i.e. at lower recycle rates the initial compartment sizes could be larger. Further research is required to optimize the design parameters for initial compartment sizing.

Table 4 presents a summary of the predominant filamentous microorganisms present in the activated sludges from various series of experiments. In activated sludge systems with F/M = 0.16 g COD removed/g TMLVSS, day, Types 0041 and 0961 were predominant until the number of compartments was increased to eight. At higher loadings and greater degrees of compartmentalization (and therefore smaller initial compartment size and higher initial F/M) Type 021N

TABLE 3. EFFECT OF RECYCLE ON DISPERSION NUMBER OF VARIOUS AERATION BASIN CONFIGURATIONS

No. of Compartments	V_T/V_i	Dispersion Number Without Recycle	 With Recycle
1	1	∞	1.532
2	2	0.330	0.921
4	4	0.226	0.515
8	8	0.147	0.458
16	16	0.054	0.386
16	32	0.085	0.456
16	74	0.088	0.509
3	64	1.523	0.649

became common. At even higher loadings (F/M $\geq$ 0.74 g COD removed/g TMLVSS, day), Type 1701 and S. natans were present.

In the experiments conducted with various selector configurations at an F/M ≈ 0.3 g COD removed/g TMLVSS, day Type 021N was the most common filamentous organism. When the 2 compartment selector was employed, Thiothrix sp. was most common in both systems with aerated and anoxic selectors. S. natans and Type 1701 generally were more frequently found in significant amounts in the CSTR control than in the compartmentalized units.

These results are generally consistent with those of Chudoba (1973a)(5) who found that bulking in a CSTR activated sludge unit was caused by a mixture of Leucothrix sp. (Type 021N?) and S. natans while bulking in a unit with an intermediate degree of mixing was caused by Leucothrix sp. (Type 021N?) alone.

CONCLUSIONS

These conclusions are specific to City of Richmond, California settled domestic sewage and settled sewage supplemented by mixing with raw sludge; they also are specific to activated sludge systems with a recycle ratio of 1.

1. Bulking at low F/M (0.05-0.25 g COD removed/g TMLVSS, day) did not occur when CSTR activated sludge systems were fed either fresh or stale unsupplemented settled domestic sewage and TMLSS was in the range 1.0-1.7 g/L.

2. As soon as supplemented settled sewage was fed to CSTR activated sludge systems at F/M in the range 0.15-0.2 g COD removed/g TMLVSS, day, bulking occurred.

3. The conditions existing in the zone of initial mixing between activated sludge and wastewater are important in determining whether or not filamentous bulking occurs at low F/M.

TABLE 4. MOST COMMON TYPES OF FILAMENTOUS MICROORGANISMS IN ACTIVATED SLUDGE SYSTEMS

		Experimental system				Control system	
Experimental series	F/M (Avg.) $\left(\frac{\text{g COD Rem.}}{\text{g TMLVSS, day}}\right)$	No. of compartments	V_T/V_I	Min. DO* (mg/L)	Filament types	Min. DO (mg/L)	Filament types
1	0.16	1	1	2.5	--	2.5	--
2	0.16	1	1	2.5	0041, 0961	2.5	0041, 0961
	0.16	2	2	2.5	0961, 0041	2.5	0041, 0961
	0.16	4	4	2.5	0961, 0041	2.5	0041, 0961
	0.16	8	8	5.5	021N, 0961	2.5	0041, 0961
	0.16	16	16	7.0	--	2.5	--
3	0.24	16	16	7.0	--	5.5	0961, 021N
	0.39	16	16	11.0	--	5.5	021N, 0961
	0.53	16	16	16.0	021N, 0961	5.5	021N, 1701
	0.74	16	16	16.0	021N, 1701	9.0	S. natans, 1701
	1.00	16	16	16.0	1701, 021N	16.0	S. natans, 1701
	1.30	16	16	24.0	021N, 1701	24.0	021N, 1701
4	0.30	16	32	4.5	Nocardia, 0041, 021N	4.5	Nocardia, S. natans, 021N
	0.30	16	16	4.5	021N, Nocardia	4.5	021N, S. natans
	0.31	16	32	4.5	021N, 0961	4.5	0961, S. natans
	0.31	16	74	4.5	H. hydrossis, 0961	4.5	021N, 1701
	0.31	16	16	4.5	021N, 0581	4.5	0581, S. natans
5	0.32	3	64	4.5	Thiothrix, 021N	4.5	Thiothrix, 021N, 0961
	0.31	3	64	0.0	Thiothrix, 021N, 0581		

---

*Min. DO in initial compartment.

4. The degree of longitudinal mixing (as measured by the dispersion number) and the soluble COD gradient throughout the reactor do not appear to be important in determining whether or not filamentous bulking occurs at low F/M.

5. The F/M in the initial aeration basin compartment was found to be consistently related to final SVI while floc loading (Eikelboom, 1981)(14) did not show such a relationship.

6. An aeration basin configuration consisting of 16 compartments, the first 8 of which are 1/32nd of the total aeration basin volume, will prevent low F/M filamentous bulking from occurring in a non-bulking sludge. This aeration basin configuration will not cure low F/M filamentous bulking in already bulking sludge. Because conditions in the initial compartment appears to be important (rather than the gradient of condition throughout the entire aeration basin) it is proposed that this conclusion can be applied to an aeration basin configuration with two initial compartments each 1/32nd of the total basin volume followed by a large CSTR with a volume equal to 32/32nds of the total basin volume.

7. An aeration basin configuration consisting of 16 compartments, configured as follows: compartments 1 and 2 equal to 1/74th of total aeration basin volume; compartments 3-8 equal to 1/32nd of total aeration basin volume and compartments 9-16 equal to 1/10th of the total aeration basin volume, will both prevent and cure low F/M bulking. Again this conclusion is postulated to apply to a system consisting of two initial basins each 1/74th of the total basin volume followed by a large CSTR with a volume equal to 72/74ths of the total basin volume.

8. An aeration basin configuration consisting of two oxygenated (DO = 4.5 mg/L) initial compartments each 1/64th of the total basin volume followed by a CSTR equal to 62/64ths of the total basin volume produced a modest reduction in the SVI (measured at 2.5 g TSS/L) of a bulking sludge from 400 mL/g to 173 mL/g at low F/M. An identically-configured system with anoxic (stirred, N_2-flushed) initial compartments did not influence bulking at low F/M any differently from a control CSTR. It is therefore concluded that initial mixing zones for control of low F/M bulking should be aerated.

9. Critical values of initial compartment parameters for control of low F/M bulking for this waste are: soluble COD $\geq$ 80 mg/L, F/M in the first reactor $\geq$ 20 g COD removed/g MLVSS, day. Further work is needed to generalize these values and account for the effect of variables such as waste characteristics, recycle ratio, MLSS concentration, etc.

10. The filamentous organisms most commonly occurring in the compartmentalized units at F/M values of approx. 0.3 g COD removed/g TMLVSS, day were Type 021N and Thiothrix sp.; in the CSTR system and the more highly loaded compartmentalized systems Type 1701 and S. natans also occurred. Both the compartmentalized systems and the CSTR systems at lower F/M values contained Types 0041 and 0961. These results generally are

consistent with those of Chudoba (1973a)(5) and also suggest that the data presented here will be generally applicable to the management of bulking caused by Type 021N.

ACKNOWLEDGMENTS

The research was conducted at the Sanitary Engineering Research Laboratory, University of California, Berkeley, with partial support from the Municipal Engineering Research Laboratory, US EPA, Cincinnati, Ohio. At the time that the research was conducted, Sang-Eun Lee was a Doctoral Candidate and Ben L. Koopman was a Post-Doctoral Research Fellow both in Sanitary Engineering. The technical assistance of John Potter and Stuart Foster is acknowledged; Drs. Michael G. Richard and Peter F. Strom are thanked for their assistance in filamentous organism identification.

REFERENCES

1. Sezgin M., Jenkins D. and Parker D. S. (1978) A unified theory of filamentous activated sludge bulking. J. Water Pollution Control Fed., 50, 362-381.

2. Palm J. C., Jenkins D. and Parker D. S. (1980) The relationship between organic loading, dissolved oxygen concentration and sludge settleability in the completely-mixed activated sludge process. J. Water Pollution Control Fed., 52, 2484-2506.

3. Strom, P. and Jenkins D. (1979) Filamentous microorganisms in activated sludge bulking in the U. S. particularly California. Paper presented at the 51st annual conference of California WPCA, San Diego, California.

4. Eikelboom, D. H. (1975) Filamentous organisms observed in activated sludge. Water Research, 9, 365-388.

5. Chudoba J., Ottova V. and Madera V. (1973a) Control of activated sludge filamentous bulking - I. Effects of hydraulic regime or degree of mixing in an aeration tank. Water Research, 7, 1163-1182.

6. Chudoba J., Grau P. and Ottova V. (1973b) Control of activated sludge filamentous bulking - II. Selection of microorganisms by means of a selector. Water Research, 7, 1389-1406.

7. Chudoba J., Blaha J. and Madera V.(1974) Control of activated sludge filamentous bulking - III. Effects of Sludge Loadings. Water Research, 8, 321-327.

8. Heide B. A. and Pasveer A. (1974) Oxidation ditch: Prevention and control filamentous sludge, H_2O, 7, 373-377.

9. Rensink J. H. (1974) New approach to preventing bulking sludge. J. Water Pollution Control Fed., 46, 1888-1894.

10. Houtmeyers J. (1978) Relations between substrate feeding patterns and development of filamentous bacteria in activated sludge processes. Agricultura, 26, 1-135.

11. Tomlinson E. J. (1976) Bulking - A survey of activated sludge plants. Technical Report TR35. Water Research Centre, Stevenage, England.

12. Tomlinson E. J. and Chambers B. (1973) The effects of longitudinal mixing on the settleability of activated sludge. Technical Report TR122. Water Research Centre, Stevenage, England.

13. Rensink J. H., Jellema K. and Ywema T. (1977) The influence of substrate gradient on the development of bulking sludge. H_2O, 10, 338-340.

14. Eikelboom D. H.(1981) Biosorption and prevention of bulking sludge by means of high floc loading. Paper 3, Water Research Centre Conference, Cambridge, England.

15. van der Laan E. T. (1958) Notes on diffusion type model for longitudinal mixing in flow. Chemical Engineering Science, 7, 187-191.

16. Levenspiel O. (1962) Chemical Reaction Engineering, Wiley and Sons, New York.

17. Standard Methods for the Examination of Water and Wastewater. (1975) 14th Edition. Amer. Public Health Assoc., New York.

18. Solorzano L. (1969) Determination of ammonia in natural waters by the phenolhypochlorite method. Limnology and Oceanology, 14, 799-801.

19. U. S. Environmental Protection Agency (1974) Manual of Chemical Analysis of Water and Wastes.

20. Tomlinson E. J. and Chambers B. (1978) The use of anoxic mixing zones to control the settleability of activated sludge. Cologne International. Traitement Combine Des Eaux usees Domestiques et Industrielles. University de Liege.

21. White, M. J. D. and Tomlinson E. J. (1978) The effect of anoxic mixing zones upon the settleability of activated sludge. Unpublished report. Water Research Centre, Stevenage, England.

Comments on
The Effect of Aeration Basin Configuration on Activated Sludge Bulking at Low Organic Loading

G. Wolfgang Fuhs
Division of Laboratories and Research
New York State Department of Health
Albany, New York

The purpose of my discussion is not to present a critique of an ongoing EPA-funded project but to discuss the results of a completed project and to make suggestions for the continuation of this work under a grant which EPA has awarded Professor Jenkins based on the recommendation of our Review Panel. I have neither had the opportunity of reviewing the past proposal or of refreshing my memory regarding the exact contents of the continuation proposal, but I have been provided with a copy of Professor Jenkins' manuscript for his presentation and I have re-analyzed some of the data for this discussion.

The paper deals with the important problem of filamentous bulking in the activated sludge process, and particularly with the bulking at low organic loadings in terms of the F/M ratio. It builds on the experience of European workers regarding the suppression of filamentous organism growth by a plug-flow arrangement or the addition of a short detention time initial compartment where sewage feed and return activated sludge mix, and addresses hypotheses advanced by these workers to explain the suppression or curing of activated sludge bulking by this arrangement. By varying basin configurations and keeping the overall F/M ratio essentially constant at the low value of 0.3 g COD removal/g TMLVSS-day, and TMLVSS at 3 g/liter the authors show that the prevention and cure of filamentous bulking is related to a high ratio of total tank volume to initial compartment volume (V_t/V_i) and associated high F/M ratios for the initial compartment and not to high "floc loading rates" (mg COD/g MLVSS) or to the degree of longitudinal mixing. Bulking occurred at V_t/V_i values of 16 or below. It was prevented at V_t/V_i = 32 and cured at V_t/V_i = 74. In the initial compartment, where supplemented sewage feed (COD around 750 mg/l) was mixed with an equal volume of return activated sludge, soluble COD was 43, between 53 and 63, and 87 mg/l for V_t/V_i values of 16, 32, and 74 respectively, while effluent COD was typically around 33 mg/l. We also note that hydraulic detention times in the initial compartments of the three configurations were 75, 37, and 16 minutes respectively. During these periods, the contact of the recycled activated sludge with the feed appears to cause or trigger an event which leads to a population imbalance in the bulking sludge leading to a reduction in filamentous growth or changed association of filaments and floc microcolonies. The result is an improvement in settling characteristics. The action undoubtedly occurs in small steps as the sludge passes repeatedly through the initial compartment.

The biomass change (dX) in an activated sludge system can be presented as the sum of several rate terms:

$$\frac{dX}{dt} = G - D - W_1 - W_2$$

where G is growth; D, decay; W_1, washout, i.e., inadvertent loss of biomass to the effluent; and W_2, deliberate wastage of excess activated sludge. Time t is in units of solids detention time. In the steady state, the sum of the rate terms over one solids cycle is zero:

$$\frac{dX}{dt} = 0$$

It is important to note that this equation also holds individually for the species comprising the biomass. The only requirement for the steady state of the individual species, again, is that the sum of the several rate terms for that species be zero. The individual terms can assume values quite different from the individual values for the total biomass. (In the steady state, the equation also holds in terms of cell numbers, N, besides biomass, X). This means that in principle the species comprising the biomass can grow, decay, and be subject to washout at different rates. Steady state is maintained when the species biomass (or cell number) remains constant in each compartment. It also follows that the species composition of the total biomass in the different compartments can be different, because the individual rate terms are species-specific. (The independence of the species is, of course reduced by metabolic mutualisms and physical association during settling of the floc.)

A population imbalance occurs if the sum of the rate terms for any species becomes non-zero. In the present case we can assume an effect on growth either alone or in combination with an effect on microcolony structure. (I remember a sludge consisting of spherical microcolonies of mixed bacteria and separate Thiothrix filaments that settled quite well.)

In the present experiments, we can estimate the effect on biomass in the initial compartment on the basis that 1 mg COD corresponds to 1.9 mg of a carbohydrate substrate which is utilized with a yield of approximately 0.6 (w/w) producing approximately 1.13 mg of biomass. The following outputs for the initial compartment are obtained with equal volumes of sewage feed (390 mg soluble COD/liter, 360 mg particulate COD/liter) and return activated sludge (6 g TMLVSS/liter and 33 mg soluble COD/liter) as inputs:

V_t/V_i	Hydraulic Detention Time, Min.	Sol. COD mg/l	TMLVSS, g/l A*	 B*	 C*
16	75	43	3.19	3.39	3.53
32	37	58	3.17	3.38	3.51
74	16	87	3.12	3.34	3.46

This corresponds to increases in the biomass according to the following table:

Biomass Increase in Initial Compartment (Percent)

V_t/V_i	Over Detention Time A*	 B*	 C*	Per Hour A*	 B*	 C*
16	6.3	13.0	17.7	5.0	10.4	14.2
32	5.7	12.7	17.0	9.2	20.6	27.6
74	4.0	11.3	15.3	15.0	42.4	57.4

*Assumptions:

A = only soluble COD converted
B = all COD converted
C = soluble COD converted, particulate
COD adsorbed

The authors did not establish a mass balance for the initial compartment. The calculations suggest that the disappearance of soluble COD alone in this compartment will increase biomass by a small but non-trivial amount (columns A), although measurements of TMLVSS would give results in the range indicated by columns B and C, depending on the degree of conversion of particulate COD to biomass. As expected, the effect on biomass increases as the size of the first compartment decreases.

Activated sludge is an assemblage of microorganisms in a state of carbon (energy) limitation. The initial effect of the addition of a soluble, biodegradable organic substrate to such an assemblage is the uptake of some of the substrate with the formation of ribonucleic acid and enzyme protein. This sequence is termed "metabolic upshift". During these events, the microorganisms increase their mass but multiplication is essentially absent. This phase is followed by the uptake of additional substrate with a partial conversion of it to CO_2 while the larger part is converted to storage products, e.g., glycogen. The term "oxidative assimilation" designates this process which, if nutrients have not become limiting, is followed by the familiar logarithmic increase in both biomass and organism numbers per unit volume of culture. If the nutrients are exhausted, nutrient uptake ceases first leading to "metabolic downshift" and continued cell multiplication until internal reserves are exhausted. The following graph illustrates this relationship between growth in terms of mass and cell numbers:

Figure 1

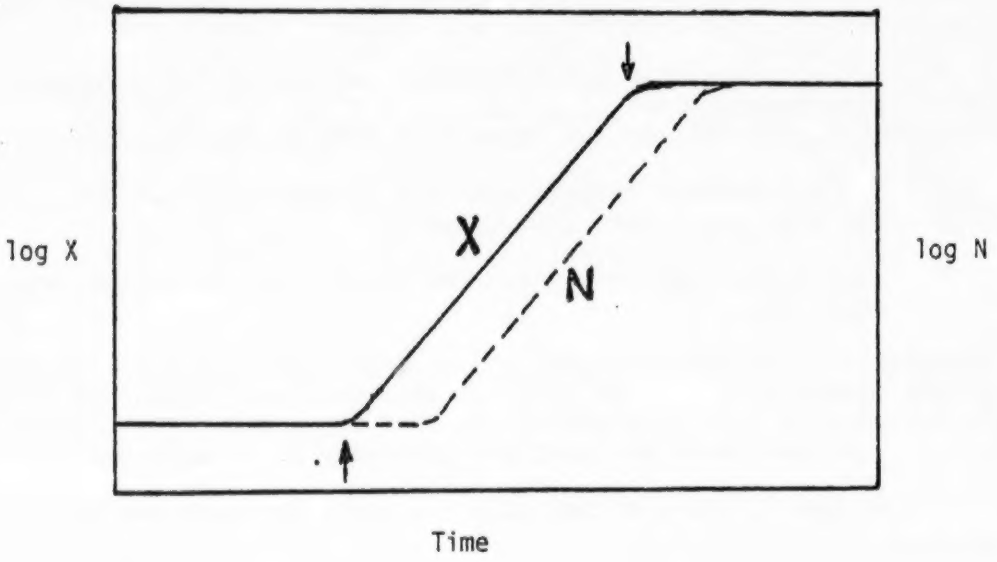

Figure 1. Relationship of microbial growth in terms of mass (X) and number (N) upon limiting nutrient addition (↑) and exhaustion (↓).

If the increase, as is the case in these experiments, is less than is required for a doubling of the biomass, the metabolic upshift nevertheless occurs at least in those organisms which can avail themselves of substrates making up the soluble COD, and the chemical composition of the cells will change. Any increase in mass may lead to the multiplication of a corresponding part of the population, i.e., cells that are ready to divide will do so, others will go through one or more cycles, and depending on their metabolic requirements and affinity to the several substrates available, will either gather more or lose stored reserves during the remainder of the activated sludge cycle.

While all this may seem very complicated, it is also a fact that methodology is presently available to measure the changes in nutritional state associated with metabolic upshift not only by macrochemical methods but also in individual members of a mixed microbial population either after appropriate separation or by cytochemical techniques. This methodology is available at several levels of sophistication depending on the degree of accuracy required in quantifying the results. Even applied in a crude fashion, it would provide clues on the species affected by nutritional imbalances associated with activated sludge bulking, be it from low F/M ratios, anoxia, or other causes.

During his presentation today Professor Jenkins put forth several ideas on approaches to a better understanding of low F/M activated sludge bulking, e.g. by examining hypotheses such as the following:

1. At low substrate concentration the filamentous organisms may grow faster than floc formers.

2. Floc formers may store substrate better than the filamentous organisms.

Consideration of surface-to-volume ratios of filaments and flocs suggest that both mechanisms may be at work. In addition, the filamentous forms could be inhibited by a component in the feed if present at high concentration. I agree that these are important questions to be addressed.

In addition, I feel that the following areas for study can be identified:

1. The sludge volume index (SVI) as a measurement of bulking should be compared with direct measurments of filament length to confirm that bulking is not caused by a change in the mechanical association of filaments and microcolonies making up the floc.

2. The effect of parameters such as reactor suspended solids, recycle rate, feed composition, and anoxia remains to be investigated.

In conclusion, Professor Jenkins should be congratulated for his and his group's success in the first part of this study and for the development of a practical approach to prevent and cure low F/M activated sludge bulking. The movement towards the inclusion of state-of-the-art measurements and real-cause variables in the modelling, design, and operation of biological wastewater treatment plants is not only important, but imperative particularly for the more advanced, and more complex, biological nutrient removal processes. This study is one that should, and according to the investigator's declared intent, would be conducted with a view on the underlying mechanisms. I feel that such an approach should be encouraged by the project officer who will oversee this work. As a member of the Review Panel I find this work very stimulating and would welcome future opportunities for briefings and discussion.

ENVIRONMENTAL ENGINEERING RESEARCH SEMINAR
July 22-24, 1981
Cincinnati, Ohio

ATTENDEES

Barry M. Austern
U.S. Environmental Protection Agency
Municipal Environmental Research Lab.
Cincinnati, Ohio 45268

William Batchelor
Texas A&M University
Civil Engineering, TAMU
College Station, Texas 77843

E. Robert Baumann
Iowa State University
496 Town Engineering Building 6
Ames, Iowa 50011

Dolloff F. Bishop
U.S. Environmental Protection Agency
Municipal Environmental Research Lab.
Cincinnati, Ohio 45268

Donald F. Carey (RD-671)
U.S. Environmental Protection Agency
401 M Street, S.W.
Washington, D.C. 20460

Keith Carswell
U.S. Environmental Protection Agency
Municipal Environmental Research Lab.
Cincinnati, Ohio 45268

William A. Cawley
U.S. Environmental Protection Agency
Industrial Environmental Research Lab.
Cincinnati, Ohio 45213

R. E. Chaddock
P. O. Box 1057
Port Orange, Florida 32019

Erik R. Christensen
University of Wisconsin
Department of Civil Engineering
Milwaukee, Wisconsin 53201

G. Lee Christensen
Civil Engineering Department
Villanova University
Villanova, Pennsylvania 19085

Jesse M. Cohen
U.S. Environmental Protection Agency
Municipal Environmental Research Lab.
Cincinnati, Ohio 45268

Sandy Cronier
University of Cincinnati
Department of Civil & Environmental Engineering
721 Rhodes Hall, #71
College of Engineering, U.C.
Cincinnati, Ohio 45221

Richard R. Dague
University of Iowa
College of Engineering
Iowa City, Iowa 52242

Chuck Darvin
U.S. Environmental Protection Agency
Industrial Environmental Research Lab.
Cincinnati, Ohio 45213

Richard M. Daum
U.S. Environmental Protection Agency
Technical Support Division
Cincinnati, Ohio 45213

Richard I. Dick
Cornell University
118 Hollister Hall
Ithaca, New York 14853

Francis A. DiGiano
University of North Carolina
ESE Department
Rosenau Hall
Chapel Hill, North Carolina 27514

Wayne F. Echelberger, Jr.
Indiana University
School of Public & Environmental Affairs
Indianapolis, Indiana 46202

Dick Eilers
U.S. Environmental Protection Agency
Municipal Environmental Research Lab.
Cincinnati, Ohio 45268

Richard Engdahl
Battelle Institute
505 King Avenue
Columbus, Ohio 43201

Peter Fedkiw
North Carolina State University
Department of Chemical Engineering
Raleigh, North Carolina 27650

Kim R. Fox
U.S. Environmental Protection Agency
Municipal Environmental Research Lab.
Cincinnati, Ohio 45268

G. Wolfgang Fuhs
New York State Department of Health
Division of Laboratories & Research
Empire State Plaza
Albany, New York 12201

Marvin C. Gardels
U.S. Environmental Protection Agency
Municipal Environmental Research Lab.
Cincinnati, Ohio 45268

A. Gehr
McGill University
Department of Civil Engineering
817 Sherbrooke St. W.
Montreal, Quebec H3A 2K6

Edwin E. Geldreich
U.S. Environmental Protection Agency
Municipal Environmental Research Lab.
Cincinnati, Ohio 45268

John Gorgol
Rutgers College of Engineering
P. O. Box 909
Piscatway, New Jersey 08854

O. J. Hahn
University of Kentucky
Mechanical Engineering Department
Lexington, Kentucky 40506

George P. Hanna, Jr.
California State University
School of Engineering
Fresno, California 93740

Stuart A. Hoenig
University of Arizona
Department of Electrical Engineering
Tucson, Arizona 85721

John Hoff
U.S. Environmental Protection Agency
Municipal Environmental Research Lab.
Cincinnati, Ohio 45268

Janet M. Houthoofd
U.S. Environmental Protection Agency
Municipal Environmental Research Lab.
Cincinnati, Ohio 45268

Chin-Pao Huang
Department of Civil Engineering
University of Delaware
Newark, Delaware 19711

J. C. Howard Huang
University of Missouri
Director of Environmental Research Center
Rolla, Missouri 65401

Jerry Huang
Associate Professor
University of Wisconsin
Department of Civil Engineering
Milwaukee, Wisconsin 53201

James R. Hunt
University of California
642 Davis Hall
Berkeley, California 94720

Walter Jakubowski
U.S. Environmental Protection Agency
Health Effects Research Laboratory
Cincinnati, Ohio 45268

Steve James
U.S. Environmental Protection Agency
Municipal Environmental Research Lab.
Cincinnati, Ohio 45268

David Jenkins
University of California - Berkeley
11 Yale Circle
Kensington, California 94708

Stephen L. Johnson (RD-672)
U.S. Environmental Protection Agency
401 M Street, S.W.
Washington, D.C. 20460

Kaz Kawata
The Johns Hopkins University
615 N. Wolfe Street
Baltimore, Maryland 21205

Hraj A. Khararjian
University of Petroleum & Minerals
Civil Engineering Department
UPM 1754
Khahran, Saudi Arabia

I. J. Kugelman
U.S. Environmental Protection Agency
Municipal Environmental Research Lab.
Cincinnati, Ohio 45268

Desmond Lawler
Department of Civil Engineering, ECJ 8-6
University of Texas at Austin
Austin, Texas 78712

James O. Leckie
Stanford University
Environmental Engineering and Science
Department of Civil Engineering
Stanford, California 94305

William W. T. Lee
University of Pennsylvania
Philadelphia, Pennsylvania 19104

Louis W. Lefke
U.S. Environmental Protection Agency
Municipal Environmental Research Lab.
Cincinnati, Ohio 45268

David Leith
Harvard University
Department of Environmental Health Sciences
665 Huntington Avenue
Boston, Massachusetts 02115

Lucille W. Light
U.S. Environmental Protection Agency
Municipal Environmental Research Lab.
Cincinnati, Ohio 45268

Hanlieh Liu
Hydronautics, Inc.
7210 Pindell Sch. Rd.
Laurel, Maryland 20810

Gary S. Logsdon
U.S. Environmental Protection Agency
Municipal Environmental Research Lab.
Cincinnati, Ohio 45268

Khalil H. Mancy
University of Michigan
2530 SPH-I
Ann Arbor, Michigan 48109

Michael P. Manning
Department of Chemical Engineering
Massachusetts Institute of Technology
Rm. 66-568
Cambridge, Massachusetts 02139

Richard Marland (RD-675)
U.S. Environmental Protection Agency
401 M Street, S.W.
Washington, D.C. 20460

R. Craig Matthiessen
U.S. Environmental Protection Agency
Office of Toxic Substances
5909 Vernons Oak Ct.
Burke, Virginia 22015

Mark A. McClanahan
U.S. Environmental Protection Agency
345 Courtland Street
Atlanta, Georgia 30365

A. Gary Meyer
U.S. Environmental Protection Agency
Municipal Environmental Research Lab.
Cincinnati, Ohio 45268

Charles R. O'Melia
Johns Hopkins University
Department of Geography & Environmental Engineering
Baltimore, Maryland 21218

Edward J. Opatken
U.S. Environmental Protection Agency
Municipal Environmental Research Lab.
Cincinnati, Ohio 45268

Robert W. Peters
Purdue University
Environmental Engineering
School of Civil Engineering
West Lafayette, Indiana 47907

James H. Porter
Energy & Environmental Engineering, Inc.
675 Massachusetts Avenue
Cambridge, Massachusetts 02139

H. William Prengle, Jr.
Professor of Chemical Engineering
Chemical Engineering Department
University of Houston
Houston, Texas 77004

Eugene W. Rice
U.S. Environmental Protection Agency
Municipal Environmental Research Lab.
Cincinnati, Ohio 45268

Chet A. Rock
Civil Engineering Department
University of Maine
457 Aubert Hall
Orono, Maine 04469

Donald R. Rowe
Western Kentucky University
Department of Engineering & Technology
Bowling Green, Kentucky 42101

Pasquale V. Scarpino
University of Cincinnati
Department of Civil & Environmental Engineering
721 Rhodes Hall, #71
Cincinnati, Ohio 45221

E. D. Schroeder
University of California
Department of Civil Engineering
Davis, California 95617

Selim Senkan
Massachusetts Institute of Technology
Rm. 66-501
Cambridge, Massachusetts 02139

Joseph H. Sherrard
Virginia Tech
Department of Civil Engineering
Blacksburg, Virginia 24061

Rolf T. Skrinde
Olympic Associates
P. O. Box 9445
Seattle, Washington 98109

Owen I. Smith
University of California
Department of Chemical Engineering
5531 Boelter Hall
Los Angeles, California 90024

Vernon L. Snoeyink
University of Illinois
208 N. Romine
Department of Civil Engineering
Urbana, Illinois 61801

Otis J. Sproul
Ohio State University
Department of Civil Engineering
2070 Neil Avenue
Columbus, Ohio 43210

Arthur C. Stern
University of North Carolina
602 Croom Court
Chapel Hill, North Carolina 27514

Mike Strutz
U.S. Environmental Protection Agency
Industrial Environmental Research Lab.
Cincinnati, Ohio 45213

J. S. Taylor
University of Central Florida
CEES Department
Orlando, Florida 32816

Dennis Tirpak
U.S. Environmental Protection Agency
401 M Street, S.W.
Washington, D.C. 20460

Richard F. Unz
Pennsylvania State University
Department of Civil Engineering
212 Sackett Building
University Park, Pennsylvania 16802

Albert D. Venosa
U.S. Environmental Protection Agency
Municipal Environmental Research Lab.
Cincinnati, Ohio 45268

Thomas C. Voice
University of Michigan
178 Engineering 1-A
Ann Arbor, Michigan 48109

Louis A. Volse
University of Detroit
Department of Civil Engineering
4001 McNichols Road
Detroit, Michigan 48221

Charles F. Walters
C.W. Associates
Drawer 246
Carrboro, North Carolina 27514

Walter J. Weber, Jr.
University of Michigan
181 Water Resources Engineering Bldg. 1-A
Ann Arbor, Michigan 48109

Constance Wells
University of Cincinnati
Department of Civil & Environmental Engineering
721 Rhodes Hall, #71
College of Engineering, U.C.
Cincinnati, Ohio 45221

Charles L. Wilkins
University of California
Department of Chemistry
Riverside, California 95021

Robert T. Williams
U.S. Environmental Protection Agency
Municipal Environmental Research Lab.
Cincinnati, Ohio 45268

George E. Wilson
Eutec Systems
4212 N. River Way
Sacramento, California 95825

Robert Wise
U.S. Environmental Protection Agency
Municipal Environmental Research Lab.
Cincinnati, Ohio 45268

Harold W. Wolf
Texas A&M University
Civil Engineering Department
College Station, Texas 77843

Yeun C. Wu
University of Pittsburgh
944 Benedum Hall
Department of Civil Engineering
Pittsburgh, Pennsylvania 15261

Ping-Yi Yang
University of Hawaii at Mamoa
Department of Agricultural Engineering
Honolulu, Hawaii 96822